Explor Anim Med Res.
Vol. 16, Issue 1, 2026
DOI: 10.52635/eamr/16.1.1-2

ISSN 2277-470X (Print), ISSN 2319-247X (Online)
Website: www.animalmedicalresearch.org

Published under the CC BY-NC 4.0 license

Editorial

UNRAVELLING THE GUT MICROBIOME: FOUNDATIONS AND FRONTIERS IN ANIMAL HEALTH AND PRODUCTIVITY

The microbiome comprises a complex community of bacteria, archaea, viruses, and eukaryotic microbes that inhabit both the internal and external surfaces of animal bodies. These microbial populations exert profound influences on animal health and disease, facilitating metabolic processes, pathogen defence, immune system modulation, and a variety of other physiological functions. Consequently, their collective impact is integral to virtually all aspects of host biology.

The gut microbiota, in particular, is a dynamic assemblage of bacteria, archaea, and eukaryotes residing within the gastrointestinal tract. Over millennia, these microorganisms have coevolved with their hosts, establishing intricate, and mutually beneficial relationships. Given the vast number of microbial cells present, the host and its resident microbes are often conceptualized as a superorganism. The gut microbiota confers numerous physiological benefits, including the maintenance of gut integrity, modulation of the intestinal epithelium, energy generation, protection against pathogens, and regulation of host immunity. However, disturbances in microbial composition, collectively referred to as dysbiosis, may compromise these critical functions. Advancements in high-throughput genomic profiling and ecosystem characterisation have highlighted the microbiota's crucial roles in a wide range of gut-related pathological conditions. The prevailing comprehension of gastrointestinal microbiota formation and composition underscores its impact on gut integrity and host health.

In livestock, the gastrointestinal microbiota is central to gut development, feed digestion and utilization, and immune responses. Patterns of microbial colonisation in early life have lasting impacts, determining the composition and functional capabilities of the microbiota and ultimately affecting host phenotypes. The gut microbiota itself is a highly diverse community, encompassing bacteria, archaea, fungi, protozoa, and viruses. The broader concept of the gut microbiome includes not only these living microorganisms but also plasmids, dead cells, extracellular DNA, and various macromolecular structures such as proteins and polysaccharides. This diversity reflects the evolutionary adaptation of the host-microbe consortium to dietary habits and environmental pressures.

While the gut microbiota is predominantly composed of bacteria, the other microbial constituents including bacteriophages and fungi play essential roles in maintaining ecosystem stability. Bacteriophages or phages, are abundant in the gastrointestinal tract and are instrumental in shaping bacterial communities through predation and horizontal gene transfer. These phage-bacteria interactions influence microbial diversity, antimicrobial resistance, and metabolic functions. In livestock, phages are increasingly viewed as potential tools for microbiota engineering. Fungi, although less prevalent, are particularly important in ruminants, where anaerobic genera such as Piromyces and Neocallimastix facilitate the breakdown of recalcitrant plant fibres by producing potent hydrolytic enzymes. These fungi interact synergistically with fibrolytic bacteria and methanogenic archaea, enhancing lignocellulose degradation in the rumen. In monogastric animals, commensal fungi such as Candida and Saccharomyces are common, though dysbiosis lead to health disorders. Further, it is vital to recognize the interdependence among bacteria, phages, and fungi in shaping microbial ecosystems in livestock. Future research integrating multi-kingdom microbial interactions will advance our understanding of microbiota function and its implications for animal health and productivity.

The composition of gut microbial communities is influenced by several environmental and physiological factors that differ across the gastrointestinal tract. The key determinants include pH, osmolarity, nutrient availability, oxygen concentration, and feed retention time, each influencing microbial selection and colonization. For example, the rumen's neutral pH favours fibre-degrading bacteria such as *Fibrobacter* and *Ruminococcus*. In contrast, the acidic environment of the monogastric stomach supports acid-resistant species like *Lactobacillus* and *Streptococcus*. Dietary composition and water intake influence gut osmolarity, with high-starch diets promoting amylolytic bacteria such as *Prevotella*. The retention time of digesta is extended in ruminants and reduced in monogastrics, influencing microbial fermentation and nutrient

absorption. Despite the gut being predominantly anaerobic, microaerophilic niches are present too, allowing facultative anaerobes like *Escherichia coli* to flourish, especially in reaction to host metabolic changes. These factors jointly promote niche specialisation and interspecies variations in microbiota composition, underscoring the complex interaction between host physiology and microbial ecology.

In recent years, the core gut microbiome has evolved from a novel concept to a central focus of biomedical research, with an exponential increase in the scientific literature on the gut microbiome in the past two decades. Although the microbiome is highly personalised, the term "core" denotes a shared set of microbial taxa, genes, or functional capabilities that are present in the vast majority of healthy individuals. The core gut microbiome in livestock consists of a stable consortium of bacteria, archaea, fungi, and protozoa shared among individuals of the same species, irrespective of diet or environment. This core community is essential for health, nutrient assimilation, and immune function, and is central to production parameters such as growth and milk yield via the breakdown of fibre and synthesis of volatile fatty acids. Core taxa also produce essential metabolites, including amino acids and vitamins, and encode key fibre-degrading enzymes critical for host nutrition. Through cross-feeding networks, core microorganisms support the broader microbial community, underpinning ecosystem stability. Manipulating these core microbial groups holds potential to enhance microbiome function and ruminant metabolism, with far-reaching implications for food security and environmental sustainability.

Identifying and characterizing the core gut microbiota established in early life represents a promising avenue for improving animal health and productivity, though significant conceptual and methodological challenges remain. Advances in multi-omics technologies, high-resolution sequencing, and artificial intelligence have opened new opportunities to elucidate microbial communities that drive growth efficiency, immune maturation, and disease resilience. However, distinguishing true "core" taxa from transient or environment-specific populations demands rigorous longitudinal and cross-cohort studies utilizing standardized sampling and analytical methods. Moreover, mechanistic insights linking microbial composition and function to host physiology and long-term performance require integrative approaches bridging microbiology, animal genetics, and nutritional sciences. The principal challenge moving forward lies in translating these insights into sustainable, microbiome-informed strategies that enhance animal production while mitigating environmental impact.

In conclusion, as our understanding evolves, it is clear that in livestock, the gut microbiome represents a highly complex and dynamic consortium of microorganisms that profoundly influence health, metabolism, immunity, and disease resistance. The gut microbiota, in particular, forms intricate and co-evolved relationships with its host, playing a pivotal role in maintaining gut integrity and overall physiological balance, and production performances. Disruptions in microbial composition, or dysbiosis, can compromise these essential functions. The gut microbiota, comprising bacteria, archaea, fungi, protozoa, and viruses, contributes to digestion, immune development, and nutrient assimilation, with its composition shaped by species, diet, and environmental factors. Ensuring the stability of the core gut microbiome is fundamental for optimal health, growth, and productivity in livestock. Advancing our understanding and management of these microbial communities offers promising avenues for enhancing animal performance and sustainability, while simultaneously addressing the intricate challenges associated with host–microbe interactions.

Dr Arindam Dhali
Head of the Station
ICAR-National Dairy Research Institute
Southern Regional Station
Adugodi, Hosur Road, Bengaluru – 560 030

Cite this article as: Dhali A. Unravelling the gut microbiome: foundations and frontiers in animal health and productivity. Explor Anim Med Res. 2026; 16(1), DOI: 10.52635/eamr/16.1.1-2.

Explor Anim Med Res.
Vol. 16, Issue 1, 2026
DOI: 10.52635/eamr/16.1.03-13

ISSN 2277-470X (Print), ISSN 2319-247X (Online)
Website: www.animalmedicalresearch.org

Published under the CC BY-NC 4.0 license

Review Article

PALEOPARASITOLOGY: A MODERN-DAY RETHINKING OF HG WELLS TIME MACHINE

Debasis Bhattacharya[1*], T. Sujatha[1], Arun Kumar De[1], Jai Sunder[1], Sharath S Yeligar[1], Sneha Sawhney[1] and Snehil Gupta[2]

Received 26 July 2025, revised 23 April 2026

ABSTRACT: This compilation deals with recent records of paleoparasitology both in Old World and New World. Paleoparasitology study has been started very recently in 1910 when M.A. Ruffer described *Schistosoma japonicum* eggs in Egyptian mummies (dated 1250-1000 BCE). Since then, paleoparasitological records have been published even if in 21st century. Three types of substrates are used for paleoparasitological diagnosis. They are coprolites (fossilized faecal samples), skeletons and mummies. With the advancement of microscopic technique, molecular biology (after standardization of extraction of ancient DNA) and immunological technique accurate diagnosis has been feasible. This compilation elaborates usefulness of paleoparasitological study in terms of understanding of (i) dietary habits and migration of ancient people, (ii) change in living pattern, (iii) archaeological doubts about prior use of an ancient structure and (iv) primate heritage of human being.

Keywords: Coprolite, Heirloom parasite, New World, Old World, Mummies, *Enterobius*, *Trichuris,* Human lice.

INTRODUCTION

Paleoparasitology is the examination of parasites found in the remains of humans and other animal species obtained from archaeological or paleontological sites, or any other preserved source. This particular scientific field banks upon interdisciplinary approaches. To mention a few are anthropology, geography, biology, medicine, genetics and obviously involvement of molecular biologists. Paleoparasitological findings also correlate with the history of medicine and disease [1].

To justify the issue on history of disease, let us cite an example on dirt-eating activity amongst shamans (individuals possessing spiritual abilities and serving as intermediates between the human and spiritual realms). Ancient literatures suggest that these individuals possess an uncivilized practice. When these individuals get distressed or disenchanted then wanted to perish. They used to take soil gradually each day until they deteriorated, resulting in facial and ocular swelling, ultimately leading to death. No one can intervene or dissuade them from their desire to death. They used to assert that the devil instructed them and manifested before them, which is the reason for their resolve to consume the earth. This particular habit and clinical symptoms refer to geophagy and hook worm infection by *Necator* sp. [2].

Therefore, this may be stated that, study on ancient parasites (specifically gastrointestinal parasites) can address (i) dietary habits of ancient people, (ii) migration of ancient people, (iii) change in living pattern, (iv) archaeological doubts about prior use of a structure and (v) primate heritage of human being. Thus, paleoparasitology explains historical development of parasite and host-parasite interaction which is the subject of choice of modern era [3].

DIETARY HABITS OF ANCIENT PEOPLE

The Samoyedic ethnic group is a native people who stay in the Far North of Russia. They are known as Nenets. An excavation study was undertaken in three different burial grounds where Nenets live (Vesakoyakha and Nyamboyto). In this study soil samples were

[1]*Animal Science Division, ICAR-Central Island Agricultural Research Institute, P.O. Bhathubasti, Sri Vijaya Puram-744 105, India.*
[2]*Department of Veterinary Parasitology, Lala Lajpat Rai University of Veterinary and Animal Sciences, Hisar, Haryana, 125004, India*
**Corresponding author. e-mail: debasis63@gmail.com*

collected from burials which were taken from intact skeletons' pelvic region (dated between 19th to early 20th centuries). From the samples of Taz Nenets, two species of parasites were recorded. They were *Taenia* sp. and *Diphyllobothrium* sp. Out of these two identified species, diphyllobothriasis infection was more common amongst Taz Nenets (dwellers of Taz of Siberia) and Nyamboyto Nenets (riverine people staying near lake of Nyamboyto of the Taz River basin). From this observation this has been postulated that, these Nenets used to consume raw fish from their very childhood. Vesakoyakha Nenets (riverine people of Siberia) used to suffer from taeniasis since they used to consume reindeer [4].

Piaui and Pernambuco are two states of Northeastern part of Brazil. Coprolites (fossilized faecal sample) of human origin (dated at least 10000 years ago) were collected during excavation from these states and were analysed. Parasite eggs (*Pharyngodonidae*) were detected. This family of parasites infect amphibians and reptiles. Therefore, it was concluded that the native people of these two states had a habit of consumption of meat of undercooked/raw reptiles and amphibians [5].

MIGRATION OF ANCIENT PEOPLE AND ANIMALS

This world is divided into two parts: (i) the Old World (refers to Africa, Asia and Europe) and (ii) the New World (refers to North and South America as well as Australia). It is said that due to human migration, many of the parasitic diseases have been transferred from the Old World to the New World after the pre-Columbian period. We take the privilege to cite an interesting example of *Entamoeba histolytica*. Its has been evidenced that, *Entamoeba histolytica* infection has been present in Western Europe since the prehistoric period. This species has been identified from samples collected from Switzerland (of Neolithic period dated 3700- and 3400-years BCE), from Greece detected in samples of early iron age and samples of Bronze age collected from France. During the Roman period, this parasite was detected from Italy, Belgium, France and Israel. From the Roman period, the situation changed. There was wide circulation of human beings and goods to most parts of the Middle East Asia. It is thought that, during the Roman period there was diffusion of this parasite from Europe to the Middle East Asian countries [6].

On the contrary, the occurrence of pathogenic amoeba in America is less compared to the countries of the Old World. But very interestingly, this parasite has been identified from human samples of pre-Columbian period (much before 15th century) and from North America (samples dated 12th to 13th centuries CE) [7]. Therefore, from these observations, this may be concluded that this particular parasite has diffused to America from the Old World before the arrival of Christopher Columbus in the New World in 1492. Some debatable historical records suggest that, migrations of human beings from the Old World to the New World occurred before the arrival of Columbus. Archaeological evidences suggest about Viking colony (dated 1000 CE) in North America through the trans-Atlantic route via Greenland [8, 9]. The parasite was introduced into America from the Old World and can travel a long way since this parasite can survive in cyst form in ordinary and freezing temperatures [10]. Moreover, as it is well known that migratory birds play a key role in dispersal of various parasites [11], including protozoa, it might be possible that amoeba parasites were transmitted from the Old World to the New World through them.

Paleoparasitological evidence exists on the roles of domestic animals and migrating birds in transmitting parasites in both humans and animals. Analysis of intestinal microbiomes preserved in coprolites of ancient birds revealed a diverse array of microorganisms, including parasites [12]. It was thought that zoonotic Trichostrongylus spp. was restricted to the New World; later, Gonçalves et al. [13] demonstrated that the species is widespread worldwide through paleoparasitological evidence. As infection of Trichostrongylus spp. is linked to the consumption of animals such as cervids, it can be postulated that the migration of the parasite happened through the migration of animals.

CHANGE IN LIVING PATTERN

The Inca civilization was initially located in Peru. As the time passed, the Inca civilization started to spread to neighbouring areas which are presently known as Argentina, Chile, Bolivia and Ecuador. A chronological study was undertaken in the Lluta area (a district situated in Chile) to know dynamics of parasitic infection in this region among people of the Lluta during the pre-Inca, Inca and Hispanic contact periods (this is a period when indigenes of America came in contact with the Europeans specifically Spanish people). Fourteen coprolites of three different periods were evaluated. During this study four parasites (*Trichuris* sp., *Enterobius vermicularis*, *Trichostrongylus* sp. and *Eimeria macusaniensis*) were detected. *Enterobius vermicularis* eggs were not detected in the coprolites of the pre-Inca period. On the contrary, intensity of infection of *Enterobius vermicularis* was more during the Inca and Hispanic contact periods. This observation may be attributed towards transition of life

pattern. During the pre-Inca period the Lluta people used to live in isolated hamlets. But during the Inca and Hispanic contact periods started to stay in densely populated villages. This may be granted as a cause of more *Enterobius vermicularis* infection through direct contact [14].

ARCHAEOLOGICAL DOUBTS ABOUT PRIOR USE OF A STRUCTURE

This is very interesting to note that, paleoparasitology can confirm some of the archaeological structures about their use during pre-historic period especially latrines and cesspit through identification of parasitic fauna [15].

PRIMATE HERITAGE OF HUMAN BEING

This is a universal truth that, human being has emerged from primates. Our family members are apes, monkeys and lemurs [16].

This is further to mention that, humans and so-called anthropomorphous monkeys *alias* big apes are similar in terms of evolution. Gorillas and chimpanzees in Africa and orangutans in Asia serve as the group's representatives. In addition to having very similar morphologies and behaviours, we share about 98% of our genetic material with the latter [17]. Many extinct branches serve as a representation of the speciation process that caused humans to diverge from our primate predecessors. We only have a rough idea of where these predecessors fit into the human lineage because fossil availability varies and some species are only preserved by a few pieces of bone or tooth. The suggested stages of hominization are based on the morphology and chronology of primates during the Pleistocene and Miocene [18].

Evolution of human being from anthropomorphous monkeys have been correlated with some commonly shared infectious and non-infectious diseases and conditions. The best examples are diseases treponematoses and rheumatism. Both the disease conditions are seen in human and non-human primates [19, 20]. This finding specifies that, these conditions have been acquired by present day *Homo sapiens* from common hominid ancestors [21, 22, 23].

Apart from these two examples, we specify three heirloom human parasites having pre-hominid ancestors with some scientific justification.

(i) *Enterobius vermicularis*

This particular species is cosmopolitan in distribution and directly transmitted between hosts. In different literatures, evolution of pinworm has been described on the basis of paleoparasitological records. Further refined cladistic analysis of *Enterobius* spp. of human and non-human primates was helpful to draw conclusion that, pinworms originated in pre-hominid human progenitors and hence predate humans as well. This particular hypothesis is popularly known as "association by descent coevolution adjunct with cospeciation" [24] . To elaborate the issue further let us describe hypothesis of Cameroon [25]. He explained that, *Enterobius anthropopitheci* (occurs in chimpanzee) is the closest relative of *Enterobius vermicularis* and *Enterobius gregorii* (affects solely human being).

Further, the results of a tree reconciliation between parasites and their host species using TREEMAP [26] showed that 64% of the trees had superimposable nodes; however, when viewed at the level of "parasite clades vs. host families," the congruence increased to 84% of superimposable nodes. A Markovian test indicates that the likelihood that such a large percentage would occur by random is $p = 0.001$ Therefore, the most likely theory to explain the genesis of human pinworm appears to be through co-evolutionary pathway.

(i) **Human lice**

Humans (*Homo sapiens*) are infested by two genera of sucking lice: one common with chimpanzees (*Pan* spp.) and the other with gorillas (*Gorilla gorilla*). Human head and body lice, along with chimpanzee lice, belong to the genus *Pediculus* (*Pediculus humanus* and *Pediculus schaeffi*, respectively). No species of *Pediculus* is known to parasitize gorillas. Human pubic lice and gorilla lice are classified within the genus *Pthirus* (*Pthirus pubis* and *Pthirus gorillae*, respectively), and no *Pthirus* species is recognized as a parasite of chimpanzees. *Pediculus* and *Pthirus* are sister taxa according to morphological and molecular evidence and primate lice have been documented to have cospeciated with their hosts for a minimum of 25 million years [27]. The intriguing distribution of these two genera prompts a compelling inquiry into the evolutionary history of primate lice. Why do humans possess both genera, while chimpanzees and gorillas possess only one genus each? The explanations are as follows:

(a) Lice infestation in primates is present since 25 million years ago. After chimpanzees and humans diverged some 6 million years ago, the two host species shared the genus *Pediculus* [28, 29].

(b) On the contrary, presence of genus *Pthirus* in man and gorilla has been explained on the basis of host switch phenomenon. A number of literatures suggest that, this phenomenon is common among lice infesting different avian and mammalian hosts [30, 31, 32]. The

Table 1. Updates on paleoparasitological records in animals and undefined samples (2000-2025)

Sl. No.	Type of Study	Brief Finding	References
1.	Analysis of cave deposits (dated 500,000 to 300,000 years BP) from Britanny, France	*Toxocara canis* was detected which most probably used to parasitize hyenas and other carnivores	[36]
2.	Paleomolecular investigation of coprolite of Iron age of banded mongoose was carried out from Tanzania	*Cryptosporidium* sp. was identified on the basis of sequence information of 18S ribosomal RNA and heat shock protein 70. New genotype of this parasite was identified which was described previously in bear.	[43]
3.	Coprolites most probably of dog of aged 6540 ± 110 years BP were examined. Material was obtained from Santa Cruz Province of Argentina	Identified parasites were *Toxocara* sp. (most probably), *Trichuris*, *Uncinaria* and *Capillaria*	[44]
4.	Rodent coprolites aged 212 ± 35 years BP were collected from archaeological site of Chubut Province of Argentina	The identified parasites were *Monoecocestus* sp., *Pterygodermatites* sp. and *Trichosomoides* sp.	[45]
5.	Diagnosis of protozoan infection in Tyrant dinosaurs (non-avian dinosaurs)	Based on lesions in the mandible *Trichomonas gallinae*-like infection was suspected	[46]
6.	Coprolite analysis of a church La Concepcion in Somta cruz de Tenerife, Spain	Detection of *Ascaris* eggs (n=344). This record seems to be the first paleoparasitological detection of *Ascaris* sp. from this species	[47]
7.	Analysis of coprolites of rodents dated around 3440-6700 years BP from Santa Cruz Province of Argentina	From 47 coprolites, 582 number of parasitic ova was detected. They were *Trichuris*, *Colodium*, *Eucoleus*, *Echinocoleusi*, unidentified capillariid eggs and cestodes of family *Anoplocephalidae*	[48]
8.	Coprolites of late Holocene period was collected from Patagonia, Argentina	Identified parasites were *Colodium* sp., *Eimeria* sp. and *Taenia* sp.	[49]
9.	Analysis of coprolites of *Kerodon rupestris*, an endemic rodent of Brazil. Approximate age of those coprolites was 5300 ± 50 years BP from Brazil	*Syphacia* sp. was detected for the first time in pre-historic rodents of America	[50]
10.	Analysis of coprolites of cervid of Pernambuco, Brazil (dated 1040 ± 50 years BP)	*Trichuris* sp. was detected	[51]
11.	Analysis of coprolites of rodents from Patagonia, Argentina	Detected *Anoplocephalidae* cestodes for the first time from this area	[52]
12.	Coprolites most probably of dog of aged 6540 ± 110 years BP were examined. Material was obtained from Santa Cruz Province of Argentina	Identified parasite was *Dioctophyma renale*	[53]
13.	Review on *Diphyllobothrium* sp. from paleoparasitological angle	This genus is present in the New World and Old World in the last 10000 years and 9500 years, respectively	[54]
14.	Examination of pellet of small mammals dated 1980 ± 80 years BP from Patagonia, Argentina	Identified *Macracanthorhynchus* in the samples	[55]
15.	Coprolites collected from sheep and dog of Bronze age were analysed. Materials were collected from Shahr-e-Sukhtch of Iran	Parasites were *Dicrocoelium dendriticum*, *Capillaria* sp., and *Taenia* sp. Albeit *Anoplocephalidae* and *Toxocara* sp. was suspected but researchers were not confident about the claim	[56]
16.	Evaluation of deer coprolites (dated between 2370 ± 70 to 580 ± 60 years BP) was done. The samples were collected from a cave of Patagonia, Argentina	*F. hepatica* like eggs detected	[57]

Sl. No.	Type of Study	Brief Finding	References
17.	Deer coprolites collected from archaeological sites of Argentina	Mixed infection of helminths and protozoa were detected	[58]
18.	Compilation of Russian scenario on paleoparasitology	(i) From young mammoth eggs of platyhelminthes and nemathelminths was detected, (ii) Mummified remains of ancient horse (37000 years older) had nematode infection (suborder: Strongylata), (iii) Intestine of mummified rodents (dated 10000-12000 years ago) had infection of *Syphacia* sp., (iv) Mummified bison of 37000 BP had *Skrjabinagia kassimov* infection, (v) Siberian goat droppings (dated 33653 ± 1638 BP) harboured *Nematodirus* sp. infection, (vi) canine samples (n=34) were collected from two different archaeological sites. Coprolites were of 7^{th} – 5^{th} millennium BC. Eggs of *Opisthorchis felineus*, *Diphyllobothrium* sp., *Spirometra* sp., *Capillaria* sp. and *Alaria alata* were detected. The most prevalent helminth infections were of *Diphyllobothrium* sp. and *O. felineus*. Infection pattern suggests that, people and dogs of Moscow and suburbs during Neolithic and Mesolithic periods used to consume raw fishes, (vii) canine coprolites (collected from Western Siberia) of transition period from Bronze to Iron age showed presence of *Strongyloides papillosus* (due to consumption of hides and intestine of cattle) and *O. felineus* (due to consumption of raw fish of carp family) and (viii) Analysis of canine coprolites and organic soil collected from Siberian Arctic-Mangazeya (claimed to be first Russian city of 17^{th} century) revealed the presence of *O. felineus*, *T. canis*, *Diphyllobothrium latum* and *Fasciola hepatica*. Therefore, this was predicted that, presence of *T. canis* on soil may be nidus for visceral larval migrans.	[59]
19.	Analysis of coprolites (70-80 million old) of crocodiles from Sao Paulo, Brazil	Two species of Ascaridoid described (*Bauruascaris* spp.) and acanthocephalan parasites detected.	[60, 61]
20.	Analysis of big size coprolite of carnivore collected from Brazil	Cysts of protozoa (order: Eucoccidiorida), and nematode (order: Ancylostomatidae) were detected	[62]
21.	Coprolite analysis of Late Triassic in Thailand	Presence of eggs belonging to Ascaridida	[63]
22.	Analysis of coprolites (n=39) of sheep by conventional and molecular methods collected from Patagonia, Argentina	Identified parasites were: *Trichuris*, *Nematodirus*, *F. hepatica*, *Eimeria* and unidentified strongyle eggs	[64]
23.	Analysis of coprolites of birds of Cenozoic and Mesozoic eras were done. The samples were collected from Brazil.	Ascaridoidea was detected.	[65]
24.	Coprolite analysis of birds of Sao Paulo, Brazil	Apicomplexa (mostly) and one cyst of Amoebozoa detected	[66]

divergence between *Pthirus pubis* and *Pthirus gorillae* is thought be more recent (<0.1 million years ago) than the chimpanzee/human split. But this prediction demands further verification [28].

This has been predicted that, host switching of the genus (*Pthirus*) has happened from gorilla to man. But very interestingly *Pthirus pubis* is transmitted from one individual to other by sexual contact. But such contact is not possible between man and gorilla. But lice may switch from one host to other unrelated host (i) prey-predator relationship [33] and through areas commonly used by different species of animals [34]. Therefore, one of the possible reasons of transmission of *Pthirus* is contact between archaic man and gorilla [28].

Table 2. Updates on paleoparasitological records in man (2000-2025)

Sl No.	Type of Study	Brief Finding	References
1.	Mummified tissues preserved in a museum of Chile (dated from 2000 years BP to 1400 AD	By PCR and using molecular probe, *Trypanosoma cruzi* was detected	[67]
2.	Screening of coprolites of archaeological sites of Chile and America	*Enterobius vermicularis* infection detected	[68]
3.	Detection of Chagas disease caused by *T. cruzi* by molecular method	Causative agent was detected from mummies of 9000 years ago. The mummies were of pre-Columbian Andean countries	[69]
4.	Evaluation of parasitic fauna in Korean mummies (Joseon dynasty) by scanning electron microscopy (SEM)	The identified parasites were *Gymnophalloides seoi*, *Paragonimus westermani*, *Metagonimus yokogawai* and *Ascaris lumbricoides*	[70, 71]
5.	Study on mummies found in Brazil (560 ± 40 BP)	Based on molecular technique *Echinostoma* sp. was detected	[72]
6.	Paleoparasitological study in Western Siberia (dated 12th centuries AD)	From the soil collected from abdomen of infant revealed infection of *O. felineus*	[73]
7.	Archaeological compilation of *Entamoeba histolytica*	From Old World (Eurasia and Africa) positive samples (n=40) recorded from prehistoric, Roman and Medieval periods. From New World (America) 31 positive samples were detected from Pre-Columbian and Colonial periods	[74]
8.	Investigation on paleoparasitological of Guanches (Canary Islands' ancient inhabitant) by analysing samples collected from mummies	Identified parasites were hook worms, *Enterobius vermicularis*, *T. trichiura* and *Ascaris* sp.	[75]
9.	Soil samples were collected from the areas of pelvic and sacrum regions from archaeological sites of Iran. The skeletons were of Bronze age.	*Physaloptera* sp. was detected in 320 skeleton samples. Authors suspected false negative cases due to presence of nematophagous fungus and faulty taphonomic processes	[76]
10.	Iranian update	(i) From mummy remains *Taenia* sp. identified, (ii) From coprolites of man *Taenia* sp., *Ascaris* sp., *Trichuris* sp. and *Enterobius vermicularis* detected, (iii) From burials and pelvic bone of adolescent male *D. dendriticum* was detected and (iv) *Enterobius* sp. and *Physaloptera* sp. detected from samples collected from sacrum and pelvic bones	[77]
11.	Compilation of Russian scenario on paleoparasitology	The first case of human *Taenia* sp. infection was detected from Russia and Western Siberia during early/ middle bronze age. The infection was acquired due to consumption of undercooked or raw roe deer and elk	[59]
12.	Review on existence of parasites in ancient Chile	Three parasites were detected. They were *Taenia* sp. *S. japonicum* and *A. lumbricoides*	[78]
13.	Study on mummies of Bolivia	The study suggested that, *Enterobius vermicularis* and *Capillaria* sp. infection was prevalent in pre-Columbian period	[79]
14.	Paleoparasitological study of gastrointestinal parasitic infection from Florence of Italy (dated 4th – 5th *c.* CE)	Detected three parasites (*D. dendriticum*, *T. trichiura* and *A. lumbricoides*)	[80]
15.	Human coprolite (dated 6040 ± 60.14 BP) was tested for parasitic ova. The study was conducted from Bonneville Estates, Rockshelter, Nevada, USA	Detected acanthocephalan eggs	[81]

Sl No.	Type of Study	Brief Finding	References
16	Compilation of human coprolite study for detection of *Cryptosporidium* sp. infection	(i) *Cryptosporidium* sp. detected from samples dated 500-3000 years old samples collected from Andean region of South America, (ii) This parasite was detected from samples of pre-Columbian Peru, ancient samples of New Zealand, Mexico and North and South America	[82]
17	Study on zoonotic parasite in 5–7-year child from Cantabrian Spain (6-7 *c.* AD)	*D. dendriticum* detected	[83]

(i) ***Trichuris***

Trichuris trichiura infects man. *T. suis* is infective for pigs. This is thought that, *T. trichiura* infection was acquired by man after domestication of pig and this species (*T. trichiura*) has evolved from *T. suis* of pigs. For that reason, both the species are almost morphologically similar [35].

But other hypotheses suggest that, *T. trichiura* has been acquired from pre-hominid hosts not from the pigs. Paleoparasitological evidence of *T. trichiura* eggs in human coprolites and mummified remains lends credence to the theory that the species existed before the estimated age of pig domestication (which occurred only 7000-12000 years ago). *T. trichiura* was present in mummified bodies discovered in European turf bogs prior to the estimated dates for pig domestication, as well as in the well-known Tyrolean Alps mummy Ötzi [36].

FEW GLIMPSES OF PALEOPARASITOLOGICAL RECORDS

M.A. Ruffer in 1910 was the first scientist to describe presence of *Schistosoma haematobium* eggs in Egyptian mummies of 1250-1000 BCE [37]. After thirty years of this publication, Lothar Szidat (1944) [38] could demonstrate *Ascaris lumbricoides* and *T. trichiura* from samples of 600 BCE (Drobnitz girl of Poland) and from 500 years BCE (one bog mummy of Karvinden man). European and American paleoparasitology emerged simultaneously between the 1950s and the 1970s. In 1979, Luiz Fernando Ferreira, Adauto Araujo, and Ulysse Confalonieri finally established a definition, scope, and limitations of paleoparasitological study [39]. The National University of Mar del Plata in Argentina, the National University of Medicine in South Korea, the University of Cambridge in England, or the University of Bourgogne Franche-Comté in France are just a few of the highly active laboratories that have since emerged after the original Brazilian, American, and French laboratories (the Oswaldo Cruz Institute, the University of Nebraska, and the University of Reims Champagne Ardenne). Lastly, various teams of archaeologists, parasitologists, or biologists in Russia, China, Iran, Denmark, England, or the Czech Republic also conduct research in paleoparasitology [40, 41, 42].

With this brief introduction of paleoparasitological investigation, we are furnishing some updates on paleoparasitological records in animals and undefined samples (Table 1) and man (Table 2).

CONCLUSION

Paleoparasitology deals with the ancient records of man and animals. Through this approach one can assess health of man and animals during pre-historic period. Not only that, this study helps to find out the pattern of evolution from apes to man exploiting “heirloom parasites” as biomarker. With the recent advancement of molecular biology and immunological approaches (specifically direct fluorescent antibody test and antigen capture ELISA) it is possible to identify the parasites up to genus, species and strain level. Thus, this approach is helpful to find out the migration of parasite from Old World to New World even before pre-Columbian era. India is home to major ancient civilizations; the best example is the Indus Valley Civilization (3300–1300 BCE), also known as the Harappan Civilization. Domestication of several domestic animal species, including zebu cattle, goats, dogs, cats, and domestic fowl, occurred during the Harappan civilization. Therefore, it will be interesting to study paleoparasitology in the Indian context.

REFERENCES

1. Nascimento DR, Carvalho DM, Marques RC. Uma História Brasileira das Doenças. 2006; Rio de Janeiro (Brazil): Mauad. Vol. 2.

2. Sousa GS. Notícia do Brasil: comentários e notas de Varnhagen, Pirajá da Silva e Edelweiss [1587]. 1974; São Paulo: MEC.

3. Le Bailly M, Maicher C, Roche K, Dufour B. Accessing ancient population lifeways through the study of gastrointestinal parasites: paleoparasitology. Appl Sci. 2021; 11:4868. DOI: 10.3390/app11114868.

4. Slepchenko SM, Ivanov SN, Nikolaevich BA, Alekseevich TA, Sergeyevich SV. Traditional living habits of the Taz tundra population: a paleoparasitological study. Korean J Parasitol. 2016; 54(5):617–623. DOI: 10.3347/kjp.2016.54.5.617.

5 Sianto L, Teixeira-Santos I, Chame M, Chaves SM, Souza SM, Ferreira LF, Reinhard K, Araujo A. Eating lizards: a millenary habit evidenced by paleoparasitology. BMC Res Notes. 2012; 5:586. DOI: 10.1186/1756-0500-5-586

6. Lavan L, Bowden W. Theory and Practice in Late Antique Archaeology. Leiden, Germany: Brill editions; 2003.

7. Le Bailly M, Romon T, Kacki S. New evidence of Entamoeba histolytica infections in pre-Columbian and colonial cemeteries in the Caribbean. J Parasitol. 2014; 100(5):684–686. DOI: 10.1645/13-476.1.

8. MacPherson AG. Pre-Columbian Discoveries and Exploration. In: Allen JL, editors. North American Exploration, Vol. 1. 1997; University of Nebraska Press: Lincoln (USA):

9. Kristinsson A, Expansions: Competition and Conquest in Europe since the Bronze Age. 2010; Reykjiavitur: Akademian Editions.

10. Acha PN, Szyfres B. Zoonoses et Maladies Transmissibles Communes Aux Hommes et Aux Animaux, Volume 3: Zoonoses Parasitaires. 2005; Paris: Office Nationale des Epizooties.

11. Tsiodras S, Kelesidis T, Kelesidis I, Bauchinger U, Falagas ME. Human infections associated with wild birds. J Infect. 2008 Feb;56(2):83-98. doi: 10.1016/j.jinf.2007.11.001.

12. Boast AP, Weyrich LS, Wood JR, Metcalf JL, Knight R, Cooper A. Coprolites reveal ecological interactions lost with the extinction of New Zealand birds. Proc Natl Acad Sci U S A. 2018;115(7):1546-1551. doi: 10.1073/pnas.1712337115.

13. Gonçalves ML, Araújo A, Ferreira LF. Human intestinal parasites in the past: new findings and a review. Mem Inst Oswaldo Cruz. 2003;98:103-18. doi: 10.1590/s0074-02762003000900016.

14. de Souza MV, da Silva LGR, Silva-Pinto V, Mendez-Quiros P, de Miranda Chaves SA, Iñiguez AM. New paleoparasitological investigations from the pre-Inca to Hispanic contact period in northern Chile. Acta Trop. 2018; 178:290–296. DOI: 10.1016/j.actatropica.2017.11.021.

15. da Rocha GC, Harter-Lailheugue S, Le Bailly M, Araújo A, Ferreira LF, da Serra-Freire NM, Bouchet F. Paleoparasitological remains revealed by seven historic contexts from “Place d’Armes”, Namur, Belgium. Mem Inst Oswaldo Cruz. 2006; 101(Suppl 2):43–52. DOI: 10.1590/s0074-02762006001000008

16. Foley R. Humans before humanity. 1995; Oxford, UK: Blackwell Publishers.

17. Fouts R. Next of kin: My conversations with chimpanzees. 1997; New York: William Morrow.

18. Foley R. Another unique species: Patterns in human evolutionary ecology. 1987; Harlow (UK): Longman Science and Technology.

19. Cockburn A. Infectious diseases: Their evolution and eradication. 1967; Springfield, IL: Charles C. Thomas.

20. Lovell NC. Patterns of injury and illness in great apes: A skeletal analysis. 1990; Washington, DC Smithsonian Institution.

21. Krause EB. Les Hommes de Néanderthal. In: Le Feu sous la Glace: 250,000 ans d’histoire européenne. 2004; Paris (France): Éditions Errance.

22. Barnes E. Diseases and human evolution. 2005; Albuquerque (NM): University of New Mexico Press.

23. Martin FD. El largo viaje: Arqueología de los orígenes humanos y las primeras migraciones. 2005; Barcelona (Spain): Ediciones Bellaterra.

24. Brooks DR, McLennan DA. Phylogeny, ecology and behaviour. 1991; 434 p. Chicago (IL): University of Chicago Press.

25. Cameron TW. The species of *Enterobius* Leach, in primates. J Helminthol. 1929; 7(3):161–182. DOI: 10.1017/S0022149X00018770.

26. Page RDM. Parallel phylogenies: reconstructing the history of host–parasite assemblages. Cladistics. 1994;10(2):155–173. DOI: 10.1111/j.1096-0031.1994.tb00170.x.

27. Reed DL, Smith VS, Hammond SL, Rogers AR, Clayton DH. Genetic analysis of lice supports direct contact between modern and archaic humans. PLoS Biol. 2004; 2(11):e304. DOI: 10.1371/journal.pbio.0020304.

28. Reed DL, Light JE, Allen JM, Kirchman JJ. Pair of lice lost or parasites regained: the evolutionary history of anthropoid primate lice. BMC Biol. 2007; 5:7. DOI: 10.1186/1741-7007-5-7.

29. Raoult D, Reed DL, Dittmar K, Kirchman JJ, Rolain JM, Guillen S, Light JE. Molecular identification of lice from pre-Columbian mummies. J Infect Dis. 2008; 197(4):535–543. DOI: 10.1086/526520.

30. Barker SC, Close RL. Zoogeography and host associations of the *Heterodoxus octoseriatus* group and *H. ampullatus* (Phthiraptera: Boopiidae) from rock-wallabies (Marsupialia: *Petrogale*). Int J Parasitol. 1990; 20(8):1081–1087, DOI: 10.1016/0020-7519(90)90053-P.

31. Johnson KP, Weckstein JD, Witt CC, Faucett RC, Moyle RG. The perils of using host relationships in parasite taxonomy: phylogeny of the Degeeriella complex. Mol Phylogenet Evol. 2002; 23(2):150–157. DOI: 10.1016/S1055-7903(02)00014-3.

32. Weckstein JD. Biogeography explains cophylogenetic patterns in toucan chewing lice. Syst Biol. 2004; 53(1):154–164, DOI: 10.1080/10635150490265085

33. Whiteman NK, Santiago-Alarcon D, Johnson KP, Parker PG. Differences in straggling rates between two genera of dove lice (Insecta: Phthiraptera) reinforce population genetic and cophylogenetic patterns. Int J Parasitol. 2004; 34(10):1113–1119, DOI: 10.1016/j.ijpara.2004.06.003.

34. Johnson KP, Adams RJ, Clayton DH. The phylogeny of the louse genus *Brueelia* does not reflect host phylogeny. Biol J Linn Soc. 2002;77(2):233–247, DOI: 10.1046/j.1095-8312.2002.00107.x

35. Samsonov, A. V. Origins of Ascaris and Trichuris of man. In: Problems in Parasitology, Part I, 1969, pp. 212–213.

36. Bouchet F, Araújo A, Harter S, Chaves SM, Duarte AN, *et al*. *Toxocara canis* (Werner, 1782) eggs in the Pleistocene site of Menez-Dregan, France (300,000–500,000 years before present). Mem Inst Oswaldo Cruz. 2003; 98(Suppl 1), 137–139, DOI: 10.1590/S0074-02762003000900020.

37. Ruffer MA. Note on the presence of "*Bilharzia haematobia*" in Egyptian mummies of the Twentieth Dynasty. Br Med J. 1910; 16:65.

38. Szidat L. Über die Erhaltungsfähigkeit von Helmintheneiern in vor- und frühgeschichtlichen Moorleichen. Z Parasitenkd. 1944; 13:265–274, DOI: 10.1007/BF03177148

39. Ferreira LF, Reinhard KJ., Araujo A. Foundations of Paleoparasitology; 2014; Rio de Janeiro (Brazil): Editora Fiocruz.

40. Paknazhad N, Mowlavi G, Dupouy-Camet J, Esmaeili Jelodar M, Mobedi I, *et al.* Paleoparasitological evidence of pinworm (*Enterobius vermicularis*) infection in a female adolescent residing in ancient Tehran (Iran) 7000 years ago. Parasites Vectors. 2016; 9:33, DOI:10.1186/s13071-016-1306-2

41. Søe MJ, Nejsum P, Seersholm FV, Fredensborg BL, Habraken R, *et al.* Ancient DNA from latrines in Northern Europe and the Middle East (500 BC–1700 AD) reveals past parasites and diet. PLoS ONE. 2018; 13(4): e0195481, DOI: 10.1371/journal.pone.0195481

42. Slepchenko S. *Opisthorchis felineus* as the basis for the reconstruction of migrations using archaeoparasitological materials. J Archaeol Sci Rep. 2020; 33: 102548, DOI: 10.1016/j.jasrep.2020.102548

43. Abe N, Takami K, Kimata I, Iseki M. Molecular characterization of a *Cryptosporidium* isolate from a banded mongoose *Mungos mungo*. J Parasitol. 2004; 90(1): 167–171, DOI: 10.1645/GE-3231RN

44. Fugassa MH, Denegri GM, Sardella NH, Araújo A, Guichón RA, *et al.* Paleoparasitological records in a canid coprolite from Patagonia, Argentina. J Parasitol. 2006; 92(5), DOI: 10.1645/GE-876R1.1.

45. Sardella NH, Fugassa MH. Parasites in rodent coprolites from the historical archaeological site Alero Mazquiarán, Chubut Province, Argentina. Mem Inst Oswaldo Cruz. 2009; 104(1): 37–42, DOI: 10.1590/s0074-02762009000100006.

46. Wolff ED, Salisbury SW, Horner JR, Varricchio DJ. Common avian infection plagued the tyrant dinosaurs. PLoS One, 2009; 4(9), e7288, DOI: 10.1371/journal.pone.0007288

47. Gijón Botella H, Afonso Vargas JA, Arnay de la Rosa M., Leles D, González Reimers E, *et al.* Paleoparasitologic, paleogenetic and paleobotanic analysis of XVIII century coprolites from the church La Concepción in Santa Cruz de Tenerife, Canary Islands, Spain. Mem. Inst. Oswaldo Cruz. 2010; 105(8):1054–1056. DOI: 10.1590/s0074-02762010000800017

48. Sardella NH, Fugassa MH, Rindel DD, Goñi RA. Paleoparasitological results for rodent coprolites from Santa Cruz Province, Argentina. Mem. Inst. Oswaldo Cruz. 2010; 105(1), 33–40, DOI: 10.1590/s0074-02762010000100004

49. Beltrame MO, Fugassa MH, Sardella NH. First paleoparasitological results from late Holocene in Patagonian coprolites. J Parasitol. 2010; 96(3), DOI: 10.1645/GE-2376.1.

50. Souza MV, Sianto L, Chame M, Ferreira LF, Araújo A. *Syphacia* sp. (Nematoda: Oxyuridae) in coprolites of Kerodon rupestris Wied, 1820 (Rodentia: Caviidae) from 5,300 years BP in northeastern Brazil. Mem Inst Oswaldo Cruz. 2012; 107(4), DOI: 10.1590/s0074-02762012000400015.

51. Sianto L, Duarte AN, Chame M, Magalhães J, Souza MV, Ferreira LF, Araújo A. *Trichuris* sp. from 1,040 +/- 50-year-old Cervidae coprolites from the archaeological site Furna do Estrago, Pernambuco, Brazil. Mem Inst Oswaldo Cruz. 2012; 107(2), DOI: 10.1590/s0074-02762012000200018.

52. Beltrame MO, Fugassa MH, Barberena R, Sauthier DE, Sardella NH. New record of anoplocephalid eggs (Cestoda: Anoplocephalidae) collected from rodent coprolites from archaeological and paleontological sites of Patagonia, Argentina. Parasitol Int. 2013; 62(5), DOI: 10.1016/j.parint.2013.04.004.

53. Fugassa MH, Gonzalez Olivera EA, Petrigh RS. First palaeoparasitological record of a dioctophymatid egg in an archaeological sample from Patagonia. Acta Trop. 2013; 128(1), DOI: 10.1016/j.actatropica.2013.06.001.

54. Le Bailly M, Bouchet F. Diphyllobothrium in the past: Review and new records. Int J Paleopathol. 2013; 3(3), DOI: 10.1016/j.ijpp.2013.05.004.

55. Beltrame MO, Fernández FJ, Sardella NH. First paleoparasitological record of acanthocephalan eggs from Northwestern Patagonia (Late Holocene, Argentina). Acta Trop. 2015; 146, DOI: 10.1016/j.actatropica.2015.02.019.

56. Makki M, Dupouy-Camet J, Sajjadi SMS, Naddaf SR, Mobedi I, Rezaeian M, Mohebali M, Mowlavi G. First Paleoparasitological Report on the Animal Feces of Bronze Age Excavated from Shahr-e Sukhteh, Iran. Korean J Parasitol. 2017; 55(2), DOI: 10.3347/kjp.2017.55.2.197.

57. María Ornela B, Eleonor T, Alberto Enrique P, Norma Haydeé S. First paleoparasitological record of digenean eggs from a native deer from Patagonia Argentina (Cueva Parque Diana archaeological site). Vet Parasitol. 2017; 235:83-85, DOI: 10.1016/j.vetpar.2017.01.011.

58. Beltrame MO, Tietze E, Pérez AE, Bellusci A, Sardella NH. Ancient parasites from endemic deer from "CUEVA PARQUE DIANA" archeological site, Patagonia, Argentina. Parasitol Res. 2017; 116(5), DOI: 10.1007/s00436-017-5429-7.

59. Slepchenko S, Reinhard K. Paleoparasitology and pathoecology in Russia: Investigations and perspectives. Int J Paleopathol. 2018; 22:39–44, DOI: 10.1016/j.ijpp.2018.03.005.

60. Cardia DFF, Bertini RJ, Camossi LG, Letizio LA. Two new species of ascaridoid nematodes in Brazilian Crocodylomorpha from the Upper Cretaceous. Parasitol Int. 2019; 72:101947, DOI: 10.1016/j.parint.2019.101947.

61. Cardia DFF, Bertini RJ, Camossi LG, Letizio LA. First record of Acanthocephala parasites eggs in coprolites preliminary assigned to Crocodyliformes from the Adamantina Formation (Bauru Group, Upper Cretaceous), São Paulo, Brazil. An Acad Bras Cienc. 2019; 91(Suppl. 2):e20170848, DOI: 10.1590/0001-3765201920170848.

62. Cardia DFF, Bertini RJ, Camossi LG, Richini-Pereira VB, Losnak DO, Francischini H, Dentzien-Dias P. Paleoparasitological analysis of a coprolite assigned to a carnivoran mammal from the Upper Pleistocene Touro Passo Formation, Rio Grande do Sul, Brazil. An Acad Bras Cienc. 2021; 93(Suppl 2):e20190876, DOI: 10.1590/0001-3765202120190876.

63. Nonsrirach T, Morand S, Ribas A, Manitkoon S, Lauprasert K, Claude J. First discovery of parasite eggs in a vertebrate coprolite of the Late Triassic in Thailand. PLoS One. 2023; 18(8):e0287891, DOI: 10.1371/journal.pone.0287891.

64. Beltrame MO, Moviglia GS, De Tommaso D, Quintana S. Gastrointestinal parasites of domestic sheep from Patagonia throughout historical times: A paleoparasitological approach. Vet Parasitol Reg Stud Rep. 2023; 44:100915, DOI: 10.1016/j.vprsr.2023.100915.

65. do Carmo GM, Luiz AHDSG, Passos JF, Lima SS, de Araújo-Júnior HI, Pereira FB. First report of a morulated Ascaridoidea (Nematoda) egg in an avian coprolite from the Paleogene of the Paraíba Valley, State of São Paulo, Brazil. J Helminthol. 2024; 98:e60. DOI: 10.1017/S0022149X24000610

66. do Carmo GM, Berto BP, Pereira FB, de Souza Lima S, de Araújo-Júnior HI, Pinheiro RM. Protozoan parasites of birds from the Tremembé formation (Oligocene of the Taubaté Basin), São Paulo, Brazil. Int J Paleopathol. 2024; 45:46–54. DOI: 10.1016/j.ijpp.2024.04.003.

67. Ferreira LF, Britto C, Cardoso MA, Fernandes O, Reinhard K, Araújo A. Paleoparasitology of Chagas disease revealed by infected tissues from Chilean mummies. Acta Trop. 2000; 75(1):79–84, DOI: 10.1016/s0001-706x(99)00095-9.

68. Iñiguez AM, Reinhard KJ, Araújo A, Ferreira LF, Vicente AC. Enterobius vermicularis: ancient DNA from North and South American human coprolites. Mem Inst Oswaldo Cruz. 2003; 98(Suppl 1):67–69, DOI: 10.1590/s0074-02762003000900013.

69. Araújo A, Jansen AM, Reinhard K, Ferreira LF. Paleoparasitology of Chagas disease—a review. Mem Inst Oswaldo Cruz. 2009; 104(Suppl 1):9–16, DOI: 10.1590/s0074-02762009000900004

70. Shin DH, Lim DS, Choi KJ, Oh CS, Kim MJ, *et al.* Scanning electron microscope study of ancient parasite eggs

recovered from Korean mummies of the Joseon Dynasty. J Parasitol. 2009; 95(1):137–145, DOI: 10.1645/GE-1588.1

71. Seo M, Oh CS, Chai JY, Jeong MS, Hong SW, *et al*. The changing pattern of parasitic infection among Korean populations by paleoparasitological study of Joseon Dynasty mummies. J Parasitol. 2014; 100(1):147–150, DOI: 10.1645/12-60.1

72. Leles D, Cascardo P, Freire A dos S, Maldonado A Jr, Sianto L, Araújo A. Insights about echinostomiasis by paleomolecular diagnosis. Parasitol Int. 2014; 63(4), DOI: 10.1016/j.parint.2014.04.005.

73. Slepchenko SM, Gusev AV, Ivanov SN, Svyatova EO. Opisthorchiasis in infant remains from the medieval Zeleniy Yar burial ground of XII-XIII centuries AD. Mem Inst Oswaldo Cruz. 2015; 110(8), DOI: 10.1590/0074-02760150156.

74. Le Bailly M, Maicher C, Dufour B. Archaeological occurrences and historical review of the human amoeba, Entamoeba histolytica, over the past 6000 years. Infect Genet Evol. 2016; 42:34–40. DOI: 10.1016/j.meegid.2016.04.030.

75. Jaeger LH, Gijón-Botella H, Del Carmen Del Arco-Aguilar M, Martín-Oval M, Rodríguez-Maffiotte C, Del Arco-Aguilar M, Araújo A, Iñiguez AM. Evidence of Helminth Infection in Guanche Mummies: Integrating Paleoparasitological and Paleogenetic Investigations. J Parasitol. 2016; 102(2):222–228, DOI: 10.1645/15-866.

76. Makki M, Dupouy-Camet J, Seyed Sajjadi SM, Moravec F, Reza Naddaf S, Mobedi I, Malekafzali H, Rezaeian M, Mohebali M, Kargar F, Mowlavi G. Human spiruridiasis due to Physaloptera spp. (Nematoda: Physalopteridae) in a grave of the Shahr-e Sukhteh archeological site of the Bronze Age (2800–2500 BC) in Iran. Parasite. 2017; 24:18, DOI: 10.1051/parasite/2017019.

77. Khodkar I, Feizhadad MH, Tavalla M. Paleoparasitology in Iran: A Review. Le Infez Med. 2018; 26(4):396–402.

78. Yeh HY, Zhan X, Qi W. A comparison of ancient parasites as seen from archeological contexts and early medical texts in China. Int J Paleopathol. 2019; 25:30–38, DOI: 10.1016/j.ijpp.2019.03.004.

79. Valverde G, Ali V, Durán P, Castedo L, Paz JL, Martínez E. First report in pre-Columbian mummies from Bolivia of *Enterobius vermicularis* infection and capillariid eggs: A contribution to Paleoparasitology studies. Int J Paleopathol. 2020; 31:34–37, DOI: 10.1016/j.ijpp.2020.08.002.

80. Kévin R, Nicolas C, Elsa P, Paolo L, Pasquino P, *et al.* Gastrointestinal parasite burden in 4th-5th c. CE Florence highlighted by microscopy and paleogenetics. Infect Genet Evol. 2021; 90:104713, DOI: 10.1016/j.meegid.2021.104713.

81. McDonough K, Johnson T, Goebel T, Reinhard K, Coe M. Paleoparasitology of human acanthocephalan infection: A review and new case from Bonneville Estates Rockshelter, Nevada, U.S.A. J Parasitol. 2023; 109(2):65–75, DOI: 10.1645/22-92.

82. Roche K, Dalle F, Capelli N, Borne R, Jouffroy-Bapicot I, Valot B, Grenouillet F, Le Bailly M. From modern-day parasitology to paleoparasitology: the elusive past record and evolution of *Cryptosporidium*. Front Microbiol. 2023; 14:1249884, DOI: 10.3389/fmicb.2023.1249884.

83. López-Gijón R, Carnicero S, Botella-López MC, Camarós E. Zoonotic parasite infection from a funerary context: A Late Antique child case from Cantabrian Spain. Int J Paleopathol. 2023; 41:55–58. DOI: 10.1016/j.ijpp.2023.03.00.

Cite this article as: Bhattacharya D, Sujatha T, De AK, Sunder J, Yeligar SS, Sawhney S and Gupta S. Paleoparasitology: A modern-day rethinking of HG Wells time machine. Explor Anim Med Res. 2026; 16(1), DOI: 10.52635/eamr/16.1.03-13.

Explor Anim Med Res.
Vol. 16, Issue 1, 2026
DOI: 10.52635/eamr/16.1.14-27

ISSN 2277-470X (Print), ISSN 2319-247X (Online)
Website: www.animalmedicalresearch.org

Published under the CC BY-NC 4.0 license

Review Article

COMPREHENSIVE REVIEW ON THE PROSPECTS AND CONUNDRUMS OF ANCIENT TO CONTEMPORARY MODERN IMMUNO-MODULATION TECHNIQUES PRACTICED IN HUMAN AND ANIMAL HEALTHCARE

Shibabrata Pattanayak[1]

Received 2 April 2026, revised 27 April 2026

ABSTRACT: Prevention of diseases by modifying the body's immune system is considered the most important aspect of healthcare from a very early stage of human civilization. Before the development of modern healthcare, nature-derived and easily available materials were used for that purpose. Along with old techniques like the use of parts of specific medicinal plants and also of some animals, the use of self or animal urine, auto-haemotherapy, autologous vaccination, etc., many modern techniques are developed to modulate the immunity of the individuals. These include techniques like vaccination by the use of weak or attenuated microorganisms of infectious diseases, their nucleic acids, artificially synthesized immunogenic proteins, etc. Research is underway for the development of vaccines to control non-infectious diseases like Alzheimer's disease, early aging (Senolytic), Type 2 diabetes, etc. Use of stem cells for different serious health problems, including cancers, is considered a highly valued area in contemporary research for modulation of immunity of the body. Along with proper validation of the commonly used techniques targeting mainly modulation of the acquired immunity, a detailed study is required on the old procedures as well as the techniques targeting modulation of the innate immunity of the body - like following of a designed lifestyle, food-drink-nature exposure-body clock maintaining style, minimizing psychological stress, etc., that influence the biological age of the individuals; effect of use of specific succulent fruits, vegetables, nuts and spice mixtures in the diet schedule as well as use of succulent biomedicines as preventive and curative medicines, etc.

Keywords: Disease susceptibility, Innate immunity, Urine therapy, Auto-vaccine, DNA vaccine, mRNA vaccine, Succulent biomedicines.

INTRODUCTION

Efforts to prevent different diseases by using available tools were perhaps started from a very early stage of human civilization. Dietary and local use of the parts of some medicinal plants, animals in their different forms, and extracts were used for that pupose. Many of such efforts were not continued afterwards, may be due to lack of availably of the items, or considering their suitability for use. From the twelfth century, modern medicine has been considered the main area of healthcare. But still today, doctors practicing modern medicine remain in a dilemma considering many aspects of that branch of science [1, 2, 3]. On the other hand, many ancient procedures of healthcare are still in practice in some parts of the world. Now, the time has come to perform a thorough investigation and analysis of such time-tested practices and procedures scientifically, without any pre-decision or prejudice to get the best possible benefits from them [2, 3]. A brief analysis of some such procedures developed and under study is performed in the light of modern medicine to find out the new avenues of research for better healthcare in the coming days.

IMMUNITY SYSTEM OF THE BODY: SOLDIERS AND WEAPONS FOR DEFENSE AND FIGHT

As per the concepts of modern medicine, the soldiers protecting the health are of different types with a variety of weapons in their stock. Broadly, the functioning immunity system of the body can be categorized into two sections: the innate and the acquired immunity. The innate immunity starts functioning from birth and has the systems and soldiers performing the first line

[1]*Assistant Director, ARD (Vet. Research & Investigation), Govt. of West Bengal, India.*
**Corresponding author e-mail: pattanayak1966@gmail.com*

of defense of the body. It is subdivided mainly into four parts: physical, physiological, cell derived, and cytokine-related immunity. This type of immunity is not generally disease-specific and can act to protect health in various aspects and from various types of diseases. The acquired immunity of the body develops as a response of encountering the disease causing agents or their parts. It is subdivided into two parts: active and passive immunity.

The active immunity is controlled by the immune system of the body after encountering the disease agents. Individuals can get such immunity after the recovery from any disease or after vaccination against any disease. It is mainly a disease-specific immunity (Fig. 1).

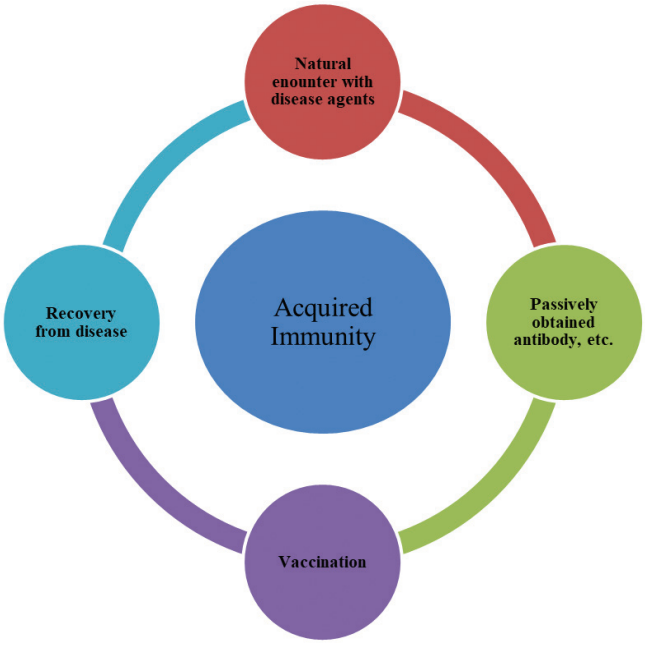

Fig. 1. Acquired Immunity factors for immunomodulation.

The passive immunity is achieved after getting antibodies, etc., from other sources, not prepared inside the body. The antibodies supplied to the babies through maternal colostrum, and the external antibodies introduced inside the body to counter some diseases are of this type [4, 5, 6].

Both innate and acquired immunity can involve immunity related cells as well as antibody, complements, etc. (cellular and humoral types of immunity) [4, 7].

USE OF URINE FOR THERAPEUTIC PURPOSES

Use of urine as a therapeutic and preventive measure against diseases in ancient times

Urine was considered "the elixir of long life" in different ancient traditions, and it was used as a therapeutic means in different ancient civilizations. Its use is noted in '*Shiwambukalpa*' (an ancient Sanskrit book) as well as documented by the philosophers of Assyrian-Babylonian, Egyptians, Sumerian, Essenians, Jewish-Christians, as well as Greek and Roman civilizations and dynasties [8, 9].

Composition of urine

As per the chemical analysis related to modern medicine, urine contains water, urea, uric acid, creatinine, various electrolytes, phosphates, organic acids, trace amounts of proteins (albumin, antibodies, enzymes), traces of hormones, glucose, and water-soluble vitamins [10].

Use of human urine

It was/is used as a drink, applied on the whole body, open skin, scalp; as a drop inside the ear or nose; on the infected wound and other affected areas, etc. Urine is used as/in asthma, allergies, arthritis, liver and other tumors, acne, indigestion, antacid, gastric ulcer, wrinkles, migraines, treating burns, sores, other early wound therapies, anal afflictions, baby rash, scorpion stings, itchy eyelids, and many other diseases [11, 12, 13].

Use of animal urine for therapeutic purposes

Like human urine, urine collected from the cow is also used for different therapeutic purposes. Oral intake and local applications are the main ways of such uses. Apart from the use of cow urine, urine collected from different animals is also used for different therapeutic purposes. These include worm infestation, abdominal enlargement, dropsy, colic, flatulence, abdominal tumor, anemia, anorexia, tuberculosis, leukoderma, leprosy, poisons, amenorrhea, hemorrhoids, etc. [11].

Research reports on urine

Urine is found to be bactericidal and effective in blocking the growth of Koch's bacilli in the laboratory [9, 14]. It possibly contains anti-cancer substances [14, 15].

The stem cells collected from the urine are a promising source for stem cell therapy, drug testing by renal toxicity study, identification of renal disease biomarker, and a potential source for tissue engineering and regenerative medicine [12, 16].

All five classes of antibodies are found in the urine samples. Disease-specific antibodies are detected from the urine of patients suffering from Dengue [17],

Covid-19, Hepatitis A [18], Strongyloidiasis [19], Human Immunodeficiency Virus type 1 [20], etc. The antibodies available in the urine may have further therapeutic as well as diagnostic value [21, 22].

Possible mechanism of action of urine therapy

Many hypotheses have been postulated to explain the therapeutic efficacy of urine. It is assumed that the components available from the urine work together to show the actual effects. The effects include re-absorption and reuse of different nutrients, hormones, and enzymes, immunological effects of some components, effect of reabsorbed urea, detoxification of the body system, bactericidal and veridical effects, transmutation effect, diuretic and psychological effects, etc. [13, 16, 21].

AUTOHEMOTHERAPY

In autohemotherapy, blood or some specific cells of the blood of the patients are collected and then reintroduced into the patients (with or without any treatment of it outside the body) as a therapeutic mean. It is either used alone or along with autologous vaccines, other pharmaceutical drugs, or surgical procedures to get the maximum beneficial effects [23, 24, 25].

In human

Use of autologous blood

Injection of autologous whole blood is performed directly to control chronic urticaria and some other diseases. In urticaria, activity of this procedure is proposed to be the modulation and control of the patients' immune response to autologous antigens involved in activation of mast cells and basophils, and also influence on other components leading to the secretion of histamine, etc. [24]. It is further suggested that such treatments can incur the activation of the T regulatory cells by Immunoglobulin G [24, 25].

Ozonated autohemotherapy

In that technique, the ozonated self-blood is reintroduced into the patients. Along with or without pharmacological therapy, that can effectively improve conditions like pain intensity, insomnia, and negative mood, as well as alleviate fatigue [25, 26]. It can induce health benefits among the patients suffering from hepatitis B, hepatitis C, and coronavirus infection [27].

In animals

In Bovine papillomatosis

Bovine papillomatosis, caused by different types of the Bovine Papilloma virus, are extensively studied to evaluate the effect of autohemotherapy. It is found effective alone [23], with an autologous vaccine prepared from the incised wart mass treated with formalin, etc. [28], or added with surgical intervention [29].

Autohemotherapy by the ozonized blood can give good result in the treatment of foot rot in animals [30].

On the health status of animals

Autohemotherapy can be used to improve the health status of the ailing animals. It can act by subsiding the biodegradation of the soft tissues to form pus, improving metabolism of the cells, influencing the immune system of the body in a positive direction, incurring homeostasis in blood and lymph circulation, etc. [30].

Requirement of a thorough investigation of the procedures practiced

Along with the development and spread of modern medicine, the applications of immunomodulation techniques involving gross materials have declined. That may be due to problems such as psychological rejection, non-acceptance of the procedures in social life (such as using urine on the scalp or skin), lack of trust due to not getting instant results like modern medicine, lack of positive reports of scientific validation of the techniques, etc.

The procedures developed for modulation of the body's immunity to reject or control different diseases requires thorough scientific investigation. These procedures are mostly cheap and easy to apply, even without taking any assistance from the costly tools and techniques used in modern medicine.

But the concept of scientific validation of all such techniques requires conceptual adjustment. Most of the time, such procedures involve gross materials and techniques, so direct study on them is to be performed for proper validation. But the combinational effect of the ingredients present in the gross materials used as some medicines is neglected in the contemporary validation techniques. Following the procedures developed to study a single molecule may not be suitable for that purpose, and so may lead to some wrong results about their actual activities. Modifications to such available analytical procedures are required for proper scientific validation of old techniques. By use of the efficient techniques and materials, the modern healthcare system may be benefitted by addition of these procedures as a principal or adjunct therapeutic system [31, 32].

VACCINATION: THE PRINCIPAL TECHNIQUE OF PREVENTIVE HEALTHCARE IN MODERN MEDICINE

In a general sense, vaccination is the introduction of foreign immunogenic materials inside the body to stimulate the body's immune system to develop protective power against those immunogenic materials. The term antigen is used to name such immunogenic materials (mainly protein). As a response against the antigen introduced in the body, some protein molecules are formed by some specific cells, called antibodies. There are involvement of different cells and their secretions in the entire procedure. Generally, the antigens of the infective microorganisms are introduced inside the body with the purpose to develop antibody against them so that the body can fight against the original microorganisms in the future. This is the main target of vaccination.

Through vaccination, the acquired immunity arm of the body is influenced for the prevention of some diseases. Vaccination has the limitation that it cannot be used to prevent all diseases, as useable vaccines are developed against some diseases only, and a very large number or quantity of vaccines cannot be introduced inside the body system of any individual [4, 33].

Sometimes, due to some reasons, the body system wrongly considers some proteins of its own as a foreign antigen and develops antibodies against its own body protein. These are antibodies called autoantibodies, and the diseases developed by them are termed as autoimmune diseases. Diseases that evolve due to the development of the autoantibody are very difficult to cure. On the other hand, due to improper development of antibodies, different hypersensitivity-related health problems can develop. When antibodies develop automatically against some antigens of the environment (available in food items, animal or insect-related materials, flowers, and other parts of some plants, etc.) in some individuals, then such antigens are termed allergens, and the hypersensitivity reactions that develop in the body due to the allergens are called allergy [4, 34].

Common vaccines used to prevent diseases

Antigen vaccines

Generally, the protein portions of any infective microorganism are considered as non-self (antigen) by the individuals if introduced in them, and so the recipient's immunity system try to remove such materials by developing antibodies along with other cellular involvement against them. Uses of a replica of antigen/s or addition of some materials with any weak antigen to stimulate the immunity system etc. techniques are also followed in some cases. These are broadly termed as antigen vaccines.

Experience of encountering such foreign antigens by the body's immunity system is utilized when facing the original infective organisms and that leads to initiating an effective fight against such agents. This general principle is followed to prepare almost all commonly used vaccines developed to prevent different diseases of infectious origin [4, 35]. Presently used bacterial and viral antigen-based vaccines are developed following that basic principle.

Anti-allergy vaccines

The allergic response of the body towards any allergen is dependent on factors like genetic predisposition, quantity of exposure to allergen/s, activity threshold of the immunity system of the body against the allergens, lifestyle, health condition of the individuals, etc. [4, 34, 36].

The anti-allergy vaccines aim to reduce the severity of the allergic response, shown by the patients due to the release of different chemicals, including some vaso-active amines, for hypersensitivity reactions. In anti-allergy vaccines, the suspected allergens, actually acting as some antigen to the body, are introduced in the body with gradually increased dose to develop tolerance of the immune system of the patients to the allergen/s. So, it may be termed as allergen-specific immunotherapy rather than vaccination, and it is not suitable for all allergens [36, 37, 38].

IMMUNO - PREVENTION AND IMMUNO-THERAPY TRIALS AGAINST CANCERS AND OTHER DISEASES

Apart from the common techniques of using the protein part of the cells of the causative organisms as an antigen to produce antibodies to protect the individuals from future attack of the same or closely related infective organisms, some other techniques of vaccine preparation are presently followed or under trials. The highest number of such research is performed on cancers, and fewer researches are performed on some other diseases. Almost similar basic principles are applied in all such efforts.

Preparation principle of recently developed anti-cancer vaccines

Protein/ peptide cancer vaccines

These are not whole cell vaccines, only some specific antigenic protein parts or even the smaller peptides of the cancer cells are used alone or in

combination with some carrier (generally some virus or some other molecules) as some anti-cancer vaccines. Vaccines of this category against some types of cancers (as for some breast cancers) are under different levels of clinical trials [39].

DNA cancer vaccines

The specific DNA associated with the targeted tumor antigens is made as DNA rings like the plasmids of bacterial cells. After entering the body cells, these rings can stimulate and use the mechanisms of the body cells to produce specific tumor antigens that ultimately trigger the body's immune system. After such stimulation, the body's own immune system is forced to recognize such antigens present in the tumor and attack them to kill. Clinical trials of DNA vaccines against prostate cancer, breast cancer, human papilloma virus cancers, melanoma, etc., are underway [40, 41].

Messenger RNA (mRNA) vaccines

Messenger RNA (mRNA) is one type of Ribonucleic acid that takes a very important part in the production of amino acid (protein) in the body. Just after production of the amino acid, the mRNA is broken down. For vaccination, a specific mRNA is prepared and introduced in the body to develop a specific antigenic protein so that the body can develop antibody against such proteins [4, 42].

Messenger RNA (mRNA) cancer vaccines

This type of vaccine may be autogenic or allogenic in nature, though both of them mainly target to stimulate cytotoxic T lymphocytes to attack and kill the tumor cells [43, 44, 45].

In autogenic mRNA cancer vaccines, the tumor sample of the suffering individuals is studied to identify cancer-causing mutations (the tumor neo-antigens). Then, specific mRNA molecules are developed artificially in the laboratory. Then these are generally introduced inside lipid nanoparticles to make an injectable vaccine [44, 46, 47].

During preparation of the allogenic mRNA vaccines, the tumor-associated antigens (TAA) common in patients suffering from the same type of cancer are identified, and the specific mRNA is synthesized artificially. Then they are generally placed under a lipid nanoparticle envelope to prepare the vaccine [48, 49, 50].

Messenger RNA antiviral vaccines

For the prevention of some viral infections, some specific mRNAs have been developed. Generally, the mRNAs coding for specific viral protein/s, mainly the viral outer membrane proteins, are developed and introduced inside the body system. The intended proteins are developed in the body, and then the immune system of the body develops antibodies against the antigen (viral outer membrane protein), making the individual ready to face the infection of the original virus.

The mRNA vaccines developed against the viral spike protein of Covid 19 virus was efficiently used to combat the Covid 19 pandemic (Comirnaty and Spikevax vaccines) [42].

Viral vector vaccines for cancer and other diseases

The engineered viruses carrying the specific genetic materials are used to instruct the recipient's cells to produce desired antigenic proteins to initiate an immune response against such antigens. Such vaccines can modulate both cellular and humoral immunity of the individuals against the specific antigens. Generally, Vaccinia virus, Adenovirus, and some oncogenic viruses are used as vectors [51, 52].

Classification of other cancer vaccines developed or under trial

The cancer vaccines developed or under different levels of trials can be categorized in different ways. Depending upon the source and the type of work they performed, the following classifications are made.

Preventive cancer vaccines

Some vaccines are developed to prevent and control the virus-induced tumors and cancers. The Hepatitis B vaccine (use of Hepatitis B virus surface antigen produced by yeast and some other cells) [53], Human papilloma vaccine (as - particles are prepared from the L1 capsid protein of different types of human papilloma viruses and placed in some specific cells to prepare the non-infectious and immunogenic vaccine) [54], prostate cancer vaccine (autologous vaccine prepared by activating the patients' white blood cells outside the body) [41, 55], BCG bladder cancer vaccine (attenuated *Mycobacterium bovis* bacteria solution is introduced inside the bladder to stimulate immunity soldiers of the body), etc. [41, 56].

Curative cancer vaccines

The main target of such vaccines is to reduce the spread and severity of the cancers by destroying existing cancer cells in the body [57, 58]. Stimulated immune cells of the patients, designed mRNA, oncolytic viruses,

etc., are used along with some sophisticated technologies like the use of virus-like particles, replication-defective viruses, the use of dendritic cells or other viruses as vectors, etc. [59, 60, 61].

Autogenic/ autologous tumor/cancer vaccines

The old, crude method of preparation of autogenic vaccine by triturating the tumor tissues (as papilloma virus-induced tumor of bovines) in normal saline, filtration of the mass, and then inactivation of the material by formalin to prepare the vaccine [62] is substituted or modified by some modern techniques. Many such vaccines are under different levels of trials and waiting for a license for marketing.

Due to the inherent genetic instability of tumor cells, expression of novel tumor antigens is common among cancer patients [46]. So, the concept of using an autologous cancer vaccine appears to be relevant in humans and even in animals [63].

In most of the autogenous vaccines, the specific type/s of immune cells are separated from the blood of the patient, stimulated artificially by specific cancer antigens and other stimulators, and then injected into the patient's body to target cancer cells. Sensitized intact lymphocytes, dendritic cells, etc., are employed for this purpose [56, 64, 65], with good safety and efficacy reports in many cases [66]. This category of vaccines is developed for treatment-resistant metastatic prostate cancer, early breast cancers, etc. [67, 68, 69].

Among the other vaccines covered in this category, Melanoma vaccine (use of oncolytic virus based vaccine to counter advanced stage Melanoma cancer), Pancreatic cancer vaccine (a mRNA vaccine), Head and neck cancer vaccine (Human papilloma virus proteins used), Intra-tumoral therapies (by injection of immune activating drugs, oncolytic viruses, some bacteria, etc. inside the tumor to activate the immunity soldiers of the body) [70, 71, 72], the lung cancer vaccines (protein based, mRNA based and mutated protein based), etc. are important [73, 74, 75].

Allogeneic cancer vaccines

These vaccines are targeted to make from the non-self cancer cells, mainly grown in the laboratory. Trials are at different stages for the development of effective vaccines against melanoma, pancreatic cancer, non-small cell lung cancer, leukemia, prostate cancer, etc. [41, 43, 76].

NEW HORIZON OF VACCINE RESEARCH

Anti-Alzheimer's vaccine

The recent efforts of preparation of an anti-Alzheimer's disease vaccine have the main target to prevent or slow down the disease. Two important abnormally configured or accumulated protein deposits of the brain of Alzheimer's disease patients, causing disruption of nerve cell functions, the Amyloid plaques and Tau tangle, are targeted by generating antibodies against them and clearing them outside the body [77, 78, 79]. The trials are performed mainly in three directions. The peptide-based vaccines, by using these two protein molecules as antigens; the DNA and mRNA vaccines generate these two proteins inside the body to act as antigens; and the genetically engineered monoclonal antibodies are directed towards these antigens [79, 80].

Malaria vaccine

The malaria vaccines aim to prevent the growth and multiplication of the malaria parasite *Plasmodium falciparum* after its introduction into the blood by the *Anopheles* mosquitoes. The circum-sporozoite proteins (CSP), the surface protein of the sporozoite stage of the malaria parasite, are neutralized by the vaccine-derived antibodies before their entry into the liver cells for further development. On the other hand, the activated T lymphocyte cells destroy the infected liver cells before their further multiplication in the cells, if some sporozoites can reach there [81, 82].

Presently, two types of malaria vaccines are used, and both follow more or less similar technology of addition of CSP fragment with a cell surface protein of hepatitis B virus, generally developed in yeast, and also have a similar type of mechanism of action. Production and use of that type of malaria vaccine has already started. Some other techniques, like attenuated malaria parasite, DNA vaccine, etc., are under different levels of trials [82, 83].

Senolytic (anti-ageing) vaccine

The senescent cells are the living, aged cells that fail to divide. Research documented that the selective elimination of the senescent cells can positively modulate the immune system of the body and can also reduce inflammation. These cells express some different types of surface antigens that are either not present or present at a very low level among the normal healthy cells. These antigens are targeted by such proposed vaccines for removal of such antigens or destruction of the cells bearing such antigens by developing antibodies against them or by stimulating the cytotoxic T lymphocytes of the body against them [84, 85, 86].

Other important diseases covered under vaccine research at present

Ongoing research is underway against some other diseases also. Chronic obstructive pulmonary disease

(COPD), Type 2 diabetes, etc., so-called lifestyle-related or age-related diseases are also targeted for prevention by vaccination. For type 2 diabetes, the targeted molecules are mainly interleukin-1 beta (IL-1β) and dipeptidyl-peptidase 4 (DPP4). Antibodies against them can be produced inside the body to prevent or reduce their activities and reduce the severity of the disease. For age-related vascular diseases like aortic aneurysm, hypertension, atherosclerosis, etc., molecules like angiopoietin 1 (Ang I) are targeted. But many problems are encountered during testing of such vaccines for use at the present stage [85].

QUESTIONS ROSE AGAINST THE CONTEMPORARY VACCINES

Many questions are raised against the modern technologies used to prepare vaccines, mainly the viral vaccines. Along with the question of possible effects of the chemical ingredients introduced inside the body with vaccine antigens, there are also questions of modification of previously considered non-pathogenic or mildly pathogenic viruses to some highly pathogenic viruses after getting new gene segments inside their genome through the genetically modified vaccines used [35, 86].

OTHER IMMUNOTHERAPY TRIALS TO CONTROL CANCERS AND OTHER IMPORTANT DISEASES

Use of Stem cells for the prevention/cure of diseases

Stem cells can be grossly categorized as embryonic or adult stem cells depending on their source. As per the ability to differentiate into various types of cells (according to the diminishing spectrum of activity), these can be categorized as totipotent, pluripotent, multipotent, oligopotent, and unipotent stem cells. Stem cells can be derived from day-old embryos, adult tissues of bone marrow, adipose tissue, blood, umbilical cord, aborted fetus, amniotic fluid, pulp of the teeth, and also by reprogramming the cells of adult persons. Stem cells can be used for different purposes related to tissue repair or tissue regeneration, drug discovery, modeling of diseases, and for other therapeutic purposes [87, 88].

So, stem cells are used to replace or repair different types of damaged tissues in the body and can assist in their proper healing. They can be used with some specific direction to modify their cellular character to fit with the specific cells of different organs and systems. They are commonly used as hematopoietic stem cells, obtained from blood or bone marrow, to treat blood cancers and some other diseases. Trials are underway to use stem cells in some heart diseases, diabetes, Parkinson's disease, spinal cord injuries, and some other neurodegenerative diseases, etc. [88, 89, 90].

Use of cytokines

Artificially prepared cytokines such as interferon, interleukins, granulocyte-macrophage colony-stimulating factor, etc., can be used to stimulate the body's immunity to attack cancer cells. These are generally applied as some adjunct therapy procedures in cancer treatment [91]. Some cytokines, like some interferones, can assist in immunomodulation for the prevention of some viral diseases also [92].

Use of monoclonal antibody

The monoclonal antibodies prepared against the specific antigen/s present in a tumor are used to attack the target so that the body's immune cells can identify them easily and can attack these cells to destroy the tumor [41, 93].

Monoclonal antibodies are also used to counter health problems like asthma, osteoporosis, autoimmune diseases, against the viruses like Hepatitis C, SARS – COV 2 Corona virus, Respiratory syncytial virus, etc. [94].

Use of immunotoxin

Sometimes the monoclonal antibody, immunoglobulin, or cytokine molecules are conjugated with some toxic substances directed to target the tumor cells with specific epitopes. After attaching to the targeted tumor antigen, the tumor cells die or become inactivated due to the effect of the toxin. These are termed as immunotoxins [95, 96, 97]. Many bacterial, fungal, or plant-derived toxins are used in different trials and research related to the use of immunotoxins. In some cancers (such as some breast cancers) and autoimmune disorders, such antibodies can be used [93, 98].

IMMUNOMODULATION BY NATURAL MEANS

Nature-derived materials have been used as a medicinal item from an early stage of human civilization. As a part of nature, people were getting some resources of nature automatically (such as sunlight, water, air, edible plants and fruits, etc.) which were beneficial to their health. From their experiences, they learned the effects of such nature-derived materials and became accustomed to many of them. Many diseases encountered nowadays were not encountered or observed rarely during that period, which may be

due to such reasons [3, 99]. Plant materials are used as medicine for the prevention of diseases at a later stage of civilization. But, for prevention and control of the severity of different diseases, vaccination is perhaps the only form considered in modern medicine [35]. For the treatment of diseases, different drugs of synthetic origin are mainly considered [3, 32]. For re-evaluation of the ancient basic concepts of using nature-derived materials (with which humans are accustomed during evolution) for staying in good health and for exploring some related effective concepts of healthcare, a few important points are analyzed in the light of modern medicine (Fig. 2).

Generally, protein, fat, and carbohydrate are considered the main items of nutrition to the body. The macro and micro minerals and the vitamins are also considered an important part of nutrition for maintaining good health.

But that concept is lacking consideration of the effects of different antioxidants and immunomodulants. To keep the body disease-free, these are very important. Most of such items can be effectively supplied to the body through nature-derived foods. The present trend of supply of some components synthesized chemically to perform the role of the nature-derived antioxidants

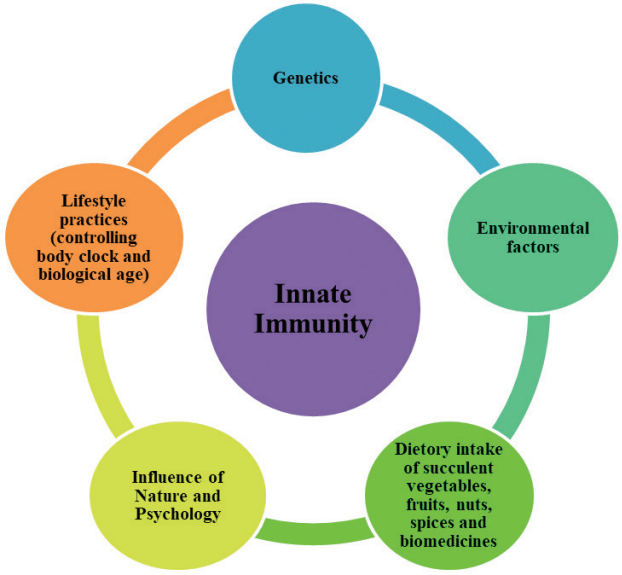
Genetics
Lifestyle practices (controlling body clock and biological age)
Environmental factors
Innate Immunity
Influence of Nature and Psychology
Dietory intake of succulent vegetables, fruits, nuts, spices and biomedicines

Fig. 2. Innate Immunity factors for immunomodulation (as described in the article).

and immunomodulants may be practically harmful to the health of the individuals [33, 32, 99].

The *Rasayana* concept of *Ayurveda*

In this concept, the rejuvenation of the body system can be performed with some specific medicines available in nature. They can modify the 'rasa's and 'dhatu's (the fluids, secretions, status of metabolic interaction influenced by metallic ions, etc.) of the body and thus can ultimately influence the disease preventive power of the body [100].

The 'Disciplined and Intelligent People's Diet' (DIP diet) concept

A specific diet plan basing mainly on vegetarian food items is advocated in this concept. As per the claims, such a diet practice can supply all essential nutrients to the body and keep individuals disease-free by modulating the immunity status of the body (https://hiims.in/dip-diet).

Use of specific millets in diet for good health - the *Siridhanya* concept

As per this concept, dietary intake of five specific nature-grown millets can control different aspects of body immunity. The unique effects of cleansing of body toxins and healing the important systemic problems of different body systems are the way to show their activities, as per the claim. The five millets advocated are – Foxtail [*Hordeum murinum* L.], Kodo [*Paspalum scrobiculatum* L.], Little millet [*Panicum sumatrense* Roth ex Roem. & Schult.], Barnyard [*Echinochloa esculenta* (A. Braun) H. Scholz], and Browntop [*Urochloa ramose* (L.) T. Q. Nguyen] [101].

The psycho-neuro-immuno-endocrinology concept of disease creation

As per this concept, the psychological status has a very strong relationship with the creation or potentiation of different diseases. The psychological stresses can influence the neuronal, immune, endocrine, etc. systems of the body, and create an environment of catching disease agents or the creation and spread of different diseases [102, 103, 104].

Lifestyle modification and use of succulent biomedicines

In this concept, following a designed lifestyle and practicing specific food habits can prevent most of the diseases.

During the evolution stage, different systems of the body of the individuals are developed with some specific characters to perform some specific functions. Some species become nocturnal, some are diurnal; some are strictly vegetarian, and others are carnivorous or omnivorous. On the other hand, one invisible clock is also working inside the body of every

individual, termed the biological clock or body clock. It is an internal timing mechanism that controls the physiological processes in a 24-hour cyclical manner. The body systems are developed as per the instructions of the biological clock of the individuals throughout the evolutionary stages.

The biological age of an individual is the overall health condition commonly found among individuals of a specific age. The biological age of an individual may not be equal to their chronological age. The lesser the biological age of an individual, the better the actual status of his or her health, and the lesser the chance of catching or suffering from any disease.

As per some recent research, lifestyle practices can influence the biological clock and biological age and thus susceptibility towards almost all diseases of the individuals [33, 99, 105].

Maintenance of the body clock and the near-nature lifestyle can influence the biological age of an individual in a positive direction and can also reduce susceptibility of various diseases [105]. By closing or restricting the entry of different synthetic or non-natural chemicals, micro- and nano-plastic particles, etc. through food, skin and lung absorption can reduce the gathering of them inside the body that can control different important parameters related with disease – from catching of the infective microbes, their growth and multiplication, severity of the diseases, initiation and expression of diseases of non-infectious origin, assisting in expression or suppression of genetic predisposition towards different diseases, etc. [106, 107, 108].

Following a lifestyle designed by considering these important aspects can influence the innate immunity of individuals and can keep them in good health [109, 110].

The addition of succulent vegetable salads, fruit salads, nut mixtures, and spice mixtures in the daily diet can modulate the immune system to a large extent. Along with modification of lifestyle, use of encapsulated biomedicines prepared from nature-derived raw, succulent herbs without addition of any synthetic chemical for control and cure of different diseases can be a good alternative to the chemical based treatment concept followed nowadays. All these procedures influence the innate or non-specific immunity arm of the body to prevent diseases, and so even a single such item may be active against a few diseases together [3, 99, 111].

CONCLUSION

From the early stage of human civilization, efforts have been made to modulate the disease preventive power of the body by different means. The natural substances, such as self or animal urine or the parts of the locally available medicinal plants, were used for such purposes. Afterwards, processes like auto-hemotherapy, auto-vaccine, etc., were developed. Vaccination by the use of parts of the infective organisms or by the use of the knowledge of genetic engineering was initiated afterwards. Not only for the prevention of infectious diseases, but even to reduce the severity of many other diseases, vaccinations are tried. Use of stem cells as some modulating agent for disease prevention and treatment is another new concept. But the parameters like biological age and its effects on expression or suppression of the genetic predisposition towards various diseases, effects of the psychological stressors, etc., of the individuals are now considered as some very important factors behind the initiation and progression of different diseases. Lifestyle-related factors like intake and gathering of different synthetic chemicals inside the body, staying away from nature, non-maintenance of the body clock, etc. are considered some very strong influencing force behind disease creation. Along with following a designed lifestyle and taking items like vegetable and fruit salads, nut mixture, spice mixture, etc., as some regular diet items, the use of disease specific succulent biomedicine capsules can be a good alternative to the chemical-based lifestyle and treatment schedules.

REFERENCES

1. Hegde BM. Doctor's dilemma. Med J Armed Forces India. 2002; DOI: 10.1016/S0377-1237(02)80078-8.

2. Hegde BM. What doctors don't get to study in Medical school. 2nd edn. 2006; Paras Medical publisher, Hyderabad, India.

3. Pattanayak S. Neglected areas of phyto-medicinal research. Explor Anim Med Res. 2025; DOI: 10.52635/eamr/15.2.155-159.

4. Tizard IR. Veterinary Immunology. 11th. edn., 2024; Saunders.

5. Innate immunity. National Cancer Institute. https://www.cancer.gov/publications/dictionaries/cancer-terms/def/innate-immunity. Accessed 19 May 2025.

6. Acquired immunity. National Cancer Institute. https://www.cancer.gov/publications/dictionaries/cancer terms/def/acquired-immunity. Accessed 20 July 2025.

7. Shishido SN, Varahan S, Yuan K, Li X, Fleming SD. Humoral innate immune response and disease. Clin Immunol. 2012; DOI: 10.1016/j.clim.2012.06.002.

8. Savica V, Calò LA, Santoro D, Monardo P, Mallamace A, Bellinghieri G. Urine therapy through the centuries. J Nephrol. 2011; DOI: 10.5301/JN.2011.6463.

9. Savica V, Ricciardi CA, Bellinghieri P, Duro G, Ricciardi B, Bellinghieri G. The historical relevance of urine and the future implications. GItal Nefrol. 2018; 35(Suppl. 70): 128-130.

10. Loeffler JM. The Golden fountain - is urine the miracle drug no one told you about? Pan Afr Medic J. 2010; 25(5): 13.

11. Thakur AN. Therapeutic use of urine in early Indian medicine. Indian J Hist Sci. 2004; 39(4): 415-427.

12. Yu P, Bosholm CC, Zhu H, Duan Z, Atala A, Zhang Y. Beyond waste: understanding urine's potential in precision medicine. Trends Biotechno. 2024; DOI: 10.1016/j.tibtech.2024.01.009.

13. Patil S. How and why urine therapy works? https://anandkunj.com/how-and-why-urine-therapy-works/. Accessed 25 June 2025.

14. Motola J. The history of urine as healing agent. J Urology. 2016; DOI: 10.1016/j.juro.2016.02.100.

15. Vaidya ADB. Urine therapy in Ayurveda: Ancient insights to modern discoveries for cancer regression. J Ayurveda Integrati Medic. 2018; DOI: 10.1016/j.jaim.2017.09.005.

16. Yu P, Opara EC, Zhang Y. Power of pee: Urine-derived stem cells in urological disorders. Uro Precision. 2023; DOI: 10.1002/uro2.16.

17. Va´zquez S, Cabezas S, Pe´rez AB, Pupo M, Ruiz D, *et al.* Kinetics of antibodies in sera, saliva, and urine samples from adult patients with primary or secondary dengue 3 virus infections. Internat J Infecti Dis. 2007; DOI: 10.1016/j.ijid.2006.05.005.

18. Rodríguez LAR, Díaz QL, Casanueva RM, Moreno AG. Anti-hepatitis A virus immunoglobulin M antibodies in urine samples for rapid diagnosis of outbreaks. Clinic Diagnost Lab Immunol, 2003; DOI: 10.1128/CDLI.10.3.492–494.2003.

19. Eamudomkarn C, Sithithaworn P, Kamamia C, Yakovleva A, Sithithaworn J, *et al.* Diagnostic performance of urinary IgG antibody detection: A novel approach for population screening of strongyloidiasis. PLoS ONE. DOI: 10.1371/journal.pone.0192598.

20. Oelemann WMR, Lowndes CM, Veríssimo da Costa GC, Morgado MG, Castello-Branco LRR, *et al.* Diagnostic detection of human immunodeficiency virus type 1 antibodies in urine: a Brazilian study. J Clinic Microbiol. 2002; DOI: 10.1128/JCM.40.3.881–885.2002.

21. Zhao H, Qiu S, Hong WX, Song KY, Wang J, *et al.* Dengue specific immunoglobulin A antibody is present in urine and associated with disease severity. Scientif Reports. 2016; DOI: 10.1038/srep27298.

22. Mohandas S, Balan S, Mourya DT. Urinary immunoglobulins in viral diagnosis: An overview. Indian J Med Res. 2022; DOI: 10.4103/ijmr.IJMR_808_18.

23. Pattanayak S. Autohaemotherapy in bovine papillomatosis. Intas Polivet. 2004; 5(1): 16-17.

24. Sheikhi A, Azarbeig M, Karimi H. Autohemotherapy in chronic urticaria: What could be the auto-reactive factors and curative mechanisms? Ann Dermatol. 2014; 26(4): 526-527.

25. Yan SH, Chen Y, Huang ZQ, Zhong WX, Wang XT, *et al.* Acupoint autohemotherapy attenuates DNCB-Induced atopic dermatitis and activates regulatory T cells in BALB/c mice. J Inflamm Res. 2024; DOI: 10.2147/JIR.S454325.

26. Shen W, Liu N, Ji Z, Fang H, Liu F, *et al.* Combining ozonated autohemotherapy with pharmacological therapy for co-morbid insomnia and myofascial pain syndrome: a prospective randomized controlled study. Pain Res Management. 2022; DOI: 10.1155/2022/3562191.

27. Niño-Sandoval TC, Rocha NS, Sarinho FW, Vasconcelos CFM, Vasconcelos AFM, Vasconcelos BC. Effect of autohemotherapy in the treatment of viral infections - a systematic review. Public Health. 2021; DOI: 10.1016/j.puhe.2021.09.024.

28. Sumitha P, Sukumar K. Bovine papillomatosis: Occurrence and its control by autogenous vaccine. Indian J Anim Health. 2021; DOI: 10.36062/ijah.2021.10821.

29. Geethanjali PV, Louis LE, Deepa PM, Vijayakumar M, Velavan A. A comprehensive treatment strategy for bovine papillomatosis: Assessing the synergistic effects of autohaemotherapy, surgical intervention, and autogenous vaccination. Internati J Vety Sci Anim Husbandry. 2024; DOI: 10.22271/veterinary.2024.v9.i1Si.1084.

30. Bhatt S, Roy K, Tiwari A, Gupta DK, Pradhan S, *et al.* Autohemotherapy in veterinary clinical practice: An update. Pharma Innovat J. 2021; SP-10(11): 482-485.

31. Pattanayak S. Neglected areas of phyto-medicinal research. Explor Anim Med Res. 2025; DOI: 10.52635/eamr/15.2.155-159.

32. Pattanayak S. Succulent biomedicines–an effective way of getting protection against diseases through immunomodulation. Explor Anim Med Res. 2020; 10(2): 112-123.

33. Pattanayak S. Limitations of the contemporary vaccines: how to overcome? Explor Anim Med Res. 2023; DOI: 10.52635/eamr/13.2.140-145.

34. Durham SR, Shamji MH. Allergen immunotherapy: past, present and future. Nat Rev Immunol. 2023; DOI: 10.1038/s41577-022-00786-1.

35. Pattanayak S, Manna S. Attenuated and modified vaccine viruses: do they act as a source of some other viral diseases? Explor Anim Med Res. 2023; DOI: 10.52635/eamr/13.1.1-7.

36. Linhart B, Valenta R. Vaccines for allergy. Curr Opin Immunol. 2012; DOI: 10.1016/j.coi.2012.03.006.

37. Akinfenwa O, Rodríguez- Domínguez A, Vrtala S, Valenta R, Campana R. Novel vaccines for allergen-specific immunotherapy. Curr Opin Allergy Clin Immunol. 2021; DOI: 10.1097/ACI.0000000000000706.

38. Dorofeeva Y, Shilovskiy I, Tulaeva I, Focke - Tejkl M, Flicker S. *et al.* Past, present, and future of allergen immunotherapy vaccines. Allergy. 2021; DOI: 10.1111/all.14300.

39. Abd-Aziz N, Poh CL. Development of peptide-based vaccines for cancer. J Oncol. 2022; DOI: 10.1155/2022/9749363.

40. Liu J, Fu M, Wang M, Wan D, Wei Y, Wei X. Cancer vaccines as promising immuno- therapeutics: platforms and current progress. J Hematology Oncology. 2022; DOI: 10.1186/s13045-022-01247-x.

41. Cancer Vaccines and Immunotherapy. https://historyofvaccines.org/vaccines-101/future-immunization/cancer-vaccines-and-immunotherapy. Accessed April 12, 2025.

42. Medline Plus (Official website of U. S. Govt.). What are mRNA vaccines and how do they work?
https://medlineplus.gov/genetics/understanding/therapy/mrnavaccines/, Accessed on 23.04.2026.

43. Srivatsan S, Patel JM, Bozeman EN, Imasuen IE, He S, *et al.* Allogeneic tumor cell vaccines: the promise and limitations in clinical trials. Hum Vaccin Immunother. 2014; DOI: 10.4161/hv.26568.

44. Stebbing J. An update on mRNA cancer vaccines. 2024; https://www.rcpath.org/resource-report/an-update-on-mrna-cancer-vaccines. html. Accessed February 12, 2025.

45. Makker S, Galley C, Bennett CL. Cancer vaccines: from an immunology perspective. Immunother Advan. 2024; DOI: 10.1093/immadv/ltad030.

46. Fritah H, Rovelli R, Chiang CL, Kandalaft LE. The current clinical landscape of personalized cancer vaccines. Cancer Treatment Rev. 2022; DOI: 10.1016/j.ctrv.2022.102383.

47. Drew L. Cancer vaccines: reasons for optimism. Nature. 2024; https://www.nature.com/articles/d41586-024-00840-z.

48. Fu Q, Zhao X, Hu J, Jiao Y, Yan Y, *et al.* mRNA vaccines in the context of cancer treatment: from concept to application. J Translational Medic. 2025; DOI: 10.1186/s12967-024-06033-6.

49. Shariati A, Khani P, Nasri F, Afkhami H, Khezrpour A, *et al.* mRNA cancer vaccines from bench to bedside: a new era in cancer immunotherapy. Biomarker Res. 2024; DOI: 10.1186/s40364-024-00692-9.

50. Sheridan, C. Individualized mRNA cancer vaccines make strides. Nat Biotechnol. 2025; DOI: 10.1038/s41587-025-02708-7.

51. Wang S, Liang B, Wang W, *et al.* Viral vectored vaccines: design, development, preventive and therapeutic applications in human diseases. Sig Transduct Target Ther. 2023; DOI: 10.1038/s41392-023-01408-5.

52. Choi Y, Chang J. Viral vectors for vaccine applications. Clin Exp Vaccine Res. 2013; DOI: 10.7774/cevr.2013.2.2.97.

53. WHO. https://www.who.int/teams/health-product-policy-and-standards/standards-and-specifications/norms-and-standards/vaccine-standardization/hep-, Accessed 24 March 2025.

54. Kumar S, Biswas M, Jose T. HPV vaccine: Current status and future directions. Med J Armed Forces India. 2015; DOI: 10.1016/j.mjafi.2015.02.006.

55. Zhou W, Lu X, Tian F, Luo Q, Zhou W, *et al.* Vaccine therapies for prostate cancer: current status and future outlook. Vaccines (Basel). 2024; DOI: 10.3390/vaccines12121384.

56. Canadian Cancer Society. Cancer vaccines. 2025; https://cancer.ca/en/treatments/treatment-types/cancer-vaccines.Accessed 11 May 2025.

57. Sobhani N, Scaggiante B, Morris R, Chai D, Catalano M, *et al.* Therapeutic cancer vaccines: From biological mechanisms and engineering to ongoing clinical trials. Cancer Treatment Rev. 2022; DOI: 10.1016/j.ctrv.2022.102429.

58. National Cancer Institute. Oncolytic virus enables the immune system to attack tumors. 2023; https://www.cancer.gov/news-events/cancer-currents-blog/2023/oncolytic-virus-. Accessed 25 May 2025.

59. Ruzzi F, Riccardo F, Conti L, Tarone L, Semprini MS, *et al.* Cancer vaccines: Target antigens, vaccine platforms and preclinical models. Molecular Aspect Medic. 2025; DOI: 10.1016/j.mam.2024.101324.

60. Liu D, CheX, Wang X, Ma C, Wu G. Tumor vaccines: Unleashing the power of the immune system to fight cancer. Pharmaceuticals. 2023; DOI: 10.3390/ph16101384.

61. Zhou Y, Wei Y, Tian X, Wei X. Cancer vaccines: current status and future directions. J Hematolo Oncolo. 2025; DOI: 10.1186/s13045-025-01670-w.

62. Ranjan R, Ghummanm SPS, Bhatt GR, Singh RS. Efficacy of autogenous vaccine and auto-hemotherapy in bovine cutaneous papillomatosis. Intas Polivet. 2013; 14(II): 411-414.

63. Lucroy MD, Clauson RM, Suckow MA, El-Tayyeb F, Kalinauskas A. Evaluation of an autologous cancer vaccine for the treatment of metastatic canine hemangiosarcoma: a preliminary study. BMC Vet Res. 2020; DOI: 10.1186/s12917-020-02675-y.

64. Liau LM, Ashkan K, Brem S, Campian JL, Trusheim JE, *et al.* Association of autologous tumor lysate-loaded dendritic cell vaccination with extension of survival among patients with newly diagnosed and recurrent glioblastoma: A phase 3 prospective externally controlled cohort trial. JAMA Oncology. 2023; 9(1): 112-121.

65. Berd D. Portrait of an autologous cancer vaccine: Then and now. Human Vacc Immunotherap. 2023; DOI: 10.1080/21645515.2023.2172925.

66. Bastin DJ, Montroy J, Kennedy MA, Martel AB, Shorr R, *et al.* Safety and efficacy of autologous cell vaccines in solid tumors: a systematic review and meta-analysis of randomized control trials. Scientif Report Nature Portfol. 2023; DOI: 10.1038/s41598-023-29630-9.

67. Marcano EG, Kröhle L, Ahlers J, Drevs J. Pilot study on outcome and antitumor efficacy of an autologous cancer cell vaccine applied in patients with advanced solid tumors. J Clinical Oncology. 2020; DOI: 10.1200/JCO.2020.38.15_suppl.3000.

68. Bobisse S, Bianchi V, Tanyi JL, Sarivalasis A, Missiaglia, *et al.* A phase 1 trial of adoptive transfer of vaccine-primed autologous circulating T cells in ovarian cancer. Nat Cancer. 2023; DOI: 10.1038/s43018-023-00623-x.

69. Fucikova J, Hensler M, Kasikova L, Lanickova T, Pasulka J, *et al.* An autologous dendritic cell vaccine promotes anticancer immunity in patients with ovarian cancer with low mutational burden and cold tumors. Clin Cancer Res. 2022; DOI: 10.1158/1078-0432.CCR-21-4413.

70. Fukuhara H, Ino Y, Todo T. Oncolytic virus therapy: A new era of cancer treatment at dawn. Cancer Sci. 2016; DOI: 10.1111/cas.13027.

71. Banda FJS, Gangane S, Raza F, Massarelli E. Current development of therapeutic vaccines in lung cancer. Vaccines. 2025; DOI: 10.3390/vaccines13020185.

72. Emmers M, Welters MJP, Dietz MV, *et al.* TEIPP-vaccination in checkpoint-resistant non-small cell lung cancer: a first-in-human phase I/II dose-escalation study. Nat Commun. 2025; DOI: 10.1038/s41467-025-60281-8.

73. Mieruszynski S. Lung cancer vaccines: How they work and the latest advances. Thoracic oncology group Australia. 2025; https://thoraciconcology.org.au/news/clinical-trials/lung-cancer-vaccines-how-they-work-and-the-latest-advances. Accessed 12 July 2025.

74. Lung Cancer Research Foundation. Vaccines for lung cancer. 2024; https://www.lungcancerresearchfoundation.org/vaccines-for-lung-cancer-.Accessed 18 July 2025.

75. Ramlogan-Steel CA, Steel JC, Morris JC. Lung cancer vaccines: current status and future prospects. Transl Lung Cancer Res. 2014; 3(1): 46-52.

76. Allogeneic tumor cell vaccine. https://www.cancer.gov/publications/dictionaries/cancer-drug/def/allogeneic-tumor-cell-vaccine.Accessed 12 June 2025.

77. Usman MB, Bhardwaj S, Roychoudhury S, Kumar D, Alexiou A, *et al.* Immunotherapy for Alzheimer's disease: current scenario and future perspectives. J Prevent Alzheimer's Dis. 2021; DOI: 10.14283/jpad.2021.52.

78. Fettelschoss A, Zabel F, Bachmann MF. Vaccination against Alzheimer disease: an update on future strategies. Hum Vaccine Immunother. 2014; DOI: 10.4161/hv.28183.

79. Hovakimyan A, Chilingaryan G, King O, Capocchi JK, Chadarevian JP, *et al.* mRNA Vaccine for Alzheimer's disease: Pilot study. Vaccines (Basel). 2024; DOI: 10.3390/vaccines12060659.

80. Bhadane P, Roul K, Belemkar S, Kumar D. Immunotherapeutic approaches for Alzheimer's disease: Exploring active and passive vaccine progress. Brain Res. 2024; DOI: 10.1016/j.brainres.2024.149018.

81. Geddes L. Two vaccines, one target: How the RTS, S and R21 Malaria vaccines work. 2024; https://www.gavi.

org/vaccineswork/two-vaccines-one-target-how-rtss-and-r21-malaria-vaccines-. Accessed 15 August 2025.

82. Laurens MB. RTS, S/AS01 vaccine (Mosquirix™): an overview. Hum Vaccin Immunother. 2020; DOI: 10.1080/21645515.2019.1669415.

83. Skwarczynski M, Chandrudu S, Rigau-Planella B, Islam MT, Cheong YS, *et al.* Progress in the development of subunit vaccines against malaria. Vaccines (Basel). 2020; DOI: 10.3390/vaccines8030373.

84. Wu R, Sun F, Zhang W, Ren J, Liu GH. Targeting aging and age-related diseases with vaccines. Nat Aging. 2024; DOI: 10.1038/s43587-024-00597-0.

85. Vasilieva MI, Shatalova RO, Matveeva KS, Shindyapin VV, Minskaia E, *et al.* Senolytic vaccines from the central and peripheral tolerance perspective. Vaccines (Basel). 2024; DOI: 10.3390/vaccines12121389.

86. Cellular Senescence. https://www.cellsignal.com/science-resources/overview-of-cellular-senescence. Accessed 12 July 2025.

87. Phillips C. National Cancer Institute. Experimental mRNA vaccine hints at potential against glioblastoma. 2024; https://www.cancer.gov/news-events/cancer-currents-blog/2024/glioblastoma-mrna-vaccine-layered-nanoparticle. Accessed 12 September 2025.

88. Stem cells: Main types, sources and uses. 2021; https://www.advancells.com/stem-cells-types-sources-and-uses/. Accessed 14 September 2025.

89. Bacakova L, Zarubova J, Travnickova M, Musilkova J, Pajorova J, *et al.* Stem cells: their source, potency and use in regenerative therapies with focus on adipose-derived stem cells - a review. Biotechnol Adv. 2018; DOI: 10.1016/j.biotechadv.2018.03.011.

90. Ghasroldasht MM, Seok J, Park HS, Ali FBL, Al-Hendy A. Stem cell therapy: from idea to clinical practice. Int J Mol Sci. 2022; DOI: 10.3390/ijms23052850.

91. Salgia R, Lynch T, Skarin A, Lucca J, Lynch C, *et al.* Vaccination with irradiated autologous tumor cells engineered to secrete granulocyte-macrophage colony-stimulating factor augments antitumor immunity in some patients with metastatic non–small-cell lung carcinoma. J Clinical Oncology. 2003; DOI: 10.1200/JCO.2003.03.091.

92. Chang D, Dela Cruz C, Sharma L. Beneficial and detrimental effects of cytokines during influenza and covid-19. Viruses. 2024; DOI: 10.3390/v16020308.

93. Khirehgesh MR, Sharifi J, Sharifi F, Akbari B. Immunotoxins and nanobody-based immunotoxins: review and update. J Drug Targeting. 2021; DOI: 10.1080/1061186X.2021.1894435.

94. Carlos WG, Gross JE, Cruz CD, Jamil S. Monoclonal antibodies: Medical uses for the prevention and treatment of disease. Am J Resp Clinical Care Medic. 2021; DOI: 10.1164/rccm.2021C3.

95. Kreitman RJ, Pastan I. Immunotoxins: From design to clinical application. Biomolecules. 2021; DOI: 10.3390/biom11111696.

96. Mazor R, Pastan I. Immunogenicity of immunotoxins containing *Pseudomonas* exotoxin A: Causes, consequences, and mitigation. Front Immunol. 2020; DOI: 10.3389/fimmu.2020.01261.

97. Wei J, Bera TK, Liu XF, Zhou Q, Onda M, *et al.* Recombinant immunotoxins with albumin-binding domains have long half-lives and high antitumor activity. Proc Natl Acad Sci. USA. 2018; DOI: 10.1073/pnas.1721780115.

98. Madhumathi J, Verma RS, Therapeutic targets and recent advances in protein immunotoxins. Current Opinion Microbiol, 2012; DOI: 10.1016/j.mib.2012.05.006.

99. Pattanayak S. Therapeutic use of plant parts as food or medicine at succulent state: an alternative healthcare system for the prevention and treatment of diseases. Discover Plants. 2025; DOI: 10.1007/s44372-025-00111-9.

100. Minakshi, Sharma R. A review article on the concept of Rasayana in Ayurveda. J AyuInt Med Sci. 2023; 8(2): 101-106.

101. The Khadar Vali Millet Lifestyle: Restoring Health Naturally. 2025; https://organicsphere.com/blogs/dr-khader-lifestyle-protocols/the-khadar-vali-millet-lifestyle-restoring-health-naturally? Accessed 17 May 2025.

102. Kim E, Zhao Z, Rzasa JR, Glassman M, Bentley WE, *et al.* Association of acute psychosocial stress with oxidative stress: Evidence from serum analysis. Redox Biol. 2021; DOI: 10.1016/j.redox.2021.102138.

103. Bechter K. Development of neuropsychiatry over the last 30 years and the new era of Immuno-psychiatry. J Affecti Disord Repo. 2023; DOI: 10.1016/j.jadr.2023.100656.

104. Pattanayak S. Psycho-neuro-immuno-endocrinology: study of the key factors of disease creation. Explor Anim Med Res. 2024; DOI: 10.52635/eamr/14.2.164-171.

105. Pattanayak S. Biological age and lifestyle: key deciding factors of aging and disease susceptibility. Explor Anim Med Res. 2024; DOI: 10.52635/eamr/14.1.1-5.

106. Pattanayak S. Processed foods - are they safe? Explor Anim Med Res. 2017; 7(2): 125-131.

107. Pattanayak S. Alternative to antibiotics from herbal origin – outline of a comprehensive research project. Current Pharmacogenom Personali Medic. 2018; DOI: 10.2174/1875692116666180419154033.

108. Pattanayak S. Trans-fats of processed and fried foods – a choice for taste or serious health problems? Explor Anim Med Res. 2019; 9(1): 5-14.

109. Hegde BM. Ideal food habits for healthy living. https://www.bmhegde.com/ideal_food.htm. Accessed on 17 September 2025.

110. Pattanayak S. Plastics and their additives reached the blood and tissue spaces: what are the possible consequences? Explor Anim Med Res. 2022; DOI: 10.5263/eamr/12.2.128-133.

111. Roy Chowdhury B. DIP Diet. https://biswaroop.com/dipdiet/, Accessed 17 October 2025.

Cite this article as: Pattanayak S. Comprehensive review on the prospects and conundrums of ancient to contemporary modern immuno-modulation techniques practiced in human and animal healthcare. Explor Anim Med Res. 2026; 16(1), DOI: 10.52635/eamr/16.1.14-27.

Explor Anim Med Res.
Vol. 16, Issue 1, 2026
DOI: 10.52635/eamr/16.1.28-39

ISSN 2277-470X (Print), ISSN 2319-247X (Online)
Website: www.animalmedicalresearch.org

Published under the CC BY-NC 4.0 license

Research Article

SINGLE NUCLEOTIDE POLYMORPHISMS APPROACH FOR GENETIC BACKGROUND OF ICR MICE USING MASSARRAY

Nopparat Phumkumarn[1*], Jarasporn Tangkhabuanbutra[1], Piyapha Hirunpatrawong[2], Panya Chariyahpongpun[1]

Received 25 March 2025, revised 23 April 2026

ABSTRACT: Single nucleotide polymorphisms (SNPs) are an effective method for determining the genetic background of ICR outbred mice in the National Laboratory Animal Center, Mahidol University. We screened 20 SNPs on all autosomes and X chromosome. This method provides fast, accurate and reliable with high confidence for assessing the genetic background of the mice used in research. The SNP markers used in this study were obtained from publicly available SNP databases of inbred mice in the ICLAS Monitoring Center and were subsequently designed using MassARRAY assay design software. Tail samples from ICR outbred mice were collected for genomic DNA extraction. We amplified gene fragments using multiplex PCR and analyzed them through allele-specific primer extension, based on matrix-assisted laser desorption/ionization-time of flight mass spectrometry (MALDI-TOF MS). We described the 20 multiplexes PCR assays for detection with the Sequenom MassARRAY® system. The genetic monitoring reference DNA samples from inbred mice were analyzed for quality control, demonstrating 100% accuracy. The MassARRAY® TYPER 4.0 genotyping software automatically determined phenotypes based on peak heights and mass. Among the analyzed SNPs, nine SNPs provided a heterozygous genotype frequency. No deviation from Hardy – Weinberg equilibrium (P_{HWE} > 0.05) was detected for all SNPs. All nine SNPs exhibited heterozygote deficiency, as indicated by positive F_{IS} values. These polymorphic SNPs offer in this study provide preliminary insights into genetic variability and may serve as candidate markers for future validation and refinement of genetic monitoring within outbred strains.

Keywords: SNP, Genetic background, MassARRAY, ICR mice.

INTRODUCTION

The management of outbred animals has become increasingly important due to their rising popularity in both academic research and commercial applications. These populations provide the genetic diversity necessary for modeling complex traits and studying natural genetic variation, making their effective management essential. Maintaining heterozygosity is a critical goal in managing outbred populations, as it ensures their health, adaptability, and long-term sustainability. Genetic monitoring plays a central role in this process, helping to preserve genetic integrity and guide breeding programs. By tracking allele frequencies and detecting deviations from genetic expectations, genetic monitoring addresses the challenges posed by genetic drift—a stochastic process that causes changes in allele frequencies due to chance rather than natural selection. As Hartl explains, genetic drift is particularly impactful in small populations, where random sampling can lead to significant fluctuations, reduced genetic diversity, and fixation of alleles, thereby compromising the population's adaptability and viability [1].

To counter these effects, robust genetic monitoring strategies must be employed to assess genetic diversity and population structure. The FELASA guidelines emphasize the importance of genetic quality assessment in maintaining the reliability and reproducibility of research outcomes, as well as the effectiveness of breeding programs [2]. Evaluating genetic diversity using tools like observed heterozygosity (*Ho*)

[1]*National Laboratory Animal Center, Mahidol University, Nakorn pathom, Thailand.*
[2]*Faculty of Medicine, Chulalongkorn University, Rama IV Road, Pathum wan, Bangkok, Thailand.*
**Corresponding author. e-mail: nopparat.phu@mahidol.ac.th*

and expected heterozygosity (*He*) is essential for understanding trends over generations and identifying any concerning patterns. The Hardy-Weinberg equilibrium (HWE) provides a theoretical framework for assessing genetic stability within populations. Deviations from HWE can signal inbreeding, genetic drift, or selection pressures, which are critical factors in maintaining the genetic health of outbred populations. Hartl underscores the importance of analyzing these metrics over successive generations to detect changes and ensure populations remain representative of their genetic pool [1]. Typically, HWE is assessed using the Chi-square test (X^2-test), which evaluates deviations from expected genetic distributions under specific assumptions. The Hardy-Weinberg principle stipulates that large populations with random mating, no selection, and no genetic drift or migration should maintain stable allele frequencies. Consequently, any significant deviations from HWE predictions may indicate violations of its assumptions, such as population stratification or genotyping errors [3]. In 1979, the ICLAS Monitoring Center established the concept of a genetic profile and a monitoring system for genetic testing, utilizing biochemical and immunologic markers for inbred strains of mice and rats [4]. Biochemical and immunological markers are complex to analyze and often require specialized equipment and techniques, which can lead to increased costs and testing times. Furthermore, some markers exhibit low genetic variability, making it challenging to effectively differentiate closely related strains [2].

Practical approaches for managing outbred populations combine genetic monitoring with advanced molecular techniques, such as genotyping-by-sequencing (GBS) and single nucleotide polymorphism (SNP) analysis. These methods enable precise assessments of genetic diversity and the identification of markers linked to desirable traits. Computational models further enhance these efforts by simulating genetic drift and predicting allele frequency distributions, providing critical insights for designing effective breeding programs. Integrating these technologies with established guidelines allows researchers and breeders to preserve the genetic diversity and integrity of outbred populations, ensuring their sustainability and utility in both research and commercial applications. SNPs, which represent single nucleotide variations in DNA sequences with typically two common alleles, have proven particularly valuable in genetic studies. Along with microsatellites, they are widely used for quality control in laboratory animals such as mice and rats. SNP analysis simplifies genotyping and facilitates high-throughput genetic assessments, making it an indispensable tool for effective population management [5]. The first published database used high-density oligonucleotide arrays to collect 2,848 SNPs located in 1,755 sequences tagged sites (STSs) identified across eight mouse strains, representing a first-generation mapping on the mouse genome [6,7]. Another experiment also developed a murine database of SNP [8]. The genotyping panel comprises 87 microsatellite markers that are polymorphic among commonly used inbred rat strains, serving applications that range from assessing genetic contamination within rat colonies [9]. Moreover, there is a genetic mapping substrains of C57BL/6 and BALB/c mice using SNPs characterization to identify the causative mutations of phenotypes induced by N-ethyl-N-nitrosourea mutagenesis [10]. The Jackson Laboratory provided baseline phenotypic data for the most common inbred mouse strains through The Mouse Genome informatics (https://www.informatics.jax.org/home/strain) which includes 420 inbred mouse and 230 inbred rat strains, complied by Dr. Micharl FW feasting. However, SNPs have not been widely utilized for genotyping outbred mice, as the data available in public databases are relatively limited compared to the extensive number of SNPs identified in inbred mouse strains. SNP markers are specific DNA sequences located at known positions on chromosomes, serving as crucial tools for genetic quality control. Outbred colonies are screened for genetic heterogeneity to identify contamination, monitor the progress of breeding programs and select future breeders.

The SNP genotyping was conducted using the MassARRAY® system coupled with matrix-assisted laser desorption/ionization time-of-flight (MALDI-TOF) mass spectrometer to provide rapid analysis of large multiplex PCR and single base extension (SBE) multiplex assays. MALDI-TOF MS is a superior technology for SNP detection, consisting of real-time TYPER software on the MassARRAY® analyzer system. This system integrates the robust multiplexed primer extension of the iPLEX® assay, achieving high accuracy in measuring molecular weight, high sensitivity for detecting both homozygosity and heterozygosity and offers a reasonable price [11]. Much research has been focused on SNP for various applications, including the identification and characterization of gene expression modulation [12], the analysis of genes that affect drug metabolism [13] and the development of human identification and sample tracking [14] by MassARRAY® system. Overall, the

combination of SNP analysis with the MassARRAY® system provides high throughput, accuracy, precision, multiplexing capability and enhanced efficiency in genetic monitoring. This study, identifies the single nucleotide polymorphism relevant to genetic quality in breeding programs. To investigate the genetic background of Institute of Cancer Research (ICR) outbred colonies at the National Laboratory Animal Center, Mahidol University (Mlac: ICR) population, we genotyped 20 SNPs located on chromosomes 1 through 19, including the X chromosome using the MassARRAY (Agena Bioscience™) platform, which combined competitive PCR with MALDI-TOF mass spectrometry. Our finding indicated that the identified SNPs exhibit susceptibility and are beneficial for genetic monitoring in outbred mice colonies.

MATERIALS AND METHODS

Samples, DNA isolation and DNA quantification

A total of 306 tail samples were collected to represent the genetic background of ICR outbred mice at the National Laboratory Animal Center, Mahidol University (Mlac: ICR). The experiment cohort was derived from parental stock maintained under a Maximum Avoidance of Inbreeding (MAI) mating scheme, yielding multiple litters with variable sizes and sex ratios. To control for litter effects and ensure balanced representation of both sexes, a sex – stratified random sampling procedure was executed within each litter across three consecutive generations. Each generation was defined as the interval between the establishment of breeders and the collection of their offspring for genotyping. Randomization was then performed within each litter, where two individuals of each sex were randomly selected to achieve a sex – balanced sampling design. In cases where all offspring in a litter were of the same sex, two individuals from that sex were randomly selected, maintaining consistency in sample size while controlling for potential litter bias. Tail samples, approximately 0.5–1 cm in length, were collected and stored in sterile 1.5 ml centrifuge tubes. DNA was isolated using the phenol-chloroform method, following the protocol described by Rupali *et al.,* 2023 [15]. The extracted DNA was eluted in 50 µl of DNase/RNase-free water, and its concentration was quantified using a NanoDrop spectrometer. The DNA concentrations ranged from 20–30 ng/µl, making the samples suitable for use with the MassARRAY® system. This sampling and extraction process ensured the representation of the genetic diversity within the ICR outbred population.

Selection of SNPs

In this study, SNPs were selected based on specific criteria to ensure accuracy and informativeness in genetic monitoring. Key factors included the distribution of SNPs across multiple chromosomes for broad genomic coverage, their polymorphic characteristics in laboratory mouse strains, and their relevance to genetic variability in both inbred and outbred populations. Priority was given to SNPs with well-documented allelic diversity and those commonly utilized in genetic studies of laboratory mice. These considerations ensured that the selected markers reliably represented the genetic variation within the Mlac: ICR population and enabled the detection of allele frequency changes across generations. Both autosomal and X-linked SNPs were included to facilitate a comprehensive analysis of genetic patterns throughout the genome. The genetic profiles of inbred mice preciously reported by the Center Institute for Experimental Medicine and Life Science (CIEM) using SNP analysis [15], this study further developed and adapted these SNP loci to assess the genetic quality of outbred mouse strains. A subset of SNP markers was selected to ensure coverage across all chromosomes. For genetic monitoring of Mlac:ICR mice, SNP databases from autosome and the X chromosome of inbred mice maintained at CIEM were utilized. The 20 selected SNPs included rs13476308, rs1347682, rs13477311, rs13477625, rs6234655, rs30716377, rs13479101, rs13479815, rs6313405, rs6208271, rs13481075, rs13481497, rs13481762, rs13482084, rs13482609, rs4217297, rs13482900, rs13483256, rs13483687, and rs13484117. These SNPs were verified using the Mouse Genome Informatics database. Primers for the Mass Extend multiplex assays were designed using MassARRAY Designer software version 4.0 (Agena Biosciences™). The SNP IDs and their corresponding extension primers are detailed in Table 1.

SNP detection

The genotype analysis was performed using iPLEX® Sample ID Plus Panel (Sequenom). The multiplex PCR of 20 SNPs, the following reaction mixture was prepared in a total volume of 5 µl per well in 96-well plates containing: 0.8 µl nuclease-free water, 0.5 µl 10X PCR buffer, 0.4 µl 25 mM $MgCl_2$, 0.1 µl 25 mM dNTP mix, 1.0 µl forward/reverse primer mix, 0.2 µl PCR enzyme and 2 µl DNA (5 – 25 ng/µl). PCR was carried out in a Bio-Rad T100 Thermal Cycler with the following conditions: initial denaturation at 95°C for 2 min followed by 45 cycles of 95°C for 30 sec, 56°C

for 30 sec, 72°C for 1 min and final step of 72°C for 5 min. The PCR products were treated with a cocktail of 1.53 µl nuclease-free water, 0.17 µl 10X SAP buffer and 0.3 µl shrimp alkaline phosphatase (1.7U/µl) (SAP) to remove excess dNTPs. The PCR cocktail was performed in the Bio-Rad T100 Thermal Cycler of 37°C for 40 min and 85°C for 5 min. The PCR products were then used as templates for the iPLEX® Pro extension reaction containing 0.62 µl nuclease-free water, 0.20 µl 10X iPLEX buffer plus, 0.20 µl 10X iPLEX termination mix, 0.94 µl extend primer mix (5 – 15 µM) and 0.04 µl iPLEX proenzyme (32 U/µl). The extension reaction cocktail was performed in the Bio-Rad T100 Thermal Cycler with the following conditions: initial denaturation at 95°C for 30 sec followed by 40 cycles of 95°C for 5 sec, followed by 5 cycles of 52°C for 5 sec and 80°C for 5 sec and a final step at 72°C for 3 min. The samples were added with 29 µl nuclease-free water and then treated with clean resin. All plates were included a negative control (no template) to confirm that there was no contamination. All the final products were spotted onto SpectroCHIP® Array using the Nano dispenser RS1000 and then transferred into the MassARRAY Compact System. Genotyping analysis was performed using the MassARRAY® analyzer 4 with an autorun system, and results were reported using Typer software.

Data analysis

The separation of the mass detector records the relative time of flight from each extension product. The results from MassARRAY Typer 4.0 genotyping software were shown in cluster analyses with signal-to-noise ratios and peak heights in real time. The Typer software generates reports indicating whether SNPs are homozygous or heterozygous. The data from the SNP call was divided into 4 groups; conservative, moderate, aggressive genotyping and low probability calls (low signal-to-noise ratios). The genotype call shows no allele when no extended primers were detected at that locus.

Statistical analysis

Genetic variation at each SNP locus was categorized into three genotypes, depending on the alleles inherited from both parents. Hardy Weinberg Equilibrium (HWE) is described by the binomial relationship $(p + q)^2 = 1$, where p and q represent the frequencies of alternative alleles [17]. In this study, the quality of all nine SNPs was assessed using genetic parameters including HWE, the inbreeding coefficient within individuals relative to their subpopulation (F_{IS}), observed heterozygosity (*Ho*), and expected heterozygosity (*He*) in PLINK 1.9 [18 - 20]. Comparison between observed and expected genotype distributions was performed to identify potential genotyping errors. Genotyping quality control (QC) included calculation of per – SNP and per – sample call rates to assess data completeness. SNPs with call rates below 95% and samples with genotyping success below 95% were excluded by comparing genotype calls across technical duplicates to ensure reliability. Principal component analysis (PCA) was performed on the genotype matrix, treating each SNP as an individual variable. This algorithm summarizes the covariance structure among SNPs and generates a series of orthogonal principal components (PCs). Each PC represents a linear combination of SNP genotypes and captures a decreasing proportion of the overall genetic variance, the first PCs reflect the major axes of genetic differentiation among individuals. SNP loadings were examined to determine the relative contribution of each locus to the observed population structure. PCA scores for each individual were visualized in R to evaluate clustering patterns and potential substructure. All QC procedures, including filtering, summary statistics, and visualization of missingness patterns, were primarily conducted in PLINK 1.9, while additional data inspection, graphical summaries, and confirmation of QC metrices were performed in R 4.3.0.

RESULTS AND DISCUSSION

Genotyping analysis using MALDI-TOF MS

In total, 306 samples from three generations of Mlac: ICR mice were successfully genotyped in this study using the MassARRAY® system. A set of 20 SNP markers, distributed across autosomes and the X chromosome, was selected from the inbred mouse genetic monitoring database of the ICLAS Monitoring Center and applied to outbred mice genetic monitoring. DNA samples were purified, genotyped, and analyzed using the MassARRAY TYPER 4.0 genotyping software. The genotyping process achieved a high average call rate of 94–100%, with only 6% of samples being classified as “no call,” indicating excellent assay performance.

The PCR extension products for the 20 SNPs were analyzed and categorized using TYPER 4.0 software, which generated outputs for various genotype classifications, including conservative, moderate, aggressive, low-probability, and no alleles. The intensities plotted against the mass signals are shown in Fig. 1. The data displayed clear and distinct peak

Table 1. PCR primers and extension primers of SNP marker using MassARRAY Design Software.

SNP ID	Chromosome	Forward primer (5' → 3')	Reverse primer (5' → 3')	UEP sequence
rs13476308	1	ACGTTGGATGCGCTGG-GTGCTCAATTCTA	ACGTTGGATGAGTCTA-CACTGATCCCCAAG	CCCAAGTAAGGATCTG
rs13476824	2	ACGTTGGATGGTG-CATTTATCTTGGTAGGG	ACGTTGGATGAAAA-CAGGCATTTGTGTGG	AAATTTAGACACTGG-TAGT
rs13477311	3	ACGTTGGATGGGCAT-GATGCGATGTTTGTG	ACGTTGGATGGGGCA-CAGTTAGAAAACAGC	ACAGTTAGAAAA-CAGCTCAATG
rs13477625	4	ACGTTGGATGTTGCT-CACTCAAAACCAGCC	ACGTTGGATGCCATGGT-GCAAGAAAAGAGC	CAGCCAAATTTCT-GTCTTCTTTCC
rs6234655	5	ACGTTGGATGTTTCA-CAGTCACACCTCTGC	ACGTTGGATGCATG-GATTGCAACTTGCCTC	TACACATACTCACTTC
rs30716377	6	ACGTTGGATGGGGAAG-GATATATTGAGCTG	ACGTTGGATGCAGCTCT-GCTATCAATGCC	CAATGCCCTCCTCA
rs13479101	7	ACGTTGGATGGACAAG-GCCACTTTTGAAG	ACGTTGGATGTCAACGT-GACCTTGACTTGC	ACTTTTGAAGAGTG-CAAACCGCCAGGCAG
rs13479815	8	ACGTTGGATGCATACAG-GCCTTTACTCAAC	ACGTTGGATG-GCTTGTTGCTTGTTTA-ATGC	CTTTACTCAA-CAATATCTTT
rs6313405	9	ACGTTGGATGTCCAT-TCTAGGTATGGTGAC	ACGTTGGATGTCATC-CCAGCTCTCCTTTAC	ATGGTGACCACATAATG-CATTATC
rs6208271	10	ACGTTGGATG-TAGCTTGTCCCCTCAGT-TAG	ACGTTGGATG-TACTTCATGTGGGAAG-ACAG	GCAGATGATAATAGGTAG
rs13481075	11	ACGTTGGATGGGTG-TAGTGGTTTTTGGAGG	ACGTTGGATGGAAA-GAGAAACCATCTCGGC	CGATACCTCTCCCAAA-GAGAACAC
rs13481497	12	ACGTTGGATGGACCTT-GAAGGCTCATAGTG	ACGTTGGATGCTGT-TATAGTACCAACAAGG	AAGAGTTAATGAAA-CAAAAGG
rs13481762	13	ACGTTGGATGAGT-TAGACCTGTGTAGGGAC	ACGTTGGATGTAATCT-CACTCTGGACTGGG	ATATATGCT-CACTTTCAACCAA
rs13482084	14	ACGTTGGATGTT-GAAACTAGCAAGTAG-CCG	ACGTTGGATGGAAGTTA-AAGAAACAGGAG	ACAGGAGTTGACAT
rs13482609	15	ACGTTGGATGGAAGAA-CAAGTGAGACGATG	ACGTTGGATGGTCAGCT-CACCTTTCAGTAG	ACGATGGTTTGTAATA
rs4217297	16	ACGTTGGATGGATA-AAAGCTGGAGTGACCG	ACGTTGGATGGACAATC-CGGCATACAGAG	CCAGTACCCTTTAGAA-CA
rs13482900	17	ACGTTGGATGTG-GCTTTTTGGTTGGTTCC	ACGTTGGATGCCAATCT-GTGGCAATAATAG	GTGATTAGGAAAACACT-TACAAAAA
rs13483256	18	ACGTTGGATGCACG-CAGCTATCATTCTTTG	ACGTTGGATGGACAGT-CAGAGTGTGGAAAG	CAAGACTCTG-CACTTGTTTCCAAGATGC
rs13483687	19	ACGTTGGATGGAAGT-GTCTGTCTCAACGTC	ACGTTGGATGCAGGGA-CATACATTACCCAC	ACGTCAGCGG-CAACTTCAGAA
rs13483842	X	ACGTTGGAT-GTTTCAGAAT-GTTCCTTGCC	ACGTTGGATGGCCA-GAGAAGAAGCAATAGG	TTCCTTGCCTTTTAAT-GAACTAGTAT

Table 2. Genotype frequencies for Mlac:ICR population (N = 306).

SNP ID	Chromosome	Allele	Genotype frequency (%)		
rs13476308	1	A/G	AA	AG	GG
			-	-	100
rs13476824	2	C/T	CC	CT	TT
			19.3	46.4	34.3
rs13477311	3	A/G	AA	AG	GG
			47	42.8	10.2
rs13477625	4	A/G	AA	AG	GG
			-	-	100
rs6234655	5	C/T	CC	CT	TT
			-	0.3	99.7
rs30716377	6	C/G	CC	CG	GG
			100	-	-
rs13479101	7	A/G	AA	AG	GG
			100	-	-
rs13479815	8	C/T	CC	CT	TT
			100	-	-
rs6313405	9	C/G	CC	CG	GG
			69.6	26.1	4.3
rs6208271	10	A/C	AA	AC	CC
		C/T	-	-	100
rs13481075	11		CC	CT	TT
		A/T	-	-	100
rs13481497	12		AA	AT	TT
		G/T	-	-	100
rs13481762	13		GG	GT	TT
		C/A	-	-	100
rs13482084	14		CC	CA	AA
		C/T	66.5	21.4	12.1
rs13482609	15		CC	CT	TT
		A/G	100	-	-
rs4217297	16		AA	AG	GG
		A/C	87.8	11.3	0.9
rs13482900	17		AA	AC	CC
		A/G	1.0	19.7	79.3
rs13483256	18		AA	AG	GG
		C/G	26.8	50.7	22.5
rs13483687	19		CC	CG	GG
		C/T	100	-	-
rs13483842	X		CC	CT	TT
			80.8	8.25	11

heights with strong signal-to-noise ratios, demonstrating the accuracy and reliability of the SNP detection process. Additionally, the genotyping data provided insights into allele frequencies and heterozygosity levels across the three generations of Mlac: ICR mice. The results demonstrated consistency in genetic variation, aligning with expectations for naturally bred, randomly mating outbred populations. These findings validate the utility of the selected SNP markers and the MassARRAY® platform for comprehensive genetic monitoring in outbred mice populations.

Table 3. Association analyses of the variants in heterozygosity population. [*Ho* (observed heterozygosity), *He* (expected heterozygosity), P_{HWE} (Hardy – Weinberg equilibrium test), and F_{IS} (inbreeding coefficient). The reported value of N/A indicates that the statistical calculation could not be performed.]

SNP ID	*Ho*	*He*	P_{HWE}	F_{IS}
rs13476824	0.46 ± 0.03	0.49 ± 0.03	0.35	0.24
rs13477311	0.43 ± 0.03	0.43 ± 0.03	0.90	0.25
rs6234655	0.01 ± 0.01	0.01 ± 0.01	1.00	1.00
rs6313405	0.26 ± 0.03	0.28 ± 0.03	0.10	0.28
rs13482084	0.21 ± 0.02	0.23 ± 0.02	0.20	0.42
rs4217297	0.11 ± 0.02	0.12 ± 0.02	0.13	0.37
rs13482900	0.20 ± 0.02	0.19 ± 0.02	1.00	0.32
rs13483256	0.51 ± 0.03	0.50 ± 0.03	0.82	0.23
rs13483842	0.12 ± 0.02	0.15 ± 0.02	0.06	N/A

Genotype frequencies

The SNPs including rs13476308, rs1347682, rs13477311, rs13477625, rs6234655, rs30716377, rs13479101, rs13479815, rs6313405, rs6208271, rs13481075, rs13481497, rs13481762, rs13482084, rs13482609, rs4217297, rs13482900, rs13483256, 13483687 and rs13484117 were genotyped in Mlac:ICR samples. Table 2 presents the allele and genotype frequencies for these SNPs. The SNPs rs13476308 and rs13477625, all genotypes across the three generations were homozygous GG genotypes. Similarly, rs1347901 consistently displayed a homozygous AA genotype. The rs30716377, rs13479815, rs13482609, rs13483867 and rs6208271 also showed homozygous CC genotype. The rs13481762, rs13481075 and rs13481497 were severally homozygous TT genotypes. In terms of heterozygosity, rs13476824 exhibited both TT and CC genotypes, resulting in a peak height ratio of CT. The rs13477311 displayed genotypes AA and GG, leading to a peak height ratio of GA. For rs13482084, the observed genotypes were AA and CC, with a peak height ratio of CA. Similarly, rs6313405 showed GG and CC genotypes with a peak height ratio of CG. The rs4217297 revealed AA and GG genotypes, resulting in a peak height ratio of GA. The genotypes for rs13482900 were AA and CC, corresponding to a peak height ratio of CA. The rs13483842 exhibited TT and CC genotypes, with a peak height ratio of CT. Lastly, rs13483256 showed AA and GG genotypes, leading to a peak height ratio of GA. The rs6234655 demonstrated a distribution of genotyping frequencies of 99.7% TT and 0.3% CT. Overall, the genotyping frequencies for rs13476308, rs13477625, rs30716377, rs13479101, rs13479815, r6208271, rs13481075, rs13481497, rs13481762, rs13482609, rs13473687 indicated a predominance of homozygous genotypes. Conversely, rs13476824, rs13477311, rs6234655, rs6313405, rs13482084, rs4217297, rs13482900, rs13483256 and rs13483842 exhibited heterozygosity within the studies population. The samples were grouped based on genotyping frequencies, and the results were analyzed across different generations for each SNP. The results are illustrated in Fig 2.

Statistical analysis

A total of nine SNPs and 306 samples were subjected to genotyping quality control. All SNPs and samples exhibited a 100% call rate, and therefore, no markers or individuals were excluded. The retained dataset provided a complete genotyping profile. Replicate concordance among technical duplicates ranged from 0–1, indicating high reliability and internal consistency of the genotyping data. PCA based on PC1 through PC3 demonstrated that samples were broadly dispersed across all three axes, indicating notable genetic variability within the dataset. The first three PCs explained 18.28%, 16.39% and 13.43% of the total genotypic variance, respectively. PCA plots showed a relatively scattered sample distribution, with most samples forming a diffuse cluster (Fig 3). A few samples fell outside this main cluster, representing outlying genotypic profiles. These patterns reflect underlying variability within the dataset rather than well – defined population substructure. Genetic parameters calculated from the SNP markers were summarized in Table 3. All nine SNPs exhibited $P_{HWE} > 0.05$, indicating that observed genotype frequencies did not significantly deviate from Hardy – Weinberg equilibrium. The overall observed heterozygosity (*Ho*) was comparable to expected heterozygosity (*He*), resulting in an inbreeding

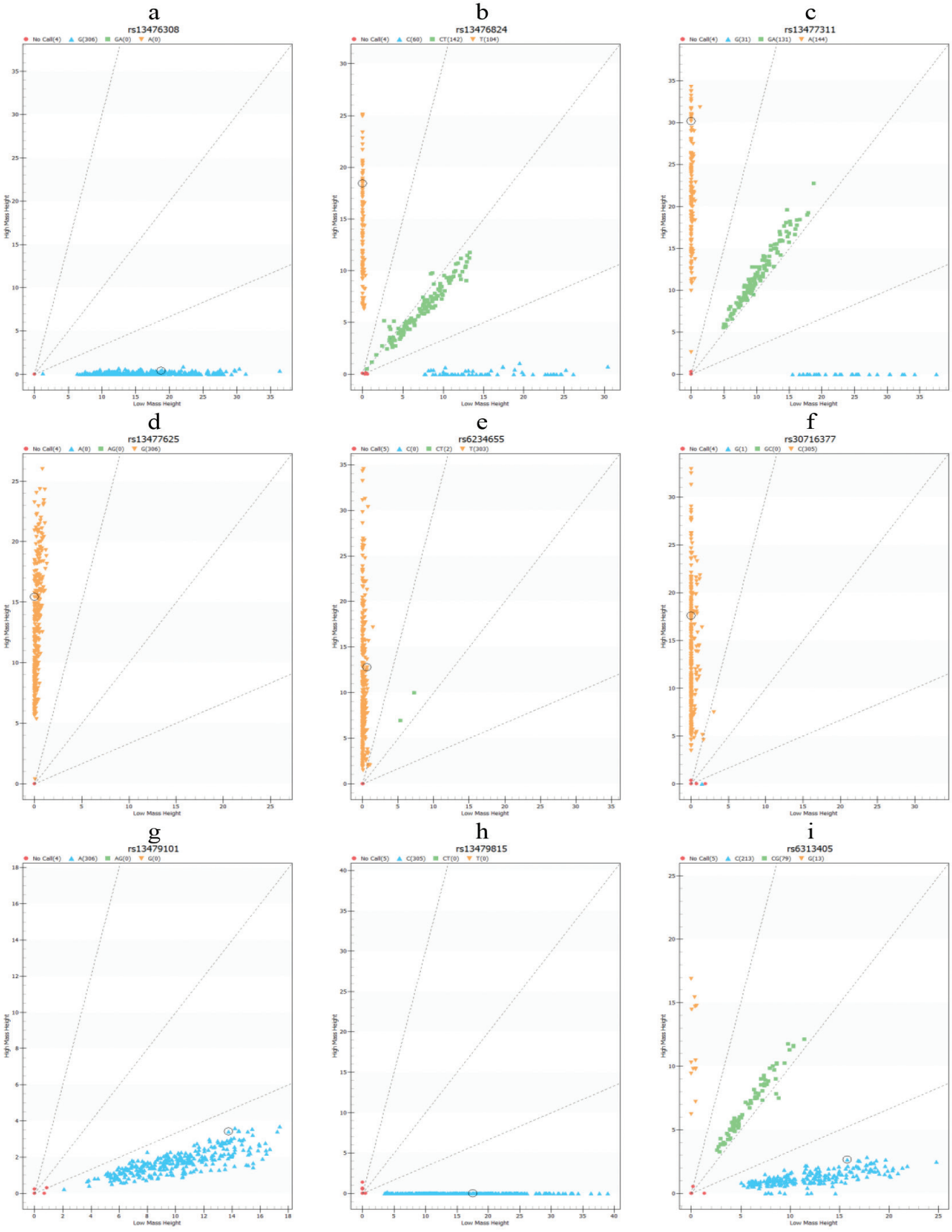

Fig. 1. Distribution of genotype calls from TYPER 4.0 software analysis. a – t show difference SNP detection. [Red spot represents No alleles, orange and blue spot represent homozygous allele and green spot represents heterozygous alleles.]

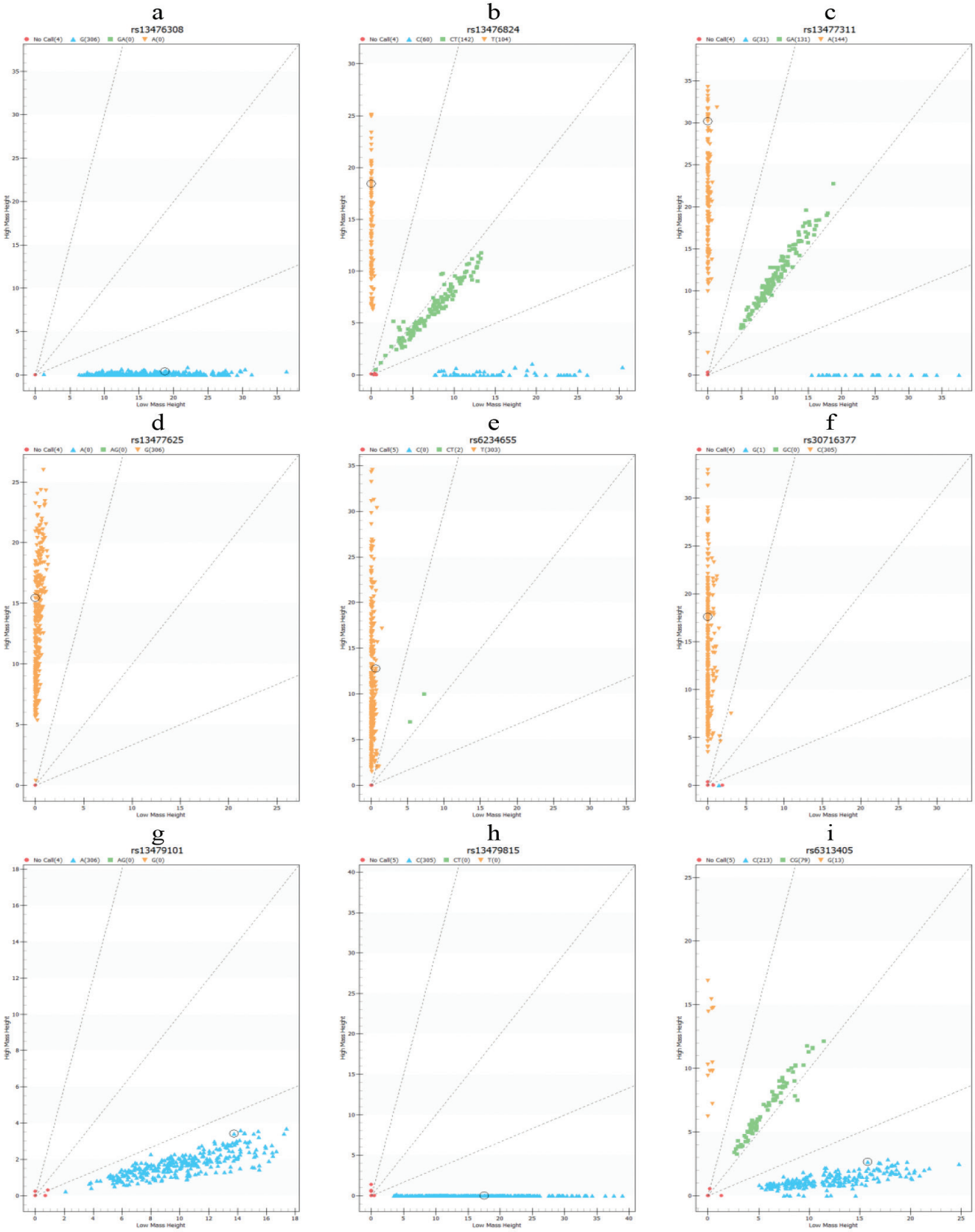

Fig. 1. (continued) Distribution of genotype calls from TYPER 4.0 software analysis. a – t show difference SNP detection. [Red spot represents No alleles, orange and blue spot represent homozygous allele and green spot represents heterozygous alleles.]

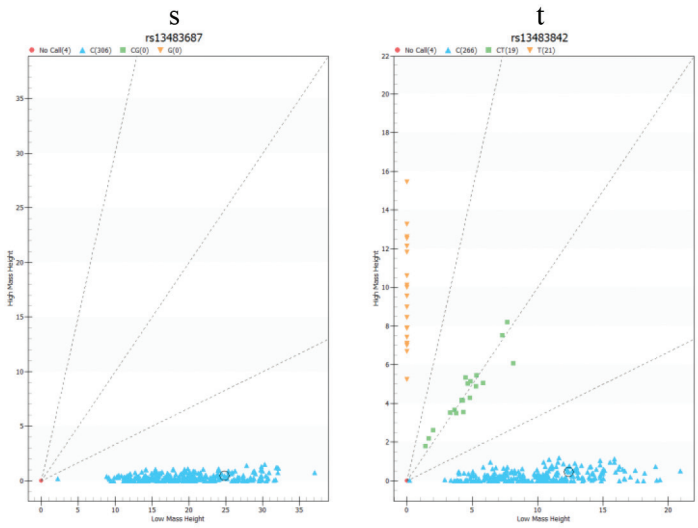

Fig. 1. (continued) Distribution of genotype calls from TYPER 4.0 software analysis. a – t show difference SNP detection. [Red spot represents No alleles, orange and blue spot represent homozygous allele and green spot represents heterozygous alleles.]

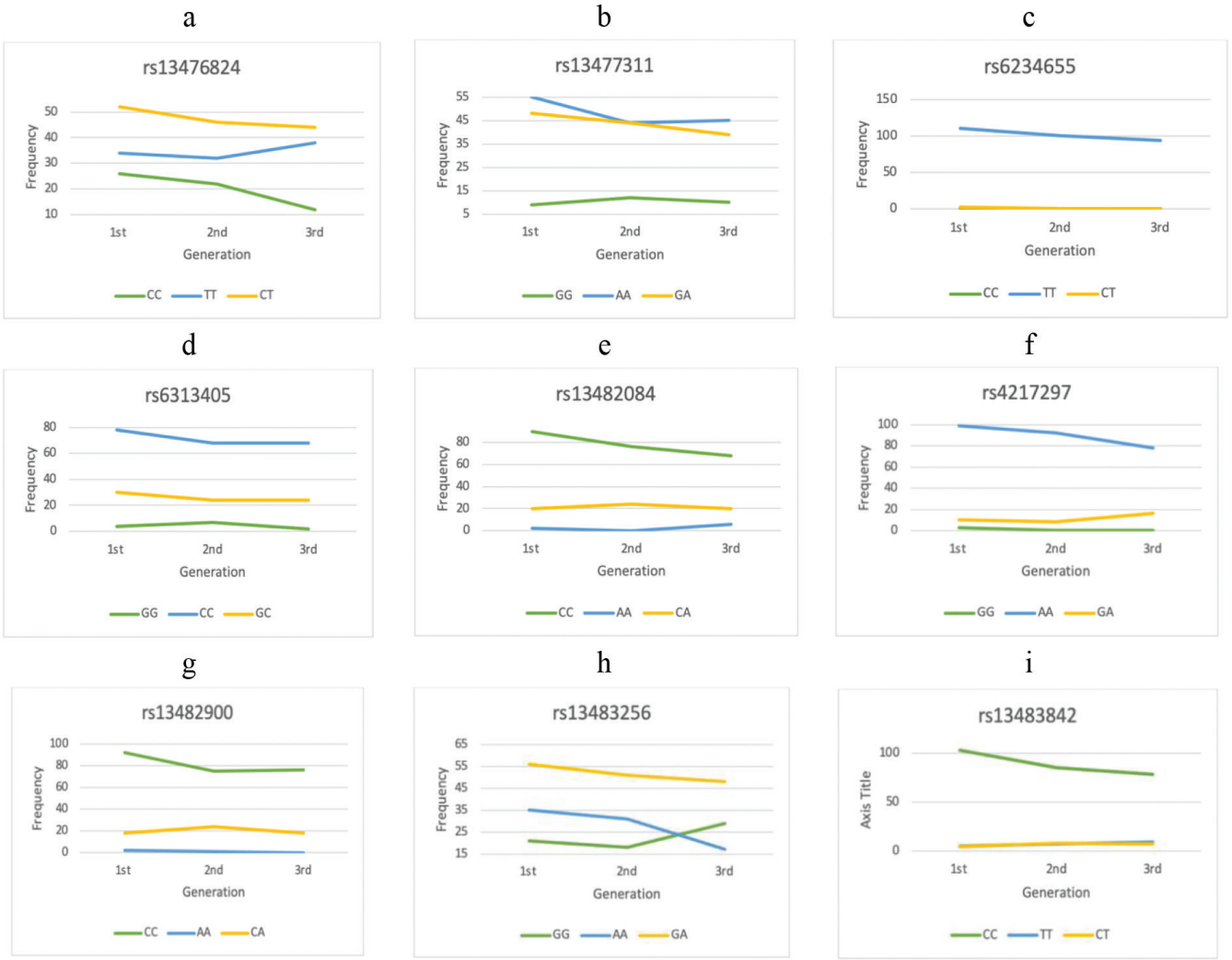

Fig. 2. Frequency of population between 1st, 2nd and 3rd generation in different genotypes of SNPs studies. a – i show difference SNP detection.

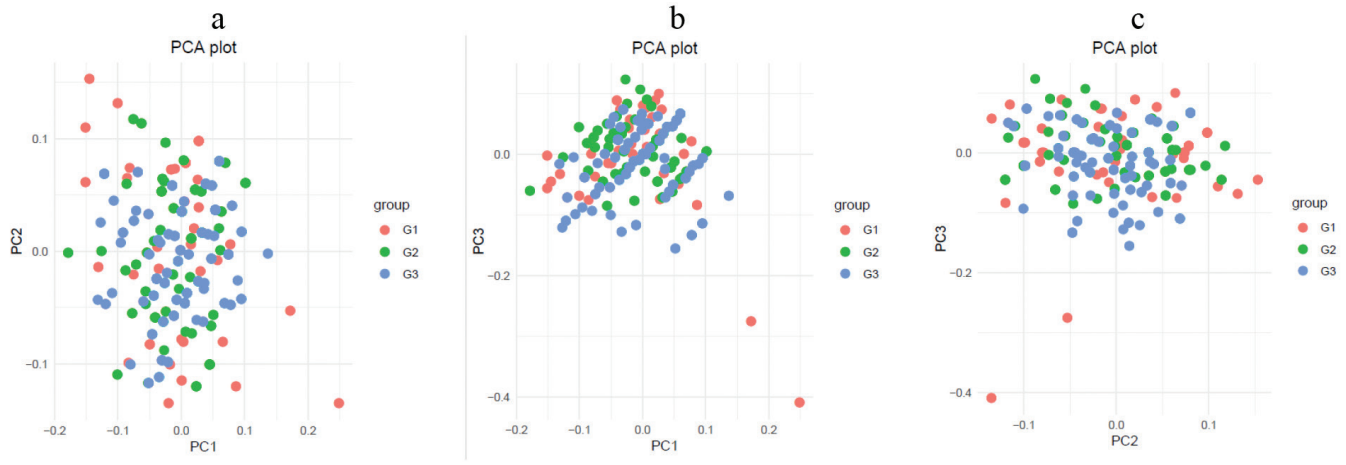

Fig. 3. Pairwise PCA scatter plots showing sample distribution along PC1 (18.28%), PC2 (16.39%) and PC3 (13.43%). a – c show PC1 vs PC2, PC1 vs PC3 and PC2 vs PC3 respectively.

coefficient (F_{IS}) of positive values for all loci. This positive F_{IS} value indicates a lower of heterozygotes in the population, suggesting high levels of inbreeding in population.

CONCLUSION

The study successfully applied a Single Nucleotide Polymorphism (SNP) – based approach to characterize the genetic background of ICR outbred mice maintained at the National Laboratory Animal Center, Mahidol University (Mlac:ICR). By utilizing twenty SNP markers distributed across all autosome and the X chromosome, the genetic quality and population structure of the Mlac:ICR stock were systematically evaluated across three generations. Genotyping was performed using the Sequenom MassARRRAY® platform integrated with matrix–assisted laser desorption/ionization time–of–flight mass spectrometry (MALDI–TOF MS), a robust and high–throughput technology that demonstrated exceptional accuracy, sensitivity, and efficiency, achieving genotyping call rates of 94–100%. Of the twenty analyzed SNPs, nine markers exhibited heterozygous genotypes, providing informative loci for assessing genetic variation. Statistical analyses confirmed that all nine loci were in Hardy – Weinberg equilibrium ($P_{HWE} > 0.05$), indicating the absence of genotyping bias, population stratification, or selection pressure. Principal component analysis (PCA) further supported these findings, revealing a coherent yet dispersed clustering pattern that reflected natural genetic variability without strong sub - structuring within the population.

Although the dataset exhibited a slight excess of homozygosity, as indicated by positive inbreeding coefficient (F_{IS}) values, this trend was not statistically significant and may reflect early signals of genetic drift or limited breeding diversity. The results emphasize the importance of ongoing genetic monitoring to preserve heterozygosity and maintain the genetic integrity of outbred colonies such as Mlac:ICR. The combination of multiplex PCR with MALDI – TOF MS genotyping proved to be a highly effective strategy for detecting genetic impurity, monitoring populations structure, and ensuring the authenticity of laboratory mouse stocks. In conclusion, the selected panel of polymorphic SNPs and the MassARRAY® genotyping system together establish a powerful and reproducible framework for routine genetic quality control in outbred mice. These findings provide a strong foundation for refining genetic monitoring strategies, enhancing colony management practices, and supporting the sustainable production of genetically diverse and reliable animal models for biomedical research.

ACKNOWLEDGMENT

This work was supported by the National Vaccine Institute as part of the Development of Monitoring Program for Laboratory Animal Quality to Support Vaccine Production (Grant No. 2566.4/1). We also thank the Mahidol University Frontier Research Facility: MU – FRF for the MassARRAY® system (Agena Bioscience, model CPM96) support.

REFERENCES

1. Hartl DL. A primer of population genetics and genomics. Oxford: Oxford University Press; 2020.

2. Benavides F, Rülicke T, Prins JB, Bussell J, Scavizzi F, Cinelli P, *et al*. Genetic quality assurance and genetic

monitoring of laboratory mice and rats: FELASA Working Group Report. Laboratory Animals. 2019; 54(2): 135–48, DOI: 10.1177/00236772198677 19.

3. Wigginton JE, Cutler DJ, Abecasis GR. A Note on Exact Tests of Hardy-Weinberg Equilibrium. The American Journal of Human Genetics. 2005; 76(5): 887–893, DOI: 10.1086/429864.

4. Nomura T. Concept for Establishment of Rat Outbred Global Standard Strains. 2000.

5. Trick M, Long Y, Meng J, Bancroft I. Single nucleotide polymorphism (SNP) discovery in the polyploid Brassica napus using Solexa transcriptome sequencing. Plant Biotechnology Journal. 2009; 7(4): 334–346, DOI: 10.1111/j.1467-7652.2008.00396.x.

6. Lindblad-Toh K, Winchester E, Daly MJ, Wang DG, Hirschhorn JN, Laviolette JP, *et al*. Large-scale discovery and genotyping of single-nucleotide polymorphisms in the mouse. Nature Genetics. 2000; 24(4): 381–386, DOI: 10.1038/74215.

7. Wade CM, Kulbokas EJ, Kirby AW, Zody MC, Mullikin JC, Lander ES, *et al*. The mosaic structure of variation in the laboratory mouse genome. Nature. 2002; 420(6915): 574–8, DOI: 10.1038/nature 01252.

8. Grupe A, Germer S, Usuka J, Aud D, Belknap JK, Klein RF, *et al*. In Silico Mapping of Complex Disease-Related Traits in Mice. Science. 2001; 292(5523): 1915–8, DOI: 10.1126/science.1058889.

9. Bryda EC, Riley LK. Multiplex microsatellite marker panels for genetic monitoring of common rat strains. PubMed. 2008.

10. MIURA I, KIKKAWA Y, YASUDA SP, SHINOGI A, USUDA D, KUMAR V, *et al*. Characterization of single nucleotide polymorphisms for a forward genetics approach using genetic crosses in C57BL/6 and BALB/c substrains of mice. Experimental Animals. 2021.

11. Gabriel S, Ziaugra L, Tabbaa D. SNP Genotyping Using the Sequenom MassARRAY iPLEX Platform. Current Protocols in Human Genetics. 2009; 60(1), 10.1002/0471142905.hg0212 s60.

12. Jurinke C, Denissenko MF, Oeth P, Ehrich M, van den Boom D, Cantor CR. A single nucleotide polymorphism based approach for the identification and characterization of gene expression modulation using MassARRAY. Mutation Research/Fundamental and Molecular Mechanisms of Mutagenesis. 2005; 573(1-2): 83–95, DOI: 10.1016/j. mrfmmm.2005.01. 007.

13. Shi Y, Xiang P, Li L, Shen M. Analysis of 50 SNPs in CYP2D6, CYP2C19, CYP2C9, CYP3A4 and CYP1A2 by MALDI-TOF mass spectrometry in Chinese Han population. Forensic Science International. 2011; 207(1-3): 183–7, DOI: 10.1016/j. forsciint.2010.10.004.

14. Johansen P, Andersen JD, Børsting C, Morling N. Evaluation of the iPLEX® Sample ID Plus Panel designed for the Sequenom MassARRAY® system. A SNP typing assay developed for human identification and sample tracking based on the SNP for ID panel. Forensic Science International: Genetics. 2013; 7(5): 482–7, DOI: 10.1016/j. fsigen.2013.04.009.

15. Sharma R, Sharad S, Minhas G, Sharma DR, Bhatia K, Sharma NK. Chapter 12 - DNA, RNA isolation, primer designing, sequence submission, and phylogenetic analysis [Internet]. Bhatt AK, Bhatia RK, Bhalla TC, editors. ScienceDirect. Academic Press; 2023. p. 197–206. Available from: https://www.sciencedirect.com/science/article/abs/pii/B978012816109800012X.

16. Yamamoto M, Hayashimoto N, Takahashi R, Seumizu H. Genetic profiles of inbred mice with the SNP analysis. Poster presentation (J-stage) May 25.

17. Utsunomiya YT, Alonso RV, Santana A, Campagnari F, José Antonio Vinsintin, Garcia JF. mendel Fix: a Perl script for checking Mendelian errors in high density SNP data of trio designs. arXiv (Cornell University). 2013 Jun 10.

18. Charlesworth B. Principles of Population Genetics. 3rd edition (1993-re-issued 1997). By Daniel L. Hartl and Andrew G. Clark. Sunderland, MA: Sinauer 519 pp. BioEssays. 1999 Jan 14;20(12):1055–5.

19. Hill WG, Mackay TFC. D. S. Falconer and Introduction to Quantitative Genetics. Genetics. 2004; 167(4): 1529–36, DOI: 10.1093/genetics/167.4.1529.

20. Slifer SH. PLINK: Key Functions for Data Analysis. Curr Protoc Hum Genet. 2018; 97(1): e59, DOI: 10.1002/ cphg.59. PMID: 30040203.

21. R Development Core Team (2023). R: A language and environment for statistical computing, reference index version 4.3.1 (Vienna, Austria: R Foundation for Statistical Computing;). Available at: http://www.R-project.org.

Cite this article as: Phumkumarn N, Tangkhabuanbutra J, Hirunpatrawong P, Chariyahpongpun P. Single nucleotide polymorphisms approach for genetic background of ICR mice using massarray. Explor Anim Med Res. 2026; 16(1), DOI: 10.52635/eamr/16.1.28-39.

Explor Anim Med Res.
Vol. 16, Issue 1, 2026
DOI: 10.52635/eamr/16.1.40-45

ISSN 2277-470X (Print), ISSN 2319-247X (Online)
Website: www.animalmedicalresearch.org

Published under the CC BY-NC 4.0 license

Research Article

DETECTION OF SINGLE NUCLEOTIDE POLYMORPHISM USING TARMS-PCR IN *TLR*2 GENE IN LOCAL CATTLE OF JAMMU

Komal Deep Kour, Dibyendu Chakraborty[1*], Nishant Kumar[1], Biswajit Brahma, Vidushi Sharma[1], Aakriti Sudan[1] and Soshthi Talwar[1]

Received 21 May 2025, revised 28 April 2026

ABSTRACT: The local cattle of Jammu is one of the unique cattle which belongs to hilly areas of Jammu. A major group of Pattern recognition receptors (PRRs) are the Toll like receptors (*TLR*s) which play a very important role in immunity of the animal. Therefore, the study was aimed to detect the polymorphism in *TLR*2 gene. The genomic DNA was isolated from blood samples of 50 unrelated local cattle of Jammu from different locations.Tetra primer amplification refractory mutation system- polymerase chain reaction (TARMS-PCR) using self-designed primers was performed to detect the SNPs. TARMS-PCR for *TLR2* revealed three bands on gel (158 bp control fragment, 120 bp B allele, 100 bp A allele). The genotypic frequencies for AA, AB and BB genotypes and allele frequency of A and B alleles were 0.12, 0.64 and 0.24, 0.44 and 0.56, respectively. The calculated observed number of alleles (n_a), effective number of alleles (n_e), observed homozygosity (H_o), expected heterozygosity (H_e), Shannon's information index (I),Wright'sfixation index (F_{IS}), PIC values were 2.00, 1.9716, 0.5022, 0.497, 0.6859,-0.2987, 0.3713, respectively. The $\chi 2$ and G^2 values for genotypes were significant. From the present study it can be concluded that there are substantial genetic variations and heterozygosity present within the local cattle population of Jammu province, which can be explored to formulate the effective breeding policies for genetic improvement, propagation and conservation of this important local cattle population.

Key words: Local Cattle, *TLR*2, TARMS-PCR, Heterozygosity, PIC, F_{IS}

INTRODUCTION

Local cattle of Jammu is one of the unique cattle which belongs to hilly areas of Jammu like Poonch, Rajouri, Ramban, Reasi, Banihal etc. They are very popular for their strength to adopt and withstand a wide range of local climatic conditions of the hilly terrain and play significant role in contributing to the local economy and livelihood security to its owners by way of providing milk, draught power and manure with minimum or zero input. Local cattle are found resistant to many diseases as compared to crossbred cattle and have the ability to withstand stressful environmental conditions [1]. The ability of a dairy cow to resist contagious disease is in part related to the activity of its immune system which consists of a variety of mechanisms and processes which are capable of both non-specifically and specifically targeting invading microorganisms [2].

Pattern recognition receptors (PRRs) are known to play an important role in the innate or nonadaptive immune response as they detect the presence of pathogens that breach an animal's surface defenses [3]. A major group of PRRs are the Toll like receptors (TLRs) which play very important role in immunity of the individual. TLR2 can sense specific structures expressed by pathogens, such as bacteria and fungi. These structures include pathogen-associated molecular patterns (PAMPs) and some endogenous ligands. The TLRs consist of a large extracellular domain responsible for PAMP binding, a transmembrane domain and an intracellular Toll/interleukin-1 receptor (TIR) domain which binds molecules and initiates cellular immune responses [4]. The extracellular domains are composed of about 20 leucine-rich repeats (LRRs) motifs of 20–30 amino acids (AA) and form a solenoid shape with the potential to bind the TLR specific PAMP [5]. After pathogen-associated molecular patterns (PAMP) recognition, TLRs activate cellular signaling pathways to induce immune response genes, including

[1]*Division of Animal Genetics & Breeding, FVSc&AH, SKUAST-Jammu, R. S. Pura, Jammu-181102, J&K, India*
[2]*Division of Livestock Production Management, FVSc&AH, SKUAST-Jammu, R. S. Pura, Jammu-181102, J&K, India*
**Corresponding author. e-mail: dibyendu_vet40@yahoo.co.in*

inflammatory cytokines [6]. Ten different Toll-like genes have been identified within the cattle genome. Among them TLR2 has been first identified as antibacterial molecule that recognizes peptidoglycan of grampositive bacteria which is activated inside the phagosome by peptidoglycans [7]. It was reported that the expression of *TLR2* gene strongly increased in different body tissue following infection in cattle [8].Toll-like receptors (TLRs) are important pattern recognition receptors and are widely expressed on the surfaces of innate immune system cells, such as monocytes and macrophages. More than 10 family members of TLRs have been identified [9] since the discovery of the first TLRs in humans [10]. *TLR*2 proteins can transmit pathogenic microorganism invasion signals, activate innate immune response generation and further induce adaptive immune response [11,12]. *TLR*2 can combine with *TLR*1 or *TLR*6 to form heterodimers, which can recognize the peptidoglycan, phosphoprotein acid and lipoprotein of Gram-positive bacteria [13]. Moreover, *TLR*2 can induce interleukin-1β production through the NF-κb pathway [14]. *TLR2* gene is located on chromosome 17 and has 2355bp long DNA. It has 6 exons.It codes a protein having 784 amino acids. Therefore, the present study was undertaken to detect the SNPs in *TLR2* gene which may be used as the main candidate gene for genetic variation studies and marker-assisted disease resistance breeding.

MATERIALS AND METHODS

Isolation of the genomic DNA and its preliminary analysis

A total of fifty (50) unrelated indigenous native cattle of Jammu region were selected randomly from natural breeding tracts i.e. different remote areas of districts of Jammu namely Poonch, Rajouri, Ramban, Doda, Udhampur. Blood samples were collected aseptically from jugular vein in 15 ml centrifuge tubes coated with 0.8MEDTA and stored at 4◦C for future use. Genomic DNA isolation was carried out by phenol-chloroform isoamyl (PCI)method.The concentration and purity of DNA was checked on Nano-drop. Samples with OD ratio from 1.7 to 1.9 were used for further study. 0.8% agarose gel was used for checking quality of DNA. The gel was photographed by UV transilluminator.

Retrieval and analysis of *TLR2* gene sequences of local cattle

The complete gene sequences of *TLR2* gene available on NCBI GenBank database [15] were retrieved for determining the consensus sequence and presence of single nucleotide polymorphisms (SNPs). Retrieved *TLR2* gene sequences of different cattle wereanalyzed for multiple sequence alignment through ClustalW Multiple alignment programme of BioEdit [16] Sequence Alignment Editor Version 7.0.

Primer Designing and TARMS PCR

The primers for TARMS PCR were designed using BioEdit software and designated as forward inner primer (FIP), reverse inner primer (RIP), forward outer primer (FOP) and reverse outer primer (ROP) as followsOuter forward 5′-ATTCCAGATCTTTAAACTC CATCCCCTCTGG-3′; 3′- Outer reverse CACTGTGTG AATTTCATTGGCCCCCAGC- 5′; 5′- Inner forward ACCTGTCCAACAACGAGATCACCTATGTCA- 3′; 3′- Inner reverse CACACCTCTGCAGGTCTCTGT TG CC-5′. TARMS-PCR reaction mixture was prepared for 15 µl comprising of master mix 6µl**,**template4µl, Outerforward primer 0.5µl, Outer reverse primer 0.5µl, Inner forward primer 1 µl, Inner reverse primer 0.5µl and distilled water 2.5µl.

PCR Amplification

Amplification reactions were carried out in Biorad thermal cycler, USA under optimized conditions which are as follows: Initial denaturation step at 95°C for 3 minutes followed by 30 cycles of cyclic denaturation at 95°C for 30 seconds, annealing at 64°C for 30 seconds, extension at 72°C for 40 seconds and final extension at 72°C for 5 minutes.

Checking of PCR product

The amplified PCR products were then checked on 3% agarose gel along with 50bp DNA ladder to know the exact size of the band.

Statistical analysis

Genotyping was done. Statistical analysis was performed using PopGene software [17] to calculate allele frequency, observed number of alleles (n_a), effective number of alleles (n_e) [18], Shannon's informative index (I) [19], observed heterozygosity (H_o), expected heterozygosity (H_e)[20],Polymorphic Information Content (PIC) and Wright's fixation indices (F_{IS}) [21]**.** Ewens-Watterson Test for neutrality was also done.

RESULTS AND DISCUSSION

DNA isolation and PCR amplification

DNA isolation was done from the venous blood samples using PCI method of isolation. Good quality bands of DNA were obtained without smearing and

Table 1: Genotype distribution and allelic frequencies at the *TLR2* gene in local Cattle population.

Locus	Genotypes			Gene/Allele		χ^2-test (HWE)	p-Value	G^2-test (HWE)	p-Value
	A/A	A/B	B/B	A	B				
TLR2	0.12 (06)	0.64 (32)	0.24 (12)	0.44	0.56	4.17	0.0412	4.27	0.0387

Figures in parentheses are number of observations.

Table 2: Summary of genetic variation statistics of *TLR2* gene in local cattle population.

Locus	n_a	n_e	I	F_{IS}
TLR2	2.00	1.97	0.6859	-0.2987

- n_a = Observed number of alleles
- n_e = Effective number of alleles [Kimura and Crow (1964)] [18]
- I = Shannon's Information index by Lewontin (1972), [19]
- F_{IS} = Fixation index of individual with sub-population by Wright's (1978) [21]

haziness on 0.8% agarose gel when viewed under UV trans-illuminator as shown in Fig 1. PCR amplification was carried out for *TLR2* genes at temperature of 64°C for 0.30sec.

TARMS PCR (Tetra amplification refractory mutation system) successfully amplified different genotypes amplicons thereby detecting SNP at 201 bp (G to A).The amplified DNA revealed 3 bands of 158bp (control fragment),120 bp (B allele) and 90bp (A allele) as shown in Fig 2. T-ARMS PCR is a relatively fast and inexpensive method for SNP genotyping. The method requires only a single PCR amplification followed by gel electrophoresis, making it relatively simple to perform. T-ARMS PCR can accurately distinguish between different genotypes, even with small amounts of DNA and can be used to genotype various SNPs in different species.

Genotype distribution and allelic frequencies at the *TLR2* gene

Genotypic distribution and allelic frequencies presented in Table 1 revealed that there are heterozygosity present in the population for *TLR*2 gene. The genotype frequencies were 0.12, 0.64 and 0.24 for AA, AB and BB genotypes, respectively. Heterozygous frequency is maximum in the population. B allele (0.56) was predominant over the A allele (0.44) in the studied population. Polymorphisms in *TLR*2 gene was reported for G and T alleles in cattle population [22], in TLR2 promoter and coding region were reported in six different cattle breeds of China using PCR-RFLF and CRS-PCR (Created Restriction Site-PCR) methods [23], HF cross bred cattle using PCR-SSCP method [24], Vietnamese Holstein Cattle [25] and crossbred cattle in India [26]. On the other hand, monomorphic *TLR*2 gene was reported in Canadian Holstein cattle [27], Italian native cattle [28]. The highest frequency of the $TLR2^T$ allele (0.99) was found in the Ayrshire breed. The herd of Ayrshire cows is close to being monomorphic for the *TLR2* gene; 98% of the animals have the homozygous $TLR2^{TT}$ genotype [29]. Similar genotype frequencies (0. 157, 0.605 and 0.236 for AA, AB and BB, respectively) and allele frequencies (0.460 for A and 0.539 for B) were reported in mastitis affected cattle [26], whereas, higher frequencies for AA genotype (0.392) and A allele (0.514) were reported in mastitis tolerant group [26]. Lower heterozygous genotype frequencies were reported in HF cross bred cattle for TLR 2 gene [24]. The allelic frequency of A and B allele were 0.5 and the genotypic frequency of the AB genotype is 1.00 without any homozygous genotype [30].In the studied population heterozygosity was more than that of the homozygosity indicates that individuals carrying different alleles which can impact the function of the TLR2 protein, potentially altering its ability to recognize and respond to pathogens.

χ^2-test and G^2-test statics in Table 1 showed significant effect ($p<0.05$) which indicates population is not in Hardy Weinberg equilibrium and evolutionary forces have acted in population. Deviation from Hardy Weinberg equilibrium might be due to use of a smaller number of breeding bulls in the population or introduction of other inheritance from the different population.Similarly,$\chi 2$ values showed a highly significantdeviation from HW equilibrium probabilitiesfor TLR2 genotypes in HF crossbred cattle [24]. On contrary, non-significant ($p> 0.05$) genotype frequencies of 15 SNPs fitted with the Hardy-Weinberg equilibrium in HF breed in China were reported [31].

Summary of genetic variation statistics of *TLR2* gene

The observed number of alleles (n_a) and effective number (n_e) of alleles for *TLR2*were 2.00 and. 1.97, respectively in local cattle of Jammu (Table 2). Lower

Table 3: Summary of Heterozygosity Statistic of *TLR2* gene in local cattle population.

Locus	Obs_Ho	Obs_He	Ho	He	Nei**	Ave_Het	PIC
TLR2	0.535	0.465	0.535	0.465	0.4928	0.4928	0.3713

- Obs_Ho = Observed homozygosity
- Obs_He= Observed heterozygosity
- Ho = Expected homozygosity,
- He = Expected heterozygosity (Levene, 1949), [20]
- ** Nei's (1973) expected heterozygosity
- Ave_Het = Average Heterozygosity
- PIC = Polymorphic information content

Table 4: Ewens-Watterson Test for neutrality of *TLR2* gene in local cattle population.

Locus	Obs. F	Min. F	Max. F	Mean	SE	L95	U95
TLR2	0.5072	0.5000	0.9802	0.8125	0.0272	0.5018	0.9802

- F- F-values.
- L95-Lower confidence limits at 95% confidence.
- U95-Upper confidence limits at 95% confidence.

estimate of n_e value was also reported in HF crossbred cattle [24].

Shannon index (I) in the studied population was 0.6859. Shannonindex value indicates the genetic diversity within a population. Specifically, it measures the allelic diversity i.e.how many different alleles are present at a locus and how evenly their frequencies are distributed. Lower Shannon index (I) values were estimated in HF crossbred cattle for different *TLR*2 SNPs [24].

Negative F_{IS} values (-0.2987) depicted in Table 2 indicates the heterozygosity excess in the population. It means there is more genetic diversity in population and less inbreeding has occurred. The negative F_{IS} value might be due to introduction of genetically dissimilar partners or admixture of populations. Higher values of F_{IS} were reported in different SNPS in *TLR*2 gene in HF crossbred cattle [24].

Summary of Heterozygosity Statistic of *TLR2* gene

For *TLR2* gene in the present study observed and expected homozygosity value was 0.535, observed and expected heterozygosity value was 0.465 and average heterozygosity was 0.4928, respectively (Table 3). The results show no overall loss of heterozygosity. The result indicates genetic diversity in the population. However, lower observed heterozygosity compared to expected heterozygosity were reported in different SNPS in *TLR*2 gene in HF crossbred cattle [24]. Observed heterozygosity (Ho) and Expected heterozygosity (He) of the loci determined from SNP frequencies ranged from 0.051 to 0.466 and from 0.060 to 0.493, respectively in cattle [32]. On the other hand, observed heterozygosity was reported to be 1.0 in Malnad Gidda cattle [30].

Nei's expected heterozygosity 0.4928 means that there is a 49.28% chance that two alleles randomly selected from the population are not the same. This reflects a moderate level of genetic variation in the population.The polymorphism information content (PIC) was 0.3713 (Table 3) showing diversity in the population.Nei's expected heterozygosity and PIC value indicates moderate level of genetic diversity within the population. Higher estimate of PIC value was reported in Malnad Gidda cattle [30]. However lower to similar PIC values were reported in cattle ranged from 0.058 to 0.372 [32].

Ewens-Watterson Test for neutrality of *TLR2* gene

Ewen Watterson test for neutrality showed F value of 0.5072 (Table 4) which is very close to lower bound (0.5018) of 95% confidence interval. Since observed F is within the confidence interval (within the range of L95-U95) it shows *TLR2* gene in consistent with neutrality. The non-significant Ewens-Watterson test suggests that the observed allele frequencies conform to expectations under neutral evolution. Therefore, no strong evidence of selection acting on this locus was detected. *TLR*2 is an immune gene often associated with disease resistance (and sometimes under selection). But the result shows that there might not be any current selective pressure which reflects the stable environment, low pathogen exposure, or historic balancing selection

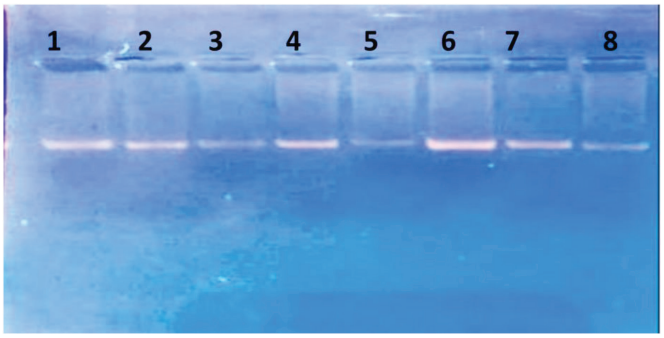

Lane: 1-8 diluted DNA
Fig1: DNA bands 0n 0.8% Agarose gel

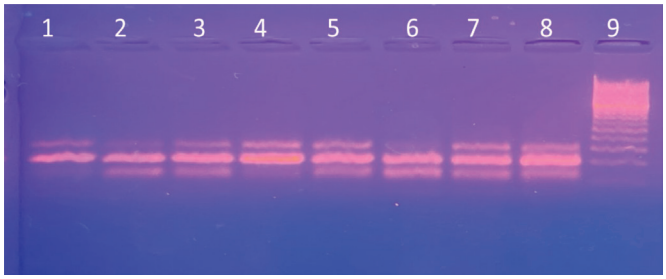

Lane 1, 4: B/B
Lane 2, 6: A/A
Lane 3, 5, 7 8: A/B
Lane 9: 50 bp DNA ladder
Fig 2: Genotyping after TARMS PCR

that has now stabilized. However, the fact that observed F is much lower than mean (0.8125) might suggest some deviation from neutrality probably indicating balancing selection, admixture, or gene flow.

However, the fact that observed F is much lower than mean (0.8125) might suggest some deviation from neutrality probably indicating balancing selection, admixture, or gene flow.

The functional details and prediction for structural model for *TLR2* in chicken model has been described earlier [33] and need to be undertaken in cattle breed.

CONCLUSION

The results from the present study showed polymorphic nature of *TLR2* gene in local cattle of Jammu that shows moderate level of genetic variation in the population and *TLR2*gene can be used for genetic improvement and marker assisted selection for disease resistance.

ACKNOWLEDGEMENT

Authors are highly thankful to the farmers for allowing to collect the samples of local cattle.

REFERENCES

1. Das DN, Rao MK, Shrihari VG, Reddy AO, Murthy, LK. Characterization of natural resistance associated macrophage protein (NRAMP1) partial gene in Malnad Gidda cattle. I J Anim Scie. 2009; 79(7):720-721.

2. Ingvartsen KL, Moyes K. Nutrition, immune function and health of dairy cattle. Anim Genet. 2013; 7:112-122.

3. Janeway CA, Medzhitov R. Innate immune recognition. Ann Rev Immunol, 2002;20: 197–216.

4. Muzio M, Polentarutti N, Bosisio D, Prahladan MK, Mantovani, A. Toll-like receptors: a growing family of immune receptors that are differentially expressed and regulated by different leukocytes. J Leukocyte Biol. 2000; 67: 450-456.

5. Jin MS, Kim SE, Heo JY, Lee ME, Kim HM, Paik SG, Lee H, Lee JO. Crystal structure of the TLR1-TLR2 heterodimer induced by binding of a tri-acylated lipopeptide. Cell. 2007;130: 1071-1082.

6. Medzhitov R, Janeway C. Innate immunity: impact on the adaptive immune response. N Engl J Med. 2000; 343:338-44.

7. Campos MA, Almeida IC, Tacheuchi O, Akira S, Valenta EP, Procopio DO, Travossos LR, Golenbock DT, Gazzinelli RT. Activation of Toll like receptor-2 by glycosyl phosphatidylinositol anchors from a protozoan parasite. J Immunol.2001; 167: 416- 423.

8. Goldammer T, Zerbe H, Molenaar A, Schuberth HJ, Brunner RM, KataSR, Seyfert, HM. Mastitis Increases Mammary mRNA Abundance of Defensin 5, Toll- Like-Receptor 2 (TLR2), and TLR4 but Not TLR9 in Cattle. Clinic Diag lab immunol.2004; 11:174–185.

9. Wang J, Li Y, Jiang Q, Wang, L. Research progress of Toll-like receptors and their agonists. Prog Phys Sci. 2018; 49(04): 289-292.

10. Medzhitov R, Preston-Hurlburt P, Janeway CA. A human homologue of the Drosophila Toll protein signals activation of adaptive immunity. Nat.1997; 388 (6640): 394-397.

11. Lin B, Lan D, Huang C, ChenY, Huang Y, Li J. Cloning and Sequence Analysis TLR2 Gene from Yak. Prog Vet Med. 2014; 35(07): 59-63.

12. Ma L, Xiao X, LiuZ. The role of Toll-like receptors in allergic asthma. Chinese J Cell Mol Immunol. 2014; 30(09): 989-992.

13. Kumar H, Kawai T, Akira S. Toll-like receptors and innate immunity. Biochem Biophys Res Commun. 2009; 388(4): 621-625.

14. Wang Y, LiuS, Li Y, Wang Q, Shao J, Chen Y, Xin J. Mycoplasma bovis- derived lipid-associated membrane proteins activate IL-1β production through the NF-κB pathway via toll-like receptor 2 and MyD88. Dev Comp Immunol.2016; 55:111-118.

15. NCBI. National Center for Biotechnology Information. http://www.ncbi.nlm.nih.gov.

16. Hall TA. BioEdit: A User-Friendly Biological Sequence Alignment Editor and Analysis Program for Windows 95/98/NT. Nucleic Acids Symposium Series, 1999; 41:95-98.

17. Yeh FC, Yang RC, Boyle T. POPGENE Version 1.32: Microsoft Window-Based Freeware for Population Genetics Analysis. University of Alberta, Edmonton.1999.

18. Kimura M, Crow JF. The number of alleles that can be maintained in a finite population. Genet.1964; 49: 725–738.

19. Lewontin RC. Testing the theory of natural selection. Nat. 1972; 236: 181-182.

20. Levene H. On a matching problem arising in genetics. The annals of mathematical statistics, 1949; 20:91-94.

21. WrightS. Evolution and the Genetics of Population, Variability Within and Among Natural Populations. The University of Chicago Press, Chicago.1978.

22. Bhaladhare A, Sharma D, Kumar A, Sonwane A, Chauhan A, Singh R, Kumar P, Yadav R, Baqir M, Bhushan B, Prakash, O. Single nucleotide polymorphisms in toll-like receptor genes and case-control association studies with bovine tuberculosis. Vet World. 2016; 9(5): 458-464.

23. Haung J, Liu L, Wang H, Zhang C, Ju Z, Wang C, Zhong, J. Variants and Gene Expression of the TLR2 Gene and Susceptibility to Mastitis in Cattle. Asian J Anim Vet Adv. 2011; 6: 51-61.

24. Jadhav PV, Das DN,Tarate SB. Genetic polymorphism in TLR2 genes of HF cross bred cattle through PCR SSCP. I J Anim Res. 2020; 54(4): 430-433.

25. Pham LD, Ba NV, Nam LQ, Tuan PV, Do, D.N. Association of Lactoferrin and Toll-like Receptor 2 Genotypes with Mastitis and Milk Components in Vietnamese Holstein Cattle. Vet Sci. 2022; 9: 379. https://doi.org/10.3390/vetsci9080379.

26. Ranjan S, Bhushan B, Gupta JP, Panigrahi M. Genotype based transcript abundance of TLR2 among crossbred cattle and their relation with mastitis. J Pharma Phytochem. 2018; SP1: 449-453.

27. Pant SD, Schenkel FS, Leyva-Baca I, Sharma BS, Karrow NA. Identification of single nucleotide polymorphisms in bovine CARD15 and their associations with health and production traits in Canadian Holsteins. BMC Genom.2007; 8:421. doi:10.1186/1471-2164-8-421.

28. Mazzone P, Di Paolo A, PetrucciL, Torricelli M, Corneli S, Sebastiani C, CiulloM, Sebastianelli M, Costarelli S, Scoccia E. Evaluation of Single Nucleotide Polymorphisms (SNPs) Associated with Genetic Resistance to Bovine Paratuberculosis in Marchigiana Beef Cattle, an Italian Native Breed. Anim.2023; 13: 587. https://doi.org/10.3390/ani13040587.

29. Kalashnikova LA, Bagal IE, Murugina NE, KalashnikovVE,SeninaRY. Evaluation of Polymorphism of the Immune System Genes TNF and TLR2 in Cattle. Rus J Genet. 2024; 60(12):1657-1664.

30. Satheesha GM, Nagaraja R, Yathish HM, Sahadev A, Jayashree R, Kotresh AM, Naveenkumar S. Molecular Characterization and Expression Profile of Partial TLR2 Gene in Malnad Gidda Cattle. Int. J. Curr. Microbiol. App. Sci. 2021; 10(01):2879-2886.

31. Bai J, Jia-peng L, Fang Y, Min H, Wen-rong L, Min-Jun L.. Association of Toll like Receptor 2 polymorphism with somatic cell score in bovine. Acta Veterinaria et Zootechnica Sinica.2011; 42 (3): 350-362.

32. Mariotti M, Williams JL, Dunner S, Valentini A, Pariset L. Polymorphisms within the toll-like receptor (TLR)-2,-4, and-6 genes in cattle. Diversity. 2009;1(1): 7-18.

33. Pal A, Pal A Jr., Mallick A. I., Biswas P. and Chatterjee P. N. 2019, Molecular characterization of Bu-1 and TLR 2 gene in Haringhata Black chicken. Genomics 112(1): 472-483. https://doi.org/10.1016/j.ygeno.2019.03.010.

Cite this article as: Kour KD, Chakraborty D, Kumar N, Brahma B, Sharma V, Sudan A and Talwar S. Detection of single nucleotide polymorphism using TARMS-PCR in *TLR2* gene in local cattle of Jammu. Explor Anim Med Res. 2026; 16(1), DOI: 10.52635/eamr/16.1.40-45.

Explor Anim Med Res.
Vol. 16, Issue 1, 2026
DOI: 10.52635/eamr/16.1.46-51

ISSN 2277-470X (Print), ISSN 2319-247X (Online)
Website: www.animalmedicalresearch.org

Published under the CC BY-NC 4.0 license

Research Article

MOLECULAR CHARACTERIZATION OF CHICKEN SHANK EXTRACTED COLLAGEN BY FOURIER TRANSFORM INFRARED (FT-IR) SPECTROSCOPY

Jigyasa Rana[1], Omshiv Keshri[2], Mayukh Ghosh[3], Anurag Mishra[4], Shailesh Kumar Patel[5]*, Shailendra Singh[5], Bhabesh Chandra Das[6]

Received 16 November 2025, revised 26 April 2026

ABSTRACT: Collagen is the most abundant protein found in bone, cartilage, tendon, skin and other connective tissues of animals and humans. Collagen is widely used in biomedical applications such as tissue engineering, wound healing and drug delivery systems owing to its biocompatibility, biodegradability and minimal immunogenicity. The collagen can be extracted by multiple extraction methods from low-value animal byproducts but the biomedical applicability mainly depends upon its structural integrity and purity which must be accessed before use. A total of 24, day-old broiler chicks were procured commercially and reared at Livestock Farm Complex, Faculty of Veterinary and Animal Sciences, RGSC, Banaras Hindu University, Mirzapur, Uttar Pradesh, India. The chicks were divided into three groups of 8 birds each viz. Group 1, Group 2 and Group 3 and were sacrificed for collagen extraction from their shank at 28, 35 and 42 days respectively. Chicken shank tissue was subjected to collagen extraction by alkali and acid treatment followed by enzymatic hydrolysis using pepsin enzyme. The lyophilized collagen samples were analyzed for different molecular vibrations and spectral analysis using a Fourier transform infrared (FT-IR) spectrometer in ATR mode. The FT-IR spectroscopy analysis of the extracted collagen from each of the study group indicated the characteristic molecular structure, as evident by the amide peaks in mid infrared region i.e. 4000-500 cm^{-1}. The study underlined the efficacy of extraction process by alkali and acid treatment followed by enzymatic hydrolysis using pepsin enzyme and suggested that chicken shank collagen extracted by this method retains normal molecular structure necessary for biomedical application. The FT-IR spectroscopy analysis of the chicken shank extracted collagen using alkali and acid treatments followed by enzymatic hydrolysis exhibited well-preserved triple-helical structure which can be potentially used as biomaterial.

Keywords: Collagen, Shank, Molecular characterization, FT-IR.

INTRODUCTION

Collagen is the most abundant protein of vertebrates and accounts for about 30% of the total protein [1]. A total of 28 collagen types have been identified based on the protein structure, amino acid sequence and molecular properties among which type I collagen is the most abundant protein of connective tissue [2, 3]. Collagen molecules form three polypeptide chains

[1]Department of Veterinary Anatomy, Faculty of Veterinary and Animal Sciences, Rajiv Gandhi South Campus, Banaras Hindu University, Barkachha, Mirzapur- 231 001, Uttar Pradesh, India.
[2]Medical Laboratory Technology, DDU Kaushal Kendra, Rajiv Gandhi South Campus, Banaras Hindu University, Barkachha, Mirzapur- 231 001, Uttar Pradesh, India.
[3]Department of Veterinary Physiology and Biochemistry, Faculty of Veterinary and Animal Sciences, Rajiv Gandhi South Campus, Banaras Hindu University, Barkachha, Mirzapur- 231 001, Uttar Pradesh, India.
[4]Department of Physics, Biophysics Laboratory, Institute of Science, Banaras Hindu University- 221 005
[5]Department of Veterinary Pathology, College of Veterinary Science and Animal Husbandry, Nanaji Deshmukh Veterinary Science University, Rewa- 486 001, Madhya Pradesh, India.
[6]Department of Veterinary and Animal Husbandry Extension Education, College of Veterinary Science and Animal Husbandry, Nanaji Deshmukh Veterinary Science University, Rewa- 486 001, Madhya Pradesh, India.
**Corresponding author. e-mail: shaileshpatel624@gmail.com*

which bind together to form a triple helix structure primarily through hydrogen bonds. Each polypeptide chain contains about 1000 amino acid residues and has an average length of 300 nm and diameter of 1.4 nm. The amino acid sequence consists mainly of (Gly-X-Y)n, where glycine (Gly) makes up about 1/3 of the collagen peptide chain and X, Y are arbitrary amino acids other than glycine. Typically, the classical composition is proline (Pro) at the X-position and 4-hydroxyproline (Hyp) at the Y-position [4]. The various types of collagen found in nature are type I collagen predominantly present in skin, bones and connective tissues; type II and type III collagen found in cartilage and reticular fibers respectively.

The primary role of collagen is to maintain tissue integrity, support cellular structures and promote elasticity in the body. In addition, collagen has a crucial role in various biological functions of cells such as cell survival, proliferation and differentiation. Collagen possesses unique properties such as biocompatibility, biodegradability and low immunogenicity, making it suitable biomaterial for a wide range of biomedical applications [5, 6].

The collagen can be extracted from skin, bone and other organs of large animals, fish and poultry. The reports on chicken shank extracted collagen are meager as most of the studies on collagen extraction have been done on large animals owing to increased yield. The extraction of collagen from chicken low-value byproducts such as bone, cartilage, stomach, feathers, shank, skin, etc. are of great importance as it has no social taboos. The extracted collagen can be utilized in various industries including food, pharmaceuticals, cosmetics, and biomedical [7]. However, for potential usage in biomedical industrythe extracted collagen must retain normal molecular structure and should be free from impurities and deformities. Therefore, it is crucial to assess the molecular structure of the extracted collagen before its commercialization and application in biomedical fields.

Fourier Transform Infrared (FT-IR) spectroscopy is widely employed to analyze the molecular structure and purity of the collagen. The FT-IR spectra provide information on the functional groups present in the collagen, which is critical for verifying its structural integrity and identifying any contaminants. Keeping the above facts in consideration, the present research work is planned to analyze molecular structure of extracted chicken shank collagen by FT-IR spectroscopy.

MATERIALS AND METHODS

Sample Collection

A total of 24, day-old broiler chicks were procured commercially from Varanasi, Uttar Pradesh and reared at Livestock Farm Complex, Faculty of Veterinary and Animal Sciences, Rajiv Gandhi South Campus, Banaras Hindu University, Mirzapur, Uttar Pradesh under standard management conditions. The study was approved by Institutional Animal Ethics Committee (IAEC) via No. IAEC/RGSC-BHU/2023-24/180. The broiler birds were divided into three study groups of 8 birds each viz. Group 1, Group 2 and Group 3 and sacrificed for extraction of collagen from shank at 28, 35 and 42 days respectively as most commercial broilers reach slaughter weight between 28-42 days of age.

Processing of collected shank for collagen extraction

The collected chicken shanks were properly cleaned, trimmed, peeled and deboned followed by mincing and grinding. Thereafter the grinded material was subjected to different dry rendering temperatures for removal of fat.

Extraction of collagen

Collected chicken shanks were subjected to extraction process by alkali and acid treatments followed by enzymatic hydrolysis as described by earlier researchers [8]. The major steps involved in the extraction process involved

I. Pre-treatments of shank tissue for collagen extraction

a) Alkali pre-treatment

The rendered shank tissue was soaked in 0.1 mol/L NaOH solution for 6 hours in a 1:10 ratio (w/v) at 4°C and 165 rpm in orbital shaker incubator (REMI RIS-24 Plus TFT) with replacement of NaOH solution at every 2 hours interval. Thereafter, washing was done with double distilled water (DDW) till neutralization.

b) Chemical de-fatting

The alkali pre-treated shank tissue was further treated with 10% butyl alcohol in 1:10 ratio (w/v) for 12 hours at 4°C and 165 rpm in orbital shaker incubator. The 10% butyl alcohol solution was replaced at every 6 hours interval followed by washing with DDW.

c) Demineralization

The chemically defatted shank tissue was further treated with 0.1 N HCl in 1:6 ratio (w/v) for 24 hours at 4°C and 165 rpm in orbital shaker incubator for removal of inorganic constituents and promotion of shank swelling. Thereafter, washing was done thrice with DDW.

II. Collagen extraction from chicken shank tissue

The pre-treated shank tissue was subjected for collagen extraction using pepsin in acetic acid under following steps:

a) Acetic acid treatment/Hydrolysis

The pre-treated shank tissue was processed in a 1:6 ratio (w/v) of 0.5 mol/L acetic acid solution for 48 hours at 4°C and 165 rpm in orbital shaker incubator.

b) Enzymatic Hydrolysis

The collagen tissue obtained after acetic acid treatment was hydrolyzed in a 1:6 ratio (w/v) of 0.5 mol/L acetic acid solution containing 0.1% pepsin (activity of 1,000.0 U/mg) (w/v) for 24 hours at 4°C and 165 rpm in orbital shaker incubator.

III. Precipitation and Dialysis of extracted collagen

The hydrolyzed, soluble collagen was filtered by a double layered nylon plastic strainer and precipitated with the help of 2.6 mol/L NaCl solution in Tris (hydroxymethyl) aminomethane hydrochloride (0.05 M) at a pH of 7.0. The precipitated collagen was sedimented at 12,000 rpm for 15 minutes at 4°C using centrifugation machine (Eppendorf centrifuge 5810R, Germany). The precipitated collagen was dialysed against 20 volume of 0.1 M acetic acid for 12 hours, followed by DDW for another 24 hours with the change of dialysis solution at every 6 hours. Dialysis was undertaken using a dialysis membrane (HIMEDIA, Dialysis membrane-50) at 4°C and 175 rpm in orbital shaker incubator. The dialyzed shank collagen was finally lyophilized (-40ºC, 100 mbar pressure, 16 hours) in a freeze dryer (MAC, MSW-137) and stored in a sealed container under room temperature.

Fourier transform infrared (FT-IR) spectroscopy

The lyophilized collagen samples extracted from Group 1, Group 2 and Group 3 were analyzed for different molecular vibrations and spectral analysis using a Fourier transform infrared (FT-IR) spectrometer (BRUKER ALPHA II, FT-IR spectrometer) in ATR mode. The FT-IR analysis was performed in the Department of Physics, Institute of Science, Banaras Hindu University, Varanasi, Uttar Pradesh, India.

RESULTS AND DISCUSSION

Macroscopic observation

Grossly, the shank extracted collagen from each of the study groups viz. Group 1, Group 2 and Group 3 revealed white colour with slightly spongy and paper like consistency with no morphological difference. Similar findings were recorded earlier in the chicken feet collagen extracted using salt, acetic acid and pepsin [9].

Fourier transform infrared (FT-IR) spectroscopy

The FTIR spectroscopy analysis of the extracted collagen from the shank samples of all age groups were acquired over the range of 4000 to 500 cm^{-1} (mid infrared region) at a resolution of 2 cm^{-1}.

In shank collagen extracted from Group 1, amide A band peak was observed at 3285 cm^{-1} (N–H stretching), and amide B band was found near 2923 cm^{-1} and 2847 cm^{-1} (asymmetric -CH_2 stretching). The amide I band region was observed at 1741 cm^{-1} (C=O stretching) whereas the amide II band region was observed at 1541 cm^{-1} (N-H bending and C-N stretching) and amide III band peak was appeared at 1229 cm^{-1}, showing vibrations of C–N stretching and N–H bending (Figure 1, Table 1).

Table 1. Fourier transform infrared (FT-IR) spectra peak locations with assignments for shank collagen extracted from Group 1.

Peak positions in wavenumber (cm^{-1})	Assignments
3285	N-H Stretching
2923	C-H Stretching
2847	C-H Stretching
1741	C=O Stretching
1621	C=C Stretching
1541	N-O Stretching
1453	C-H Bending
1328	O-H Bending
1229	C-N Stretching
1151	C-O Stretching
1066	C-O Stretching
958	C=C Bending
865	C=C Bending

In shank collagen extracted from Group 2, amide A band peak (N–H stretching) was detected at 3302 cm^{-1}, and amide B band peak (-CH_2 stretching) appeared at 2920 cm^{-1} and 2845 cm^{-1}. The amide I (C=O stretching), amide II (N-H bending and C-N stretching) and amide III (C–N stretching and N–H bending) band peaks was found near 1739 cm^{-1}, 1531 cm^{-1} and 1235 cm^{-1} respectively (Figure 2, Table 2).

In shank collagen extracted from Group 3, amide A band peak (N–H stretching) was detected at 3280 cm^{-1} whereas amide B band peak (-CH_2 stretching) appeared at 2920 cm^{-1} and 2852 cm^{-1}. The amide I band peak (C=O stretching) was found near 1744 cm^{-1}, amide II

(N-H bending and C-N stretching) was seen at 1531 cm^{-1} and the amide III band peak (C–N stretching and N–H bending) was seen around at 1404 cm^{-1} and 1233 cm^{-1} (Figure 3, Table 3).

Table 2: Fourier transform infrared (FT-IR) spectra peak locations with assignments for shank collagen extracted from Group 2.

Peak positions in wavenumber (cm^{-1})	Assignments
3302	N-H Stretching
2920	C-H Stretching
2845	C-H Stretching
1739	C=O Stretching
1636	C=C Stretching
1531	N-O Stretching
1450	C-H Bending
1325	O-H Bending
1235	C-N Stretching
1149	C-O Stretching
1017	C-O Stretching
875	C=C Bending

The FT-IR spectra of shank extracted collagen from Group 1, Group 2 and Group 3 showed the preservation of characteristic molecular structure of collagen as indicated by the occurrence of distinct amide bands. The Amide bands A, B, I, II and III in our study confirms the proper extraction of collagen from chicken feet, which was similar to the previous findings [9-12]. In a previous study [10] the amide A band (N–H stretching) was found near 3412 cm^{-1} and 3338 cm^{-1} whereas the Amide B band region (-CH_2 asymmetrical stretching) was observed near 2925 cm^{-1}. In addition, Amide I band (C=O stretching), Amide II band (N-H bending and C-N stretching) and Amide III bands (C–N stretching and N–H bending) were appeared around 1745 cm^{-1}, 1550 - 1600 cm^{-1} and 1220 - 1320 cm^{-1} to 1451-1450 cm^{-1} respectively. The shifting of absorption peak towards lower wavenumbers (cm^{-1}) for amide I and amide II in our study denotes the existence of more and stronger hydrogen bonds in the collagen structure which further suggests a more stable and robust triple-helical conformation.

The collagen extracted from Group 1, Group 2 and Group 3 revealed no significant molecular differences suggesting collagen from the different age group included in the present study mainly represents type I collagen with high degree of structural integrity.

The FT-IR spectrum analysis was used as a quantitative method for confirmation of retention of the triple helix structure in extracted collagen. The confirmation was derived from the earlier described method [13, 14] based on the ratio of the peak intensities of amide III and 1450 cm^{-1} (amide III/1450 cm^{-1}), which should be equal to 1 for well-preserved collagen. The present study showed that the ratio of amide III/1450 cm^{-1} for Group 1, Group 2 and Group 3 was found as 0.84, 0.85 and 0.85 - 0.96 respectively which indicated that extracted collagen from all the study groups maintained well-preserved triple-helical

Table 3: Fourier transform infrared (FT-IR) spectra peak locations with assignments for shank collagen extracted from Group 3.

Peak positions in wavenumber (cm^{-1})	Assignments
3280	N-H Stretching
2920	C-H Stretching
2852	C-H Stretching
1744	C=O Stretching
1629	C=C Stretching
1531	N-O Stretching
1453	C-H Bending
1404	C-N Stretching (Amide III band)
1338	O-H Bending
1233	C-N Stretching (Amide III band)
1149	C-O Stretching
1070	C-O Stretching
873	C=C Bending
709	C=C Bending
581	C-I Stretching

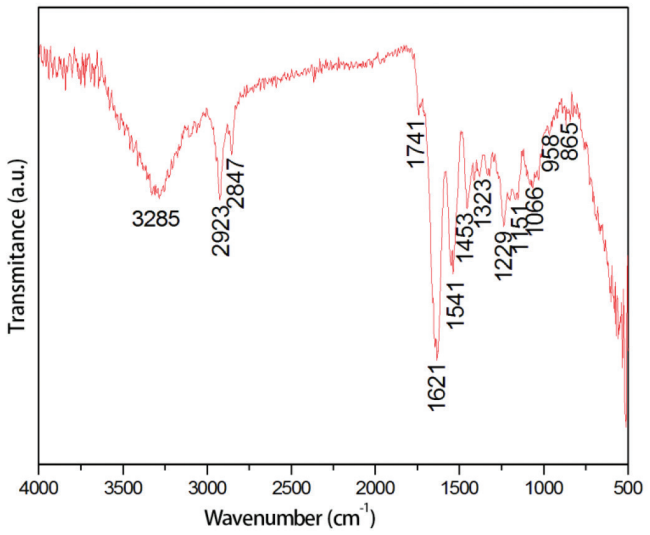

Fig. 1. Fourier transform infrared (FT-IR) spectra of shank collagen extracted from Group 1.

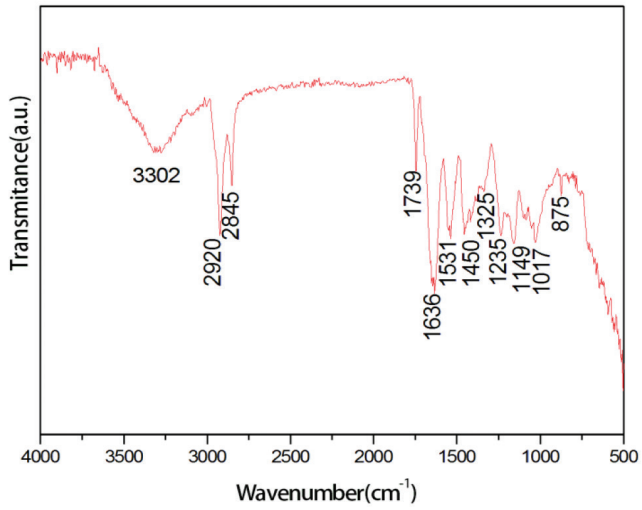

Fig. 2. Fourier transform infrared (FT-IR) spectra of shank collagen extracted from Group 2.

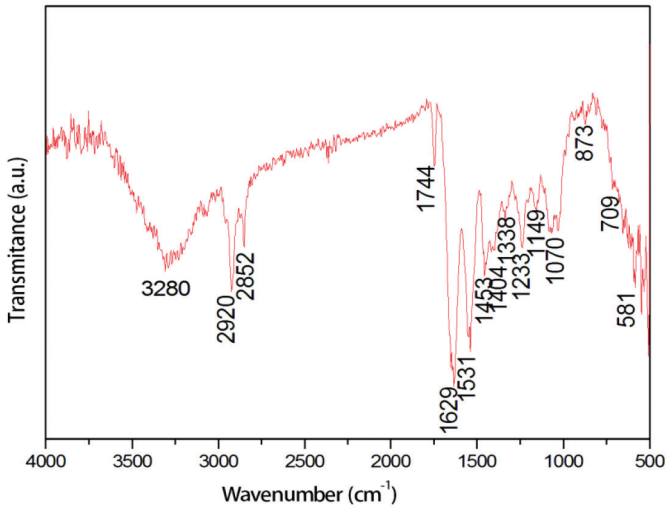

Fig. 3. Fourier transform infrared (FT-IR) spectra of shank collagen extracted from Group 3.

structure. In some studies [12], researchers found that amide III defines integrity of helix structure in collagen, with a ratio value close to 1.0 in our study we might say that the method of collagen extraction used in this study provides well preserved biomedical grade collagen from chicken feet. The triple helix structure is responsible for the biological and mechanical function of collagen and plays a crucial role in forming higher order structures by virtue of its inherent amino acid-amino acid interactions [15]. Therefore, the structural integrity of the extracted collagen is crucial for its commercialization as biomaterial.

The result of this study showed the extraction process by alkali and acid treatments followed by enzymatic hydrolysis provides collagen with higher structural integrity, with minimal contamination from other biological materials. This confirms the effectiveness of the isolation process and supports the potential use of this shank collagen in biomedical applications where structural integrity and purity are crucial.

CONCLUSION

The FT-IR spectroscopy analysis of the chicken shank extracted collagen using alkali and acid treatments followed by enzymatic hydrolysis exhibited well-preserved helical structure. The study further underlined the advantages of extraction process and suggested that chicken shank collagen extracted by this method retains normal molecular structure necessary for biomedical application. In addition, molecular characterization of the collagen extracted by other available methods may be done to strengthen the existing information on collagen extraction for biomedical use.

Financial support

This work was financially supported by Seed Grant/ Incentive to faculty members under IoE Scheme, Banaras Hindu University in the form of a project (IoE/ Seed Grant/21757) entitled “Synthesis of collagen based tissue Implant and its application in wound healing”.

ACKNOWLEDGEMENT

The authors sincerely acknowledge the Head, Department of Physics, Institute of Science, BHU for providing instrumentation for FT-IR spectroscopy. The authors are thankful to the Coordinator, IoE Cell, BHU, the Director, Institute of Agricultural Sciences, BHU and Dean, FVAS, RGSC, BHU, Varanasi for providing the funds and facilities to carry out this research work.

ETHICS APPROVAL

The experimental work was approved by the Institutional Animal Ethics Committee (IAEC) with IAEC No. IAEC/RGSC-BHU/2023-24/180.

REFERENCES

1. Gelse K, Pöschl E, Aigner T. Collagens--structure, function, and biosynthesis. Adv Drug Deliv Rev. 2003; 55(12): 1531-1546. https://doi.org/10.1016/j.addr.2003.08.002.

2. Srinivasan S, Durairaj B. Collagen isolation and characterization from *Sardinella longiceps*. J Adv Vet Anim Res. 2021; 8(4): 679-686. https://doi.org/10.5455/javar.2021.h560.

3. Espinales C, Romero-Peña M, Calderón G, Vergara K, Cáceres PJ, Castillo P. Collagen, protein hydrolysates and chitin from by-products of fish and shellfish: An overview.

Heliyon. 2023; 9(4): e14937. https://doi.org/10.1016/j.heliyon.2023.e14937.

4. Campos LD, Santos Junior VA, Pimentel JD, Carregã GLF, Cazarin CBB. Collagen supplementation in skin and orthopedic diseases: A review of the literature. Heliyon. 2023; 9(4): e14961. https://doi.org/10.1016/j.heliyon.2023.e14961.

5. Lim YS, Ok YJ, Hwang SY, Kwak JY, Yoon S. Marine Collagen as A Promising Biomaterial for Biomedical Applications. Mar Drugs. 2019; 17(8): 467. https://doi.org/10.3390/md17080467.

6. Sorushanova A, Delgado LM, Wu Z, Shologu N, Kshirsagar A *et al*. The Collagen Suprafamily: From Biosynthesis to Advanced Biomaterial Development. Adv Mater. 2019; 31(1): e1801651. https://doi.org/10.1002/adma.201801651.

7. Gojkovic Z, Marova I, Matouskova P, Obruca S, Miloslav P. Use of ultrasonic spectroscopy and viscosimetry for the characterization of chicken skin collagen in comparison with collagens from other animal tissues. Prep Biochem Biotechnol. 2014; 44(8): 761-71. https://doi.org/10.1080/10826068.2013.867869.

8. Rana J, Keshri OS, Rahman CKF, Kumar V, Patel SK *et al*. Extraction and evaluation of collagen as biomaterial from chicken shank. Indian J Anim Res. 2024; (Online first article). http://dx.doi.org/10.18805/IJAR.B-5502.

9. Zhou C, Li Y, Yu X, Yang H, Ma H et al. Extraction and characterization of chicken feet soluble collagen. LWT - Food Science and Technology. 2016; 74: 145-153. https://doi.org/10.1016/j.lwt.2016.07.024.

10. Hashim P, Ridzwan MM, Bakar J. Isolation and characterization of collagen from chicken feet. International Journal of Bioengineering and Life Sciences. 2014; 8(3): 250-254.

11. Potti RB, Fahad MO. Extraction and characterization of collagen from broiler chicken feet (gallus gallus domesticus) - biomolecules from poultry waste. J Pure Appl Microbiol. 2017; 11(1): 315-322.

12. Suparno O, Prasetyo NB. Isolation of collagen from chicken feet with hydro-extraction method and its physico-chemical characterisation. In IOP Conference Series: Earth and Environmental Science. 2019; 335(1): 012018.

13. Doyle BB, Bendit EG, Blout ER. Infrared spectroscopy of collagen and collagen-like polypeptides. Biopolymers. 1975; 14(5): 937-957. https://doi.org/10.1002/bip.1975.360140505.

14. Gao LL, Wang ZY, Zheng LI, Zhang CX, Zhang DQ. The characterization of acid and pepsin soluble collagen from ovine bones (Ujumuqin sheep). J Integr Agric. 2018; 17(3): 704-711. https://doi.org/10.1016/S2095-3119(17)61751-9.

15. Fernandes LL, Resende CX, Tavares DS, Soares GA, Castro LO et al. Cytocompatibility of chitosan and collagen-chitosan scaffolds for tissue engineering. Polímeros. 2011; 21(1): 1-6.

Cite this article as: Rana J, Keshri O, Ghosh M, Mishra A, Patel SK, Singh S, Das BC. Molecular characterization of chicken shank extracted collagen by fourier transform infrared (FT-IR) spectroscopy. Explor Anim Med Res. 2026; 16(1), DOI: 10.52635/eamr/16.1.46-51.

Explor Anim Med Res.
Vol. 16, Issue 1, 2026
DOI: 10.52635/eamr/16.1.52-62

ISSN 2277-470X (Print), ISSN 2319-247X (Online)
Website: www.animalmedicalresearch.org

Published under the CC BY-NC 4.0 license

Research Article

EVALUATION OF THE ANTIMICROBIAL EFFICACY OF *CUPRESSUS MACROCARPA* AND *THYMUS VULGARIS* ESSENTIAL OILS AGAINST SELECTED MULTIDRUG-RESISTANT PATHOGENS OF VETERINARY AND HUMAN ORIGIN

Renas Ihsan Abdulkarim[1] and Nawzat Aboziad Issa[1, *]

Received 12 April 2025, revised 23 April 2026

ABSTRACT: This study evaluated the antimicrobial efficacy of essential oils (EOs) extracted from *Cupressus macrocarpa* (*C. macrocarpa*) and *Thymus vulgaris* (*T. vulgaris*) against selected multidrug-resistant (MDR) bacterial and fungal isolates originating from both veterinary and human sources. Using agar disc diffusion and broth dilution methods, we evaluated their potential as alternatives to conventional antimicrobials by determining the minimum inhibitory concentration (MIC), minimum bactericidal concentration (MBC), and minimum fungicidal concentration (MFC). Time-kill kinetics and antibiotic interaction assays were also conducted. Both EOs exhibited notable antimicrobial activity against the selected MDR pathogens. Notably, *T. vulgaris* demonstrated superior antimicrobial efficacy, with lower MIC (9–25 µL/mL) and MBC (12–40 µL/mL) values compared to *C. macrocarpa* (MIC: 12–40 µL/mL; MBC: 15–50 µL/mL). It also showed potent antifungal activity, achieving the lowest MFC (30 µL/mL) against yeast isolates. Time-kill assays revealed that *T. vulgaris* eradicated most pathogens within 2 hours, while *C. macrocarpa* requires up to 24 hours. Furthermore, antibiotic interaction studies indicated that *T. vulgaris* enhanced the efficacy of conventional antibiotics synergistically, whereas *C. macrocarpa* exhibited antagonistic interactions that may compromise antibiotic effectiveness. These findings underscore the therapeutic potential of *T. vulgaris* as a promising candidate for treating MDR infections and as a valuable adjunct to antibiotic therapy. However, caution is warranted when co-administering *C. macrocarpa* with antibiotics due to its antagonistic effects. Overall, this study highlights the potential role of essential oils, particularly *T. vulgaris*, in addressing antimicrobial resistance (AMR) in both veterinary and human medicine.

Keywords: Multidrug-resistant, Veterinary and human isolates, *Cupressus macrocarpa*, *Thymus vulgaris*, Time-kill assay and Required dose.

INTRODUCTION

In recent years, the search for innovative and naturally derived antimicrobial agents has intensified in response to the growing challenge of drug-resistant pathogens [1] having saved millions of lives from infectious diseases. Microbes have developed acquired antimicrobial resistance (AMR). Among these natural alternatives, essential oils have garnered significant attention due to their potent bioactive properties and broad-spectrum activity against bacteria and fungi [2]. Derived from various plant parts such as leaves, seeds, flowers, and bark, essential oils are complex mixtures of volatile aromatic compounds known for their distinctive fragrances and multifaceted biological activities [3]. Their antimicrobial properties make them promising candidates as natural alternatives to synthetic agents

Essential oils of particular interest are Lemon Cypress oil, derived from *Cupressus macrocarpa* 'Goldcrest' [4] and thyme oil, extracted from *T. vulgaris* [5]. Both have demonstrated remarkable efficacy against a wide range of bacterial and fungal pathogens, attributed to their rich composition of bioactive compounds [6]. *C. macrocarpa* EO is characterized by its high concentration of monoterpenes, sesquiterpenes, and other volatile organic compounds, such as limonene, α-pinene, β-pinene, δ-3-carene, and myrcene, which contribute to its strong

[1]*Surgery and Internal Medicine department, College of Veterinary Medicine, University of Duhok, Kurdistan region, Iraq*
**Corresponding author. e-mail: nawzat.issa@uod.ac*

antimicrobial properties [7]. These compounds exert their effects by disrupting microbial cell membranes, inhibiting essential enzymes, and interfering with genetic material, ultimately leading to cell death [8].

Similarly, *T. vulgaris* EO is renowned for its antimicrobial activity, primarily due to its major bioactive components, thymol and carvacrol [9]. These phenolic monoterpenoids exhibit broad-spectrum antimicrobial effects against bacteria, fungi, and even certain viruses. Their mechanisms of action include membrane disruption, enzyme inhibition, and interference with genetic material, resulting in microbial cell death [10].

Despite the growing interest in these essential oils, a comprehensive analysis of their antimicrobial activities against clinically significant bacterial and fungal isolates from both human and veterinary sources was lacking. This study aimed to address this gap by evaluating the antibiotic sensitivity profiles of these isolates and assessing the antimicrobial efficacy of *C. macrocarpa* and *T. vulgaris* essential oils. Specifically, the study determined their minimum inhibitory concentration (MIC), minimum bactericidal concentration (MBC), and minimum fungicidal concentration (MFC), and performed time-kill assays to evaluate their antimicrobial kinetics. Additionally, the study conducted a direct comparative analysis of the two essential oils, explored their potential synergistic effects with conventional antimicrobials, and assessed their cross-species applicability.

MATERIALS AND METHODS

Ethical approval

The study was approved by the Ethical Committee of the College of Veterinary Medicine, University of Duhok, Iraq (Permit number: CVM2024/0110UoD).

Study period and location

The research was conducted at the College of Veterinary Medicine, University of Duhok, Iraq, from September 2024 to February 2025.

Tree Materials and Essential Oil Extraction

Samples of *C. macrocarpa* and *T. vulgaris* were collected from farms in Duhok Province, Iraq. The plant species were identified by a taxonomist at the University of Duhok. The samples were air-dried indoors, and essential oils (EOs) were extracted using a Clevenger apparatus, achieving a purity of ≥ 99%.

Antimicrobial and Essential Oil Sensitivity Profiling

Antimicrobial susceptibility testing was performed using the disc diffusion method. Nine antibiotics were tested on animal bacterial isolates, and 13 antibiotics were tested on human isolates, along with six antifungal discs for *Candida albicans* (*C. albicans*).

Animal bacterial isolates were sourced from veterinary cases at the College of Veterinary Medicine, University of Duhok, Iraq, including *E. coli*, *Pasteurella multocida* (*P. multocida*), *Klebsiella pneumonia* (*K. pneumoniae*), and *Proteus mirabilis* (*P. mirabilis*) from pneumonic sheep and goats [11], MRSA strains from Rasol and Abdulrahman, (2023) [12] sheep, and goats using traditional and molecular characterization. The study was conducted in Duhok province during the period from November 2021 to March 2022. Furthermore, the isolates were screened for the presence of MRSA using the standard Kirby-Bauer disk diffusion method (oxacillin discs, and *Corynebacterium pseudotuberculosis* (*C. pseudotuberculosis*) and *Streptococcus agalactiae* (*S. agalactiae*) from infected sheep and cattle [13]. Human isolates were identified using the VITEK system at Zariland Medical Laboratories/ Duhok province, Iraq.

The Kirby-Bauer method was modified by applying 15 µL of *C. macrocarpa* and *T. vulgaris* essential oils to culture plates, which were incubated at 37°C for 24-48 hours. Results were interpreted according to CLSI guidelines for both human [14] and animal isolates [15]. Isolates were classified as susceptible or resistant, with intermediate sensitivity categorized as resistant.

MIC, MBC, and MFC Determination

The MIC, MBC, and MFC of the tested EOs were determined using broth dilution testing [2]. Various EO concentrations were tested against bacterial and fungal isolates. For each, 1 ml of 5×10^6 CFU/ml bacteria or yeast was added to 1.5 ml microtubes, followed by EO. The microtubes were vortexed and incubated in a shaker incubator at 37°C for 24-48 hours. The MIC was the lowest EO concentration preventing visible growth. MBC/MFC were determined by subculturing 20 µl from MIC tubes onto MHA for bacteria (blood agar for *Corynebacterium pseudotuberculosis*) and Sabouraud Dextrose Agar (SDA) or blood agar for yeast. MBC/MFC were confirmed by the absence of growth on agar plates after incubation at 37°C for 24-48 hours.

Time-Kill Assay

The antimicrobial activity of selected essential oils (EOs) was assessed using a time-kill kinetic assay, following standardized microbiological procedures outlined by Hulankova (2024)[16]. Briefly, quantification of viable microbial cells was performed

by determining colony-forming units (CFU/mL) for bacterial isolates and *C. albicans*, using a combination of optical density (OD) measurements and two-fold serial dilution, as outlined by Mira, Yeh, and Hall (2022)[17].

Microbial cultures were grown in Mueller–Hinton Broth (MHB) under aerobic conditions at 37 °C in a shaker incubator (Forma orbital shaker Thermo, UK) at 150 rpm until reaching the logarithmic growth phase. The optical density of bacterial cultures was measured at 600 nm [18], whereas *C. albicans* suspensions were measured at 550 nm [19] (CFU, using a spectrophotometer (Libra S22, Biochrom, Scientific Laboratory Suppliers, UK). OD–CFU calibration curves were generated to determine CFU/mL and to prepare standardized challenge inocula. For inoculum preparation, 1 mL of a culture adjusted to 1×10^8 CFU/mL was transferred into sterile 15 mL centrifuge tubes and centrifuged at 1000 × g for 10 min. Supernatants were discarded, and the pellets were resuspended in sterile phosphate-buffered saline (PBS) to obtain a final concentration of 5×10^6 CFU/mL. Microbial suspensions (5×10^6 CFU/mL) were treated with EO at MBC/MFC concentrations and incubated at 37°C with shaking. Aliquots were taken at 2, 4, and 24 hours, plated onto agar, and incubated to determine viable counts. Controls without EO were included.

Synergistic and Antagonistic Effects of EO and Antibiotics:

The study investigated the combined effects of essential oils (EOs) from *C. macrocarpa* and *T. vulgaris* with antibiotics or antifungals on bacterial and yeast isolates to assess interactions with antimicrobials that did not individually reach the sensitivity threshold. A 6 µl concentration of EO (0.5 × MIC) was used to evaluate synergistic or antagonistic effects. Bacterial and fungal cultures were grown on Mueller-Hinton and blood agar, with antibiotic discs saturated with EOs (6 µl)[20]. Synergy was indicated by an increase of >2 mm in the inhibition zone compared to either antimicrobial or EO alone [21]. Antagonism was observed if the inhibition zone was reduced by >2 mm when used in combination [22]0.5, 1, and 2 µg/ml of vancomycin. and the zones of inhibition were measured at 24 h. The CLSI-recommended checkerboard method was used as a reference to detect synergy.

Statistical Analysis

Significant differences in inhibition zones between EOs and effective antibiotics against veterinary bacterial strains were analyzed using one-way ANOVA in GraphPad Prism 8.0.1. Additionally, Fisher's Exact Test was applied to assess the antibacterial efficacy of *C. macrocarpa* and *T. vulgaris* at 2 and 4 hours post-treatment. Results were presented as mean ± SE from three independent experiments, with statistical significance set at $p < 0.05$.

RESULTS

Susceptibility patterns to antibiotics, antifungals, and essential oils:

The antibiotic susceptibility testing of veterinary isolates revealed widespread resistance to penicillin and tetracycline, with all isolates except *C. pseudotuberculosis* showing resistance (Table 1). Methicillin-resistant *Staphylococcus aureus* (MRSA) strains (CTI, D, and C) and *E. coli* were resistant to streptomycin, while *C. pseudotuberculosis* and *S. agalactiae* remained susceptible. *P. multocida* exhibited resistance to chloramphenicol. Amoxicillin-clavulanic acid demonstrated variable efficacy, with resistance observed in *P. multocida*, *P. mirabilis*, and MRSA-D and MRSA-C. The emergence of multidrug resistance in veterinary clinical isolates is further evidenced by the prevalence of ceftiofur resistance in *E. coli* and MRSA-C, as well as sulfamethoxazole-trimethoprim resistance in *E. coli*, *P. mirabilis*, and *Streptococcus agalactiae*. In contrast, *S. agalactiae* and *K. pneumoniae* remained highly susceptible to sulfamethoxazole-trimethoprim. These findings underscore the need for targeted antibiotic use in veterinary medicine.

The essential oils of *C. macrocarpa* and *T. vulgaris* demonstrated potent antibacterial activity against all tested veterinary isolates, including MRSA strains (Table 1). The inhibition zones ranged from 26.7 ± 0.9 mm to 34.0 ± 0.6 mm, with the most pronounced activity observed against the MRSA- CTI isolate (*C. macrocarpa*: 34.0 ± 0.6 mm; *T. vulgaris*: 32.0 ± 2.1 mm). This indicates a strong inhibitory effect of both EOs, particularly against resistant Gram-positive pathogens.

Human bacterial and fungal isolates displayed varying resistance patterns. *E. coli* and *K. pneumonia* were resistant to ampicillin, cefepime, and ceftazidime, while *S. aureus* and *S. haemolyticus* exhibited variable resistance profiles. Ciprofloxacin and gentamicin were effective against *E. coli*, *E. faecalis*, and *S. aureus* but showed limited efficacy against *K. pneumonia* and *S. haemolyticus*. Tigecycline demonstrated broad susceptibility across isolates, whereas vancomycin resistance was observed in multiple strains. Antifungal

testing of *C. albicans* revealed resistance to azole such as itraconazole, fluconazole, ketoconazole, and miconazole, raises significant concerns for the future of antifungal therapy, though amphotericin B and nystatin remained effective (Table 2).

Similarly, both essential oils exhibited substantial antibacterial and antifungal activity against human clinical isolates. In this group, *C. macrocarpa* produced inhibition zones ranging from 22.7 ± 2.9 mm to 28.1 ± 0.1 mm, while *T. vulgaris* showed slightly higher zones of inhibition, ranging from 27.7 ± 0.3 mm to 28.3 ± 0.9 mm (Table 2).

Minimum Inhibitory Concentration (MIC), Minimum Bactericidal Concentration (MBC), and Minimum Fungicidal Concentration (MFC)

The MIC, MBC, and MFC values varied depending on the essential oil used. *T. vulgaris* consistently exhibited lower MIC and MBC values compared to *C. macrocarpa*, indicating stronger antibacterial activity. Similarly, *T. vulgaris* demonstrated greater antifungal efficacy, as evidenced by lower MFC values against yeast isolates (Table 3). The lowest MIC and MBC values for *T. vulgaris* were observed against *E. coli* and MRSA (*S. aureus*), with values as low as 9–12 µL/mL. In contrast, *C. macrocarpa* required higher concentrations (12–15 µL/mL) for the same isolates.

Time-Kill Assay at MBC/MFC

The time-kill assay demonstrated that *T. vulgaris* EO exhibited a faster and more potent bactericidal and fungicidal effect compared to *C. macrocarpa*. Within 2 hours of treatment, *T. vulgaris* eliminated all bacterial and fungal isolates except *P. mirabilis*, *E. faecalis* and *C. albicans*. In contrast, *C. macrocarpa* only eradicated *K. pneumoniae* and *MRSA-C*.

Fisher's Exact Test revealed a significant difference in the antimicrobial efficacy between the two oils. At 2 hours, the odds ratio was 0.033 ($p = 0.00024$), indicating that *C. macrocarpa* was significantly less effective than *T. vulgaris* in inhibiting bacterial growth. After 4 hours, *T. vulgaris* achieved complete inhibition of bacterial growth in all tested isolates, whereas some isolates remained viable when treated with *C. macrocarpa* (odds ratio = 0.0, $p = 0.0177$). By 24 hours, *C. macrocarpa* also achieved complete inhibition of all isolates (Table 4). These findings underscore the strong antimicrobial potential of *T. vulgaris* as a viable alternative therapeutic agent for tackling multidrug-resistant infections where conventional treatments fail.

Interactions Between Essential Oils and Antibiotics

The study also assessed the interaction between antibiotics and the EOs of *C. macrocarpa* and *T. vulgaris* against various bacterial isolates (Table 5). *T. vulgaris* consistently exhibited synergistic effects, enhancing antibiotic efficacy, while *C. macrocarpa* showed antagonistic interactions when combined with chloramphenicol, streptomycin, amoxicillin-clavulanic acid (AMC/AUG), and penicillin against *P. multocida, P. mirabilis, K. pneumoniae*, and MRSA-C and MRSA-D, resulting in reduced inhibition zones. Additionally, an indifferent effect was observed when *C. macrocarpa* was combined with azithromycin against MRSA-D, indicating no significant enhancement in antimicrobial activity.

DISCUSSION

The findings of this study highlight the alarming prevalence of antimicrobial resistance in bacterial isolates from both animals and humans, underscoring the urgent need for robust antimicrobial stewardship programs and the development of alternative treatments. The antibiotic susceptibility testing of veterinary isolates revealed widespread resistance to penicillin and tetracycline. The widespread resistance to commonly used antibiotics, such as penicillin and tetracycline, observed in animal isolates, reflects the declining efficacy of these drugs [23, 24]. Notably, *E. coli*, *P. mirabilis*, and MRSA exhibited resistance to streptomycin, while *P. mirabilis*, MRSA, and *P. multocida* showed resistance to amoxicillin-clavulanic acid. This resistance is likely driven by the improper use of antibiotics by local farmers, who often store and administer drugs like oxytetracycline, tylosin, streptomycin, and penicillin without veterinary oversight. Such practices, including underdosing, overuse, and premature cessation of treatment, facilitate bacterial adaptation through mechanisms such as aminoglycoside-modifying enzymes, ribosomal mutations, and efflux pumps, ultimately reducing antibiotic efficacy [25]. The prominent cause contributing to the current crisis remains to be the overuse and misuse of antimicrobials, particularly the inappropriate usage of antibiotics, increasing the global burden of antimicrobial resistance. The global consumption and usage of antibiotics are therefore closely monitored at all times. Additionally, resistance to amoxicillin-clavulanic acid in *P. mirabilis* and MRSA is primarily attributed to β-lactamase production, which degrades the antibiotic despite the presence of clavulanic acid [26].

Table 1: Antibiotic sensitivity profiles of veterinary isolates, highlighting resistance and susceptibility patterns across various bacterial strains.

Antimicrobiials	*E. coli*	*P. multocida*	*P. mirbilis*	*K.pneumonia*	*C. pseudotuberculosis*	*Strept agalactiae*	*MRSA- CTI (Cattle isolate)*	*MRSA -CTII (Cattle isolate)*	*MRSA- D (Dog isolate)*	*MRSA- C (Cat isolate)*
Penicillin	R	R	R	R	S	R	R	R	R	R
	0	6.3 ± 0.3	4.0 ± 0.6	13.0 ± 1.5	30.7 ± 1.2	10.3 ± 0.3	0	0	0	0
Tetracycline (TE)	R	R	R	R	S	R	R	R	R	R
	5.3 ± 0.3	0	0	0	26.7 ± 3.3	0	9.0 ± 0.6	11.3 ± 3.0	13.3 ± 0.9	6.7 ± 1.3
Streptomycin (S)	R $^{Cu**\ T**}$	S ^{Cu***}	R	S $^{Cu\ T}$	S	S $^{Cu**\ T**}$	R	S $^{Cu***\ T***}$	R	R
	15.5 ± 0.5	16.3 ± 2.6	14 ± 1.2	17.0 ± 1.5	25.7± 3	20.3 ± 1.5	9.0 ± 0.6	16.0 ± 1.0	15.0 ± 0.6	10.0 ± 1.0
Chloramphenicol (C)	S	R	R	S	S	S	S $^{Cu***\ T**}$	S	S $^{Cu**\ T**}$	S $^{Cu***\ T**}$
	27.5 ± 2.5	12.3 ± 0.3	12.3 ± 0.3	30.0 ± 1.7	28.3 ± 1.7	22.7 ± 0.3	23.3 ± 0.9	24.7 ± 2.7	21.0 ± 0.6	21.0 ± 0.6
AMC or AUG	S	R	R	S	S	S	S	S	R	R
	23 ± 2.5	16.7 ± 0.7	16.7 ± 0.7	24.3 ± 1.2	25.0 ± 2.9	21.0 ± 0.6	30.3 ± 0.3	30.7 ± 0.7	15.3 ± 0.3	13.0 ± 0.6
Ceftiofur (CFT)30µg	R	S	S	S	S	S $^{Cu*\ T*}$	S ^{Cu**T*}	S	S	R
	6 ± 0.6	26.0 ± 3.1	23.5± 0.5	27.5 ± 2.5	31.5 ± 1.5	27.3 ± 1.5	26.0 ± 0.6	30.7 ± 0.7	23.0 ± 1.2	0
SMX-TMP	R	S	R	S	S	R	S ^{Cu*}	S	S $^{Cu*\ T*}$	S ^{Cu**}
	0	27.0 ± 1.5	0	29.5 ± 2.5	29.3 ± 0.7	0	27.3 ± 1.5	28.3 ± 1.7	22.3 ± 1.5	25.7 ± 1.3
AZM	R	S	S $^{Cu\ T}$	S	S	R	R	R	R	R
	1.3 ± 0.7	23.3 ± 2.0	19.3 ± 1.8	23.0 ± 2.0	27.3 ± 1.5	0	4.7 ± 2.9	7. ± 1.5	10. ± 2.9	0
Tylosin 30µg	R	R	R	R	S	R	R	S	R	R
	0	0	0	0	35.7 ± 4.7	7.3 ± 3.7	3.3 ± 1.7	27.3 ± 1.5	13.5 ± 1.5	10.5 ± 0.5
Cupressus macrocarpa	S	S	S	S	S	S	S	S	S	S
	28.7 ± 0.7	29.7 ± 0.9	28.7 ± 0.7	28.7 ± 0.7	26.7 ± 0.9	27.7 ± 0.3	34.0 ± 0.6	31.3 ± 1.2	26.7 ± 0.9	32.0 ± 0.6
Thyme vulgaris	S	S	S	S	S	S	S	S	S	S
	27.7 ± 1.5	28.3 ± 0.9	27.3 ± 0.7	28.7 ± 0.7	27.0 ± 0.6	27.7 ± 0.3	32.0 ± 2.1	31.7 ± 0.9	27.0 ± 0.6	27.7 ± 0.3

The superscripts “Cu” and “T” indicate significant differences in the inhibitory zones (in mm) between the essential oils (EOs) of Cupressus macrocarpa and Thymus vulgaris, as well as antibiotics. Asterisk notations (*, **, ***) correspond to the following levels of significance: $p < 0.05$, $p < 0.01$, and $p < 0.001$, respectively.

Table 2: Antibiotic and antifungal sensitivity profiles of human-origin bacterial and fungal isolates, with resistance (R) and susceptibility (S) observed across various agents.

Antibiotics	*Bacterial and fungal isolates of human origion*					
	E. coli	***E. faecalis***	***K. pneumoniae***	***S. aureus***	***S. haemolyticus***	***C. albican***
Ampicillin	R	-	R	-	-	-
Cefepime	R	-	R	R	R	-
Ceftazidime	R	-	R	-	R	-
Ciprofloxacin	S	S	R	S	R	-
Clindamycin	-	S	-	S	R	-
Erythromycin	R	R	-	-	R	-
Gentamicin	S	S	S	R	S	-
Imipenem	S	-	S	-	-	-
Meropenem	S	-	S	-	-	-
Tetracycline	S	R	R	S	R	-
Tigecycline	S	S	S	S	S	-
(SMX-TMP)	S	-	R	S	S	-
Vancomycin	-	R	-	R	R	-
Itraconazole	-	-	-	-	-	R
Amphotericin B	-	-	-	-	-	S
Fluconazole	-	-	-	-	-	R
Ketoconazole	-	-	-	-	-	R
Nystatin (NS)	-	-	-	-	-	S
Miconazole	-	-	-	-	-	R
Cupressus macrocarpa	**S** 28.1 ± 0.1	**S** 26.± 2	**S** 26± 2	**S** 22.7 ±2.9	**S** 26.7 ± 3.5	**S** 26. ± 3.
Thyme vulgaris	**S** 28.2 ± 0.2	**S** 28.3 ± 0.3	**S** 27.7 ± 0.3	**S** 28.3 ±0.3	**S** 28.3 ± 0.9	**S** 27.7 ± 0.3

The emergence of multidrug resistance in veterinary clinical isolates is further evidenced by the prevalence of ceftiofur resistance in *E. coli* and MRSA-C, as well as sulfamethoxazole-trimethoprim resistance in *E. coli*, *P. mirabilis*, and *Streptococcus agalactiae*. The high resistance to azithromycin in *E. coli* and MRSA, coupled with the limited efficacy of tylosin, underscores the escalating challenge of AMR in veterinary medicine [26]. These findings emphasize the need for ongoing surveillance and judicious antibiotic selection in veterinary practices [27].

Human bacterial and fungal isolates displayed varying resistance patterns. Concerning resistance patterns, with *E. coli* and *K. pneumonia* showing significant resistance to ampicillin, cefepime, and ceftazidime, complicating treatment options [28]. Similarly, diverse resistance patterns in *S. aureus* and *S. haemolyticus* highlight the importance of personalized antibiotic therapy based on specific resistance profiles [29]. While ciprofloxacin and gentamicin remain effective against *E. coli*, *E. faecalis*, and *S. aureus*, their limited efficacy against *K. pneumoniae* and *S. haemolyticus* underscores the need for targeted antimicrobial strategies [30]. Tigecycline demonstrated broad susceptibility, consistent with findings by Kenza El Bazi *et al.*, (2022) [26]. However, widespread vancomycin resistance across multiple bacterial strains raises serious concerns for managing severe infections, necessitating continuous monitoring and adaptable treatment protocols [32]. Addressing these challenges requires a multifaceted approach, including the development of novel antibiotics, strengthened infection control measures, and robust antimicrobial stewardship programs [33].

The high resistance of *Candida albicans* to azole antifungals, such as itraconazole, fluconazole, ketoconazole, and miconazole, raises significant concerns for the future of antifungal therapy. While amphotericin B and nystatin retain efficacy, the increasing prevalence

Table 3: Minimum inhibitory concentration (MIC) and minimum bactericidal concentration (MBC) values for bacterial and fungal isolates of animal and human origin against *Cupressus macrocarpa* and *Thyme vulgaris.*

Bacterial Isolates-Animal Origion	*Cupressus macrocarpa*		*Thyme vulgaris*	
	MIC	**MBC**	**MIC**	**MBC**
Escherichia coli	12	15	9	12
P. multocida	12	15	12	15
P. mirbilis	40	50	25	40
K.pneumonia	12	12	12	15
C. pseudotuberculosis (Sheep isolate)	15	18	15	18
Streptococcus agalactiae	40	50	15	20
Staph aureus MRSA CTI (Cattle isolate)	12	15	9	12
Staph aureus MRSA CTII (Cattle isolate)	12	15	9	12
Staph aureus MRSA D (Dog isolate)	12	15	9	12
Staph aureus MRSA C (Cat isolate)	12	15	9	12
Bacterial and fungal Isolates-human Origion				
Escherichia coli	12	15	9	12
K.pneumonia	12	15	9	12
Staphylococcus aureus	12	15	9	12
Staphylococcus haemolyticus	12	15	9	12
Enterococcus faecalis	35	50	15	18
Candida albicans	30	40	15	30

Table 4: Time required to kill bacterial and fungal isolates at the minimum bactericidal concentration (MBC) for various bacterial isolates, using *Cupressus macrocarpa* and *Thyme vulgaris.* Time to bacterial death was recorded at 2 hours, 4 hours, and 24 hours post-treatment.

Bacterial Isolates	2h post-treatment		4h post-treatment		24h post-treatment
	C. macrocarpa	*T. vulgaris*	*C. macrocarpa*	*T. vulgaris*	*C. macrocarpa*
Animal Isolates					
E. coli	G	NG	G		NG
K. pneumoniae	NG	NG	-		
P. multocida	G	NG	NG		
P. mirabilis	G	G	NG	NG	
C. pseudotuberculosis	G	NG	NG		
S. agalactiae	G	NG	G		NG
Staph aureus MRSA CTI (Cattle isolate)	G	NG	G		NG
Staph aureus MRSA CTII (Cattle isolate)	G	NG	G		NG
Staph aureus MRSA D (Dog isolate)	G	NG	NG		
Staph aureus MRSA C (Cat isolate)	NG	NG	-		-
Human Isolates					
E.coli	G	NG	NG		
K. pneumoniae	G	NG	G		NG
Staphylococcus aureus	G	NG	NG		
Staphylococcus hamolyticus	G	NG	G		NG
Enterococcus faecalis	G	G	NG	NG	
Candida albicans	G	G	NG	NG	

G = growth and NG = no growth

Table 5: Antimicrobial activity of *Cupressus macrocarpa* and *Thyme vulgaris*, alone and in combination with antibiotics, against bacterial isolates from animals. The inhibition zone diameters (mm) are presented as mean ± standard error. Results are classified as antagonistic (A) when the combination produced a smaller inhibition zone than either agent alone, synergistic (S) when the combination produced a larger inhibition zone, and indifferent (I) when there was no significant difference.

Bacteria-Animal Isolates	Antibiotic	Alone	*Cupressus macrocarpa*			*Thyme vulgaris*		
			Alone	Combination	results	Alone	Combination	results
		mm	mm	mm		mm	mm	
P. multocida	Chloramphenicol	12.3 ± 0.3	29.7 ± 0.9	21.5± 1.5	A	28.3 ± 0.9	36.5 ±1.5	S
	AMC or AUG	16.7 ± 0.7		16.5± 1.5	A		31.5±1.5	S
P. mirabilis	Streptomycin	14 ± 1.2	28.7 ± 0.7	17.5± 0.5	A	27.3 ± 0.7	35.5±2.5	S
	AMC or AUG	16.7 ± 0.7		18	A		36±2	S
K. pneumoniae	Penicillin	13.0 ± 1.5	28.7 ± 0.7	11± 1	A	28.7 ± 0.7	37.5±2.5	S
S. agalactiae	Penicillin	10.3 ± 0.3	27.7 ± 0.3	37.5± 0.5	S	27.7 ± 0.3	38.6±2.3	S
MRSA CTII (Cattle isolate)	Tetracycline	11.3 ± 3.0	31.3 ± 1.2	35.5± 2.5	S	31.7 ± 0.9	34+1	S
MRSA-D (Dog isolate)	Tetracycline	13.3 ± 0.9	26.7 ± 0.9	29.5± 0.5	S	27.0 ± 0.6	36.5± 1.5	S
	Streptomycin	15.0 ± 0.6		23± 0.1	A		38	S
	Azithromycin	10. ± 2.9		27.5	I		38	S
MRSA- C (Cat isolate)	Streptomycin	10.0 ± 1.0	32.0 ± 0.6	16± 1	A	27.7 ± 0.3	35±2.5	S
	AMC or AUG	13.0 ± 0.6		24± 1	A		31.5± 1.5	S

of azole-resistant strains underscores the need for novel antifungal compounds [34].

The routine use of antibiotics in animals for growth promotion, disease prevention, and treatment drives bacterial adaptation, leading to the emergence of resistant pathogens [25]. These resistant bacteria can transfer to humans through direct contact, contaminated food, or environmental exposure, complicating treatment options [35]. The widespread use of antibiotics in food-producing animals exerts selective pressure, promoting the persistence and spread of resistant strains, which are then transmitted to humans [36]. This highlights the urgent need for enhanced antimicrobial stewardship and surveillance to curb the transfer of resistance from animal reservoirs to human clinical settings [32, 33]

The essential oils of *C. macrocarpa* and *T. vulgaris* exhibit potent antibacterial activity against multidrug-resistant isolates, including MRSA, from both veterinary and human sources, demonstrating their potential as alternative antimicrobial agents. These findings are consistent with earlier reports suggesting the broad-spectrum efficacy of plant-derived EOs against resistant pathogens [2, 34]. *T. vulgaris* demonstrated superior efficacy compared to *C. macrocarpa*, with pronounced inhibition of MRSA likely due to mechanisms such as membrane disruption and metabolic interference [40].

The antimicrobial efficacy of these essential oils was further confirmed by MIC, MBC, and MFC assessments. *T. vulgaris* exhibited lower MIC and MBC values, indicating potent bactericidal properties, as well as reduced MFC values, suggesting enhanced fungicidal activity [41].

Time-kill assays at MBC/MFC concentrations revealed that *T. vulgaris* exerted rapid and potent bactericidal and fungicidal effects, eliminating most isolates within two hours. In contrast, *C. macrocarpa* exhibited slower antimicrobial activity, with complete inhibition observed only after 24 hours. These findings underscore the strong antimicrobial potential of *T. vulgaris* as a viable alternative therapeutic agent for tackling multidrug-resistant infections where conventional treatments fail.

This study also highlights the complex interactions between essential oils and antibiotics. *T. vulgaris* consistently exhibited synergistic effects, enhancing antibiotic efficacy, while *C. macrocarpa* showed antagonistic interactions. These contrasting outcomes are likely due to differences in their chemical composition. The high levels of thymol and carvacrol in *T. vulgaris* may enhance membrane disruption and antibiotic uptake [37, 38]. In contrast, antagonism observed with *C. macrocarpa* may result from compounds that interfere with antibiotic permeability

or alter bacterial metabolism [44]. Thus, while *T. vulgaris* holds promise as an antibiotic adjuvant, caution is warranted when combining *C. macrocarpa* with conventional antimicrobials. Further studies are needed to clarify the mechanisms underlying these interactions.

In conclusion, this study underscores the growing threat of antibiotic resistance, particularly against commonly used antibiotics, with multidrug-resistant strains posing significant challenges. *T. vulgaris* essential oil demonstrated strong antimicrobial activity against multidrug-resistant bacterial and fungal pathogens from both veterinary and human sources, exhibiting superior efficacy (lower MIC, MBC, and MFC values) and rapid killing kinetics. Its synergistic interactions with antibiotics suggest its potential as an adjunct therapy for multidrug-resistant infections. While *C. macrocarpa* also showed antimicrobial activity, its antagonistic effects with certain antibiotics warrant caution in combination treatments. Overall, *T. vulgaris* holds promise as a natural antimicrobial agent in combating resistance in clinical and veterinary medicine.

Authors contribution: Renas Ihsan Abdulkarim and Nawzat Aboziad Issa conceived and designed the study. NAI and RIA executed the experiment and analysed the data. All authors interpreted the data, critically revised the manuscript for important intellectual contents and approved the final version.

REFERENCES

1. Salam MA, Al-Amin MY, Salam MT, Pawar JS, Akhter N, Rabaan AA, *et al.* Antimicrobial Resistance: A Growing Serious Threat for Global Public Health. Healthcare (Switzerland), 2023; 11(13):1946, DOI: 10.3390/healthcare11131946.

2. Issa NA. Evaluation the Antimicrobial Activity of Essential Oils against Veterinary Pathogens, Multidrug-resistant Bacteria and Dermatophytes. Pak Vet J., 2024; 44(2): 260-265, DOI: 10.29261/pakvetj/2024.165.

3. Mohamed AA, Alotaibi BM. Essential oils of some medicinal plants and their biological activities: a mini review. J Umm Al-Qura Univ Appl Sci, 2023; 9: 40–49, DOI: 10.1007/s43994-022-00018-1.

4. Sherif AE, Amen Y, Rizk DE, Abdelwahab G. Chemical compositions and antimicrobial activities of three lemon odor essential oils of Cupressus macrocarpa, Cymbopogon citratus. and Citrus limon. Egypt J Basic Appl Sci, 2023; 10(1): 894–905, DOI: 10.1080/2314808X.2023.2291245.

5. Posgay M, Greff B, Kapcsándi V, Lakatos E. Effect of Thymus vulgaris L. essential oil and thymol on the microbiological properties of meat and meat products: A review. Heliyon, 2022; 8(10):e10812, DOI: 10.1016/j.heliyon.2022.e10812.

6. Sriti J, Haj Salem M, Aidi Wannes W, Bachrouch O, Mejri H, Belloumi S, *et al.* Antioxidant, antibacterial and insecticidal activities of cypress (Cupressus sempervirens L.) essential oil. Int J Environ Health Res. 2024; 34(2): 1168–1179, DOI: 10.1080/09603123.2023.2207475.

7. Semerdjieva I, Cantrell CL, Zheljazkov VD, Radoukova T, Koleva-Valkova LH, Astatkie T, *et al.* Chemical profile, antioxidant and antimicrobial activity of Pinus heldreichii Christ. Distributed in Bulgaria. Heliyon. 2024; 10;10(1):e22967, DOI: 10.1016/j.heliyon.2023.e22967.

8. Pedroso MB, Scariot FJ, Rocha RKM, Echeverrigaray S, Delamare APL. Antifungal activity and mechanism of action of monoterpenes against Botrytis cinerea. Cienc e Agrotecnologia. 2024; 48: 1-8, DOI: 10.1590/1413-7054202448018823.

9. Halat DH, Krayem M, Khaled S, Younes S. A Focused Insight into Thyme: Biological, Chemical, and Therapeutic Properties of an Indigenous Mediterranean Herb. Nutrients. 2022; 8;14(10):2104, DOI: 10.3390/nu14102104.

10. Imran M, Aslam M, Alsagaby SA, Saeed F, Ahmad I, Afzaal M, *et al.* Therapeutic application of carvacrol: A comprehensive review. Food Science and Nutrition. 2022; 3;10(11):3544-3561, DOI: 10.1002/fsn3.2994.

11. Ahmed B. Abdullah M. Isolation and molecular diagnosis of the main bacterial species causing Pneumonia in small ruminants in the Duhok Abattoir-Kurdistan region of Iraq. Microb Biosyst. 2022; 7(2): 66-73, DOI: 10.21608/mb.2023.193960.1069.

12. Rasol VA, Abdulrahman RF. Detection and Molecular Characterization of Staphylococcus aureus and Methicillin-Resistant Staphylococcus aureus (MRSA) Nasal Carriage Isolates from Healthy Domestic Animal in Duhok Province. Egypt J Vet Sci. 2023; 54(2): 263-273, DOI: 10.21608/ejvs.2022.168434.1404.

13. Khanamir RA, Issa NA, Abdulrahman RF. First study on molecular epidemiology of caseous lymphadenitis in slaughtered sheep and goats in Duhok Province, Iraq. Open Vet J. 2023; 13(5): 588-598, DOI: 10.5455/OVJ.2023.v13.i5.11.

14. Weinstein MP, Lewis JS. The clinical and laboratory standards institute subcommittee on Antimicrobial susceptibility testing: Background, organization, functions, and processes. Journal of Clinical Microbiology. 2020; 58(3), DOI: 10.1128/JCM.01864-19.

15. Clinical and L. S. Institute. Performance standards for antimicrobial disk and dilution susceptibility tests for bacteria isolated from animals. VET01S-Ed5. *CLSI Suppl. VET08*, 2022.

16. Hulankova, R. Methods for Determination of Antimicrobial Activity of Essential Oils In Vitro—A Review, Plants, 2024; 13(19):2784, DOI: 10.3390/plants13192784.

17. Mira, P, Yeh, P. and B. Hall, G. Estimating microbial population data from optical density. PLoS One, 2022; 17: 1-8, DOI: 10.1371/journal.pone.0276040.

18. Wacogne, B.*et al.*,. Concentration vs. Optical Density of ESKAPEE Bacteria: A Method to Determine the Optimum Measurement Wavelength," Sensors, 2024; 24(24), DOI: 10.3390/s24248160.

19. Sahu, S. R. Utkalaja, B. G Patel, S. K. and Acharya, N. Spot Assay and Colony Forming Unit (CFU) Analyses–based sensitivity test for Candida albicans and Saccharomyces cerevisiae," Bio-protocol. 2023; 13(21), DOI: 10.21769/BioProtoc.4872.

20. Caballero Gómez, N. Manetsberger, J. Lavilla Lerma, L. Martínez Martos, J. M. Benomar , N. and Abriouel, H. Exploring synergistic effects of essential oils compounds with antibiotics and biocides against multidrug-resistant foodborne pathogens, Appl. Food Res., 2024; 4(2), DOI: 10.1016/j.afres.2024.100581.

21. Khleifat, K. M. Matar, S. A. Jaafreh, M. Qaralleh, H. Al-Limoun, M. O.and Alsharafa, K. Y. Essential oil of centaurea damascena aerial parts, antibacterial and synergistic effect. J. Essent. Oil-Bearing Plants. 2019; 2(2): 356-367, DOI: 10.1080/0972060X.2019.1626292.

22. Sy C. L.*et al.* Synergy of β-Lactams with Vancomycin against Methicillin-Resistant Staphylococcus aureus: Correlation of Disk Diffusion and Checkerboard Methods. J. Clin. Microbiol.. 2016; 54(3): 565-568, DOI: 10.1128/JCM.01779-15.

23. Haulisah, N. A. Hassan, L. Bejo, S. K. Jajere, S. M., and Ahmad, N. I. High Levels of Antibiotic Resistance in Isolates From Diseased Livestock. Front. Vet. Sci. 2021; 8, DOI: 10.3389/fvets.2021.652351.

24. Egyir B, Dsani E, Owusu-Nyantakyi C, Amuasi GR, Owusu FA, Allegye-Cudjoe E, et al. Antimicrobial resistance and genomic analysis of staphylococci isolated from livestock and farm attendants in Northern Ghana. BMC Microbiol. 2022; 22(1), DOI: 10.1186/s12866-022-02589-9.

25. Tang KWK, Millar BC, Moore JE. Antimicrobial Resistance (AMR). British Journal of Biomedical Science. 2023; 80:11387, DOI: 10.3389/bjbs.2023.11387.

26. Maddock KJ, Bowden R, Cole SD, Diaz-Campos D, Daniels JB, Lecuyer TE, et al. Current state and future directions for veterinary antimicrobial resistance research. Am J Vet Res. 2024; 85(3), DOI: 10.2460/ajvr.23.12.0294.

27. Caneschi A, Bardhi A, Barbarossa A, Zaghini A. The Use of Antibiotics and Antimicrobial Resistance in Veterinary Medicine, a Complex Phenomenon: A Narrative Review. Antibiotics. 2023; 12(3):487, DOI: 10.3390/antibiotics12030487.

28. Castanheira M, Simner PJ, Bradford PA. Extended-spectrum β-lactamases: An update on their characteristics, epidemiology and detection. JAC-Antimicrobial Resistance. 2021; 3(3): dlab092, DOI: 10.1093/jacamr/dlab092.

29. Abdulmanea AA, Alharbi NS, Somily AM, Khojah OT, Farrag MA, Alobaidi AS, et al. Prevalence and antibiogram pattern of multidrug-resistant Staphylococcus aureus infections in individuals with sickle cell disease. A retrospective study, hematological and genetic analysis. J King Saud Univ - Sci [Internet], 2024;36(11):103542. Available from: https://doi.org/10.1016/j.jksus.2024.103542.

30. Halawa EM, Fadel M, Al-Rabia MW, Behairy A, Nouh NA, Abdo M, et al. Antibiotic action and resistance: updated review of mechanisms, spread, influencing factors, and alternative approaches for combating resistance. Front Pharmacol. 2023; 14:1-17, DOI: 10.3389/fphar.2023.1305294.

31. Kenza El Bazi, Mouhcine Miloudi, Youssef El Kamouni, Said Zouhair, Lamiae Arsalane. Tigecycline susceptibility among multi-drug resistant bacteria: A 7-year retrospective study. GSC Adv Res Rev. 2022; 11(1): 079-083, DOI: 10.30574/gscarr.2022.11.1.0096.

32. Li G, Walker MJ, De Oliveira DMP. Vancomycin Resistance in Enterococcus and Staphylococcus aureus. Microorganisms. 2023; 11(1):24, DOI: 10.3390/microorganisms11010024.

33. Oliveira M, Antunes W, Mota S, Madureira-Carvalho Á, Dinis-Oliveira RJ, Dias da Silva D. An Overview of the Recent Advances in Antimicrobial Resistance. Microorganisms. 2024; 12(9):1920, DOI: 10.3390/microorganisms12091920.

34. Teixeira MM, Carvalho DT, Sousa E, Pinto E. New Antifungal Agents with Azole Moieties. Pharmaceuticals. 2022; 15(11):1427, DOI: 10.3390/ph15111427.

35. Endale H, Mathewos M, Abdeta D. Potential Causes of Spread of Antimicrobial Resistance and Preventive Measures in One Health Perspective-A Review. Infection and Drug Resistance. 2023; 16: 7515—7545, DOI: 10.2147/IDR.S428837.

36. Sharma S, Chauhan A, Ranjan A, Mathkor DM, Haque S, Ramniwas S, et al. Emerging challenges in antimicrobial resistance: implications for pathogenic microorganisms, novel antibiotics, and their impact on sustainability. Front Microbiol. 2024; 15:1403168, DOI: 10.3389/fmicb.2024.1403168.

37. Darby EM, Trampari E, Siasat P, Gaya MS, Alav I, Webber MA, et al. Molecular mechanisms of antibiotic resistance revisited. Nature Reviews Microbiology. 2023; 21(5):280-295, DOI: 10.1038/s41579-022-00820-y.

38. Kaur K, Singh S, Kaur R. Impact of antibiotic usage in food-producing animals on food safety and possible antibiotic alternatives. The Microbe [Internet]. 2024; 4: 100097, DOI: 10.1016/j.microb.2024.100097.

39. Serag M, Daadeer D, Elfayoumy R. Antibacterial potential of essential oils extracted from three medicinal plants against some foodborne bacteria. Catrina Int J Environ Sci. 2023; 28(1): 73-91, DOI: 10.21608/cat.2023.220193.1179.

40. Sateriale D, Forgione G, De Cristofaro GA, Pagliuca C, Colicchio R, Salvatore P, et al. Antibacterial and Antibiofilm Efficacy of Thyme (Thymus vulgaris L.) Essential Oil against Foodborne Illness Pathogens, Salmonella enterica subsp. enterica Serovar Typhimurium and Bacillus cereus. Antibiotics. 2023; 12(3):485, DOI: 10.3390/antibiotics12030485.

41. Blanc AR, Sortino MA, Butassi E, Svetaz LA. Synergistic effects of Thymus vulgaris essential oil in combination with antifungal agents and inhibition of virulence factors of Candida albicans. Phytomedicine Plus. 2023; 16(1):149, DOI: 10.1016/j.phyplu.2023.100481.

42. Hajibonabi A, Yekani M, Sharifi S, Nahad JS, Dizaj SM, Memar MY. Antimicrobial activity of nanoformulations of carvacrol and thymol: New trend and applications. OpenNano. 2023; 13: 100170, DOI: 10.1016/j.onano.2023.100170.

43. Khwaza V, Aderibigbe BA. Antibacterial Activity of Selected Essential Oil Components and Their Derivatives: A Review. Antibiotics. 2025; 14(1):68, DOI: 10.3390/antibiotics14010068.

44. Muteeb G, Rehman MT, Shahwan M, Aatif M. Origin of Antibiotics and Antibiotic Resistance, and Their Impacts on Drug Development: A Narrative Review. Pharmaceuticals. 2023; 16(11):1615, DOI: 10.3390/ph16111615.

Cite this article as: Abdulkarim RI and Issa NA. Evaluation of the antimicrobial efficacy of *Cupressus macrocarpa* and *Thymus vulgaris* essential oils against selected multidrug-resistant pathogens of veterinary and human origin. Explor Anim Med Res. 2026; 16(1), DOI: 10.52635/eamr/16.1.52-62.

Explor Anim Med Res.
Vol. 16, Issue 1, 2026
DOI: 10.52635/eamr/16.1.63-70

ISSN 2277-470X (Print), ISSN 2319-247X (Online)
Website: www.animalmedicalresearch.org

Published under the CC BY-NC 4.0 license

Research Article

PROTECTIVE EFFECT OF *PUNICA GRANATUM* PEEL EXTRACT AGAINST FIPRONIL INDUCED THYROID TOXICITY IN MALE WISTAR ALBINO RATS

P. Nakul[1*], K. Sujatha[2*], A. Anand Kumar[3] and S. Vijayalakshmi[4]

Received 28 February 2025, revised 23 April 2026

ABSTRACT: The present study was carried out to check the thyroid toxicity induced by fipronil in male Wistar albino rats and its amelioration with pomegranate peel extract. A total of 24 male Wistar rats were grouped in to 4 groups (Group I, II, III and IV) with 6 animals in each group. Fipronil was administered orally @ 10 mg/kg b. wt. in distilled water for a period of 45 days in group II rats and group IV rats fed with both fipronil (@ 10mg/kg b. wt.) and pomegranate peel extract (@ 200mg/kg b. wt.) for a period of 45 days. Group I and III animals were treated as vehicle (distilled water) and *Punica granatum* (pomegranate) peel extract control respectively. Pooled serum samples were collected at fortnight interval for checking the thyroid hormonal status. Fipronil treated rats showed significant (*P<0.05*) decrease in the serum T3 and T4 levels and increased levels of serum TSH. Histopathologically, severe degenerated and disrupted follicular lining epithelium with complete loss of architectural details of thyroid follicles and immunohistochemically, increased expression of BAX antigen was observed in the fipronil treated animals. Co-administration of *Punica granatum* (pomegranate) peel extract along with fipronil resulted in the increased T3, T4 levels and decreased TSH levels compared to fipronil treated group and near to control rats value. Histologically, thyroid gland of rats treated with fipronil along with *Punica granatum* peel extract showed restoration of thyroid architecture with minimal inflammatory changes, normal follicular epithelium and lumen filled with colloidal secretions. Immunohistochemically, ameliorative group showed mild immunoreactivity and decreased expression of BAX antigen. This study highlights the protective role of pomegranate peel extract in reducing fipronil-induced thyroid damage.

Keywords: BAX antigen, Histopathology, Hormonal status, Immunohistochemistry, *Punica granatum*, Thyroid toxicity, Wistar albino rats.

INTRODUCTION

Fipronil is broad-spectrum phenylpyrazole insecticide commonly used in veterinary, agricultural and household purposes. In order to increase the crop yield and to reduce harvest loss, agricultural field workers were forced to use different kinds of pest control methods in fields. One of the common ways is the use of broad-spectrum insecticides. Indiscriminate use of these pesticides results in accidental poisoning in agricultural community [1]. Discussion being going on among the scientific community regarding the extensive use of fipronil and its toxicity in different organisms. Fipronil is reported to be highly toxic to aquatic invertebrates and fishes and moderately toxic to rats and mice [2].

Fipronil acts on central nervous system of insects by inhibiting the GABA-A receptors and glutamate-activated chloride channels. Inhibition of g-aminobutyric acid receptors results in hyperexcitation and death of insects [3]. Fipronil also induce oxidative damage by generating excess free radicals which damages biological membranes and organ toxicity [4]. Other than nervous system, fipronil also cause multisystem impairments in animals which affects hepatic, respiratory, cardiac,

[1,3]*Department of Veterinary Pathology, College of Veterinary Science, Sri Venkateswara Veterinary University, Tirupati- 517502, Andhra Pradesh.*
[2*]*Coordinator, Centre for Continuing Veterinary Education and Communication*
[4]*Associate Professor, Department of Veterinary Microbiology, C. V. Sc. Tirupati*
**Correspondence author. e-mail: nakulperayil1995@gmail.com, karamalasujatha@gmail.com*

gastro-intestinal and reproductive systems [5,6,7]. Still, the research on the toxic effects of fipronil on endocrine functions is not widely discussed. So the current study focussed on checking the extend of endocrine disruptive effects of fipronil in Wistar albino rats.

Usage of herbal medicine has been widely recommended in toxicity studies because of their less side effects, easily availability, cheaper rate and long-standing effects. In developed countries also, herbal plant extracts have been in use as complementary and alternative medicines [8,9]. Different varieties of herbal plants have been used in many agro-chemical toxicity studies. In this study, we incorporated the peel extract powder of pomegranate (*Punica granatum*). Because of its easy availability, higher anti-oxidant potential and less side effects, *Punica granatum* has got worldwide recognition. It also contains polyphenolic compounds like catechins, quercetin, anthocyanidin which are responsible for the antioxidant potential of peel extract of pomegranate [10]. Hence, our study focussed on checking the ameliorative effects of *Punica granatum* peel extract against fipronil induced thyroid toxicity.

MATERIALS AND METHODS

Experimental animals, fipronil and pomegranate peel extract procurement

Male Wistar albino rats used for this study was procured from Sri Venkateshwara Enterprises, Bangalore. Acclimatization for the procured rats were provided in a standard polypropylene rat cages for two days and further maintenance given at 25ºC ± 1ºC and a 12:12 hour interval light/ dark cycle for 6 weeks by following all standard laboratory hygienic conditions and *ad libitum* feed and water. Technical-grade fipronil (99% purity; Batch No. FIP92B5266) was sourced from Gharda Chemicals Ltd., Mumbai, while *Punica granatum* peel extract (Product No. Dadim LC23030077) was obtained from Chemiloids Life Science Pvt. Ltd., Vijayawada, Andhra Pradesh.

Animal ethical committee approval

The Institutional Animal Ethical Committee (IAEC) approval was obtained prior to the commencement of the experiment. (Wide no 281/ go/ ReBi/ S/ 2000/ CPCSEA/ CVSc/ TPTY/ 010/ Veterinary Pathology/ 2023 dated: 08.05. 2023).

Reagents

Primary (BAX) and secondary antibodies for immunohistochemistry were procured from Elabscience Company

Study trial

Study was designed such a way that a total of 24 male Wistar rats were randomly assigned in to four groups with six animals in each group. Group I animals were considered as control group provided them with normal laboratory animal feed and *ad libitum* water. Group II animals were treated with technical grade fipronil (99% pure) @ 10mg/kg b. wt. orally for a period of 45 days of experimental duration. Group III animals served as *Punica granatum* (pomegranate) peel extract control providing them pomegranate peel extract @ 200 mg/kg b. wt. orally for a period of 45 days. Group IV animals were treated with both fipronil and pomegranate peel extract @ 10 mg/kg b. wt. and 200 mg/kg b. wt. orally for checking the ameliorative effect of *Punica granatum* peel extract. Pooled blood samples were collected from all experimental rats at fortnight interval for hormonal assay. Animal sacrifice was done at 6th week (after the end of experimental period) and representative tissue sample of thyroid was collected in 10% neutral buffered formalin for histopathological and immunohistochemical studies.

Hormonal assay

At fortnight intervals, pooled blood samples were collected from all groups directly in to serum vial and allowed to clot for serum separation. This separated serum was centrifuged at 4000 rpm for 20 mins and stored at –20ºC for the estimation of T3, T4 and TSH levels. All hormonal estimations were carried out in Siemens centor 100 automatic biochemical analyzers procured from siemens, Germany using the chemiluminescence immunoassay (CLIA) method.

Histopathology

Detailed post-mortem examination was conducted during sacrifice and representative tissue pieces from thyroid was collected and preserved in 10% neutral buffered formalin for histopathological studies. Dehydration process was done manually by keeping the tissues in different grades of alcohol followed by clearing using xylene. The paraffin infiltration process was carried out by keeping the cleared tissue in paraffin wax bath overnight. Embedding should be completed within 4 to 5 hrs after completion of the paraffin infiltration. Sections of 5-6 (μ) thickness was cut and stained with routine Hematoxylin and Eosin (H&E) stain [11].

Immunohistochemistry

Paraffin sections of thyroid were cut into 3-4 μ thickness and then mounted onto Amino Propyl Ethoxy

Silane (APES) coated slides for overnight incubation at 37ºC. By passing through 2 changes of xylene for 15 minutes each, sections were deparaffinized followed by dipping in 2 changes of absolute alcohol to remove xylene. Under running tap water, the obtained sections were washed for 10 minutes and then rinsed in distilled water for 5 minutes. The sections were kept in a 3:1 (preheated) antigen retrieval solution and kept in a pressure cooker for 3 whistles. Sections were removed from the heat and kept until the retrieval solution was lukewarm (around 45 minutes). Later, sections were kept in distilled water followed by Tris EDTA buffer for 5 minutes each. The slides were kept in the humid chamber and to block the endogenous peroxidase, peroxidase block solution (freshly prepared 3% hydrogen peroxide) was added for 10 min. Washed the sections in Tris EDTA buffer 3 times 5 minutes each. Above these tissue sections, the power block solution was poured and kept for 10 min. Primary antibody (BAX) was added to the thyroid sections, and slides were kept at room temperature for 30 min. Washed the slides in Tris EDTA buffer for 5 minutes each in 3 changes. Super enhancer solution was added and kept for 20 minutes followed by washing in Tris EDTA buffer. A secondary antibody with poly HRP (Horseradish peroxidase) was added and incubated for 20 minutes. Then washed in acid Tris EDTA buffer for 5 minutes each in 3 changes. Working colouring reagent was prepared from Diamino benzidine (DAB) by adding one drop of DAB into 1 ml of the substrate (supplied with kit). The sections were kept in the colouring reagent for 5-8 minutes followed by washing in Tris EDTA and tap water for 2 min each. The staining of sections was done by using Harris haematoxylin for 2 minutes followed by tap water wash for 5 min. Blueing was done by dipping the slides in lithium carbonate solution twice and washing them in tap water. The sections were mounted in DPX after air drying.

Statistical analysis: By performing one-way ANOVA, the results were statistically analysed using SPSS software [12].

RESULTS AND DISCUSSION

The mean serum T_3 values were 154, 82.52, 161.80, and 148.28 (ng/dl) in Group I to IV respectively, and are given in Table. 1. There was a significant ($P<0.05$) decrease in serum T_3 values in fipronil treated groups when compared to the control. Whereas significant improvement ($P<0.05$) in T_3 values was observed in *Punica granatum* ameliorated rats (Group IV) when compared to fipronil treated rats. Similarly, a significant decrease in serum T4 values was observed in fipronil treated (Group II) rats when compared to the control group. The mean serum T_4 values in in Group I to IV rats were 9.53, 4.26, 8.43, and 8.5 (µg/dl) respectively, and are given in Table2. Significant improvement ($P<0.05$) in T_4 values was observed in *Punica granatum* ameliorated rats (Group IV) when compared to fipronil treated rats. These observations were in line with [13,14,15] in their work. The decrease in the serum T3 and T4 levels in fipronil treated rats might be due to the induction of hepatic microsomal enzymes by fipronil which results in excessive catabolism and increased clearance of T3 and T4 levels from the body [5]. Fipronil is known to induce hepatic microsomal enzymes, particularly those involved in phase II metabolism, such as UDP-glucuronosyltransferases and sulfotransferases [16]. This enzymatic induction accelerates the glucuronidation and sulfonation of thyroid hormones, which are critical rate-limiting steps in their biliary excretion [17,18]. Consequently, the enhanced metabolism and clearance of T3 and T4 lead to a reduction in their serum concentrations. Hepatic microsomal enzymes play a major role in glucuronidation and sulfonation, which are limiting steps in the biliary excretion of T4 and T3 hormones [19]. Secondly, fipronil disrupts the normal functioning of the hypothalamus-pituitary-thyroid (HPT) axis [20]. It impairs the feedback regulation between thyroid hormone levels and pituitary secretion of thyroid-stimulating hormone (TSH), thereby contributing further to hypothyroxinaemia. This dual effect enhanced peripheral metabolism and impaired central regulation collectively result in significant reductions in serum T3 and T4 levels in fipronil-exposed animals [20].

In contrary to serum T3 and T4 levels, we observed a significant ($P<0.05$) increase in serum TSH values in fipronil treated groups when compared to the control group and a significant decrease in mean TSH values of Group IV rats compared to the fipronil treated rats. The mean serum TSH values in Group I to IV rats were 4.11, 7.93, 4.08, and 5 (µIU/ ml) respectively, and are given in Table 3. This might be due to reduced T4 concentration which will gradually suppress the negative feedback of T4 on TSH secretion, thereby increasing the plasma TSH concentration [13]. This finding was contrary with [21] who noticed declined serum TSH level along with serum T3 and T4 levels in MSG toxicity case.

In *Punica granatum* ameliorated group showed significant improvement in serum T3 and T4 values

than fipronil treated group. Similar observation was reported by [21]. This might be due to the scavenging effects of different polyphenolic compounds present in *Punica granatum* such as ellagic acid, punicalagin, gallic acid, and flavonoids [22]. These molecules exhibit strong antioxidative properties by scavenging reactive oxygen species (ROS), reducing oxidative stress in the hypothalamus, pituitary, and thyroid tissues [23]. Oxidative stress plays a critical role in damaging thyrotroph cells of the anterior pituitary and thyrocytes, leading to impaired synthesis and secretion of thyroid hormones [24]. *Punica granatum* components upregulate the expression of nuclear factor erythroid 2–related factor 2 (Nrf2) and its downstream antioxidant response element (ARE)-regulated genes [25]. Nrf2 activation leads to increased transcription of antioxidant enzymes like superoxide dismutase (SOD), catalase, and glutathione peroxidase, thereby mitigating ROS-induced cellular apoptosis in endocrine tissues and supporting the functional preservation of the hypothalamic-pituitary-thyroid (HPT) axis [26]. Moreover, polyphenolic compounds in *Punica granatum* may directly influence deiodinase enzymes, particularly type 2 deiodinase (DIO2), which converts T4 into its more active form, T3 in peripheral tissues [27]. Preservation of DIO2 activity ensures proper peripheral activation of thyroid hormones even under toxic conditions.

Histopathological examination of thyroid gland of group II animals revealed a complete loss of architectural details of thyroid follicles with a lack of colloid and interfollicular blood vessel congestion (Fig: 1A). The majority of fipronil treated rats showed severe degeneration and disrupted follicular lining epithelium with desquamation of epithelial cells into the lumen and variation in the sizes of follicles (Fig: 1B). Few follicles with pale pink colloidal secretions in the lumen, and severe disruption and complete architectural loss of remaining follicles (Fig: 1C) were also noticed in some rats. Similar findings were reported by [14,28]. These alterations might be due to fipronil impaired hypothalamus-pituitary thyroid (HPT) axis,

Table 1: Mean values of serum T3 (ng/dl) in rats of different experimental groups.

Experimental Period (weeks)	GROUP I	GROUP II	GROUP III	GROUP IV
2	152.98	100.30	159.05	154.36
4	153.77	79.03	161.11	151.04
6	155.26	68.25	165.26	139.46
Mean ± SE	154 ± 0.66^{a}	82.52 ± 9.41^{b}	161.80 ± 1.82^{a}	148.28 ± 4.51^{a}

Mean values with different superscripts differ significantly ($P < 0.05$), ANOVA, S.E – Standard Error

Table 2: Mean values of serum T4 (µg/dl) in rats of different experimental groups.

Experimental Period (weeks)	GROUP I	GROUP II	GROUP III	GROUP IV
2	9.3	6.9	8.2	10
4	9.5	3.8	8.5	8.8
6	9.8	2.1	8.6	6.7
Mean ± SE	9.53 ± 0.14^{a}	4.26 ± 1.40^{b}	8.43 ± 0.12^{a}	8.5 ± 0.96^{a}

Mean values with different superscripts differ significantly ($P < 0.05$), ANOVA, S.E – Standard Error

Table 3: Mean values of serum TSH (µIU/ ml) in rats of different experimental groups

Experimental Period (weeks)	GROUP I	GROUP II	GROUP III	GROUP IV
2	4.09	7.42	4.11	5.01
4	4.12	7.92	4.08	5.31
6	4.13	8.46	4.06	4.68
Mean ± SE	4.11 ± 0.01^{c}	7.93 ± 0.30^{a}	4.08 ± 0.01^{c}	5 ± 0.18^{b}

Mean values with different superscripts differ significantly ($P < 0.05$), ANOVA, S.E – Standard Error

which reduces the secretion of thyroid hormones like T3, and T4. In addition to hormonal imbalance, free radicals produced by fipronil sulfone cause increased peroxidation of thyroid follicular membrane. These imbalances inhibit the inorganic iodate transfer to the interior of follicles, inhibit colloid conversion into T3 and T4, and various histological alterations in the thyroid gland [13]. Microscopically, similar lesions were observed in ameliorated rats with reduced intensity. Most of the follicles restored their normal architecture with the presence of colloidal secretions inside the follicle, mild congestion, and mild degenerative changes (Fig: 1D). Similar findings were noticed by another author with [21]. It might be due to its free radical scavenging and antioxidant activity [29,30,31] which protects the thyroid gland from oxidative damages induced by fipronil. *Punica granatum* exerts potent anti-inflammatory effects by inhibiting the nuclear factor kappa B (NF-κB) signaling pathway. Polyphenols in the peel inhibit NF-κB activation, leading to a reduction in the production of pro-inflammatory cytokines such as tumor necrosis factor-alpha (TNF-α), interleukin-1 beta (IL-1β), and interleukin-6 (IL-6) [32]. This suppression of inflammatory mediators helps maintain the basement membrane integrity of thyroid follicles and prevents inflammatory-mediated destruction of thyroid parenchyma. Restoration of the cellular redox balance and improvement of mitochondrial function support the normal biosynthesis of thyroglobulin and promote the re-secretion of colloidal material into the follicular lumen [32]. The reduced oxidative and inflammatory stress allows thyrocytes to re-differentiate into their normal cuboidal morphology, leading to normalization of thyroid follicular architecture.

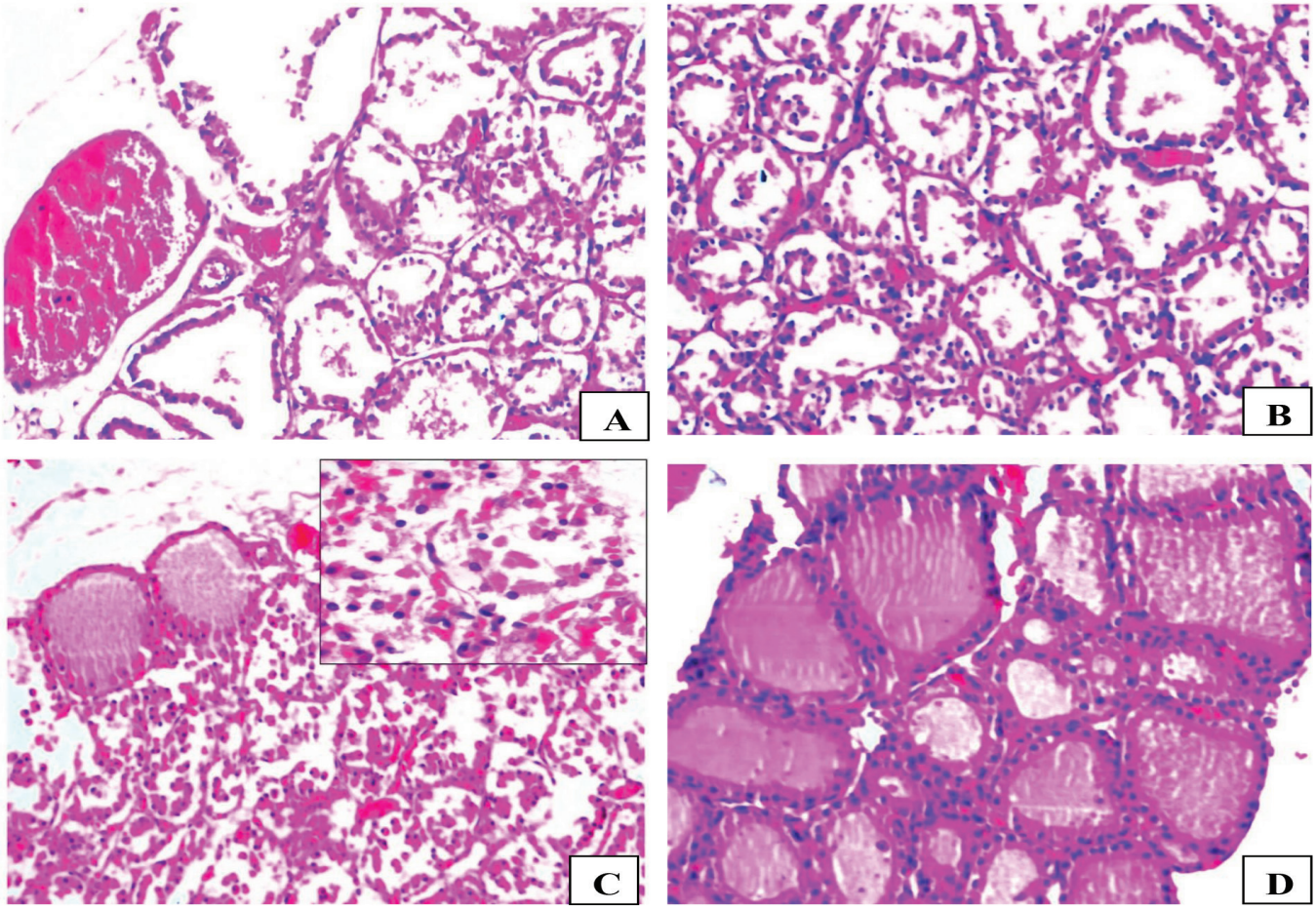

Fig. 1. Histopathological changes of thyroid gland in different experimental groups: (A) Complete loss of architectural details of thyroid follicles with a lack of colloid and interfollicular blood vessel congestion in Group II rats. H & E: x 100. **(B) Severe degeneration and desquamation of thyroid follicles with desquamated cellular debris inside the lumen and variation in the size of follicles in Group II rats.** H & E: x 100. **(C) Severe disruption and complete architectural loss of follicles in Group II rats.** H& E: x 100 (Insight microphotograph x 400). **(D) Restoration of normal architecture with presence of colloidal secretions inside the follicle, mild congestion, and mild degenerative changes in Group IV rats.** H & E: x 100.

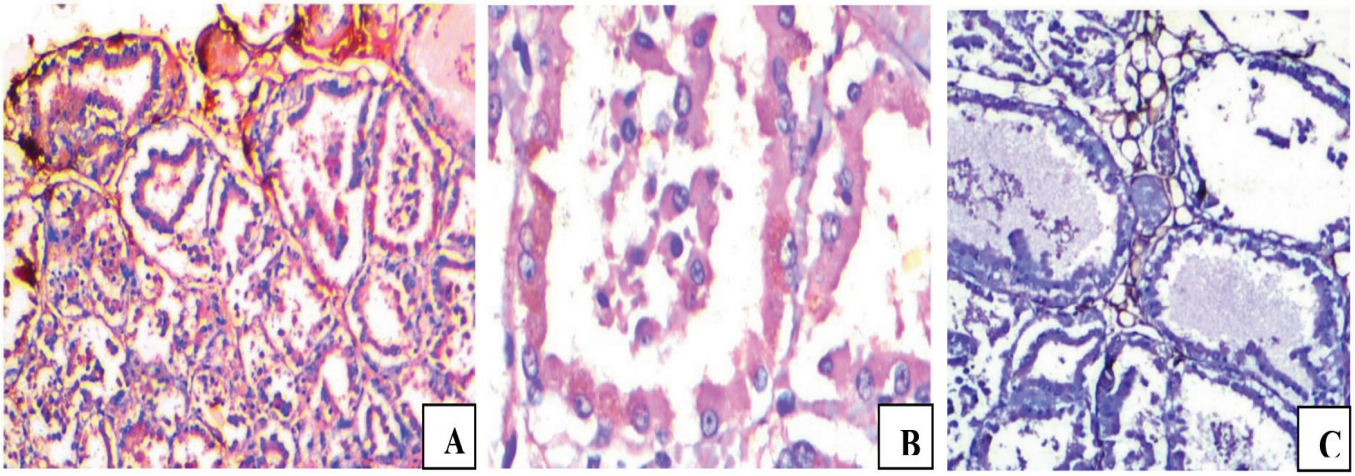

Fig. 2. Immunohistochemistry with BAX marker to check the apoptosis level: (A) Increased reaction in lining epithelium of thyroid follicles of Group II animals. BAX marker x 100; **(B) Increased reaction in lining epithelium of thyroid follicles in Group II animals.** BAX marker x 400; (**C) Negative immunoreactivity of thyroid follicles in Group IV rats.** BAX marker x 100.

Immunohistochemistry was done for the detection of apoptotic changes in thyroid by using monoclonal antibodies against BAX antigen in which brown colour develops indicates the presence of antigen. Immunohistochemically, BAX antigen was detected in the lining epithelium of thyroid follicles (Fig 2A, B) of fipronil treated rats (Group II). The similar observations were made by [33,34,35]. The findings might be due to fipronil induced alteration in the mitochondrial membrane integrity and inhibition of energy transport chain. In addition to decreased ATP production, it also activates the apoptotic enzymes like caspases 3 and 7 which initiates cell damage [2]. *Punica granatum* ameliorated rats (Group IV) showed mild immunoreactivity and decreased expression of BAX antigen (Fig 2C).This might be due to presence of ellagic acid and gallic acid present in pomegranate peel extract which exhibit antioxidant properties and powerful free radical scavengers which supresses lipid peroxidation and apoptotic damage of tissues by restoring the antioxidant enzyme activities like catalase, peroxidase and superoxide dismutases [36,37]. Punicalagin and ellagic acid downregulate the expression of the pro-apoptotic protein BAX while upregulating the anti-apoptotic protein Bcl-2, thereby improving the Bcl-2/BAX ratio [38]. This alteration in the expression of apoptotic regulators prevents mitochondrial outer membrane permeabilization and inhibits the downstream caspase cascade, ultimately reducing thyrocyte apoptosis and preserving the structural integrity of the follicular epithelial lining [21].

CONCLUSION

The present study was caried out to check the effects of fipronil toxicity in thyroid gland of Wistar albino rats and to check the ameliorative effect of *Punica granatum* peel extract in it. The observations made in this study indicates that fipronil @ 10 mg/kg b. wt. /day orally for a period of 6 weeks induces toxic effects on thyroid gland in rats due to accumulation of fipronil metabolites in these organs and associated oxidative damage. Alterations of thyroid hormones indicating that fipronil has an endocrine disruptive action. Co-administration of *Punica granatum* peel extract along with fipronil resulted in a significant improvement of hormonal status and restored histologic structures of thyroid gland near to normal which clearly supports the ameliorative potential of *Punica granatum* (pomegranate) peel extract for fipronil induced endocrine disruptions.

ACKNOWLEDGEMENT

All the authors are highly thankful to Sri Venkateswara Veterinary University, Tirupati for providing all facilities for the successful conduction of this research work.

REFERENCES

1. Eisenstein M. Pesticides: Seeking answers amid a toxic debate. Nature. 2015; 521(7552): 52-55, DOI:10.1038/521 S52a.

2. Das PC, Cao Y, Cherrington N. Fipronil induces CYP isoforms and cytotoxicity in human hepatocytes. Chem Biol Interact. 2006; 164 (3): 200–214, DOI: 10.1016/j. cbi.2006.09.013.

3. Hainzl D, Cole LM, Casida JE. Mechanisms for selective toxicity of fipronil insecticide and its sulfone metabolite and desulfinyl photoproduct. Chem Res Toxicol. 1998; 11 (12): 1529–1535, DOI: 10.1021/tx980157t.

4. Scandalios JG. Oxidative stress: molecular perception and transduction of signals triggering antioxidant gene defenses. Braz J Med Biol Res. 2005; 38: 995–1014, DOI: 10.1590/S0100-879X2005000700003.

5. Leghait J, Gayrard V, Toutain PL, Picard-Hagen N, Viguié C. Is the mechanism of fipronil-induced thyroid disruption specific to the rat: re-evaluation of fipronil thyroid toxicity in sheep? Toxicol Lett. 2010; 194 (3): 351–357.

6. De Oliveira PR, Bechara GH, Denardi SE, Oliveira RJ, Mathias MI. Cytotoxicity of fipronil on mice liver cells. Microsc Res Tech. 2012; 75: 28–35, DOI:10.1002/jemt.21018.

7. Khan S, Jan MH, Kumar D, Telang AG. Fipronil induced spermotoxicity is associated with oxidative stress, DNA damage and apoptosis in male rats. Pestic Biochem Physiol. 2015; 124: 8–14, DOI: 10.1016/j.pestbp.2015.03.010.

8. Calapai G. European legislation on herbal medicines: a look into the future. Drug Saf. 2008; 31: 428–431, DOI: 10.2165/00002018-200831050-00009.

9. Braun LA, Tiralongo E, Wilkinson JM, Spitzer O, Bailey M, Poole S. Perceptions, use and attitudes of pharmacy customers on complementary medicines and pharmacy practice. BMC Complement Altern Med. 2010; 10: 38, DOI: 10.1186/1472-6882-10-38.

10. Gil MI, Tomás-Barberán FA, Hess-Pierce B, Holcroft DM, Kader AA. Antioxidant activity of pomegranate juice and its relationship with phenolic composition and processing. J Agric Food Chem. 2000; 48: 4581–4589, DOI: 10.1021/jf000404a.

11. Culling CFA. Handbook of Histopathological and Histochemical Techniques (Including Museum Techniques). 3rd ed. 1974; p. 361.

12. Snedecor WG, Cochran GW. Statistical Methods. 6th ed. Oxford and IBH Publishing Company, New Delhi. 1967; 258–268.

13. Hurley PM. Mode of carcinogenic action of pesticides inducing thyroid follicular cell tumours in rodents. Environ Health Perspect. 1998; 106: 437- 45, DOI: 10.1289/ehp.98106437.

14. Leghait J, Gayrard V, Picard-Hagen N, Camp M, Perdu E, Toutain PL, Viguié C. Fipronil-induced disruption of thyroid function in rats is mediated by increased total and free thyroxine clearances concomitantly to increased activity of hepatic enzymes. Toxicology. 2009; 255(1-2): 38-44, DOI: 10.1016/j.tox.2008.09.026.

15. Tukhtaev KR, Zokirova NB, Tulemetov SK, Tukhtaev NK. Effect of prolonged exposure to low doses of fipronil on thyroid function of pregnant rats and their offspring. Internet J Toxicol. 2013; 10(1).

16. Gupta RC. Toxicology of organophosphate and carbamate compounds. Academic Press; 2012; pp. 209-216.

17. Köhrle J. Local activation and inactivation of thyroid hormones: the deiodinase family. Mol Cell Endocrinol. 1999; 151: 103–119, DOI: 10.1016/S0303-7207(99)00040-4.

18. Schmutzler C, Bacinski A, Gotthardt I, Huhne K, Ambrugger P, Wallaschofski H, et al. The role of environmental chemicals in thyroid hormone dysfunction in humans. Eur J Endocrinol. 2007; 157: 603–616.

19. Shelby MK, Cherrington NJ, Vansell CD, Klaassen CD. Tissue mRNA expression of the rat UDP-glucuronosyltransferase gene family. Drug MetabDispos. 2003; 31: 326–333, DOI: 10.1124/dmd.31.3.326.

20. Zhao Y, Tan YS, Dai J, Chen H. Fipronil exposure induces thyroid hormone disruption through multiple mechanisms in zebrafish. Environ Pollut. 2016; 219: 456–464.

21. Noya DAE, Soliman MAE, Bashandi MA. Light and electron microscopic study on the possible protective effect of pomegranate peel extract on the pituitary-thyroid axis exposed to monosodium glutamate in adult male albino rats. Egypt J Histol. 2022; 45: 667–686.

22. Viuda-Martos M, Fernandez-Lopez J, Perez-Alvarez JA. Pomegranate and its many functional components as related to human health: a review. Compr Rev Food Sci Food Saf. 2010; 9: 635–654, DOI: 10.1111/j.1541-4337.2010.00131.x.

23. Ismail T, Sestili P, Akhtar S. Pomegranate peel and fruit extracts: a review of potential anti-inflammatory and anti-infective effects. J Ethnopharmacol. 2012; 143: 397–405, DOI: 10.1016/j.jep.2012.07.004.

24. Silva JE, Bianco SDC. Thyroid-adrenergic interactions: physiological and clinical implications. Thyroid. 2008; 18: 157–165, DOI: 10.1089/thy.2007.0252.

25. Xu J, Wang C, Jiang H, Dai H. Ellagic acid alleviates oxidative stress and inflammation via Nrf2/ARE signaling in a model of Parkinson's disease. Food Chem Toxicol. 2014; 70: 151–160, DOI: 10.3389/fphar.2021.757161.

26. Saha P, Das S, Das S. Silymarin: the hepatoprotective agent. Nat Prod Radiance. 2011; 3: 66–70.

27. Bianco AC, Kim BW. Deiodinases: implications of the local control of thyroid hormone action. J Clin Invest. 2006; 116: 2571–2579, DOI: 10.1172/JCI29812.

28. Roques BB, Lacroix MZ, Puel S, Gayrard V, Picard-Hagen N, Jouanin I, Viguié C. CYP450-dependent biotransformation of the insecticide fipronil into fipronil sulfone can mediate fipronil-induced thyroid disruption in rats. Toxicol Sci. 2012; 127(1): 29-41, DOI: 10.1093/toxsci/kfs094.

29. Shiban M, Al-Otaibi M, Al-Zoreky N. Antioxidant activity of pomegranate (Punica granatum L.) fruit peels. Food Nutr Sci. 2012, DOI: 10.4236/fns.2012.37131.

30. Dkhil MA. Anti-coccidial, anthelmintic and antioxidant activities of pomegranate (Punica granatum) peel extract. Parasitol Res. 2013; 112: 2639-2646, DOI: 10.1007/s00436-013-3430-3.

31. Hasan S, Elrahman A, Abou-Rawash A, Bekheet M, Abou-Rawash R, Hassan S. Protective role of an aqueous extract of Punica granatum (pomegranate) peel on lead-induced anemia in rats. 2016, DOI: 10.5455/ajvs.228349.

32. Larrosa M, Tomas-Barberan FA, Espin JC. The dietary hydrolysable tannin punicalagin releases ellagic acid that induces apoptosis in human colon cancer Caco-2 cells by using the mitochondrial pathway. J Nutr Biochem. 2010; 17: 611–625, DOI: 10.1016/j.jnutbio.2005.09.004.

33. Abdel-Daim MM, Abdeen A. Protective effects of rosuvastatin and vitamin E against fipronil-mediated oxidative damage and apoptosis in rat liver and kidney. Food Chem Toxicol. 2018; 114: 69-77, DOI: 10.1016/j.fct.2018.01.055.

34. Sayed AA, El-Desouky MA, Ibrahim KA. Garlic and allopurinol attenuate hepatic apoptosis induced by fipronil in male albino rats. RegulToxicolPharmacol. 2019; 107: 104400, DOI: 10.1016/j.yrtph.2019.05.025.

35. Tohamy HG, El-Kazaz SE, Alotaibi SS, Ibrahiem HS, Shukry M, Dawood MA. Ameliorative effects of boswellic acid on fipronil-induced toxicity: antioxidant state, apoptotic markers, and testicular steroidogenic expression in male rats. Animals. 2021; 11(5): 1302, DOI: 10.3390/ani11051302.

36. Ashoush IS, El-Batawy OI, El-Shourbagy GA. Antioxidant activity and hepatoprotective effect of pomegranate peel and whey powders in rats. Ann Agric Sci. 2013; 58(1): 27-32, DOI: 10.1016/j.aoas.2013.01.005.

37. Sayed S, Alotaibi SS, El-Shehawi AM, Hassan MM, Shukry M, Alkafafy M, Soliman MM. The anti-inflammatory, anti-apoptotic, and antioxidant effects of a pomegranate-peel extract against acrylamide-induced hepatotoxicity in rats. Life. 2022; 12(2): 224, DOI: 10.3390/life12020224.

38. Lei F, Zhang XN, Wang W, Xing DM, Xie WD, Su H, Du LJ. Evidence of anti-obesity effects of the pomegranate leaf extract in high-fat diet induced obese mice. Int J Obes. 2007; 31: 1023–1029, DOI: 10.1038/sj.ijo.0803502.

Cite this article as: Nakul P, Sujatha K, Kumar AA, Vijayalakshmi S. Protective effect of *Punica granatum* peel extract againts fipronil induced thyroid toxicity in male wistar albino rats. Explor Anim Med Res. 2026; 16(1), DOI: 10.52635/eamr/16.1.63-70.

Explor Anim Med Res.
Vol. 16, Issue 1, 2026
DOI: 10.52635/eamr/16.1.71-76

ISSN 2277-470X (Print), ISSN 2319-247X (Online)
Website: www.animalmedicalresearch.org

Published under the CC BY-NC 4.0 license

Research Article

EFFECT OF BAEL AND CURRY LEAVES ON THE REPRODUCTIVE PERFORMANCE OF ANESTROUS BINJHARPURI CATTLE

K. Sethy*, A.K. Nahak, R.D. Mukherjee, N. Panda, V.T. Andhale, and D. Thakur

Received 26 June 2025, revised 26 April 2026

ABSTRACT: Medicinal plants have shown promising potential in treating reproductive disorders in livestock. Bael and curry leaves are an excellent source of calcium, phosphorus, iron and other minerals, which sensitizes the activity of reproductive hormones enhancing fertility in animals. 32 Anestrous Binjharpuri heifers were randomly assigned into four dietary treatment groups, with 8 cattle in each group. The treatments were T1: basal diet, T2: basal diet + bael leaves (50g/ day / animal), T3: basal diet + curry leaves (50g/ day/ animal), T4: basal diet + bael leaves (50g/ day/ animal) + curry leaves (50g/ day/ animal). The trial continued for 60 days, body weight was measured on the first and last day of the experiment. Blood samples were collected at the end to assess the blood chemistry, antioxidants and serum minerals concentration of the animals. Onset of oestrous and conception rate was assessed throughout the experiment. Results revealed that supplementation of bael and curry leaves significantly (P<0.05) improved body weight gain, antioxidants, mineral status and conception rate in Binjharpuri anestrous cattle. Serum triglycerides and total cholesterol were significantly (P<0.05) reduced in treated animals compared to control animals.

Keywords: Anestrous, Bael, Binjharpuri cattle, Body weight, Curry, Stress, Reproduction.

INTRODUCTION

Binjharpuri cattle is one of the important indigenous cattle breeds of the state of Odisha serving to the farming community as dual-purpose cattle. It still exists in its purest form after so long use of artificial insemination. It is also known as "Deshi", in its native tract of the Jajpur district of Odisha state [1]. This breed of cattle is mainly reared by marginal farmers and poorer sections of the people for production of the milk and agricultural operations like ploughing. Reproductive health issues pose significant challenges to the Binjharpuri cattle affecting the economic status of poor farmers [2]. Reproductive health concerns negatively impact the reproductive rate of heifers, causing delays in their integration into breeding herds and reducing the overall number of calves and milk production per cow. This results in substantial financial losses for small and marginal farmers [3]. Anestrous is the one of important reproductive cycle functional abnormality characterized by the lack of an apparent sign of estrus, either expressed or not recognized. A variety of treatment options, including both hormonal and non-hormonal approaches, are utilized to effectively manage this problem. However, the majority of synthetic medications have been met with reluctance from Binjharpuri dairy farmers due to substantial financial outlay and inconsistent outcomes. Alternative, more affordable, and safer options are available instead of more expensive hormones. Various medicinal plants have shown promising potential in treating reproductive disorders in livestock [4]. The plants curry (*Murraya koenigii*) and bael (*Aegle marmelos*) leaf have been individually studied for their potential to enhance fertility in laboratory animals, and anoestrous goats [5,6]. There is limited research on Binjharpuri cattle. This research intends to improve our understanding of this field, so contributing to the preservation and advancement of the Binjharpuri breed's productivity and sustainability. Using the aforementioned information into consideration, a planned study has been designed to evaluate the effectiveness of *Murraya koenigii* and *Aegle marmelos*, separately and in combination, in inducing estrus in Anestrous Binjharpuri cattle in field conditions.

AICRP on NPAERPA, Department of Animal Nutrition, C.V.Sc. &A.H., OUAT, Bhubaneswar, India
**Corresponding author. e-mail: ksethy@ouat.ac.in*

MATERIALS AND METHODS

Selection of animals and dietary treatments

For the trial, 32 anoestrous Binjharpuri heifers with age more than 3 years with no physiological or anatomical abnormalities and normal genital tracts were selected from the Binjharpur block of Jajpur district, Odisha.

The study was carried out as per the guidelines laid down by the Institutional Animal Ethics Committee (433/GO/Re/S/01CCSEA). The animals were dewormed prior to the trial with fenbendazole, a broad-spectrum anthelmintic, at a dose of 10 mg/kg body weight. For the trial, the animals were randomly assigned to four treatment groups, each comprising 8 heifers following a completely randomized design. Treatment groups were T1: basal diet, T2: basal diet + bael leaves (50g/ day / animal), T3: basal diet + curry leaves (50g/ day/ animal), T4: basal diet + bael leaves (50g/ day/ animal) + curry leaves (50g/ day/ animal). The animals were offered a diet with concentrate + paddy straw (basal diet) and were managed in accordance with standard husbandry practices. 32% crushed maize, 26% soybean, 39% wheat bran, 2% mineral mixture, and 1% salt were used to make the concentrate mixture. The animals were given individual feed and clean water on a regular basis, two to three times daily, without access to outdoor grazing. The trial was carried out over a span of 60 days.

Preparation of bael and curry powder

Fresh, mature green leaves of *Aegle marmelos* and *Murraya koenigii* were collected in and around Bhubaneswar. The leaves underwent a thorough washing process and were subsequently left to dry in the shade for 48 hours at ambient temperature. Following the drying process, the leaves were separated from their stems and ground into a fine powder using a vertical grinder. Subsequently, 50 grams of each powdered sample were carefully stored in sealed plastic bags under ambient temperature conditions. Prior to administration to the animals, the powdered leaves were combined with jaggery. The proximate composition of the basal diet along with *Aegle marmelos* and *Murraya koenigii* samples were determined in accordance with [7] guidelines.

Body weight gain

The body weight was measured using Johnson's formula [8] at 0 and 60 days of the experiment. The BW gain was assessed by subtracting initial from final weight and average daily gain (ADG) was calculated.

Estimation of blood chemistry

Blood samples from each animal were collected at 60 days of the experiment through jugular vein puncture in a 20 ml test tube. The tubes were then placed for 3-4 hours in a slanted position to ease the serum separation. Subsequently, the blood clot was carefully detached from the tube walls using an applicator stick, ensuring the prevention of haemolysis. The serum was then carefully extracted using an auto-pipette and transferred to labelled, capped glass vials. These serum samples were then placed in a thermocol container with ice for transportation and subsequently stored at -40°C for future analysis. An automated biochemistry analyser was used to assess the serum glucose, total protein, urea, triglycerides, and total cholesterol.

Estimation of antioxidant enzymes

According to [9], lipid peroxidation in RBC hemolysate was measured. The extinction coefficient of 1.56×10^8 was used to compute malondialdehyde (MDA) concentration in haemoglobin [10]. The Bergmeyer [11] method was used to measure the amount of catalase (CAT) in erythrocytes. Nitro blue tetrazolium was used as a substrate to evaluate the superoxide dismutase (SOD) activity following appropriate dilution in accordance with Marklund and Marklund [12], with some adjustments recommended by Minami and Yoshikawa [13].

Estimation of serum minerals

Triple acid mixture (nitric acid, sulphuric acid and perchloric acid at a ratio of 4:2:1) was used to digest the serum samples and the concentration of Ca, P, Fe, Zn, and Cu was measured using ICP-OES (Toplab India, Mumbai).

Reproductive status

For the onset of heat, the animals were observed on a regular basis. Behavioural signs were used to identify the heat [14]. The local veterinary assistant surgeon artificially inseminated animals showing signs of heat using the semen of a Binjharpuri bull. After 45 days of insemination, a routine pregnancy diagnosis was performed per rectally.

Statistical analysis

Software Package for Social Sciences (SPSS) version 17.0 [15] was used to do a one-way analysis of variance on the collected data, and Duncan [16] was used to compare the means at a significance level of $P<0.05$.

RESULTS AND DISCUSSION

Chemical composition of basal diet

The concentrate mixture and paddy straw had crude protein (CP) contents of 19.35% and 2.15 percent, respectively (Table 1). The CP, crude fiber (CF) and total ash content of bael leaves were 5.70%, 18.70%, 9.50% respectively, whereas curry leaves had CP 7.20 %, CF 12.80 %, and TA 10.60 %. (Table 1).

Similar to our result [17] observed 5.90 % CP, 1.80 % ether extract and 9.20 % total ash in bael leaf powder. It was also found that *Murraya koenigii* have CP content between 2.1–12.5%, TA content in the range of 9.70–13.06%, and acid insoluble ash (AIA) ranging from 1.35–1.82% [18].

Body weight and average daily gain

BW gain and ADG were significantly ($P < 0.05$) higher in all the treated groups than control group (Table 2) indicated that addition of leaves of bael and curry improved the BW gain of anoestrous Binjharpuri

Table 1. Chemical composition of the basal diet (% DM basis)

Attributes	Concentrate mixture	Paddy straw	Bael leaves	Curry leaves
Organic matter	89.90	88.50	90.50	89.40
Crude Protein	19.35	2.15	5.70	7.20
Crude fibre	12.20	39.20	18.70	12.80
Nitrogen Free extract*	55.45	45.10	64.25	64.90
Ether extract	2.90	2.05	1.85	4.50
Total Ash	10.10	11.50	9.50	10.60

*Calculated value

Table 2. Body weight (Kg) Changes in Binjharpuri cattle.

Days	Treatments				P value
	T1	T2	T3	T4	
Initial (0 day)	199.50± 3.90	199.90± 4.60	199.50± 3.50	200.00± 4.00	0.930
Final (60 days)	205.70± 3.70	208.50± 3.00	208.00± 4.01	210.20± 4.10	0.068
Gain (Kg)	6.20^{a}±0.60	8.60^{b}±0.55	8.50^{b}±0.49	10.20^{c}±0.58	0.031
ADG (g)	103.33^{a}±12.16	143.33^{b}±12.50	141.67^{b}±11.90	170.00^{c}±10.20	0.017

^{ab}Values bearing different superscripts in a row differ significantly ($P<0.05$)

Table 3. Serum biochemical profile of Binjharpuri cattle

Parameter	Treatments				P value
	T1	T2	T3	T4	
Glucose(mg/dl)	50.52±3.90	52.60±3.07	53.05±3.10	52.94±3.50	0.885
Total Protein (g/dl)	6.60±0.27	6.85±0.05	6.80±0.18	6.69±0.16	0.601
Urea (mg/dl)	33.55±5.11	32.05±3.12	32.20±5.20	31.90±3.64	0.147
Triglyceride (mg/dl)	80.20^{a}±1.25	74.90^{b}±1.50	75.10^{b}±1.74	71.57^{b}±1.02	<0.01
Total cholesterol (mg/dl)	160.30^{a}±7.28	140.50^{b}±5.00	134.45^{b}±6.30	121.03^{b}±4.70	<0.01

^{ab}Means bearing different superscripts in a row differ significantly ($P < 0.05$)

Table 4. Antioxidant enzyme status (U/ mg haemoglobin) of Anestrous Binjharpuri cattle.

Parameter	Treatments				P value
	T1	T2	T3	T4	
Catalase	1.80^{a}±0.05	2.18^{b}±0.04	2.05^{b}±0.08	2.42^{c}±0.20	0.012
SOD	19.50^{a}±1.90	25.90^{c}±2.05	22.70^{b}±1.70	26.88^{c}±2.10	<0.01
LPO	3.57^{c}±0.21	2.85^{ab}±0.10	3.00^{b}±0.12	2.47^{a}±0.05	0.020

^{abc}Means bearing different superscripts in a row differ significantly ($P < 0.05$)

Table 5. Mineral status of experimental animals

Minerals	Treatments				P value
	T1	T2	T3	T4	
Ca (mg/dl)	7.60^{a}±0.31	8.90^{b}±0.52	8.60^{b}±0.57	9.15^{bc}±0.49	<0.01
P(mg/dl)	4.17^{a}±0.15	5.03^{b}±0.17	5.11^{b}±0.10	5.48^{c}±0.23	0.005
Fe (ppm)	19.15^{a}±1.05	23.52^{b}±0.98	28.51^{c}±1.57	29.56^{c}±1.06	<0.01
Zn (ppm)	4.40^{a}±0.31	5.67^{b} ±0.26	5.80^{b}±0.32	5.92^{b}±0.24	0.013

^{abc}Values bearing different superscripts in a row differ significantly (P<0.05).

cattle. Combined supplementation has shown better response compared to individual supplementation.

This result corresponds with the findings where rats' body weight significantly increased upon feeding of powdered bael leaves [19]. Significantly (P<0.05) higher BW was observed in kids supplemented with polyherbal preparation containing *Withania somnifera, Ocimum tenuiflorum, Tinospora cordifolia* and *Aegle marmelos* to Black Bengal goats [20]. Contrary to this, [21] noticed non-significant difference in body weight gain in crossbred heifers supplemented with bael and curry leaves. This may be due to a different breed of cattle compared to the present experiment. Increased gain might be due to better nutrient digestion and availability in supplemented animals compared to the control [22].

Blood biochemicals

The values of blood glucose, total protein, and urea at 2-month experimental period showed non-significant (P>0.05) difference among the treatments, whereas significant (P<0.05) decreased in serum triglycerides and total cholesterol was seen in treated animals than the control (Table 3).

Similar to our observation, Priyadarshinee *et al.* [21] observed similar serum glucose, total protein concentration and decreased serum total cholesterol and triglycerides in cross bred cows supplemented with bael and curry leaves. *Murraya koenigii* is rich in genistein, diphenolic phytoestrogens which reduces the cholesterol and triglycerides in animals [23]. [24] also proposed that bioactive compounds found in a variety of plants were in charge of lowering total cholesterol levels by boosting fat excretion into faeces and decreasing fat absorption in the digestive tract. According to [25], *A. marmelos* and *M. koenigii* contain secondary plant metabolites such as flavonoids, which are responsible for monitoring the normal lipid profile in animals due to strong lecithin acetyl transferase activity.

Antioxidant status

Supplementing with bael and curry leaves significantly (P<0.05) raised catalase and SOD levels and lowered (P<0.05) LPO, as seen by a drop in MDA levels (Table 4). Similarly, [26] observed increased catalase and SOD activity in rats supplemented with curry leaves extract. Curry and bael leaves give protection against oxidative damage to the living cells. Various chemical analysis suggest that these plants are abundant in flavonoids, alkaloids, polyphenols, and chlorophyll [17]. These substances acted as antioxidants to combat oxidative stress in animals [27, 28].

Serum minerals

The serum concentration of Ca, P and Fe and Zn was significantly (P<0.05) improved due to bael and curry supplementation in experimental animals (Table 5). The bael and curry leaves are very good sources of Ca, P and Fe and other minerals [29]. Presence of these minerals enhances the utilization of other microminerals and sensitizes various reproductive hormones for better fertility in animals [30]. Similarly, [31] and [32] also observed higher serum Ca and P concentration in animals supplemented with *Murraya koenigii* and *Aegle marmelos*

Reproductive status

The percentage of animals that came into oestrus (oestrus %) and overall conception rates in various treatments were significantly higher in combined bael and curry supplemented animals compared to other treatments. It was also observed that bael and curry supplementation alone improved the reproductive performance of animals compared to non-supplemented control animals (Fig 1).

The results of [33] in delayed pubertal heifers and [34] in Anestrous buffaloes support the result that the conception rate was improved when either

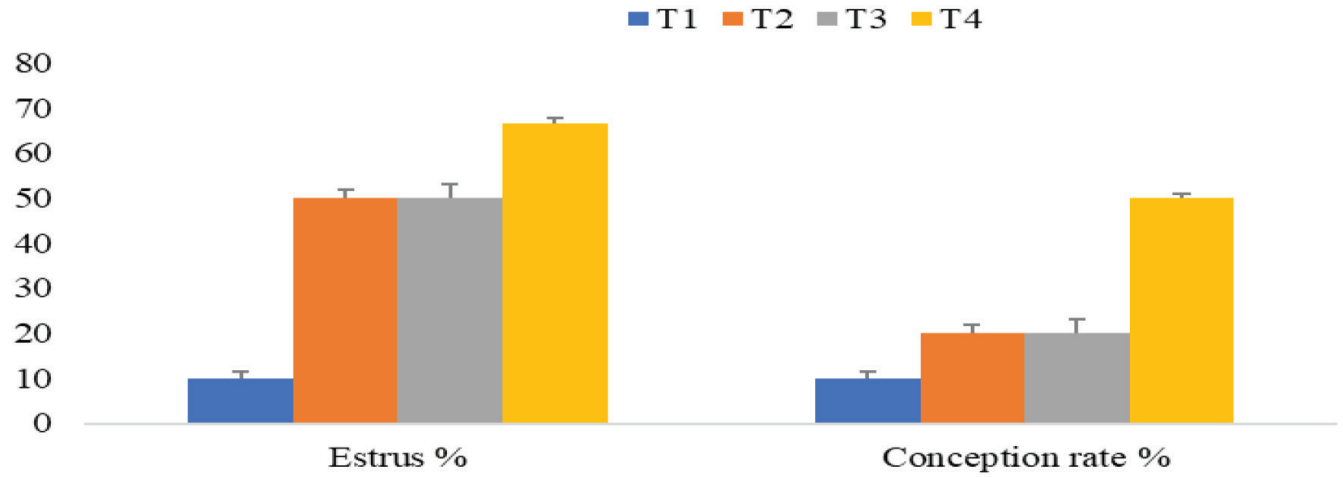

Fig. 1. Reproductive performance in experimental animals.

curry or bael was supplemented. The plant *Murraya koenigii* plays an important role as it may enhance follicular growth and steroidogenesis, thereby leading to induce estrous in Anestrous heifers [31]. Higher antibacterial, anti-inflammatory, and antioxidant qualities of pharmacologically active substances such as koenimbine, murrayacine, girinimbine, koenigine, koenine, mahanimbine, murrayanol, and mahanine may be the cause of treated animals' enhanced conception rates [35]. The plant's genistein content may bind to the estrogen receptor, promoting the growth and development of reproductive organs through the induction of estrous [36].

CONCLUSION

Combined supplementation of dried bael and curry leaves enhanced the body weight gain, antioxidant, mineral status, conception rate and decreased the blood cholesterol and triglyceride levels of anoestrous Binjharpuri cattle.

ACKNOWLEDGEMENT

The authors are grateful to the AICRP on "Nutritional and Physiological Approaches for Enhancing Reproductive Performance in Animal" OUAT, Bhubaneswar, Odisha for this research work.

REFERENCES

1. Dash SK, Sethi BP, Rao PK. Evaluation of Binjharpuri cattle of India in the native tract. Int. J. Livest. Prod. 2013; 4:102–105, DOI: 10.5897/IJLP10.005.

2. Nayak S, Goswami RN, Das GC, Zaman G, Das B, Phookan A, Khanikar D. Evaluation of production performance of Binjharpuri cattle of Odisha. Indian J. Anim. Sci. 2023; 93:100-104, Doi.org/10.56093/ijans.v93i1.128486.

3. Chaudhari CF, Suthar BN, Sharma VK, Dabas VS, Chaudhari NF, Panchsara HH. Estrus induction and fertility response in delayed pubertal Kankrej heifers treated with norgestomet ear implant. Vet. World. 2012; 5:453-458, DOI:10.5455/vetworld.2012.453-458.

4. Khade NB, Patel DM, Naikoo M, Dhami AJ, Sarvaiya NP, Gohel MM. Estrus induction in pubertal anestrus Gir heifers using different hormone protocols. Indian J. Field Vet. 2007; 7:4-8.

5. Kumar R. Effect of *Aegle Marmelos* (Bel) and *Ficus Religiosa* (Pipal) on reproductive performance in anestrus goat and buffalo (Doctoral dissertation). IVRI; 2008.

6. Jondhale NS, Shanker U, Mehrotra S, Agarwal SK, Singh SK, Das GK, Deori S. Effect of *Aegle marmelos* and *Ficus religiosa* leaves extracts on the ovarian function in rats. Indian Vet J.. 2009; 86:1141-1144.

7. AOAC. Official methods of analysis of the Association of Official Analytical Chemistry (16th ed.). AOAC International, Washington, USA; 1995.

8. Johnson DW. Livestock Weights from Measurements. Minnesota Agricultural Experiment Station Folder 70; 1940.

9. Placer ZA, Cushman LL, Johnson BC. Estimation of product of lipid peroxidation (malonyl dialdehyde) in biochemical systems. Anal. Biochem. 1966; 16:359-364, Doi. org/10.1016/0003-2697(66)90167-9.

10. Utley HG, Bernheim F, Hochsein P. Effect of sulphydril reagents on per-oxidation of microsomes. Arch. Biochem. Biophys. 1967; 118:29–32, Doi.org/10.1016/0003-9861(67)90273-1.

11. Bergmeyer HU. U.V. method of catalase assay. In Methods of Enzymatic Analysis (Vol. 3, pp. 273). Wenheim Deerfield Beach, Florida; 1983.

12. Marklund S, Marklund G. Involvement of the superoxide anion radical in the autoxidation of pyrogallol and a convenient assay for superoxide dismutase. Eur. J. Biochem. 1974; 47:469–474, Doi.org/10.1111/j.1432-1033.1974.tb03714.x.

13. Minami M, Yoshikawa H. Simplified assay method of superoxide dismutase activity of clinical use. Clin. Chim. Acta. 1979; 92:337–342, Doi.org/10.1016/0009-8981(79)90211-0

14. Layek SS, Mohanty TK, Kumaresan A, Behera K, Chand S. Behavioural signs of estrus and their relationship to time of ovulation in Zebu (Sahiwal) cattle. Anim. Reprod. Sci. 2011; 129:140-145, DOI: 10.1016/j.anireprosci.2011.11.006.

15. SPSS. Statistical Packages for Social Sciences, Version 20.0. International Business Machines Corporation, IBM SPSS Inc., New York, USA; 2011.

16. Duncan DB. Multiple range and multiple F tests. Biom. 1955; 11:1-42. http://dx.doi.org/10.2307/3001478.

17. Singh AK, Singh S, Saroj PL, Krishna H, Singh RS, Singh RK. Research status of bael (*Aegle marmelos*) in India: A review. Indian J. Agric. Sci. 2019; 89(10):1563-1571.

18. Jain M, Gilhotra R, Singh RP, Mittal J. Curry leaf (*Murraya koenigii):* A spice with medicinal property. MOJBM. 2017; 2(3):236-256, DOI:10.56093/ijas.v89i10.94576.

19. Asghar N, Mushtaq Z, Arshad MU, Imran M, Ahmad RS, Hussain SM. Phytochemical composition, antilipidemic and antihypercholesterolemic perspectives of Bael leaf extracts. Lipids Health Dis. 2018; 17:1-9, DOI:10.1186/s12944-018-0713-9.

20. Sahoo N, Behura NC, Mishra J. Effects of Immu-21 on certain blood biochemicals, milk, colostrum, body weight gain and livability in goats. Phytomedicine. 2001; 2:69-76.

21. Priyadarshinee P, Sethy K, Swain RK, Mishra SK, Behera K, Pradhan SK, Tripathy S. Combined effect of Bel and curry leaves supplementation on the performance of anestrous cattle. Indian J. Anim. Nutr. 2021; 38:240-245, DOI: 10.5958/2231-6744.2021.00035.9.

22. Singh U, Kocher A, Boora R. Proximate composition, available carbohydrates, dietary fibres and anti-Nutritional factors in Bael (*Aegle marmelos L.)* leaf, pulp and seed powder. IJSRP. 2012; 2(4):1-4.

23. Ramadan AA, Afifi NA, Erian EY, Saleh DO, Sedik AA. Beneficial effect of trigonelline on the metabolic changes associated with insulin resistance in rats. World J. Pharm. Pharm. Sci 2015;5(2):1238-1250.

24. Thomas Z, Pertiwi D, Bagus SA, EM BJ, Alfiza NS. Effect of tender coconut water on blood lipid levels in high fat diet fed male rats. JKIMSU. 2017;6(2):63-68.

25. Krupanidhi AM, Kalleshappa CM, Chanchi AR. Antihyperlipidemic activities of isolated bio compounds of *Aegle marmelos*. J. Pharm, Biol. Sci. 2012; 11:42-45. DOI: 10.9790/3008-1105024245

26. Khan BA, Abraham A, Leelamma S. Role of *Murraya koenigii* (curry leaf) and *Brassica juncea* (Mustard) in lipid peroxidation. Indian J. Physiol. Pharmacol. 1996; 40:155-158.

27. Ningappa MB, Dinesha R, Srinivas L. Antioxidant and free radical scavenging activities of polyphenol-enriched curry leaf (*Murraya koenigii L.*) extracts. Food Chem. 2008; 106:720-728. Doi.org/10.1016/j.foodchem.2007.06.057.

28. Tachibana Y, Kikuzaki H, Lajis NH, Nakatani N. Antioxidative activity of carbazoles from *Murraya koenigii* leaves. J. Agric. Food Chem. 2001; 49:5589-5594, DOI: 10.1021/jf010621r.

29. Shanthala M, Prakash J. Acceptability of curry leaf (*Murraya koenigii)* incorporated products and attitude toward consumption. J. Food Process. Preserv. 2005;29(1):33-44, Doi.org/10.1111/j.1745-4549.2005.00011.x.

30. Dutta A, Baruah B, Sharma BC, Baruah KK, Goswami RN. Serum macro mineral profiles in cyclic and anoestrus local heifers in lower Brahmaputra valley of Assam. Indian J. Anim. Res. 2001; 35:44-46.

31. Das AK, Rajkumar V, Dwivedi DK. Antioxidant effect of curry leaf (*Murraya koenigii*) powder on quality of ground and cooked goat meat. Int. Food Res. J. 2011;18(2):563-569.

32. Satheshkumar S, Punniamurthy N. Estrus induction by supplementation of *Murraya koenigii* in anestrus heifers. Indian J. Anim. Reprod. 2009; 30(2):66-67.

33. Das GK, Mehrotra S, Narayanan K, Kumawat BL, De Kumar U, Khan TA. Estrus induction response and fertility performance in delayed pubertal heifers treated with *Aegle marmelos* and *Murraya koenigii*. J. Anim. Res. 2016; 6:151-156, DOI:10.5958/2277-940X.2016.00025.5.

34. Kumar R, Mehrotra S, Shanker U, Barshney VP, Dutt R, Agarwal SK, Das GK, Singh SK. Effect of *Aegle marmelos* and *Ficus religiosa* on endocrine profile and reproductive performance in anoestrus buffaloes. XXV Annual Convention and National Symposium of ISSAR, Namakkal, Tamil Nadu, India, 10-12, Compendium and Souvenir. p. 55; 2009.

35. Handral H, Hoti SL, Shruthi SD. In vitro evaluation of antimicrobial activities of crude extracts from *Murraya koenigii* against pathogenic bacteria. Int J Pharm Pharm Sci. 2012; 4:74-76.

36. Kumi-Diaka J, Rodriguez R, Goudaze G. Influence of genistein (4′, 5, 7-trihydroxyisoflavone) on the growth and proliferation of testicular cell lines. Biol. Cell. 1998; 90:349-354, Doi.org/10.1016/S0248-4900(98)80015-4.

Cite this article as: Sethy K, Nahak AK, Mukherjee RD, Panda N, Andhale VT, and Thakur D. Effect of bael and curry leaves on the reproductive performance of anestrous Binjharpuri cattle. Explor Anim Med Res. 2026; 16(1), DOI: 10.52635/eamr/16.1.71-76.

Explor Anim Med Res.
Vol. 16, Issue 1, 2026
DOI: 10.52635/eamr/16.1.77-84

ISSN 2277-470X (Print), ISSN 2319-247X (Online)
Website: www.animalmedicalresearch.org

Published under the CC BY-NC 4.0 license

Research Article

THE EFFECT OF PLATELET-RICH-PLASMA SUPPLEMENTED EXTENDER ON POST-THAW FERTILITY OF SIROHI AND BARBARI BUCK SEMEN

Arya Mahesh Narkhede[1], Satya Nidhi Shukla[1*], Shivika Chouksey[1] and Anand Kumar Jain[2]

Received 7 April 2025, revised 26 April 2026

ABSTRACT: The freezing and thawing process during cryopreservation of semen decreases motility, compromises membrane integrity and impairs cell function, along with the fertilizing capacity of the spermatozoa. The present study aimed to evaluate the efficacy of platelet-rich plasma (PRP) as a supplement in semen extenders to improve post-thaw fertility of Barbari and Sirohi buck semen. For this study, 288 ejaculates were collected from both breeds, of which 30 best ejaculates from each breed were processed and cryopreserved using a standard protocol. Each ejaculate was divided into three equal aliquots. A tris egg-yolk citrate extender was utilized for dilution, to which varying percentages of PRP were incorporated. The first aliquot of semen was diluted with extender containing 0% PRP (G-I), the second with extender containing 7% PRP (G-II) and the third with extender containing 10% PRP (G-III), respectively. All the ejaculates were evaluated at pre-freeze, equilibration and post-thaw stages. At the pre-freeze stage, semen parameters did not vary significantly across different extenders. However, significantly higher ($p<0.05$) percentage of progressive motility (54.00±1.54,53.66±1.49), sperm viability (62.73±1.54,58.36±1.44) and plasma membrane integrity (51.63±1.85,50.23±2.43) was recorded during post post-thaw stage in Barbari and Sirohi bucks extender supplemented with 7 % PRP. The inclusion of 7% PRP enhanced post-thaw fertility and had a beneficial impact on the semen freezability of Barbari and Sirohi bucks.

Keywords: Cryopreservation, Platelet-rich plasma [PRP], Buck semen, Sirohi, Barbari.

INTRODUCTION

Cryopreservation of semen is essential for maintaining sperm motility and viability for extended periods. However, it is a complex process that can damage the various aspects of the cell membrane along with its function, ultimately diminishing its overall functionality. Cryoinjuries primarily affect sperm motility, plasma membrane functionality and acrosome integrity [1]. Platelet–Rich Plasma (PRP) is a substance, abundant in growth factors that are compatible, homogeneous and non-antigenic. Platelets contain α granules, which on activation release seven fundamental protein growth factors, viz. epidermal growth factor, insulin-like growth factor, vascular endothelial growth factor, transforming growth factor β, nerve growth factor, hepatocyte growth factor and fibroblast growth factor, respectively [2]. Platelets also contain dense platelet granules consisting of histamine, zinc ions, calcium ions, superoxide dismutase, serotonin and adenosine triphosphate, all of which play a crucial role in maintaining cellular and tissue homeostasis [3].

Numerous preventive procedures are implemented to minimize the detrimental effects of semen cryopreservation, including optimizing freezing protocols, engineering freezing apparatus and improving the freezing medium [4]. The addition of cryoprotectants has become the most scientifically researched method, along with antioxidants, peptide molecules, fatty acids, animal serum, nanoparticles, plant essential oils and bioactive analogues. This has proven beneficial for improving sperm quality and viability after cryopreservation. The formulation of the semen extender used in cryopreservation plays a vital role in preserving the integrity of spermatozoa [5].

[1]*Department of Veterinary Gynaecology and Obstetrics, College of Veterinary Science and Animal Husbandry, Nanaji Deshmukh Veterinary Science University, Jabalpur- 482 001, Madhya Pradesh, India.*
[2]*Department of Veterinary Physiology and Biochemistry, College of Veterinary Science and Animal Husbandry, Nanaji Deshmukh Veterinary Science University, Jabalpur- 482 001, Madhya Pradesh, India.*
**Corresponding author. e-mail: snshukla2@gmail.com*

Supplementation of PRP in semen extender at various concentrations has been validated to enhance sperm quality in both fresh and post-thawed conditions in ram at 5% PRP [6], buck at 10% PRP [7], buffalo bull at 10% PRP [8] and human at 5% PRP [5]. The growth factors present in PRP protect the sperm from cryodamage during cryopreservation, which helps maintain sperm viability, acrosomal integrity, plasma membrane integrity and fertility. It also improves both *in vivo* and *in vitro* fertilization, making it a highly effective technique for enhancing fertility [7, 8]. The present study aims to investigate the effectiveness of PRP in preserving sperm fertility during cryopreservation by examining its impact on various physiological parameters. No literature could be traced regarding the potential effects of incorporating Platelet-Rich Plasma (PRP) concentrations into a semen extender on sperm quality and functionality in Indian goat breeds. Therefore, this study was formulated to evaluate the post-thaw fertility of PRP-supplemented buck semen and its effect on the post-thaw recovery rate.

MATERIALS AND METHODS

Animals and semen collection

Six sexually mature adult bucks of each Barbari and Sirohi breeds were selected for this study. The bucks were maintained under a semi-intensive system in the University Goat Farm, NDVSU, Jabalpur, Madhya Pradesh. For six months, routine semen samples were collected with the help of an artificial vagina and rapid testing was done at the field level for assessment of freezability. Ejaculates fulfilling minimum standards were selected for further dilution and then cryopreservation.

PRP preparation

The PRP was prepared by the modified double centrifugation protocol adopted from Salama and co-workers [7]. Briefly, 3ml of whole blood was collected in anticoagulant acid citrate dextrose-A (ACD-A) coated tubes from four additional, sexually mature bucks of both breeds on the day of semen collection and centrifuged initially at 2450 rpm for 5 mins. The supernatant and buffy coat were transferred to another sterile anticoagulant-free tube and re-centrifuged at 3300 rpm for 17 mins to obtain pure PRP. The manual smear slide method was used to calculate platelets in PRP, and a concentration of 10^9 cells/ml PRP was maintained [9]. PRP activation was done by adding 10% calcium chloride in a 1:10 ratio, and the supernatant was used for this study.

Ethical Consideration

The Institutional Animal Ethical Committee of the College of Veterinary Science and Animal Husbandry, Jabalpur, Madhya Pradesh, approved all the animal experiments conducted in this study (certificate no: 13/IAEC/Vety./2024)

Extender preparation

A tris-based semen extender was prepared using tris, citric acid, fructose, 6% glycerol, 10% egg yolk, streptomycin and penicillin dissolved in double-distilled water to make 100ml volume as standardized in the Semen processing lab of the Department of Veterinary Gynaecology and Obstetrics, Jabalpur. The pH was adjusted to 7.0 to 7.2. PRP was added in concentrations of 7%(G-II) and 10%(G-III) to 100 ml of semen extender; the control (G-I) was devoid of PRP.

Semen handling and cryopreservation

The freshly collected semen ejaculates were divided into three equal aliquots. The initial dilution of 1:3 was performed at the farm upon evaluation, followed by a final dilution depending on the sperm concentration in the lab at 4°C before cryopreservation. Post dilution, followed by 4 hours of equilibration, the filling and sealing of semen straws was done. After that, straws were positioned on a freezing rack, 4 cm above the static liquid nitrogen vapor. After seeding for 10 minutes, the straws were immediately plunged into liquid nitrogen and stored at -196°C until further evaluation. A total of 288 ejaculates were collected from both breeds throughout the study interval, out of which the best 60 ejaculates (30 of each breed) were used to assess the effect of PRP as a semen extender at different semen processing stages. Post-thaw semen assessment was done after thawing at 40ºC for 45 sec.

Evaluation of semen

The collected semen samples were evaluated for sperm individual motility, viability, plasma membrane integrity, abnormalities and acrosomal integrity at three stages of semen processing, i.e., pre-freeze, equilibrated and post-thaw stage.

Individual motility (%)

Initial individual motility was evaluated by placing a 10µl drop of diluted semen on a sterilized pre-warmed (37 °C), clean, grease-free glass slide. It was observed under the high-power objective lens (400X) of the compound phase contrast microscope. The percentage of motile spermatozoa was calculated subjectively by

observing the direction and movement of each sperm. Further processing was done on ejaculates that exhibited at least 70% motility [10].

Sperm Viability (%)

The sperm viability (%) was evaluated using the method described by Blom [11]. A small drop of diluted semen was mixed with an equal amount of Eosin-Nigrosin stain in a 1:4 ratio, and a thin, uniform tongue-shaped smear was prepared. After drying, a total of 200 sperms were counted in various fields under a high-power objective lens (400X) of the compound phase contrast microscope. Unstained spermatozoa heads were considered live and partially /completely stained as dead [Figure 1a].

Sperm plasma membrane integrity (%)

The evaluation of sperm plasma membrane integrity was done by the hypo-osmotic swelling (HOS) test as per the method described by Revell and Mrode [12]. Briefly, 0.1ml of diluted semen sample was mixed with 1ml of HOS solution and incubated in a water bath at 37°C for 1 hour. Post incubation, a 10µl drop of sperm suspension was placed on a clean, grease-free glass slide and covered with a coverslip. Two hundred sperms were examined in various fields under a high-power objective lens (400X) of the compound phase contrast microscope for sperm tail swelling. Spermatozoa showing any kind of swelling or curling of the tail were considered as HOST-reacted sperm [Figure 1b] and expressed in percentage. The osmolarity of the HOS solution differed during the pre-freeze (150mOsmol/L) and post-thaw stages (75mOsmol/L) as per the method adopted by Gangwar and co-workers [10].

Acrosomal integrity (%)

The acrosomal integrity percentage was assessed using the Giemsa staining technique as per the method given by Gangwar and co-worker [10]. On a sterilized glass slide, a thin smear of each dilution was prepared and immediately fixed in methanol for thirty minutes after drying. The fixed semen smear was then stained for 90 minutes using freshly made Giemsa working solution (3ml Giemsa stock solution + 2ml Sorensen's phosphate buffer + 45ml distilled water). Spermatozoa having dark purple heads with visible acrosomal ridges were counted as live intact acrosomes, and spermatozoa with light purple/ white heads, remaining unstained or without an acrosomal cap, were counted as dead or non-intact spermatozoa [Figure 1c] and were expressed in percentage. 200 sperms were examined in various fields under a high-power objective lens (400X) of the compound phase contrast microscope.

Sperm abnormalities (%)

The morphological sperm abnormalities were studied using the Rose-Bengal staining technique [10]. A small drop of diluted semen was taken on a clean, grease-free glass slide and a thin, uniform smear was prepared. After drying, the slide was immersed in Rose-Bengal stain for 7 minutes. Following that, it was washed with tap water and air-dried. Two hundred sperm were examined in each smear at a magnification of 400X to determine the incidence of various sperm abnormalities classified as head, mid-piece and tail abnormalities [Figure 1d].

Statistical analysis

The data obtained during the study was subjected to statistical analysis with the help of the statistical software "R" Studio, Package. Data from different experiments were presented as Mean±SE and analyzed by Two-way ANOVA, and Tukey's range test as described by Snedecor and Cochran [13]. The difference at $p \leq 0.05$ was considered satisfactory significant.

RESULTS

Effect of supplementation of PRP in buck semen extender during different processing stages

Individual motility (%)

The individual motility percentage varied among groups across all stages, with a significant ($p < 0.05$) difference observed only at the post-thaw stage. The highest motility was recorded in 7% PRP-supplemented semen extender, followed by 10% and 0%, respectively [Tables 1 and 2].

Sperm viability (%)

For both breeds, sperm viability remained comparable during the pre-freeze and equilibration stages but showed a significant ($p < 0.05$) increase post-thaw in the 7% PRP-supplemented group [Tables 1 and 2].

Plasma membrane integrity (%)

Plasma membrane integrity was assessed by the proportion of HOS-positive spermatozoa and did not differ significantly between the pre-freeze and equilibration stages. However, significant difference ($p < 0.05$) was observed with the 7% PRP-supplemented semen extender, followed by 10% and 0%, as illustrated in Tables 1 and 2 in both breeds.

Acrosomal integrity (%)

The acrosomal integrity followed a similar trend and no significant ($p > 0.05$) difference was seen during pre-freeze and equilibration stage However, a higher value was seen in 7% PRP-supplemented semen extender, followed by 10% and then 0% in both breeds [Table 1 and 2].

Table 1. Seminal parameters in Sirohi buck semen supplemented with PRP at different stages (Mean±SE).

Parameters	Semen processing stages	Sirohi buck semen		
		0% PRP	7% PRP	10% PRP
Individual motility	**Pre-freeze**	$84.40^{a}\pm0.84$	$84.40^{a}\pm0.84$	$84.40^{a}\pm0.84$
	Equilibrated	$78.33^{a}\pm1.36$	$78.33^{a}\pm1.44$	$78.00^{a}\pm1.61$
	Post-thaw	$33.00^{bB}\pm1.92$	$53.66^{bA}\pm1.49$	$48.16^{bA}\pm2.19$
Viability	**Pre-freeze**	$87.96^{a}\pm0.90$	$87.96^{a}\pm0.90$	$87.96^{a}\pm0.90$
	Equilibrated	$83.86^{a}\pm1.14$	$86.30^{a}\pm0.96$	$82.63^{a}\pm1.40$
	Post-thaw	$41.86^{bB}\pm2.12$	$58.36^{bA}\pm1.44$	$51.96^{bA}\pm2.48$
HOS positive	**Pre-freeze**	$82.23^{a}\pm1.06$	$82.23^{a}\pm1.06$	$82.23^{a}\pm1.06$
	Equilibrated	$73.40^{a}\pm1.61$	$75.73^{a}\pm1.30$	$70.50^{a}\pm1.42$
	Post-thaw	$38.43^{bB}\pm2.39$	$50.23^{bA}\pm2.43$	$40.43^{bB}\pm2.40$
Acrosomal Integrity	**Pre-freeze**	$84.36^{a}\pm0.85$	$84.36^{a}\pm0.85$	$84.36^{a}\pm0.85$
	Equilibrated	$76.83^{a}\pm1.30$	$79.03^{a}\pm1.15$	$77.03^{a}\pm1.28$
	Post-thaw	$46.66^{bB}\pm2.21$	$62.93^{bA}\pm1.68$	$54.16^{bB}\pm2.42$
Abnormalities	**Pre-freeze**	$3.96^{c}\pm0.28$	$3.96^{c}\pm0.28$	$3.96^{c}\pm0.28$
	Equilibrated	$5.80^{b}\pm0.35$	$5.50^{a}\pm0.33$	$5.96^{b}\pm0.42$
	Post-thaw	$7.83^{aA}\pm0.43$	$6.16^{aB}\pm0.31$	$7.73^{aA}\pm0.47$

Mean value bearing different superscripts of the same parameter (a,b,c) within the group and (A,B,C) in between groups differ significantly ($p<0.05$).

Table 2. Seminal parameters in Barbari buck semen supplemented with PRP at different stages (Mean±SE).

Parameters	Semen processing stages	Barbari buck semen		
		0% PRP	7% PRP	10% PRP
Individual motility	**Pre-freeze**	$86.66^{a}\pm0.87$	$87.00^{a}\pm0.85$	$87.33^{a}\pm0.82$
	Equilibrated	$80.66^{a}\pm1.26$	$81.00^{a}\pm1.29$	$81.33^{a}\pm1.14$
	Post-thaw	$31.33^{bC}\pm2.29$	$54.00^{bA}\pm1.54$	$45.50^{bB}\pm2.27$
Viability	**Pre-freeze**	$90.83^{a}\pm0.64$	$90.83^{a}\pm0.64$	$90.80^{a}\pm0.63$
	Equilibrated	$87.16^{a}\pm0.93$	$87.13^{a}\pm0.93$	$86.76^{a}\pm0.74$
	Post-thaw	$39.50^{bB}\pm2.26$	$62.73^{bA}\pm1.54$	$56.00^{bA}\pm2.21$
HOS positive	**Pre-freeze**	$86.13^{a}\pm0.82$	$86.13^{a}\pm0.82$	$86.13^{a}\pm0.82$
	Equilibrated	$81.36^{a}\pm1.21$	$83.26^{a}\pm0.96$	$82.96^{a}\pm1.11$
	Post-thaw	$35.36^{bC}\pm2.27$	$51.63^{bA}\pm1.85$	$42.73^{bB}\pm2.36$
Acrosomal Integrity	**Pre-freeze**	$87.40^{a}\pm0.92$	$87.40^{a}\pm0.92$	$87.40^{a}\pm0.92$
	Equilibrated	$81.60^{a}\pm0.99$	$81.70^{a}\pm0.96$	$80.66^{a}\pm0.76$
	Post-thaw	$47.33^{bC}\pm2.25$	$68.90^{bA}\pm1.44$	$59.26^{bB}\pm2.15$
Abnormalities	**Pre-freeze**	$5.13^{b}\pm0.30$	$5.13^{b}\pm0.30$	$5.13^{b}\pm0.30$
	Equilibrated	$5.36^{b}\pm0.35$	$5.23^{a}\pm0.25$	$5.13^{b}\pm0.26$
	Post-thaw	$7.90^{aA}\pm0.32$	$5.76^{aB}\pm0.26$	$6.30^{aB}\pm0.33$

Mean value bearing different superscripts of the same parameter (a,b,c) within the group and (A,B,C) in between groups differ significantly ($p<0.05$) .

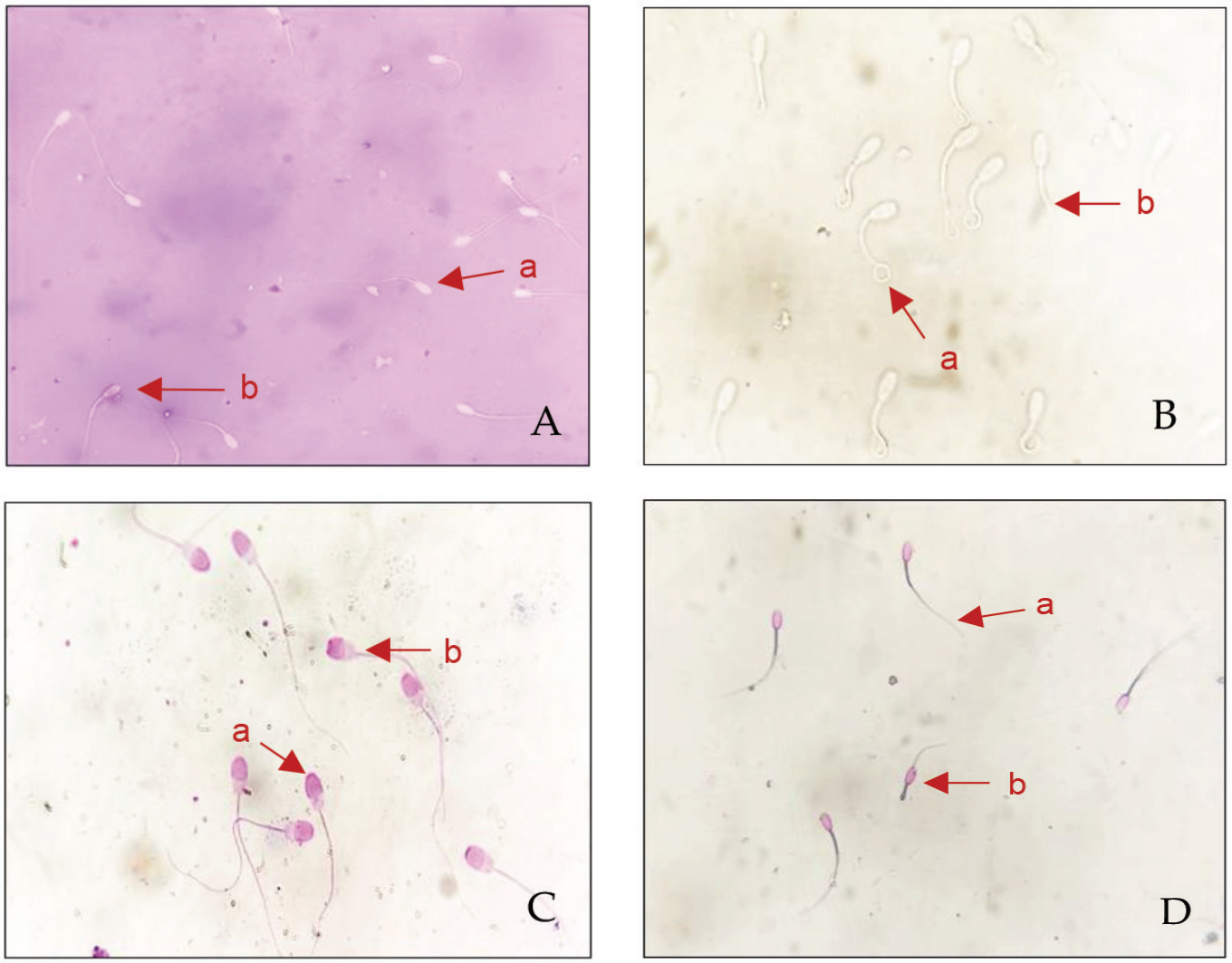

Fig. 1.A. Evaluation of viability of sperm. (a) Live – head colorless/white (b) Dead – pink/purple head. **B. Evaluation of plasma membrane integrity by HOST.** (a) Tail coiled - HOS reacted sperm (b) Tail no coiled - no reaction. **C. Evaluation of acrosome integrity of sperm.** (a) Acrosome intact (b) Acrosome reacted. **D. Evaluation of abnormalities.** (a) Abnormality absent (b) Abnormality present

Sperm abnormalities (%)

No significant ($p > 0.05$) differences were observed during early stages. Post-thaw, abnormalities were significantly ($p < 0.05$) lower in the 7% PRP group compared to 10% and control [Table 1 and 2].

Recovery rate percentage of semen parameters in PRP-supplemented semen extender of both breeds

The recovery rate percentage was calculated between the pre-freeze to post-thaw stage and the equilibrated to post-thaw stage, and the highest values of motility, viability, plasma membrane integrity, acrosomal integrity, and abnormality were found in the group supplemented with 7% PRP, followed by 10% PRP and then 0% PRP in both breeds (Figure 2).

DISCUSSION

The improvement in post-thaw sperm motility, viability, and membrane integrity may be attributed to the bioactive components of PRP, including insulin-like growth factor-1 (IGF-1), transforming growth factor (TGF), serotonin, and nerve growth factor (NGF). These molecules have been reported to enhance sperm function by improving calcium transport, reducing oxidative stress, and maintaining membrane stability. IGF-1 increases intracellular calcium levels, promoting flagellar activity and sperm survival [14], while TGF provides anti-inflammatory protection during cryopreservation [15]. Serotonin is known to improve sperm kinematics [16], and NGF enhances motility and viability by interacting with its receptor on the sperm mid-piece [17].

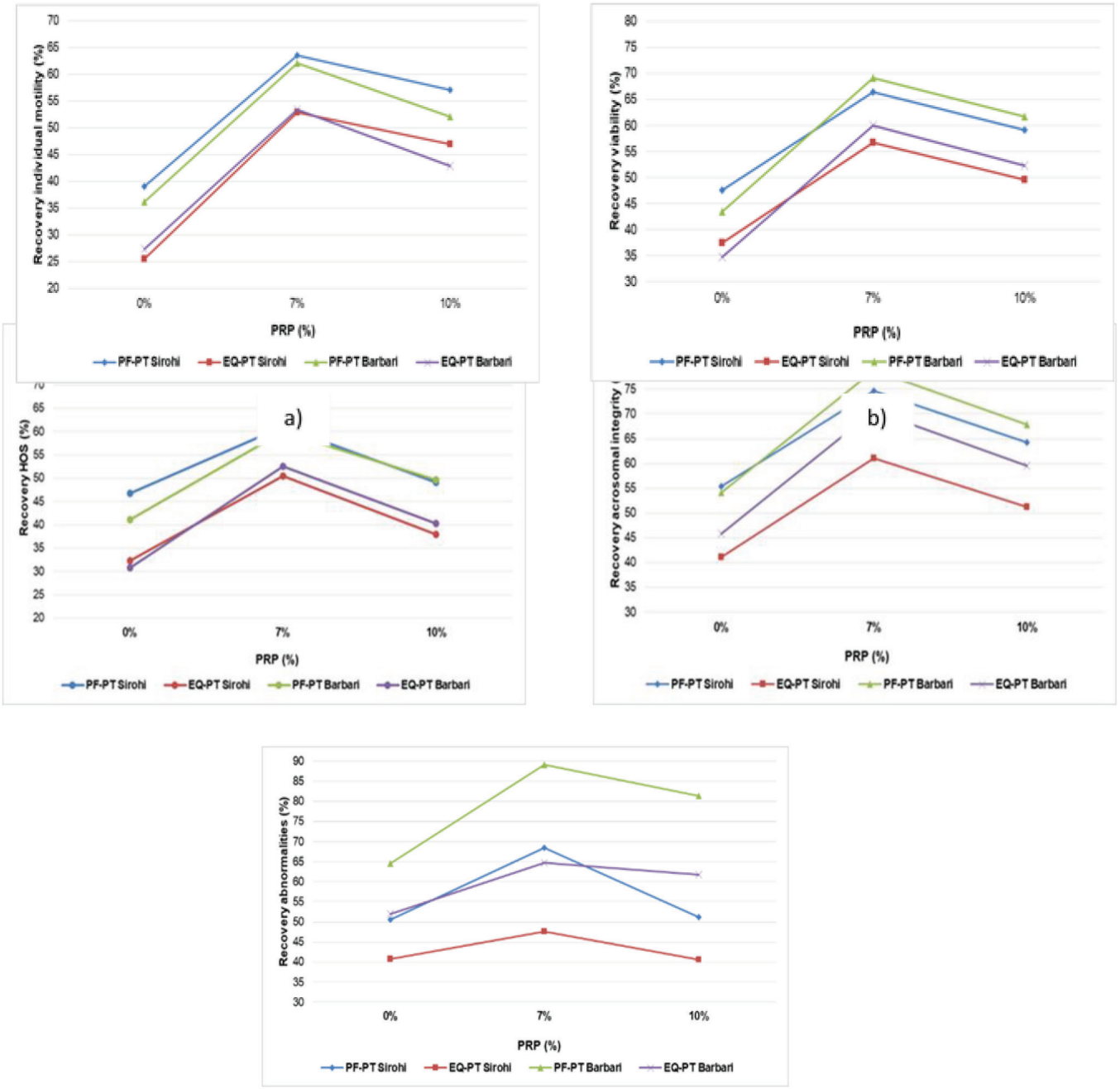

Fig. 2. Recovery percentage of spermatozoa in PRP-supplemented semen extender at different stages in both breeds. a) Individual motility, b) Sperm viability, c) Plasma membrane integrity by HOS, d) Acrosomal integrity and e) abnormalities. PF- pre-freeze, PT- post-thaw, EQ- equilibrated.

During freezing, spermatozoa are exposed to osmotic and thermal stresses, resulting in lipid phase separation, cholesterol efflux, and protein migration in the plasma membrane [18]. These changes reduce motility, viability, and fertilizing capacity by disturbing membrane integrity [19]. The protective role of PRP may stem from NGF-mediated activation of MAP kinase signaling, which preserves membrane architecture [20], and IGF-1–mediated stabilization of acrosomal membrane proteins [22]. The protein content of PRP likely acts as a colloidal buffer, reducing osmotic stress and minimizing ice crystal formation during freezing and thawing [23].

However, excessive PRP 10% showed reduced efficacy. Higher concentrations may cause over-release of platelet-derived factors, increasing reactive oxygen

species (ROS) generation and oxidative stress. Elevated protein content can raise extender viscosity, interfere with cryoprotectant penetration, and create osmotic imbalance, leading to plasma and acrosomal membrane destabilization [5,7,8]. Overstimulation of growth factor pathways may also induce premature capacitation or acrosomal exocytosis, explaining the decline in post-thaw quality at higher PRP levels.

Differences in seminal parameters among breeds and individuals can result from factors such as age, nutritional status, season, hormonal balance, and overall reproductive health [24]. Despite these variations, the consistent superiority of 7% PRP supplementation across breeds in the present study suggests that moderate PRP inclusion effectively minimizes cryoinjury and enhances post-thaw semen quality.

CONCLUSIONS

The addition of PRP into the semen extender at different concentrations positively affected the freezability of semen in Barbari and Sirohi bucks. The addition of 7% PRP in the semen extender proved to be better in improving the post-thaw fertility of buck sperm, followed by 10%.

CONFLICTS OF INTEREST

The authors have declared that there are no conflicts of interest concerning this study.

ACKNOWLEDGEMENT

We acknowledge the Department of Animal Husbandry and Dairying, Government of India, for fully funding the project titled 'Optimizing Superior Buck Use in Up-Gradation of Non-Descript Goats with Seasonal Fertility Investigation and Semen Cryopreservation' Under the scheme, National Livestock Mission.

REFERENCES

1. Johnson LA, Weitze KF, Fiser P, Maxwell WM. Storage of boar semen. Animal Reproduction Science. 2000; 62(3):143-172. DOI: 10.1016/s0378-4320(00)00157-3.

2. Marx RE. Platelet-rich plasma: evidence to support its use. Journal of oral and maxillofacial surgery. 2004; 62(4): 489-496. DOI: 10.1016/j.joms.2003.12.003.

3. Hezavehei M, Sharafi M, Kouchesfahani HM, Henkel R, Agarwal A *et al.* Sperm cryopreservation: A review on current molecular cryobiology and advanced approaches. Reproductive biomedicine online. 2018; 37(3): 327-339. DOI: 10.1016/j.rbmo.2018.05.012.

4. Alcay S, Gokce E, Toker MB, Onder NT, Ustuner B *et al*. Freeze-dried egg yolk-based extenders containing various antioxidants improve post-thawing quality and incubation resilience of goat spermatozoa. Cryobiology. 2016; 72(3): 269-273. .DOI: 10.1016/j.cryobiol.2016.03.007.

5. Yan B, Zhang Y, Tian S, Hu R, Wu B. Effect of autologous platelet-rich plasma on human sperm quality during cryopreservation. Cryobiology. 2021; 98: 12-16. .DOI: 10.1016/j.cryobiol.2021.01.009.

6. Alcay S, Aktar A, Koca D, Kilic MA, Akkasoglu M *et al.* Autologous platelet-rich plasma has a positive effect on ram spermatozoa during cryopreservation in the non-breeding season. Kafkas Univ Vet Fak Derg. 2022; 28(2): 229-234. DOI: 10.9775/kvfd.2021.26763.

7. Salama MS, Shehabeldin AM, Ashour MA, Al-Ghadi MQ, Marghani BH *et al*. Effect of the addition of platelet-rich plasma to Boer buck semen on sperm quality and antioxidant activity before and after cryopreservation and *in vivo* fertility. Small Ruminant Research. 2024; 230: 107167. DOI: 1016/j.smallrumres.2023.107167.

8. El-Sherbiny HR, Abdelnaby EA, Samir H, Fathi M. Addition of autologous platelet-rich plasma to semen extender enhances cryotolerance and fertilizing capacity of buffalo bull spermatozoa. Theriogenology. 2022; 194: 104-109. DOI: 10.1016/j.theriogenology.2022.09.029.

9. Gole SG, Krishna M, Gole GN. Comparison study of platelet count estimation by two methodologies: An automated hematology analyzer and peripheral blood smear examination. Indian J. Pathol. Res. Pract. 2018; 7(8): 905-909. DOI: 10.21088/ijprp.2278.148X.7818.3.

10. Gangwar C, Kharche SD, Pourouchottamane R, Ranjan R, Chatli MK *et al*. Advances in Artificial Insemination in Goats, 1st ed.; New India Publishing Agency: New Delhi, India, 2023; pp-183-189.

11. Blom, E. A One-minute live-dead sperm stain by means of eosin–nigrosine. Journal of Fertility and Sterility, 1950; 1(2): 176–177. DOI: 10.1016/S0015-0282(16)30125-X.

12. Revell SG, Mrode RA. An osmotic resistance test for bovine semen. Animal Reproduction Science. 1994; 36(2): 77–86. DOI: 10.1016/0378-4320(94)90055-8.

13. Snedecor GW, Cochran WG. Statistical Methods, 6th ed.; Oxford and IBH Publishing Co.: Calcutta, India. 1994; pp-105.

14. Miah AG, Salma U, Takagi Y, Kohsaka T, Hamano KI *et al.* Effects of relaxin and IGF-I on capacitation, acrosome reaction, cholesterol efflux and utilization of labeled and

unlabeled glucose in porcine spermatozoa. Reprod Med Biol. 2008; 7(1): 29–36. DOI: 0.1111/j.1447-0578.2007.00198.x.

15. Sharkey DJ, Tremellen KP, Briggs NE, Dekker GA, Robertson SA. Seminal plasma transforming growth factor-β, activin A and follistatin fluctuate within men over time. Human Reproduction. 2016; 31(10): 2183–2191.DOI: 10.1093/humrep/dew185.

16. Jimenez-Trejo F, Tapia-Rodríguez M, Cerbón M, Kuhn DM, Manjarrez-Gutierrez *et al*. Evidence of 5-HT components in human sperm: implications for protein tyrosine phosphorylation and the physiology of motility. Reproduction. 2012; 144(6): 677–685. DOI: 10.1530/REP-12-0145.

17. Castellini C, Mattioli S, Bosco AD, Cotozzolo E, CartoniMancinelli A *et al*. Nerve growth factor receptor role on rabbit sperm storage. Theriogenology. 2020; 153:54–61. DOI: 10.1016/j.theriogenology.2020.04.042.

18. Purdy PH. A review of goat sperm cryopreservation. Small Ruminant Research. 2006; 63(3): 215–225. DOI: 10.1016/j.smallrumres.2005.02.015.

19. Jeyendran RS, Der V, Perez-Pelaez M, Crabo BG, Zaneveld LJD. Development of an assay to assess the functional integrity of the human sperm membrane and its relationship to other semen characteristics. Reproduction. 1984; 70(1): 219–228. DOI: 10.1530/jrf.0.0700219.

20. Li C, Sun Y, Yi K, Ma Y, Sun Y *et al*. Detection of nerve growth factor (NGF) and its specific receptor (TrkA) in ejaculated bovine sperm, and the effects of NGF on sperm function. Theriogenology. 2010; 74(9): 1615–1622. DOI: 10.1016/j.theriogenology.2010.06.033.

21. Drobnis EZ, Crowe LM, Berger T, Anchordoguy TJ, Overstreet JW *et al*. Cold shock damage is due to lipid phase transitions in cell membranes: a demonstration using sperm as a model. The Journal of Experimental Zoology. 1993; 265(4): 432–437. DOI: 10.1002/jez.1402650413.

22. Selvaraju S, Krishnan BB, Archana SS, Ravindra JP. IGF1 stabilizes sperm membrane proteins to reduce cryoinjury and maintain post-thaw sperm motility in buffalo (*Bubalus bubalis*) spermatozoa. Cryobiology. 2016; 73(1): 55–62. DOI: 10.1016/j.cryobiol.2016.05.012.

23. Taher-Mofrad SMJ, Topraggaleh TR, Ziarati N, Bucak MN, Nouri M *et al*. Knockout serum replacement is an efficient serum substitute for cryopreservation of human spermatozoa. Cryobiology. 2020; 92(1): 208–214. DOI: 10.1016/j.cryobiol.2020.01.013.

24. Chouksey S, Shukla SN, Dubey A, Soni Y, Mandal S *et al*. Detection of Mitochondrial-Derived Peptide Humanin in Semen and Reproductive Tract of Caprine Along with Its Relation to Seasonality. Reproduction in Domestic Animals. 2025; 60: e70113. DOI: https://doi.org/10.1111/rda.70113.

Cite this article as: Narkhede AM, Shukla SN, Chouksey S, Jain AK. The effect of platelet-rich-plasma supplemented extender on post-thaw fertility of sirohi and barbari buck semen. Explor Anim Med Res. 2026; 16(1), DOI: 10.52635/eamr/16.1.77-84.

Explor Anim Med Res.
Vol. 16, Issue 1, 2026
DOI: 10.52635/eamr/16.1.85-93

ISSN 2277-470X (Print), ISSN 2319-247X (Online)
Website: www.animalmedicalresearch.org

Published under the CC BY-NC 4.0 license

Research Article

PREVALENCE OF *KLEBSIELLA PNEUMONIAE* AND ANTIMICROBIAL RESISTANCE GENES IN BOVINE MASTITIS IN CAUVERY DELTA REGION OF TAMIL NADU

Jayalakshmi K[1]*, Palanivel K.M[2], Sumathi D[3], Vijayarajan A[1], Babu Prasath N[4], Sangeetha A[5] and Veeraselvam M[6]

Received 13 June 2025, revised 28 April 2026

ABSTRACT: *Klebsiella pneumoniae* is emerging as a major environmental mastitis pathogen, often linked with poor cure rates. The studies of *K. pneumoniae* associated mastitis in dairy cattle are very limited. The study was carried out to assess the prevalence, antimicrobial resistance pattern and biofilm forming capacity of *K. pneumoniae* in bovine mastitis in the Cauvery delta region of Tamil Nadu, India. A total of 155 milk samples were collected from mastitis cases and bacterial culture was performed. The bacteria was identified based on colony characters and confirmed by PCR. Further, the antimicrobial sensitivity assay, minimum inhibitory concentration and biofilm assay was performed in *K. pneumoniae* isolates to determine the antimicrobial resistance, and its resistance genes were confirmed by PCR. Among 155 milk samples, bacterial growth was observed in 123 samples, of which 78 (63%) samples had *K. pneumoniae*. The antimicrobial sensitivity assay revealed that the 91.25% of *K. pneumoniae* isolates were sensitive to enrofloxacin, ciprofloxacin, ceftriaxone and co-trimoxazole and 62.50% were sensitive to oxytetracycline and 100% were resistant to ampicillin and methicillin. The MIC of amoxicillin-cloxacillin, amoxicillin-sulbactam, gentamicin and oxytetracycline against *K. pneumoniae* were ranged between 125-500, 25-220, 200-400 and 75-500 µg/ml, respectively. All *K. pneumoniae* isolates from mastitis cases were moderate to strong biofilm formers. All *K. pneumoniae* isolates contained ESBL genes, specifically bla_{TEM} and bla_{SHV}. Among these, 66% of isolates had a combination of both bla_{TEM} and bla_{SHV} genes, 24% of isolates had bla_{SHV} and 10% had the bla_{TEM}. The aminoglycoside resistant gene was detected in two isolates only. None of the isolates had the fluoroquinolone resistance gene (*gyr*A and *gyr*B), cefotaxime resistance gene ($bla_{CTX\text{-}M\text{-}G1}$ and $bla_{CTX\text{-}M\text{-}G2}$), sulfonamide resistance gene (*sul1),* tetracycline resistance gene (*tet*A and *tet*M) and the multidrug efflux pump gene (*acrAKp)*. The *K. pneumoniae* was highly prevalent in clinical mastitis cases, and the isolates exhibited high MIC, biofilm forming ability and carriage of AMR genes. An integrated AMR surveillance to be implemented in future.

Keywords: AMR, Biofilm, ESBLs, *Klebsiella pneumoniae*, Mastitis, MIC

INTRODUCTION

Mastitis is one of the major production losses causing disease in the dairy animals throughout the world. It is most commonly caused by contagious and environmental pathogens. Nowadays, the incidence of environmental mastitis gradually increases with the decline of contagious mastitis [1]. The large proportion of environmental mastitis in cattle is caused by *Escherichia coli, Klebsiella* spp and *Enterobacter* sp [2, 3], and which are found in soil, feed, drinking water, faeces, rumen contents, bedding material, sewage, surface water and plants, which is transmitted at any time, during milking, between milking, dry period and prior to calving in heifers [4, 5]. The intramammary infection of *Klebsiella pneumoniae* commences as subclinical in the early dry period and progresses to

[1]*Veterinary Clinical Complex, Veterinary College and Research Institute, Orathanadu-614 625, TANUVAS, India*
[2]*Department of Veterinary Medicine, Veterinary College and Research Institute, Namakkal-637 002, TANUVAS, India*
[3]*Department of Clinics, Madras Veterinary College, Chennai-600 007, TANUVAS, India*
[4]*Department of Veterinary Pathology, Veterinary College and Research Institute, Orathanadu-614 625, TANUVAS, India*
[5]*Department of Veterinary Public Health and Epidemiology, Veterinary College and Research Institute, Orathanadu-614 625, TANUVAS, India*
[6]*Department of Veterinary Medicine, Veterinary College and Research Institute, Orathanadu-614 625, TANUVAS, India*
**Corresponding author. e-mail: jayalkshm22@gmail.com*

clinical mastitis during lactation [6]. The increased production of inflammatory cytokines (IL-1, IL-6, IL-8 and TNFα) during an infection induces a severe systemic inflammatory reaction and strong immune response, the damaged mammary epithelial cells undergoes apoptosis [5]. The *Klebsiella* spp more often causes severe long lasting intramammary infection and persists for more than 200 days and more often detrimental effects on milk production and increased premature culling in dairy cattle [3,4,7]

The *K. pneumoniae* is a large capsulated gram negative bacilli that encodes major virulence factors, viz., fimbriae, capsules, lipopolysaccharides and siderophores [5]. The *K. pneumoniae* is classified as classical and hypervirulent based on virulence [8]. The capsular serotype is usually associated with hypervirulence and emerging as multidrug resistance [9, 10]. The biofilm formation is a key virulence mechanism responsible for antimicrobial resistance and poor response to treatment [11]. The *K. pneumoniae* inherently resistant to penicillin and ampicillin through the production of extended spectrum β-lactamase (ESBL) [5]. The rate of antimicrobial resistance (AMR) among *K. pneumoniae* isolates in dairy herds varied with the regions [12]. The documentation of region-wise AMR pattern of *K. pneumoniae* is utmost importance to select the choice of antibiotics for treatment to improve the recovery rate. The present article described the prevalence and antimicrobial resistance patterns of *K. pneumoniae* isolated from bovine mastitis cases in the Cauvery delta region of Tamil Nadu.

MATERIALS AND METHODS

A total of 155 milk samples were collected from dairy cows affected with clinical mastitis, which was presented to the large animal medicine unit of the Veterinary Clinical Complex, Veterinary College and Research Institute, Orathanadu. The colour and consistency of milk varied from yellow serous fluid with fibrin clots, yellowish milk with flakes, watery milk with flakes and brown coloured fluid.

Isolation of bacteria

The isolation of bacteria in milk samples was performed as per standard procedures [13]. The milk samples were inoculated into sterile nutrient broth and incubated at 37°C for 12-24 hrs. The broth culture was streaked into MacConkey agar (MA) and Eosin and Methylene Blue (EMB) agar by using a sterile inoculation loop and incubated at 37°C. The colony characters of bacteria were examined after 24 hrs. The biochemical tests, like indole, methyl red, citrate and Voges-Proskauer test were done to identify the bacteria.

Antibacterial sensitivity test

The antimicrobial sensitivity pattern of *K. pneumoniae* isolates were performed as per the Kirby Bauer disc diffusion method [14]. A single *K. pneumoniae* colony from each isolate was inoculated into nutrient broth and incubated at 37°C for 12 hrs. The broth culture was swabbed in Muller Hinton agar and antibiotic impregnated disc such as ciprofloxacin (5 µg), enrofloxacin (5 µg), gentamicin (10 µg), amikacin (30 µg), ampicillin (10 µg), ceftriaxone (30 µg), ampicillin/ sulbactam (10/10 µg), methicillin (5 µg), co-trimoxazole (25 µg) and oxytetracycline (30 µg) were placed at equal distance and incubated at 37°C for 24 hrs. The zone of inhibition for each antibiotic was measured and recorded.

Determination of minimum inhibitory concentration (MIC)

The MIC of antibiotics were carried out as per the method described by Eroglu *et al.* (2024) [15]. Frozen cultures of *K. pneumoniae* isolates were thawed to room temperature and inoculated 100 µl in sterile nutrient broth (5ml), incubated at 37°C for 24 hrs and observed for growth based on turbidity appearance. This culture (100 µl) again inoculated in sterile nutrient broth and incubated at 37°C for 24 hrs. Thereafter, bacterial culture was centrifuged at 3000 rpm for 10 minutes, the supernatant was discarded and the bacterial pellet was washed twice with phosphate buffered saline (pH 7.2). Then bacterial pellet was reconstituted in sterile nutrient broth and 200 µl of culture transferred to a 96 well sterile microtitre plate and antibiotics (amoxicillin cloxacillin, amoxicillin sulbactam, gentamicin and oxytetracycline) were added in different concentrations separately for each isolates and incubated at 37°C for 24 hrs along with a negative control (nutrient broth culture without antibiotics). The absorbance was measured on 0 and 24 hrs at 570 nm to determine the inhibition of growth using a spectrophotometer. The MIC of antibiotics (amoxicillin-cloxacillin, amoxicillin-sulbactam, gentamicin and oxytetracycline) were tested in the range of 0.1-1000 µg/ml.

Biofilm assay

The overnight nutrient broth culture (100 µl) of *K. pneumoniae* isolates were inoculated in 10 ml of brain heart infusion (BHI) broth enriched with sucrose (2%) and incubated at 37°C for 6-8 hrs. The log phase BHI enriched

broth culture (1:100 dilution) 200 µl was transferred to a sterile 96 well microtitre plate and incubated at 37°C for 48 hrs, the liquid phase was decanted and plate was washed with 200 µl of phosphate buffered saline for three times. Thereafter, 200 µl of 0.1% crystal violet dye was added and incubated at room temperature for 15 minutes, then the contents were decanted and washed with distilled water for three times, the plate was dried by blotting on tissue paper. The glacial acetic acid (30%) 100 µl was added to each well to solubilize the biofilm, allowed to stand for 15 minutes and measured the absorbance at 570 nm using a spectrophotometer. The biofilm was graded as weak, moderate and strong based on biofilm forming capacity [16].

Extraction of bacterial DNA

The bacterial DNA was extracted by the boiling and lysis method [17]. A single pure colony was transferred into a 1.5 ml microcentrifuge tube containing 500 µl of sterile distilled water, mixed well, boiled for 10 minutes and cooled at room temperature. The sample was centrifuged at 8000 rpm for 6 minutes, and the clear supernatant was carefully aspirated and stored at -20ºC for PCR analysis.

Molecular detection of bacteria and AMR genes

The genotypic identification of *Klebsiella* spp was done by PCR. The primer sequences of target bacteria and antimicrobial resistance genes are given in table 1 [18, 19] and table 2 [20, 21, 22, 23]. The PCR was carried out with optimized thermal cycling conditions of initial denaturation at 94ºC for 10 minutes followed by 35 cycles of denaturation at 94ºC for 1 minute, annealing at 55ºC for 1 minute, extension for 1 minute and final extension at 72ºC for 10 minutes. The PCR confirmed field isolate of *K. pneumoniae* was used as a positive control, and the PCR reaction without a DNA template was used as a negative control. The amplified PCR products were electrophoresed in 1.5 % agarose with 1X TAE buffer at 60 V for 45 minutes, visualized under a UV transilluminator and documented in the Gel Doc system.

RESULTS AND DISCUSSION

In bacterial culture, out of 155 milk samples, the growth was observed in 123 samples, of which 78 samples were positive for *Klebsiella* spp (63%). In MacConkey agar, the *Klebsiella* spp exhibited lactose-fermenting small to large dome shaped glistening pink to yellow mucoid colonies with smooth edges. The colonies had a pink centre and pink edges or yellow centre with pink edges (Fig. 1). In the biochemical test, the *Klebsiella* spp showed a positive reaction to citrate, acid production with gas in triple sugar iron agar and a negative reaction to indole. The PCR amplification confirmed the presence of *Klebsiella* spp and *K. pneumoniae* and its expected amplicon sizes were 441 and 130 bp, respectively (Fig. 2).

In this study, the prevalence of *K. pneumoniae* was 63%. This finding was in concordance with the report of Salauddin *et al*. (2019) [24], who reported that 62.5% of bovine mastitis in Bangladesh due to *Klebsiella* spp. The country-wise reported prevalence of *K. pneumoniae* in clinical mastitis cases of dairy cows in Japan (38.8%), Asia (14.26%), China (7.49%), sub-saharian Africa (8.6%), South Africa (18.5%), Kenya (23%) and Nigeria (11.1%), Northwestern Iran (40%) and European countries (0.73%). Among Asian countries, the higher prevalence of *K. pneumoniae* was reported in Bangladesh followed by Iran and Japan. The least prevalence was reported in European countries [3, 25, 26, 27].

In ABST, the *K. pneumoniae* isolates of bovine mastitis showed 91.25% sensitivity to enrofloxacin, ciprofloxacin, ceftriaxone and co-trimoxazole, 62.5% sensitivity to oxytetracycline and 100% resistance to ampicillin and methicillin (Fig. 3). These finding were in concordance with the report of Fu *et al*. (2022) [5], who reported that the *K. pneumoniae* was highly sensitive to enrofloxacin (92.31%) followed by tobramycin and cefoxitin (73.85%). Arya *et al.* (2020) [28] reported that the *K. pneumoniae* isolates in bovine milk samples were highly susceptible to the quinolone group of antibiotics and resistant to ampicillin. Yadav *et al*. (2021) [29] reported that *K.*

Table 1. Primer sequence of *Klebsiella* spp.

S. No.	Name of the bacteria	Target gene	Primer sequence	Amplicon size (bp)	Reference
1.	*Klebsiella* spp	*gyr*A	F-5'-CGCGTACTATACGCCATGAACGTA-3′ R-5′-ACCGTTGATCACTTCGGTCAGG-3′	441	18
2.	*K. pneumoniae*	*16S−23S* rDNA	Pf 5'- ATTTGAAGAGGTTGCAAACGAT-3' Pr1 5'-TTCACTCTGAAGTTTTCTTGTGTTC-3'	130	19

Table 2. Primer sequence of antimicrobial resistance genes.

S. No.	Antibiotics	Target gene	Primer sequence	Amplicon size (bp)	Reference
1.	Ampicillin	bla_{TEM}	F- 5' TCCGCTCATGAGACAATAACC-3' R 3' ATAATACCGCACCACATAGCAG-5'	296	20
2.	Ampicillin	bla_{SHV}	F 5' –TACCATGAGCGATAACAGCG-3' R 3' – GATTTGCTGATTTCGCTCGG-5'	450	20
3.	Cefotaxime	$bla_{CTX\text{-}M\text{-}G1}$	F- 5'- GTTACAATGTGTGAGAAGCAG-3' R-5'- CCGTTTCCGCTATTACAAAC-3'	1000	21
4.	Cefotaxime	$bla_{CTX\text{-}M\text{-}G2}$	F-5'-CGTTAACGGCACGATGAC-3' R-5'-CGATATCGTTGGTGGTRCCA-3'	404	21
5.	Aminoglycoside	*aac* (6')-*aph*(2")	F- 5'-TTGGGAAGATGAAGTTTTTAGA-3' R- 5'-CCTTTACTCCAATAATTTGGCT-3'	174	22
6.	Quinolones	*qnr*A	F-5'-ATTTCTCACGCCAGGATTTG-3' R- 5'-GATCGGCAAAGGTTAGGTCA-3'	516	18
7.	Tetracycline	*tet*A	F-5'-GGTTCACTCGAACGACGTCA-3' R-5'-CTGTCCGACAAGTTGCATGA-3'	577	18
8.	Tetracycline	*tet*M	F-5′-GTGGACAAAGGTACAACGAG-3' R-5′-CGGTAAAGTTCGTCACACAC-3'.	403	23
9.	Sulfonamide	*sul1*	F-5'-TTCGGCATTCTGAATCTCAC-3' R-5'-ATGATCTAACCCTCGGTCTC-3'	822	18
10.	Multi-drug efflux pump	*acrAKp*	F-5'-ATTTCTCACGCCAGGATTTG-3' R-5-GATCGGCAAAGGTTAGGTCA-3'	940	18

Table 3. Minimum inhibitory concentration (MIC) of antibiotics for *Klebsiella pneumoniae* isolated from mastitis cases.

Mastitis conditions	No. of isolates	Minimum inhibitory concentration of antibiotics (µg/ml)			
		Amoxicillin-cloxacillin	Amoxicillin-sulbactam	Gentamicin	Oxytetracycline
Mastitis without systemic involvement	11	125	25	200	50
Mastitis with systemic involvement	35	500	50-100	240	75-125
Mastitis with severe systemic involvement	32	>1000	220	400	500

pneumoniae isolates of bovine mastitis milk were 100% susceptible to chloramphenicol, 83.30% to enrofloxacin, 72.20% to oxytetracycline and 55.60% to gentamicin and all isolates were resistant to the penicillin group of antibiotics. The *K. pneumoniae* isolates from mastitis milk samples in China showed resistant to sulphonamides (45.07%), tetracycline (36.18%), aminoglycosides (27.47%), β-lactams (27.35%) amphenicols (26.82%), macrolides (20.98%), lincosomides (21.24%), polypeptides (15.31%) and quinolones (7.80%) [25]. The low level of resistance has been reported to tetracycline (5.6-19.5%), and β-lactams (0-6.9%) in Europe and the United States [12].

The MIC of *K. pneumoniae* isolates against amoxicillin-cloxacillin, amoxicillin-sulbactam, gentamicin and oxytetracycline were ranged between 125- 500 (isolates of mild to moderate cases), 25-220, 200-400 and 75-500 µg/ml, respectively (Table 3). *K. pneumoniae* isolates (11) from animals without systemic involvement showed MICs of 125, 25, 200 and 50 µg/ml, respectively for amoxicillin-cloxacillin, amoxicillin-sulbactam, gentamicin and oxytetracycline. The *K. pneumoniae* isolates (35) from systemic involvement like anorexia, reduced feed intake and yellowish milk with flakes showed MICs of 500, 50-100, 240 and 75-125 µg/ml, respectively for amoxicillin-cloxacillin, amoxicillin-sulbactam, gentamicin and oxytetracycline, respectively. The *K. pneumoniae* isolates (32) from

animals with severe systemic involvement like pyrexia, lameness, anorexia, and reduced feed intake and yellow serous fluid with fibrin clots from affected mammary quarters had MICs of 220, 400 and 500 µg/ml, respectively for amoxicillin-sulbactam, gentamicin and oxytetracycline, whereas, no MIC was observed for amoxicillin-cloxacillin @ 1000 µg/ml. (Fig. 4). The MIC of amoxicillin-cloxacillin for *K. pneumoniae* was similar to the report of CLSI (2020) [14], reported that the MIC of amoxicillin for *K. pneumoniae* was >128 µg/ml. The result of MIC of amoxicillin-sulbactam was corroborates with the report of Mukherjee *et al.* (2013) [30], who opined that the MIC of sulbactam against *K. pneumoniae* was 25 µg/ml. In this study, the MIC of gentamicin (200-400 µg/ml) was higher than the report of Eroglu *et al.* (2024) [15], who reported that the MIC of gentamicin against *K. pneumoniae* was 0.09 µg/ml. In this study, the MIC of oxytetracycline for *K. pneumoniae* was similar to the report of Mosallam and Elshimy, (2024) [31], who reported that the MIC of oxytetracycline against *K. pneumoniae* was more than 100 µg/ml. The high MIC of amoxicillin-cloxacillin and gentamicin indicated the resistance status of *K. pneumoniae* in bovine mastitis.

Fig. 1. Colony character of *K. pneumoniae* in MacConkey agar- pink to yellow mucoid colonies.

Out of 78 isolates, 23 and 55 isolates had moderate (OD value - 0.175-0.230) and strong biofilm formation (OD value - 0.421-0.658), respectively (Fig.5). The *K. pneumoniae* isolates from clinical mastitis cases were 100% biofilm formers. The virulent *K. pneumoniae* (isolates of milk from yellow serous fluid with fibrin clots) strongly produced biofilm and exhibited a high MIC value and poorly responded to treatment. This finding indicated that a strong correlation exists between biofilm forming *K. pneumoniae* and antimicrobial resistance. The similar results were reported by

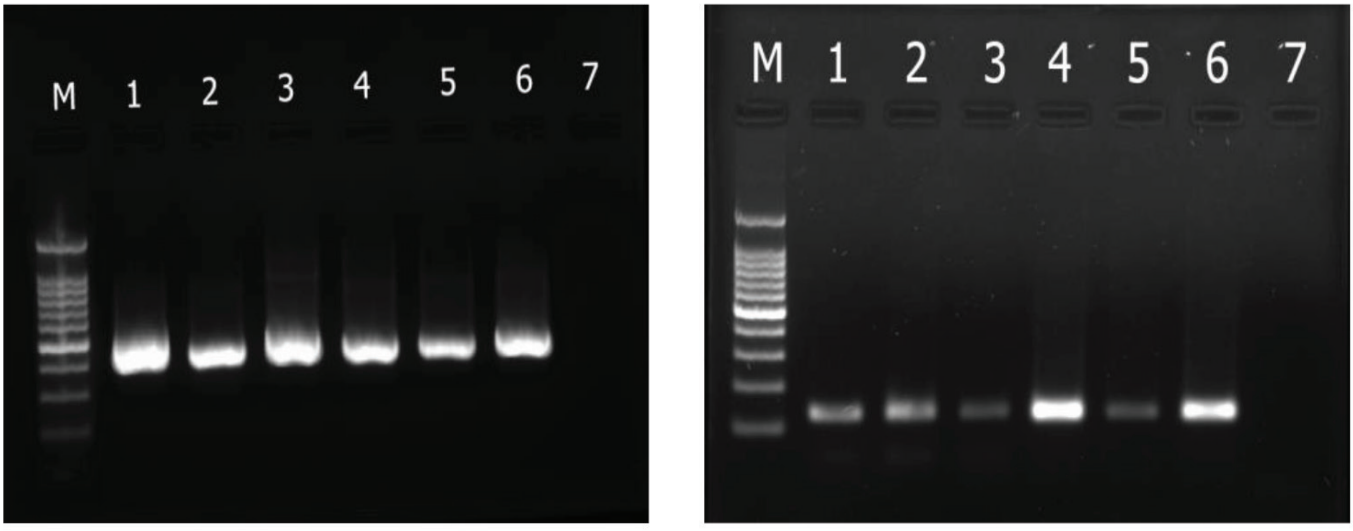

(a)

M	-	DNA marker (100 bp)
Lane 1		Positive control
Lane 2-6	-	Positive field samples
Lane 7	-	Negative control

(b)

M	-	DNA marker (100 bp)
Lane 1		Positive control
Lane 2-6	-	Positive field samples
Lane 7	-	Negative control

Fig. 2. Molecular confirmation of bacteria isolated from mastitis milk sample (a) *gyr* A of *Klebsiella* spp (441 bp) and (b) *16S-23SrDNA* gene of *Klebsiella pneumoniae* (130 bp).

Shadkam *et al*. (2025) [32], who opined that the antimicrobial resistance was higher in biofilm forming *K. pneumoniae* than non-biofilm formers.

In this study, the *K. pneumoniae* isolates harboured 100% ESBLs genes, bla_{TEM} (Fig. 6a) and bla_{SHV} genes (Fig. 6b). Among these 66% of isolates had both bla_{TEM} and bla_{SHV} genes, 24% isolates had bla_{SHV} and 10% had the bla_{TEM} gene alone. The similar findings were reported by Nahar *et al*. (2021) [33], who opined that the *K. pneumoniae* isolates exhibited 50% bla_{TEM}, 15% bla_{SHV} and 35% combination of bla_{TEM} and bla_{SHV} genes. The extended spectrum β-lactamase (ESBL) and carbapenemase were most common resistant mechanisms in Enterobacteriaceae bacteria and confer resistance against penicillin, cephalosporins, monobactams, meropenem and imipenem antibiotics. The most frequently reported variants of ESBL were TEM (Temoneira), SHV (sulfhydryl reagent variable) and CTX-M (cefotaxime-hydrolysing beta-lactamase) [34]. The carbapenemases encoded by the bla_{KPC}, bla_{NDM} and bla_{OXA-48} genes, as well as the plasmidic AmpC usually associated with the bla_{CMY} genes [35, 36].

In the present study, the aminoglycoside resistant gene was detected in two isolates only. None of the isolates carried the quinolone resistance gene (*qnr*A), cefotaxime resistance gene ($bla_{CTX-M-G1}$ and $bla_{CTX-M-G2}$), sulfonamide resistance gene (*sul1),* tetracycline resistance gene (*tet*A and *tet*M) and the multidrug efflux pump gene (*acrAKp)*, whereas Tran *et al.* (2023) [18] reported that the *K. pneumoniae* isolates in Vietnam carried 100% multidrug efflux pumps and the *tet*A gene, 94% had bla_{SHV} and 8% harboured bla_{NDM} and none of the isolates carrying the *tet*B and *qnr*A genes. This variation indicated the presence or absence of antimicrobial resistance in bacteria varied with geographical area and antimicrobial usage [34]. The distribution of AMR genes in *K. pneumoniae* isolates of China had bla_{SHV} (100%) and bla_{TEM} (64.7%), bla_{NDM-1} (36.8%), bla_{VIM} (17.6%) and bla_{OXA-10} genes (19.1%) and the presence of bla_{OXA-10} was positively associated with tetracycline resistance [37]. *K. pneumoniae* isolates that carrying the CTX-M-15 and SHV-12 β-lactamases exhibit resistance to both ceftiofur and cefquinome [38]. *K. pneumoniae* isolates from bovine mastitis were multidrug resistance and carried bla_{CTX-M}, bla_{SHV}, and bla_{TEM}, quinolone and tetracyclines resistance genes [12]

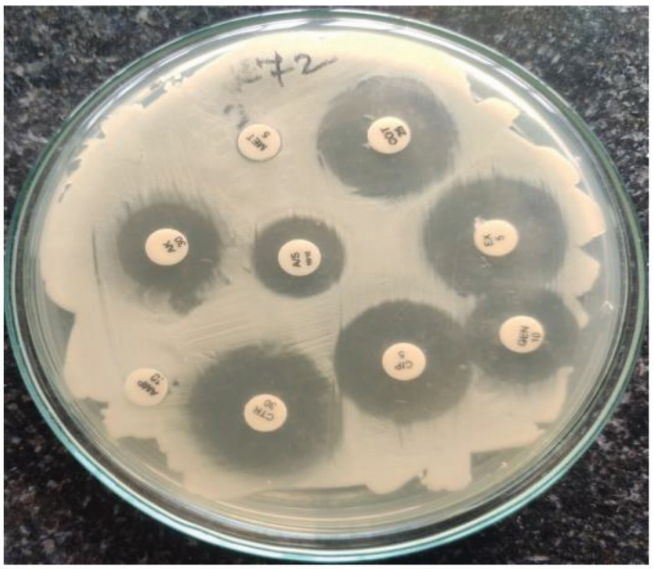

Fig. 3. Antimicrobial susceptibility test of *K. pneumoniae* on Muller Hinton agar.

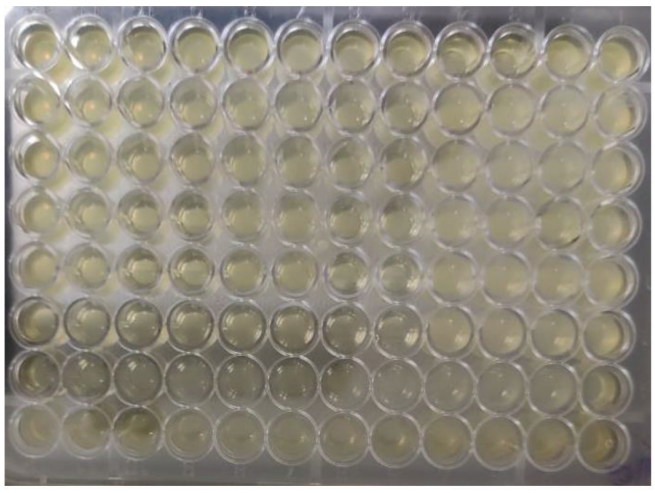

Fig. 4. Determination of minimum inhibitory concentration of *K. pneumoniae* by microtitre plate method.

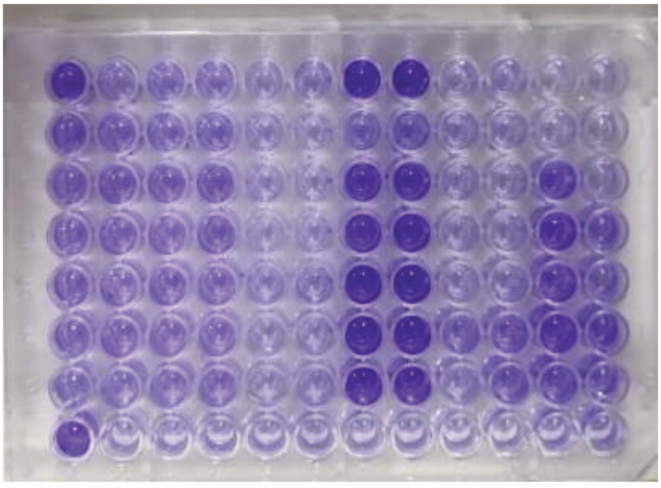

Fig. 5. Determination of biofilm assay of *K. pneumoniae* by microtitre plate method.

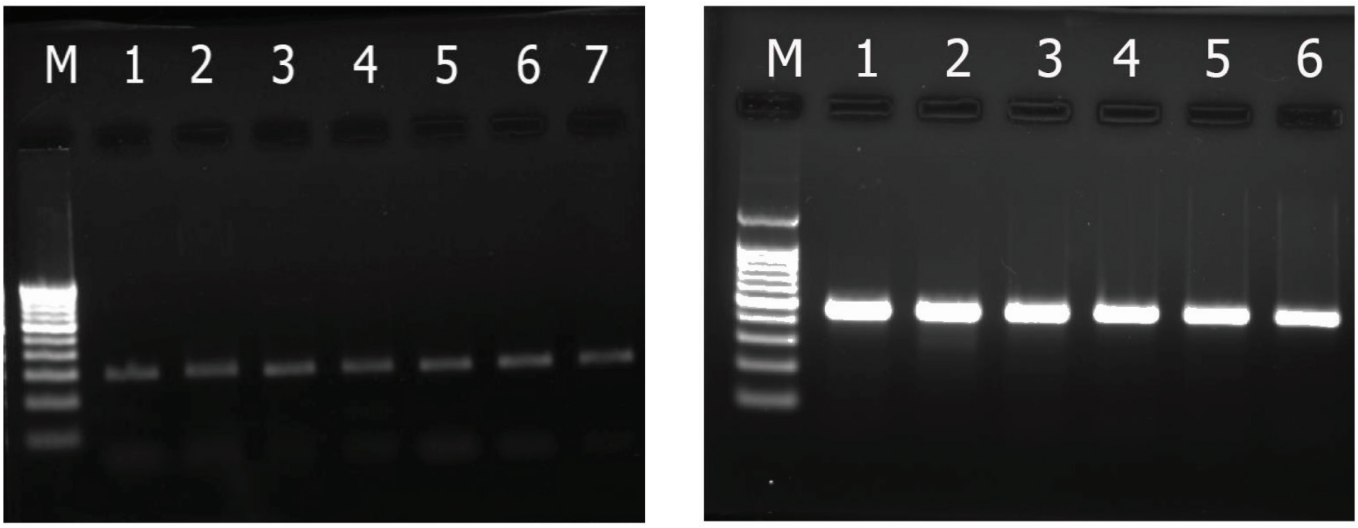

(a) M- DNA marker (100 bp), Lane 1- 7 bla_{TEM} gene

(b) M- DNA marker (100 bp), Lane 1- 6 bla_{SHV} gene

Fig. 6. Molecular detection of antimicrobial resistance gene in *K. pneumoniae* (a) bla_{TEM}- 296 bp and (b) bla_{SHV}-450 bp.

and a higher prevalence of aminoglycoside resistance gene *aac*(3)-iv (77.4%) and tetracycline genes *tet*A (76.7%) was reported in Bangladesh [39].

Based on observation, enrofloxacin could be used as the choice of antibiotic for klebsiella mastitis in dairy cows. The similar finding was reported by Fu *et al.* (2022) [5], who opined that *K. pneumoniae* showed 92.31% sensitive to enrofloxacin. In this study, the animals were treated with Inj. enrofloxacin @ 5 mg/Kg IM along with supportive therapy. Out of 78 animals, 23 (29.48%) animals were completely recovered, 47 (60.25%) animals infected quarters progressed to fibrosis and 8 (10.25%) animals quarter were progressed to gangrene. The gangrenous changes (3-6 days of initial symptoms) were observed in the affected quarter of some of the animals with yellow serous fluid with fibrin clots and anorexia.

The clinical outcome of enrofloxacin was 29.48%. These results were contradictory to the report of Sugiyama *et al*. (2022) [3], who reported that the enrofloxacin was effective in 76.70% of *K. pneumoniae* mastitis cases. The lower clinical outcome of enrofloxacin in this study might be due to the strong biofilm forming *K. pneumoniae* limiting the efficacy of the antibiotic.

The *K. pneumoniae* poses challenges for veterinarians and physicians because of treatment failure, which is a major transporter of resistance genes from the environment to clinically important bacteria through plasmids/horizontal gene transfer mechanisms. The community acquired *K. pneumoniae* was hypervirulent and multidrug resistance led to serious clinical invasion in animals and humans [40]. The integrated AMR surveillance and control across animals, humans and the environment are needed to curb its spread and resistance.

CONCLUSION

The *Klebsiella pneumoniae* isolates from bovine mastitis had high MIC, biofilm former and carried AMR genes (bla_{TEM} and bla_{SHV} genes). The intramammary infection with *K. pneumoniae* not only caused the loss of milk yield in the affected quarter, but it resulted in generalized loss of milk secretion in all quarters and also increased culling percentage. Improving the health and immune status of the animal during the transition period could helps to reduce the economic losses associated with mastitis.

ACKNOWLEDGEMENT

The authors are thankful to the Dean, Veterinary College and Research Institute, Orathanadu, Department of Veterinary Medicine and Department of Veterinary Public Health and Epidemiology, Veterinary College and Research Institute, Orathanadu, Tamil Nadu Veterinary and Animal Sciences University, Chennai-51, Tamil Nadu for providing facilities to carried out the research.

ETHICS APPROVAL

Not applicable

REFERENCES

1. Cobirka M, Tancin V, Slama P. Epidemiology and classification of mastitis. Animals (Basel). 2020; 10(12):2212, DOI: 10.3390/ani10122212.

2. Wenz JR, Barrington GM, Garry FB, McSweeney KD, Dinsmore RP, Goodell G, Callan RJ. Bacteremia associated with naturally occurring acute coliform mastitis in dairy cows. J Am Vet Med Assoc. 2001; 219: 976- 981, DOI:10.2460/ javma.2001.219.976.

3. Sugiyama M, Watanabe M, Sonobe T, Kibe R, Koyama S, Kataoka Y. Efficacy of antimicrobial therapy for bovine acute *Klebsiella pneumoniae* mastitis. J Vet Med Sci. 2022; 84(7): 1023-1028, DOI: 10.1292/jvms.21-0617.

4. Smith KL, Hogan JS. Environmental mastitis. Vet Clin North Am Food Anim Pract. 1993; 9(3):489-498

5. Fu S, Wen C, Wang Z, Qiu Y, Zhang Y, Zuo J, Xu Y, Han X, Luo Z, Chen W, Miao J. .Molecular epidemiology and antimicrobial resistance of outbreaks of *Klebsiella pneumoniae* clinical mastitis in Chinese dairy farms. Microbiol Spectr. 2022; 10(6), DOI: 10.1128/spectrum.02997-22.

6. Bradley AJ, Green MJ. A study of the incidence and significance of intramammary enterobacterial infections acquired during the dry period. J Dairy Sci. 2000; 83(9):1957-1965, DOI: 10.3168/jds.S0022-0302(00)75072-7.

7. Grohn YT, Wilson DJ, Gonzalez RN, Hertl JA, Schulte H, Bennett G. Effect of pathogen-specific clinical mastitis on milk yield in dairy cows. J Dairy Sci. 2004; 87:3358-3374, DOI: 10.3168/jds.S0022-0302(04)73472-4.

8. Guerra MES, Destro G, Vieira B, Lima AS, Ferraz LFC, Hakansson AP, Darrieux M, Converso TR. *Klebsiella pneumoniae* biofilms and their role in disease Pathogenesis. Front Cell Infect Microbiol. 2022; 12:877995, DOI: 10.3389/ fcimb.2022.877995.

9. AL-Busaidi B, AL-Muzahmi M, AL-Shabibi Z, Rizvi M, AL-Rashdi A, AL-Jardani A, Farzand R, AL-Jabri Z. Hypervirulent capsular serotypes K1 and K2 *Klebsiella pneumoniae* strains demonstrate resistance to serum bactericidal activity and *Galleria mellonella* lethality. Int J Mol Sci. 2024; 25, DOI: 10.3390/ijms25031944.

10. Cai K, Xu M, Liu L, Zhao, H. Molecular epidemiology and antimicrobial resistance of *Klebsiella pneumoniae* strains isolated from dairy cows in Xinjiang, China. Vet Med Sci. 2025; 11(1):e70120, DOI: 10.1002/vms3.70120.

11. Kang, HJ, You JY, Kim SH, Moon JS, Kim HY, Kim JM, Kang HM. Genetic diversity, virulence genes, antimicrobial resistance, and biofilm formation of *Klebsiella pneumoniae* isolated from bovine mastitis milk in South Korea Microbiol Spectr. 2025; 13(11):e0134325, DOI: 10.1128/ spectrum.01343-25.

12. Song S, He W, Yang D, Benmouffok M, Wang Y, Li J, Sun C, Song X, Ma S, Cai C, Dang S, Wu C, Shen Z, Wang Y. Molecular Epidemiology of *Klebsiella pneumoniae* from Clinical Bovine Mastitis in Northern Area of China (2018-2019). Engineering, 2022; 10: 146-154, DOI:10.1016/j.eng.2021.01.015

13. Hogan JS, Gonzalez RN, Harmon RJ, Nickerson SC, Oliver SP, Pankey JW, Smith KL. Laboratory Handbook on Bovine Mastitis. Third Edn. 2017, National Mastitis Council, USA.

14. Clinical and Laboratory Standard Institute (CLSI). Performance Standards for Anti-Microbial Susceptibility Testing. 30th Edition, M100. 2020. Available from: https://clsi.org/ media/3481/ m100ed30_sample.pdf.

15. Eroglu B, Delik E, Tefon-Ozturk ET. Antibiotic concentrations affect the virulence of *Klebsiella quasipneumoniae* subsp. *similipneumoniae* isolates. Cell Microbiol. 2024; 920468, DOI: 10.1155/2024/5920468.

16. Triveni AG, Suresh Kumar M, Manjunath, C, Shivnnavar CT, Gaddad SM. Biofilm formation by clinically isolated *Staphylococcus aureus* from India. J Infect Dev Ctries. 2018; 12(12): 1062-1066, DOI:10.3855/jidc.10671.

17. Munoz MA, Francis L. Welcome FL, Schukken YH, Zadoks RN. Molecular epidemiology of two *Klebsiella pneumoniae* mastitis outbreaks on a dairy farm in New York State. J Clin Microbiol. 2007; 45(12): 3964-3971, DOI: 10.1128/ JCM.00795-07.

18. Tran MT, Vu DM, Vu MD, Bui TP, Dang BX, Dang LTM, Le TV. Antimicrobial resistance and molecular characterization of *Klebsiella* species causing bovine mastitis in Nghe An province, Vietnam. J Adv Vet Anim Res. 2023; 10(1): 132-143, DOI: 10.5455/javar.2023.j662.

19. Osman EA, El-Amin N, Adrees EAE, Al-Hassan L, Maowia Mukhtar M. Comparing conventional, biochemical and genotypic methods for accurate identification of *Klebsiella pneumoniae* in Sudan. Access Microbiol. 2020; 10;2(3), DOI: 10.1099/acmi.0.000096.

20. Doosti A, Pourabbas M, Arshi A, Chehelgerdi M, Kabiri H. TEM and SHV Genes in *Klebsiella pneumoniae* isolated from cockroaches and their antimicrobial resistance pattern. Osong Public Health Res Perspect. 2014; 6(1): 3-8, DOI: 10.1016/j. phrp.2014.10.011.

21. Diagbouga S, Salah FD, Sadji AY, Dabire AM, Nadembega C, Kere AB, Soubeiga ST, Ouattara AK, Zohoncon T, Belemgnegre M, Karou S, Simpore J. Detection of high prevalence of TEM/SHV/CTX-M Genes in ESBL producing and multidrug resistant *Klebsiella Pneumoniae* and *Klebsiella Oxytoca.* J Clin Diagn Res, 2016; 4:1, DOI: 10.4172/2376-0311.1000130.

22. Martineau F, Picard FJ, Lansac, N, Menard C, Roy PH, Ouellette M, Bergeron MG. Correlation between the resistance genotype determined by multiplex PCR assays and the antibiotic susceptibility patterns of Staphylococcus aureus

and Staphylococcus epidermidis. Antimicrob Agents Chemother. 2000; 44(2): 231-238, DOI: 10.1128/AAC.44.2.231-238.2000.

23. Jose KR, Vijayakumar K. Antimicrobial resistance profiling of coagulase negative staphylococci isolated from bovine mastitis. Indian J Anim Sci. 2024; 94 (4): 308-314, DOI: 10.56093/ijans.v94i4.129868.

24. Salauddin M, Akter MR, Hossain, MK, Rahman MM. Isolation of multi-drug resistant *Klebsiella* sp. from bovine mastitis samples in Rangpur, Bangladesh. J Adv Vet Anim Res. 2019; 6(3): 362-365, DOI: 10.5455/javar.2019.f355.

25. Liu K, Zhang L, Gu X, Qu W. The prevalence of Klebsiella spp. associated with bovine mastitis in china and its antimicrobial resistance rate: A Meta-analysis. Front Vet Sci. 2022; 9:75750, DOI: 10.3389/fvets.2022.757504.

26. Song J, Xiang W, Wang Q, Yin J, Tian T, Yang Q, Zhang M, Ge G, Li J, Diao N, Liu F, Shi K, Cai R, Du R, Gong Q. Prevalence and risk factors of *Klebsiella* spp. in milk samples from dairy cows with mastitis-A global systematic review. Front Vet Sci. 2023; 10:1143257, DOI:10.3389/fvets.2023.1143257.

27. Olaitan MO, Orababa OQ, Shittu RB, Oyediran AA, Obunukwu GM, Arowolo MT, Kade AE, Yahaya KI, Yusuff RA. Extended-spectrum beta-lactam-resistant *Klebsiella pneumoniae* in sub-Saharan Africa: A systematic review and meta-analysis from a One Health perspective. BMC Infect Dis. 2025: 25(1):843, DOI: 10.1186/s12879-025-11276-9.

28. Arya LK, Manoj Kumar, Priya P, Saurabh K, Kumari N. Isolation and Identification of *Klebsiella pneumoniae* from a milk sample. Indian Vet J. 2020; 97 (01): 15-17.

29. Yadav R, Chhabra R, Singh M, Shrinet G, Talukdar SJ. Antibiogram of *Klebsiella pneumoniae* isolated from mastitic milk samples of cattle and buffalo. Haryana Vet. 2021; 60(2): 195-197.

30. Mukherjee S, Chaki, S, Pal TK, Mookerjee M, Das S, Dastidar SG. Experimental studies on synergism between meropenem and sulbactam. Afr J Microbiol Res. 2013; 7(27): 3461-3465, DOI: 10.5897/AJMR12.497.

31. Mosallam FM, Elshimy, R. Eradication of Klebsiella pneumoniae pulmonary infection by silver oxytetracycline nano-structure. AMB Expr. 2024; 14(1):62, DOI:10.1186/s13568-024-01720.

32. Shadkam S, Goli HR, Mirzaei B, Gholami M, Ahanjan M. Correlation between antimicrobial resistance and biofilm formation capability among *Klebsiella pneumoniae* strains isolated from hospitalized patients in Iran. Ann Clin Microbiol Antimicrob. 2021; 20(1): 13, DOI: 10.1186/s12941-021-00418-x.

33. Nahar AK, Islam MA, Islam MN, Alam MM. ESBL-producing Klebsiella sp. isolated from raw milk of healthy cow in small holder dairy farms of Mymensingh district in Bangladesh. Bangladesh J Vet Med. 2021;19 (2): 141-150, DOI: 10.33109/bjvmjd2021amrt1.

34. Gelalcha BD, Dego OK. Extended-spectrum beta-lactamases producing *Enterobacteriaceae* in the USA dairy cattle farms and implications for public health. Antibiotics (Basel). 2022; 11(10), DOI: 10.3390/antibiotics11101313.

35. Lalak A, Wasyl D, Zajac M, Skarzynska, M, Hoszowski A, Samcik I, Wozniakowski G, Szulowski K. Mechanisms of cephalosporin resistance in indicator Escherichia coli isolated from food animals. Vet Microbiol. 2016; 194: 69-73, DOI: 10.1016/j.vetmic.2016.01.023.

36. King DT, Sobhanifar S, Strynadka, NCJ. The Mechanisms of resistance to β-Lactam antibiotics. In Handbook of Antimicrobial Resistance, 2017;1-22pp, DOI:10.1007/978-1-4939-0667-3-10-1.

37. Cao W, Xu Y, Huang Y, Xu T. Isolation of pathogenic bacteria from dairy cow mastitis and correlation of biofilm formation and drug resistance of *Klebsiella pneumoniae* in Jiangsu, China. Agriculture. 2023; 13, DOI:10.3390/agriculture13101984.

38. Timofte D, Maciuca IE. Evans NJ, Williams H, Wattret A, Fick JC, Williams NJ. Detection and molecular characterization of *Escherichia coli* CTX-M-15 and *Klebsiella pneumoniae* SHV-12 –β-lactamases from bovine mastitis isolates in the United Kingdom**.** Antimicrob Agents Chemother. 2014; 58(2): 789-794, DOI: 10.1128/AAC.00752-13.

39. Chowdhury MSR, Hossain H, Rahman MN, Rahman A, Ghosh PK, Uddin MB, Hoque MN, Hossain MM, Rahman MM. Emergence of highly virulent multidrug and extensively drug resistant *Escherichia coli* and *Klebsiella pneumoniae* in buffalo subclinical mastitis cases. Sci Rep. 2025; 15:11704, DOI:10.1038/s41598-025-95914-x.

40. Wyres KL, Holt KE. *Klebsiella pneumoniae* as a key trafficker of drug resistance genes from environmental to clinically important bacteria. Curr Opin Microbiol. 2018; 45:131-139, DOI: 10.1016/j.mib.2018.04.004.

Cite this article as: Jayalakshmi K, Palanivel KM, Sumathi D, Vijayarajan A, Babu Prasath N, Sangeetha A, Veeraselvam M. Prevalence of *Klebsiella pneumoniae* and antimicrobial resistance genes in bovine mastitis in cauvery delta region of Tamil Nadu. Explor Anim Med Res. 2026; 16(1), DOI: 10.52635/eamr/16.1.85-93.

Explor Anim Med Res.
Vol. 16, Issue 1, 2026
DOI: 10.52635/eamr/16.1.94-101

ISSN 2277-470X (Print), ISSN 2319-247X (Online)
Website: www.animalmedicalresearch.org

Published under the CC BY-NC 4.0 license

Research Article

OCCURRENCE OF *BABESIA* SPP. INFECTION IN DOMESTIC CATS (*FELIS CATUS*) OF ASSAM, INDIA

Pooja K. Marwaha[1], Arabinda Phukan[1], Nagendra N. Barman[2], Deepa Lahkar[3], Ditul Barman[1], Bendangla Changkija[1], Mrinal K. Nath[3], Utpal Barman[1], Prerona Patowary[1], Tinku Das[3] and Syed A. Arif [4]*

Received 14 April 2025, revised 22 April 2026

ABSTRACT: Babesiosis in cats is a relatively unexplored tick-transmitted clinical entity, however, increasing numbers of cases highlight the growing importance of disease. The study was conducted from June 2020 to May 2021 to assess the hospital-based occurrence and clinical-pathological alterations linked to *Babesia* infections in domestic cats of Assam presented to Veterinary Clinical Complex (VCC), College of Veterinary Science, Khanapara, Guwahati. Suspected cats (n=50) were screened for *Babesia* infection by conventional microscopy followed by molecular testing. Additionally, the haemato-biochemical alterations in affected cats were also analyzed. An occurrence of 52.00% (26/50) was recorded for babesiosis in cats. Risk factor analysis revealed age to be significantly correlated with the infection, being highest in cats of >2 years while the other associated factors were statistically non-significant. Most consistent clinical manifestations were lethargy/weakness, fever, dark yellow urine and/or stool, diarrhoea, pale mucous membranes, dry muzzle, rough coat and inappetence. Hematobiochemical analysis revealed decreased haemoglobin, total erythrocyte and platelet counts, increased ALT, AST and bilirubin in affected cats, with data being statistically significant ($p<0.05$). Combined treatment of diminazene diaceturate and clindamycin along with supportive therapy led to recovery in affected cats except two with the cerebral form and severe anaemia. The present findings will assist clinician and field veterinarians while managing similar type of clinical cases and serves as valuable baseline data to conduct further research. Although treatment of these cases can be very challenging, but with proper evaluation of the haemato-biochemical findings, along with other diagnostic tests, can help in delivering rational treatment, especially in field condition.

Keywords: Assam, *Babesia*, Cat, Haemoprotozoa, PCR

INTRODUCTION

The domestic cat (*Felis catus*) evolved from the Middle Eastern wildcat (*Felis silvestris*) about 70,000 to 100,000 years ago. Today, there are about 600 million domestic cats worldwide, however, their population in India is currently unreported [1].

Feline babesiosis, caused by several species of *Babesia* such as *Babesia felis*, *B. herpailuri*, *B. cati*, *B. pantherae*, *B. canis* subsp. *presentii*, *B. canis* subsp. *canis*, and *B. microti*, is transmitted through tick bites and is frequently diagnosed in the clinical veterinary practice [2]. In acute cases, anaemia is the primary symptom, however, cats often show signs like lethargy, loss of appetite, rough coat, exercise intolerance, weight loss, weakness, pale gums, rapid heart rate and breathing, pica, vomition, and diarrhoea. Blood tests typically reveal regenerative anaemia, reduced platelet along with variable white blood cell counts [3]. The rise in cases of babesiosis is attributed to the growing feral cat population and their interactions with stray dogs, which facilitate the spread of these parasites [4]. Diagnosis of infection ranges from direct microscopy to more sensitive molecular techniques such as PCR assays, which are effective in detecting low

[1]*Department of Veterinary Clinical Medicine, Ethics & Jurisprudence,* [2]*Department of Veterinary Microbiology,* [3]*Department of Veterinary Epidemiology & Preventive Medicine,*
College of Veterinary Science, Assam Agricultural University, Khanapara, Guwahati-781022, Assam, India.
[4]*Division of Veterinary Medicine, ICAR-IVRI, Izatnagar, Bareilly, Uttar Pradesh, India.*
**Corresponding author. e-mail: syed.arif@aau.ac.in*

levels of parasitaemia. The treatment options include administration of drugs like primaquine phosphate and diminazene aceturate, though their efficacy remains under-studied [5].

The current work aims to explore status of babesiosis in cats of Assam, India, a region with favorable conditions for the disease with a focus on clinical presentations, molecular diagnosis, and therapeutic management of the infection.

MATERIALS AND METHODS

Study area

The current study was carried out for a period of 12 months from June, 2020 to May, 2021 in Veterinary Clinical Complex (VCC), College of Veterinary Science, Assam Agricultural University, Khanapara, Guwahati, Assam. The state usually experiences hot and humid climatic condition with long summers, short winter, and heavy rainfall which make its highly conducive for the development and propagation of various ticks that acts as a natural vector for transmitting various haemoparasitic diseases in animals.

Study animals

Domestic cats were attended as routine clinical inspection at the OPD unit of VCC and suspected cases for *Babesia* infection irrespective of age, sex and breed were selected based on history and clinical symptoms. as, reduced activity, rough coat, inappetence, anorexia, weakness, fever, subnormal temperature, diarrhoea, recumbency, dry muzzle, sunken eyeballs, vomiting, pale-whitish/icteric mucous membranes, dark yellow urine and/or stool colour, respiratory distress, nervous symptoms, increased capillary refill time (CRT) and skin tent test (STT).

Collection of blood samples

Around 2mL of whole blood in EDTA and 3mL in clot activator tubes were collected aseptically by venipuncture of cephalic and/or saphenous veins for microscopy, haemato-biochemical and molecular tests. The parasitological and haemato-biochemical testing were conducted on same day of collection while part of samples was preserved at -20°C until further processing for molecular tests.

Diagnosis

Microscopic detection

The microscopy was conducted on Giemsa-stained thin blood smears as per standard protocol [6]. A sample was recorded negative if no parasites were detected after examining at least 50 oil immersion fields for duration of 20-30 minutes [7]. Additionally, for accurate microscopic diagnosis of blood parasites, Giemsa working solution was optimized to pH 7.0–7.2 [8]. Buffered distilled water at this pH produced more uniform staining and improved smear clarity.

Molecular detection

Extraction of DNA

The DNA extraction was carried out from the blood samples using DNeasy Blood and Tissue Kit® (QIAGEN, Hilden, Germany) as per manufacturer's protocol. Molecular testing was conducted to detect presence of *Babesia* spp. by using a genus specific primer as per method described by Birkenheuer and coworkers [9].

DNA Amplification for *Babesia* spp.

The extracted DNAs were subjected to PCR reaction to amplify *18S rRNA* gene fragment of 340 bp with published primers [9]. The PCR assay was performed in reaction volume of 25µL with mixture comprising of 5µL DNA template, 12.5µL DyNAzyme II PCR mix (Sapphire Fast PCR mix, Takara), 5.5µL nuclease-free water (NFW) and 1 µL each (10 pmol) of *Babesia* genus specific forward and reverse primers. The reaction was performed with 35 cycles with each cycle consisting of 45s for denaturation at 98ºC, 56°C each for annealing, and 72°C for extension. A final extension step was performed at 72°C for 5 min, followed by a hold at 4°C, in a semi-automated thermal cycler (TC-5000; Bibby Scientific, Burlington, USA). The positive control for was obtained from repository of Department of Veterinary Parasitology, CVSc, AAU, Khanapara, Guwahati, India. Distilled water was used as no template control. The PCR product was subjected to agarose gel electrophoresis and visualized under UV transilluminator.

Haemato-biochemical parameters

Haematological and biochemical assessments were performed by using a semi-automated blood analyser (MS4-e,MeletSchloesing Lab, France) and biochemical analyzer (C-61; Benesphera®, Avantor, Mumbai, India) as per manufacturer's instructions. Blood parameters, including total red blood cell count (TEC), haemoglobin level (Hb), packed cell volume (PCV), total white blood cell count (TLC), differential white blood cell count (DLC), and platelet count were evaluated. Additionally, serum biochemical markers such as total protein, albumin, alanine aminotransferase (ALT), aspartate

aminotransferase (AST), alkaline phosphatase (ALP), total bilirubin (direct and indirect), total serum protein (TSP), blood urea nitrogen (BUN) and creatinine were also studied and compared between babesiosis affected cats and healthy control.

Statistical analysis

Data obtained were analyzed for age, sex and season wise (pre-monsoon, monsoon, post-monsoon and winter) as risk factors to understand their correlation with occurrence of babesiosis in cats. The whole period of observation was divided into four seasons as per Indian Meteorological Department (IMD), Airport, Guwahati-15, Assam, India.

Additionally, to perform comparative evaluation of healthy cats and *Babesia*-positive cats for haematological and biochemical analyses, out of 26 cats diagnosed as positive for *Babesia* infection, only 14 cases were included based on sample adequacy, completeleness of records and owners consent. The data generated were analyzed using the Chi-square (χ^2) test, with significance assessed at 1% and 5%. Twenty-one cats were divided into two groups: Group I (7 healthy cats) and Group II (14 cats with babesiosis). Mean values, standard error, and significant differences ($p<0.05$) between the groups were determined using one-way ANOVA. All tests used a significance level of $p=0.05$. SPSS version 20.0 was used for analysis.

RESULTS

During the study period, a total of two-hundred fifty (250) domestic cats were presented to the VCC of which 50 were clinically suspected to have haemoprotozoan infection based on observed symptoms as described earlier. A total of 20 cats were detected positive for *Babesia* spp. via microscopy (Figure 1). However, the PCR assay conducted on all the blood samples (n=50) detected 6 more positive cases, as confirmed by the amplification of expected 340 bp product (Figure 2), in addition to the 20 cases positive by microscopy. Hence, in the present study, an occurrence of 52.00% (26/50) was recorded for babesiosis in cats of Assam, India.

All the cats found positive for *Babesia* spp. were treated with a combination of diminazine diaceturate @3.5mg/kg BW, deep I/M (2 doses at 48-hour interval) and clindamycin @ 10mg/kg body weight P.O. (twice daily for 2 weeks). Supportive treatment comprising of intravenous fluids, multivitamins, acid blockers, anti-emetics, haematinics and platelet booster formulations were instituted whenever necessary. Twenty-three cats (88.46%) recovered uneventfully whereas two cats who exhibited cerebral form of the disease with head tilting or apathetic/ataxic behavior (Figure 9) and one presented lately with severe signs of anaemia, unfortunately succumbed to the infection within two days of starting treatment.

The TEC, Hb, and platelet count, were significantly lower ($p<0.01$), while TLC was significantly higher ($p<0.01$) in cats infected with babesiosis compared to healthy controls (Table 2). Statistical non-significant ($p>0.05$) elevation was recorded for lymphocytes, monocytes, neutrophils, eosinophils, basophils in babesiosis infected cats in comparison to healthy control. Non-significant lower PCV values were also recorded in babesiosis infected cats ($p>0.05$) (Table 2). The biochemical analysis showed that the average levels of TSP, BUN, and creatinine were significantly lower ($p<0.01$), while the mean levels of ALT ($p<0.01$), AST ($p<0.01$), direct serum bilirubin, indirect serum bilirubin, and total serum bilirubin were significantly higher ($p<0.05$) in cats diagnosed with babesiosis (Table 2).

DISCUSSION

This is the first report on occurrence and clinico-pathological changes associated with naturally occurring babesiosis in domestic cats of Assam, India. Similar findings have been reported by other workers [10, 11] who reported an occurrence of feline babesiosis of upto 77%. On the other hand, some reports suggested lower prevalence rates of 9% and 3.14% respectively [12,13]. In addition to this, variation in sample size [14], and geo-climatic location could be one of the reasons for this finding. On contrary, the lower rate of occurrence of babesiosis in cats may be attributed to their grooming behaviour, which significantly lessens the exposure to the ectoparasitic vectors thereby reducing transmission [15]. At the same time, the higher occurrence in our study could be a result of the pre-immunity concept, where contracting infection in the early days of life, especially in endemic areas, leads to subclinical carrier status without manifesting any clinical signs [11]. No statistical difference was noted in occurrence of the disease in relation to gender which corroborates with the findings of Vilhena and co-workers [12]. However, non-significant higher infection was found in males (53.85%) than females (50.00%) [15,16]. The increased susceptibility may be attributed to factors such as variations in environmental exposure, including more frequent roaming behavior, or sex-

Table 1. Age, season and sex-wise occurrence of *Babesia* infection in domestic cats

	Frequency	Total no. of cases	Number of positive cases	Occurrence (%) (95% CI)[a]	Chi-Sq	p-value
Age	<6 months	15	5	33.33 (0.095-0.571%)	10.037	0.018*
	6-12 months	13	8	61.50 (0.350-0.880%)		
	13-24 months	12	4	33.33 (0.066-0.600%)		
	>24 months	10	9	90.00 (0.714-1.086%)		
Season	Pre-monsoon (March to May)	10	8	80.00 (0.553-1.000%)	4.174	0.241
	Monsoon (June to September)	12	6	50.00 (0.218-0.782%)		
	Post-monsoon (October & November)	18	8	44.44 (0.215-0.673%)		
	Winter (December to February)	10	4	40.00 0.096-0.704%)		
Gender	Male	26	14	53.85 (34.70-73.00%)	0.073	0.786
	Female	24	12	50.00 (38.20-65.80%)		
	Total	50	26	52.00		

[a] *Confidence interval; result is significant at ($p<0.05$)*

related genetic and hormonal influences on the disease [16]. A higher rate of occurrence was observed in cats older than 2 years of age can be explained by the behavioural and hunting activity of the animal that brings them in close contact with vectors of the disease, thereby making them easy targets of infestation. Similar findings were also suggested elsewhere [13].

Occurrence of the disease was recorded to be the highest (80.00%) in pre-monsoon and lowest (40.00%) in the winter season. This finding can be correlated with the fact that warm and moist conditions are highly conducive for the growth and multiplication of vectors [13]. PCR-based diagnosis of babesiosis was found to be more sensitive than traditional microscopic detection. This can be attributed to the fact that conventional Giemsa stained microscopy usually fails to detect the parasite in case of low parasitemia in naturally infected animals/or chronic carriers. Similar reports were published by other workers [17, 18, 19].

In this study, the primary clinical signs observed in cats affected by babesiosis included increased lethargy/weakness (100%) followed by fever (84.62%), dark yellow urine and/or stool (76.92%), diarrhoea (69.23%), dry muzzle (57.69%), recumbency (57.69%), prolonged capillary refill time (53.85%), dehydration (53.85%), rough coat (46.15%), inappetence (42.31%) anaemia (34.62%), vomition (30.78%), sunken eyeballs (30.78%), sub-normal temperature (15.38%), respiratory distress (11.58%) and ataxia (7.69%). Corneal opacity was detected in two cats (7.69%), possibly resulting from the formation of immune complexes [20]. Weakness/ lethargy, pyrexia and pale mucous membranes were the most prominent clinical feature of feline babesiosis. Development of anaemia followed by icteric condition is might be due to the destruction of parasitized erythrocytes by macrophage-monocyte system. Fever reaches its peak during the initial phase of parasitemia, likely due to the release of pyrogens during erythrolysis [21]. Nervous symptoms typically appear in the later stages of the disease and may result from the parasites invading the central nervous system [22]. Clinical symptoms such as vomiting and respiratory distress recorded in this study could possibly related to systemic inflammatory response syndrome (SIRS) due to release of different chemical

Table 2. Comparison of haemato-biochemical parameters between babesiosis affected cats and healthy control.

Parameter	Infected (n=14)	Healthy control (n=7)	*p*-value	Reference range*	Key findings
TEC (×10^6/µL)	4.94±0.55	7.53±0.21	0.007**	5.5-10.0	Severe anaemia
TLC(×10^3/µL)	36.07±5.88	11.09±0.44	0.001**	5.5-19.5	Leucocytosis
PCV (%)	28.86±2.45	36.14±1.73	0.154^{NS}	30-45	-
Hb (g/dL)	8.24±0.1	11.13±0.42	0.002**	9.8-15.4	-
Thrombocytes (×10^3/µL)	79.07±11.46	215.86±18.85	0.007**	120-500	Thrombocytopenia
Lymphocytes (%)	41.7±2.51	35.58±3.68	0.944^{NS}	27-36	Lymphocytosis
Monocytes (%)	2.9±0.32	0.96±0.17	0.566^{NS}	0-5	-
Neutrophils (%)	59.97±3.76	56.87±2.5	0.772^{NS}	45-64	-
Eosinophils (%)	1.05±0.38	0±0	0.099^{NS}	0-4	-
Basophils (%)	0.5±0.07	0.47±0.03	0.724^{NS}	0-1	-
ALT (IU/L)	83.11±9.77	58.31±2.46	0.004**	25-97	Hepatic damage
AST(IU/L)	51.99±5.66	36.19±0.63	0.008**	7-38	-
Serum direct bilirubin (mg/dL)	0.85±0.37	0.26±0.03	0.041*	<0.3	Haemolytic anaemia
Serum indirect bilirubin (mg/dL)	0.46±0.11	0.19±0.04	0.037*	0.1-0.4	-
Serum total bilirubin (mg/dL)	1.31±0.46	0.46±0.07	0.047*	0.15-0.8	Hyperbilirubinemia
TSP(g/dL)	6.34±0.17	6.74±0.08	0.910^{NS}	5.4-7.9	-
BUN (mg/dL)	37.77±5.91	24.73±0.75	0.061^{NS}	19-34	Azotaemia
Creatinine (mg/dL)	2.64±0.94	1.29±0.09	0.179^{NS}	0.8-1.8	-

p<0.05 Significant; *p<0.01* Highly significant; *p>0.05* Non-significant. ** indicates highly significant (*p<0.01*), ^{NS}indicates non-significant difference (*p<0.05*).
*Normal reference range: The Merck Veterinary Manual, 11th edition (2016)

mediators of inflammation [23], and as a result of inflammatory response, animal can develop gastritis, pancreatitis and pulmonary dysfunction. This may lead to multiple organ dysfunction syndrome as the chief mechanism responsible for most of the clinical signs of feline babesiosis [23].

The mean values of Hb, TEC and thrombocytes showed highly significant changes (p<0.01) in babesiosis affected cats and the present finding is in agreement with previous reports [22,24]. The precise mechanism behind anaemia is not fully comprehended. However, Anaemia in cats infected with Babesia spp. could be caused by haemolysis and mechanical destruction of the affected erythrocytes. Additionally, the production of serum haemolytic factors [25], oxidative damage to erythrocytes, and changes in erythrocyte osmotic fragility [22,25] contribute to enhanced phagocytosis of red blood cells, leading to anaemia. Haemolysis can occur either intravascularly or extravascularly, typically caused by the attachment of the parasite to the erythrocyte membrane or by biologically active molecules produced by the pathogen, whether alive or dead. The severity of anaemia is usually a reflection of the intensity and duration of parasitemia [23]. On the other hand, PCV values were found to be lower but statistically insignificant (p>0.05) in babesiosis affected cats than to normal. The reduced values observed in affected cats align with the results reported earlier [2, 22]. The decrease in PCV could be due to the immune-mediated deconstruction of erythrocytes caused by binding of antibodies on to blood cells activating the compliment system.

The leucocytosis and granulocytosis observed in this study are consistent with previous report [3]. This could be due to recruitment of immune cells in response to chemical mediators of inflammation due to ongoing infection. However, it was found that white blood cell counts to be variable and inconsistent in cats suffering from babesiosis [2]. On the other hand, both leucopaenia and leucocytosis are associated with babesiosis [24]. Insignificant lymphocytosis observed in the cats affected with *Babesia* spp. infection is explained by generalized hyperplasia of the lymphoid tissue in response to pathogen during the acute phase of a disease [25].

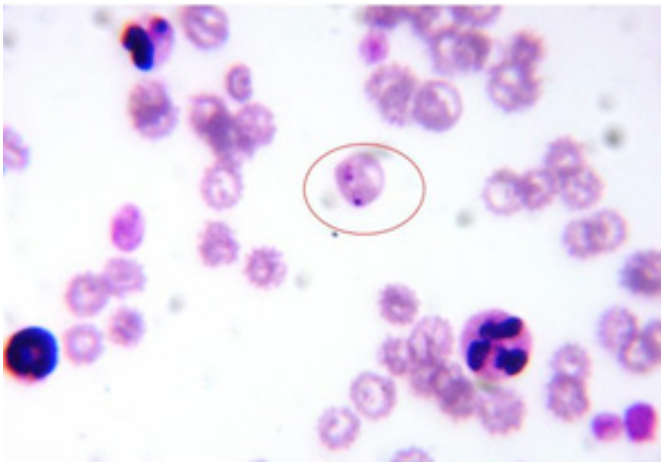

Fig.1: Photomicrograph showing *Babesia organism* in erythrocytes, Giemsa stain (x100 magnification).

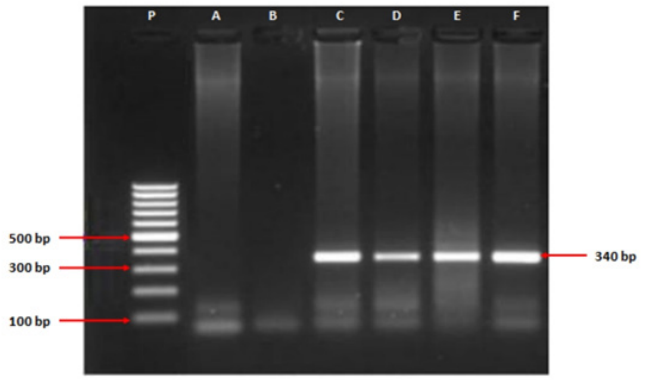

Fig. 2 Agarose gel electrophoresis of 340bp fragments of Babesia spp. DNA; Lane P: 100bp DNA ladder;
Lane A: Negative sample; Lane B: Non template control;
Lane C: Positive control; Lane D, E & F: PCR product of Babesia spp. sample.

Fig. 3 (A & B)

Fig. 4

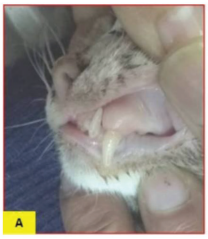

Fig. 5 (A & B)

Fig. 6

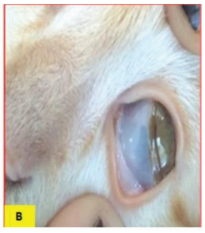

Fig. 7 (A & B)

Fig. 8 (A & B)

Fig.9 (A & B)

Fig. 3 (A) and **(B)** Mentation- depressed and lethargic; **Fig. 4** Diarrhoea; **Fig. 5 (A)** and **(B)** Pale mucous membrane of gums;Figure 6: Rough body hair coat; **Fig.7 (A)** and **(B)** Sunken eyeball with pale mucous membrane; **Fig. 8 (A)** and **(B)** Visible yellow discolouration of skin & mucous membranes (icterus); **Fig. 9 (A)** and **(B)** Head tilting and circling gait seen due to nervous system involvement –cerebral form of feline babesiosis.

ALT is an enzyme found in the liver that aids in converting proteins into energy within hepatocytes, whereas AST have a role in metabolism of amino acids. Normally, these enzymes are present in the bloodstream at low levels under physiological conditions. However, during liver diseases, their levels increase, serving as indicators of hepatic injury. Elevated AST levels can also indicate muscle damage. The mean values of ALT and AST were significantly ($P<0.01$) higher in the babesiosis affected cats in the study and it could be due to tissue hypoxia, hepatocellular injury and necrotic damage to liver and skeletal muscles [3,]. Bilirubin is a breakdown product of erythrocytes. Increased bilirubin levels may suggest hepatic injury, haemolytic anaemia, or biliary obstruction. The hyperbilirubinemia observed in cats with babesiosis could be attributed to excessive red blood cell destruction by the invading pathogen or increased fragility of the erythrocytes, intrahepatic cholestasis and subsequently, excessive production of bilirubin (both direct and indirect) [3, 23]. Further, values for TSP, BUN and creatinine in the babesiosis affected cats were slightly elevated in comparison to healthy cats, but they did not show significant difference ($p>0.05$) which might be possibly due to the infection not being very severe in the affected cats. Similar reports were also published by other workers [22].

CONCLUSION

This study provides the first report on the occurrence and clinicopathological changes associated with babesiosis in domestic cats from Assam, India. An occurrence of 52.00% was recorded during the study period from June 2020 to May 2021. Common clinical signs included lethargy, fever, icterus, diarrhoea, and inappetence, while rare cerebral involvement was noted in two cases. Affected cats exhibited severe anaemia, leukocytosis, lymphocytosis, thrombocytopenia, and elevated ALT, AST, and bilirubin levels, indicating hepatic dysfunction. Mean TSP, BUN, and creatinine levels were insignificantly higher than in healthy cats. It was also found that while PCR proved to be more sensitive and reliable for diagnosing the infection, optimizing the buffer pH during staining could be promising, especially under field conditions. Findings of the present study shall help the clinicians in diagnosing and treating similar clinical cases. Combined therapy with diminazene diaceturate and clindamycin showed excellent recovery outcomes.

Conflict of interest

The authors declare that there is no conflict of interest.

Acknowledgements

The authors expresses sincere gratitude to the authority of College of Veterinary Science, Assam Agricultural University, Khanapara, Guwahati-781022, Assam for providing the necessary facilities and acknowledges the sincere support extended by all the technical and non-technical staffs under DBT-ADMaC (Advanced Animal Diagnostics and Management Consortium) for carrying out the research work.

Ethical clearance

This study was approved by the Institutional Animal Ethics Committee with the approval number: 770/Go/Re/S/03/CPSCEA/FVSc/AAU/IAEC/773.

REFERENCES

1. Driscoll CA, Clutton-Brock J, Kitchener AC, O'Brien, SJ. The taming of the cat. Sci Am. 2009; 300(6): 68-75.

2. Kumar M, Shekhar P, Haque S, Mahto D. Feline babesiosis. Vet World. 2008; 1(4): 120-121.

3. Ayoob AL, Prittie J, Hackner SG. Feline babesiosis. J Vet Emerg Crit Care. 2010; 20(1): 90-97. DOI: 10.1111/j.1476-4431.2009.00493.x.

4. Bhattacharjee K, Sarmah PC. Prevalence of haemoparasites in pet, working and stray dogs of Assam and North-East India: A hospital based study. Vet World. 2013; 6(11): 874-878. DOI: 10.14202/vetworld.2013.874-878.

5. Lewis KM, Cohn LA, Marr HS, Birkenheuer AJ. Failure of efficacy and adverse events associated with dose-intense diminazene diaceturate treatment of chronic *Cytauxzoon felis* infection in five cats. J Feline Med Sur. 2014; 16(2): 157-163. DOI: 10.1177/1098612X13502974.

6. Soulsby EJL. Helminthes, Arthropods and Protozoa of domesticated animals, 7th ed.; Lea & Febiger: London, United Kingdom, 1982; pp.728-737.

7. Kakati P, Sarmah C, Ray D, Bhattacharjee K, Sharma R, *et al*. Emergence of oriental theileriosis in cattle and its transmission through *Rhipicephalus (Boophilus) microplus* in Assam, India. Vet World. 2015; 8: 1099-1104. DOI: 10.14202/vetworld.2015.1099-1104.

8. Arif SA, Mahato G, Barman NN, Islam S, Das T, *et al*. Epidemiological studies on pathogenic Theileria infection in the goat population of Assam, India. J Livest Sci, 2025; 16: 127-135. DOI: 10.33259/JLivestSci.2025.127-135.

9. Birkenheuer AJ, Levy MG, Breitschwerdt EB. Development and evaluation of a seminested PCR for detection and differentiation of *Babesia gibsoni* (Asian genotype) and B. canis DNA in canine blood samples. J Clin Microbiol. 2003; 41(9): 4172-7. DOI: 10.1128/JCM.41.9.4172-4177.2003.

10. Futter, GJ and Belonje, P. Studies on feline babesiosis. J S Afr Vet Assoc. 1980; 51(3): 143-146.

11. Schoeman T, Lobetti RG, Jacobson LS, Penzhorn, BL. Feline babesiosis: Signalment, clinical pathology and concurrent infections. J S Afr Vet Assoc. 2001; 72(1): 4-11. DOI: 10.4102/jsava.v72i1.601.

12. Vilhena H, Martinez-Díaz VL, Cardoso L, Vieira L, Altet L, *et al*. Feline vector-borne pathogens in the north and centre of Portugal. Parasit Vectors. 2013; 6: 99. DOI: 10.1186/1756-3305-6-99.

13. Ahmad SS, Khan MS, Khan MA, Ahmad N. Prevalence of Babesiosis in cats in Lahore. Pakistan J Anim Plant Sci.,2011; 21(2): 354-357.

14. Sarma K, Eregowda CG, Roychoudhury P, Borthakur SK, Jawalagatti V, *et al.* A 5-Year Prospective Study on Incidence and Clinico-pathological Changes Associated with Naturally Occurring Trypanosomosis in

Dogs of Mizoram, India. Acta Parasitol. 2022; 67(1):61-71. DOI: 10.1007/s11686-021-00425-0.

15. Eckstein RA, Hart BL. Grooming and control of fleas in cats. Appl Anim Behav.Sci. 2000; 68: 141-150. DOI: 10.1016/s0168-1591(00)00095-2.

16. Mellanby RJ, Handel IG, Clements DN, Bronsvoort BM, Lengeling A, Schoeman JP. Breed and sex risk factors for canine babesiosis in South Africa. J Vet Intern Med. 2011; 25(5):1186-9. DOI: 10.1111/j.1939-1676.2011.00779.x

17. Rucksaken R, Maneeruttanarungroj C, Maswanna T, Sussadee, M, Kanbutra P. Comparison of conventional polymerase chain reaction and routine blood smear for the detection of *Babesia canis*, *Hepatozoon canis*, *Ehrlichia canis*, and *Anaplasma platys* in Buriram Province, Thailand. Vet World. 2019; 12(5):700-705. DOI: 10.14202/vetworld.2019.700-705.

18. Sindhu B, Shobhamani B, Suresh K, Chengalva, RV. Diagnosis of Babesiosis by Conventional Microscopy and PCR. Int J Curr Microbiol App Sci. 2020; 9(09): 345- 350. DOI: https://DOI.org/10.20546/ijcmas.2020.909.044

19. Arif SA, Lahkar D, Gogoi SM, Changkija B, Kakati P, *et al*. The molecular detection and therapeutic management of pathogenic *Theileria luwenshuni* infection in a goat: A case report. Iranian J Parasitol. 2024; 9(4): 1-8. DOI: 10.18502/ijpa.v19i4.17173.

20. Joshi V, Alam S, Dimri U, Bhanuprakash AG, Gopalakrishnan A, Ajith, Y. A rare case of *Theileria annulata* induced corneal opacity in a calf. J Parasit Dis. 2016; 41(2):442-445. DOI: 10.1007/s12639-016-0824-z.

21. Breitschwerdt EB. Clinical Microbiology and Infectious Diseases of the Dog and Cat. Philadelphia: WB Saunders. 1984; pp. 796-805.

22. Hartmann K, Addie D, Belák S, Baralon CB, Egberink H, *et al.* Babesiosis in cats: ABCD guidelines on prevention and management. J Feline Med Sur. 2013; 15: 643-646. DOI: 10.1177/1098612X13489230.

23. Taboada J, Merchant SR. Babesiosis of companion animals and man. Vet Clinics North America: Small Animal Practice. 1991; 21(1): 103-122.DOI: 10.1016/s0195-5616(91)50011-5.

24. Vilhena H, Tvarijonaviciute A, Ceron JJ, Vieira L, Pastor J, Silvestre-Ferreira AC. Acute phase proteins response in cats naturally infected with *Hepatozoon felis* and *Babesia vogeli*. Vet Clinical Pathol. 2017; 46(1): 72-76. DOI: 10.1111/vcp.12451.

25. Onishi T, Ueda K, Horie M, Kajikawa T, Ohishi I. Serum hemolytic activity in dogs infected with *Babesia gibsoni*. J Parasitol. 1990; 76: 564-567.

Cite this article as: Marwaha PK, Phukan A, Barman NN, Lahkar D, Barman D, Changkija B, Nath MK, Barman U, Patowary P, Das T, Arif SA. Occurrence of *Babesia* spp. infection in domestic cats (*Felis catus*) of Assam, India. Explor Anim Med Res. 2026; 16(1), DOI: 10.52635/eamr/16.1.94-101.

Explor Anim Med Res.
Vol. 16, Issue 1, 2026
DOI: 10.52635/eamr/16.1.102-107

ISSN 2277-470X (Print), ISSN 2319-247X (Online)
Website: www.animalmedicalresearch.org

Published under the CC BY-NC 4.0 license

Research Article

INFLUENCE OF UREA ON *IN VITRO* METHANOGENESIS AND FERMENTATION OF FEED WITH BUFFALO RUMEN LIQUOR

P. N. Chatterjee[1]*, D. N. Kamra[2], N. Agarwal[2] and Aruna Pal[1]

Received 24 March 2025, revised 8 April 2026

ABSTRACT: Four wheat straw-based iso-nitrogenous and iso-caloric complete feeds were formulated from commonly used feed ingredients containing graded levels of urea so as to replace 0 (U0), 15 (U15), 30 (U30) and 45 (U45) per cent protein. There was no effect on *in vitro* gas production, but methane production was decreased (P<0.05) by 10.6% at the highest level of urea inclusion in the ration (U45). The loss of GE in the form of methane was 9.25, 14.95 and 18.74 per cent less in U15, U30 and U45 rations, respectively, as compared to control (U0). The production of VFA was not affected but acetate: propionate ratio decreased with increasing level of urea in the diet. No difference was observed in protozoa population except total holotrichs, which was significantly higher (P<0.05) in the U0 ration. There was no effect of the urea levels on *in vitro* true digestibility of feed and the activities of different enzymes like Carboxymethyl cellulose, xylanase and protease. It can be concluded that upto 30 percent of replacement of feed nitrogen by urea, methanogenesis can be reduced leaving any adverse effect in rumen fermentation.

Keywords: Buffalo, Feed fermentation, Methane, Protozoa, Urea

INTRODUCTION

Rumen is a unique fermentation vat in the gastro-intestinal tract of ruminants in which a consortium of microbes acts upon the lignocellulosic feed and bioconverts it into volatile fatty acids, microbial protein, carbon dioxide and methane. In the rumen, methanogenesis is an essential metabolic process for the utilization of molecular hydrogen generated during fermentation of feed; otherwise, the accumulation of hydrogen would result in limiting the rate of feed fermentation [1]. The synthesis of methane in the rumen accounts for 2-12% of the gross energy of feed taken by the animal [2]. Further, methanogenesis by the livestock is also of great concern due to its global warming potential, which is 23 times higher than that of CO_2 [3]. Ruminants are responsible for the production of 20% of the global methane emission [4]. Therefore, methane mitigation will improve the feed efficiency of the animals as well as reduce the environmental pollution thus can make livestock production more economical and eco-friendlier.

Diet and feeding schedules have a considerable impact on rumen fermentation pattern and methane generation [5] as molar proportions of different VFA influence the amount of metabolic hydrogen generation [6]. Inclusion of feed additives based on plant secondary metabolites and inorganic compounds also affect production of methane and fermentation of feed [7, 8, 9. 10]. Feeding of urea is commonly recommended as non-protein nitrogen source and has been reported to be economically feasible and has no adverse effect when fed below the toxic levels [11, 12]. The influence of dietary urea on ruminal methanogenesis depends on the level of supplementation, diet composition, and synchronization of nitrogen with energy sources available in the rumen [13]. In recent days attempts are in vogue to devise different slow-release urea compounds that can regulate ruminal fibrolytic bacteria and redirect hydrogen utilization away from methanogenesis [14]. The level of supplementation of urea in practical diet need to be determined to chalk out a strategic feeding regime to boost the rumen

[1] *West Bengal University of Animal and Fishery Sciences, Belgachia, Kolkata-700037, India*
[2] *Animal Nutrition Division, ICAR-Indian Veterinary Research Institute, Izatnagar, UP-243122, India*
**Corresponding author. e-mail: chatterjeenutrition@gmail.com*

fermentation. In the present study, we planned to investigate the effect of urea inclusion in feed on *in vitro* methanogenesis and fermentation of feed in the rumen with buffalo rumen liquor as inoculum.

MATERIALS AND METHODS

Preparation of rations

Four iso-nitrogenous and iso-caloric complete feeds, namely U0, U15, U30 and U45 were prepared wherein 0, 15, 30 and 45 per cent of feed nitrogen was replaced with urea (Table 1). Urea was sprinkled over the respective feeds carefully and mixed well for homogeneity. Ingredients of feeds were properly ground, screened through 1 mm sieve and mixed thoroughly and used for the *in vitro* evaluation. Proximate constituents of ration and NDF and ADF contents were estimated as per AOAC [15]. Gross energy content of feeds was estimated by Gallenkamp adiabatic bomb calorimeter (Fischer Scientific Company, USA).

Feeding of animals and sampling of rumen liquor

Rumen liquor was collected from two adult fistulated buffaloes maintained at Animal Nutrition Shed of the institute, and fed on a diet of concentrate mixture (maize, 320 g; solvent extracted soybean meal, 200 g; wheat bran, 450 g; mineral mixture, 20 g and salt, 10 g per kg) and wheat straw (1:1). The wheat straw contained 909 g organic matter (OM); 31 g crude protein (CP); 15 g ether extract (EE); 835 g neutral detergent fibre (NDF) and 535 g acid detergent fibre (ADF) per kg of DM whereas, the concentrate mixture contained 895 g OM; 195 g CP; 40 g EE; 385 g NDF and 164 g ADF per kg of DM. The animals were fed at the rate of 2.5 kg DM/100 kg BW. Rumen liquor sample was collected just before feeding and was transported immediately to the laboratory under anaerobic conditions in insulated flasks, pooled in equal proportion and used as a source of inoculum.

In vitro gas production test

The *in vitro* gas production test was carried out as per Menke and Steingass [16]. The air-dried substrate samples (200±10 mg) from the four rations were weighed and placed in the graduated glass syringes (100 mL), and 30 mL of the incubation medium was dispensed anaerobically into each syringe followed by incubation at 39°C for 24 h. A similar set of syringes was run separately for estimation of *in vitro* true digestibility (IVTD) after termination of incubation, samples were collected for various analyses.

After 24 h of incubation, the gas production was recorded. For methane estimation, 100 µL of headspace gas from the syringe was injected in gas chromatograph (NUCON 5765, AIMIL, New Delhi, India) equipped with stainless steel Porapak-Q column and flame ionization detector (FID). Gas mixture (Spancan, England) consisted of 50% methane and 50% CO_2 was used as standard. Flow rates of nitrogen, hydrogen and air were kept as 20, 30 and 320 mL/min and the oven, injector and detector temperatures were 40, 50 and 50°C, respectively.

Estimation of enzyme activity and metabolites

The contents of the syringes were treated with carbon tetrachloride and lysozyme solution (0.4%) each at the rate of 5 mL per 30 mL of medium and incubated for 3 h at 39°C. The samples were sonicated for 6 min with 30 sec pulse rate in ice bath followed by centrifugation at 27000 × g for 30 min at 4°C. The clear supernatant was used as enzyme source. The activities of carboxymethyl cellulase (CMCase) and xylanase were estimated using Carboxymethyl cellulose and xylan as substrate as described elsewhere [17]. The reducing sugars produced due to enzyme activity were estimated as described by Miller [18]. A unit of enzyme activity was defined as the enzyme which produced one nanomole of reducing sugar per min under assay conditions. Protease activity was measured by using azocaesin as substrate [19]. The enzyme activity was expressed as microgram of azocaesin hydrolyzed per hour.

The ammonia nitrogen in the fermented medium was estimated as per the method of Weatherburn [20]. For estimation of volatile fatty acids, 1ml of the fermented medium was mixed with 0.20 ml metaphosphoric acid (25 ml/100 ml). The mixture was allowed to stand for 2 h at room temperature and centrifuged at 5000×*g* for 20 min. The 1μl supernatant was injected in a chromosorb 101 glass column (4 ft length and 1.8 mm diameter) fitted in gas chromatograph (Nucon-5765) equipped with FID [21]. Microscopic counting of protozoa was done as described earlier [22].

In vitro digestibility

Another parallel set of syringes was run to estimate *in vitro* true digestibility (IVTD) of feed. After 24 h incubation, contents of the syringe were transferred to a spoutless beaker by repeated washings with 100 mL neutral detergent solution. The flask contents were refluxed for 1 h and filtered through pre-weighed Gooch crucibles (Grade G1). The DM content of the residue was weighed and IVTD of the feed was calculated as follows [23].

Statistical analysis

The data were analyzed using Generalized Linear Model ANOVA procedures and differences between the means were compared by Duncan's Multiple Range Test [24].

RESULTS AND DISCUSSION

The chemical composition of different feeds is presented in Table 1, all of which were iso-caloric and iso-nitrogenous having 11.8-12.1% CP and 58.9-60.0% TDN. The NDF was reduced and acid ADF increased with increasing level of urea.

Gas and methane production per gram DM of feed are presented in Table 2. Gas production was not affected (P≥0.05) with inclusion of urea in the feed. Methane production decreased with increasing level of urea in the feed and was significantly (P< 0.05) lower with the U45 feed where 45% of the nitrogen was replaced with urea. There was 1.6, 7.1 and 10.6% less methane production in U15, U30 and U45 feeds, respectively. A distinct significant correlation (r=0.99) was observed between hemicellulose content of feeds and methane production. In the present study, methane production was decreased with increasing levels of maize in the feeds. The results of the *in vivo* experiments also indicated that less methane was generated with increasing level of concentrate in the diet and on replacing fibrous diet with starchy diet [25] [26]. A significant correlation (r=0.95) was observed between total gas and methane production in the present experiment. Chatterjee *et al.* [6] reported a relationship between TDN level in the feed and methane production. The *in vitro* methane production (ml/g DM) was similar in 80 and 100% TDN diets but methane production (ml/g DDM) was lower in 100% TDN feed. In the present study though, the rations were iso-caloric, maize grain was of variable levels.

Gross energy content of diet was higher in high urea containing rations. The per cent loss of GE as methane was in the range of 8.43-6.85% (Table 2) as described by earlier reports [27]. Loss of GE was 18.74, 14.95 and 9.25% in rations U45, U30 and U15, respectively, where 45, 30 and 15% nitrogen was replaced with urea. No difference (P>0.05) was observed in IVTD of rations on urea inclusion in the rations (Table 2). Toppo *et al*. [28] also did not find any difference in digestibility of urea supplemented and the control feeds in adult crossbred cattle.

There was no difference in microbial enzyme activities (Table 3) among the feeds. However, better

Table 1. Ingredients and chemical composition of the rations.

Ingredients	Rations†			
	U0	U15	U30	U45
Ingredients (% as fed basis)				
Maize	8.28	23.77	39.28	50.0
Wheat straw	3.41	15.53	27.66	41.65
Wheat Bran	85.32	57.70	30.06	5.35
Min. mix	2	2	2	2
Salt	1	1	1	1
Urea (g)	0	0.625	1.250	1.875
Chemical composition (% on DM basis)				
Dry matter	96.39	96.64	96.09	95.19
Crude protein	11.89	12.05	11.79	11.99
Total ash	8.25	8.20	8.08	8.46
Organic matter	91.75	91.80	91.92	91.54
Neutral detergent fibre	61.58	60.76	56.93	55.96
Acid detergent fibre	22.81	26.09	29.49	31.75
Hemicellulose	38.77	34.67	27.44	24.21

†Compete feeds containing graded levels of urea replacing 0 (U0), 15 (U15), 30 (U30) and 45 (U45) per cent of feed nitrogen

Table 2. Gas and methane (mL/g DM) production and *in vitro* true digestibility (%) of feed at 24h.

	Ration†			
	U0	U15	U30	U45
Total gas, mL/g DM	214.4±5.80	209.2±4.62	203.9±3.13	202.5±6.22
Methane, mL/g DM	37.44±0.99[a]	36.83±1.33[ab]	34.79±1.05 [ab]	33.47±1.10[b]
IVTD, %	66.49±0.64	66.42±0.57	66.31±0.40	64.42±0.86
NDF digestibility, %	47.55±0.99 [a]	46.59±0.91[ab]	43.14±0.67[bc]	41.45±1.42[c]
GE (kcal/g DM)	4.1983	4.5524	4.5867	4.6194
Energy loss as methane† (kcal/g DM)	0.3538	0.3480	0.3287	0.3163
GE loss as methane (%)	8.43	7.65	7.17	6.85

†Compete feeds containing graded levels of urea replacing 0 (U0), 15 (U15), 30 (U30) and 45 (U45) per cent of feed nitrogen.
[abc]Means with different superscripts in a column differ significantly (P<0.05)
†GE value of methane was considered as 9.45 kcal/L

Table 3. Effect of urea on microbial enzymes activity and rumen metabolites.

	Rations†			
	R1	R2	R3	R4
CMCase, nmoL/min/mL	46.42±1.39	47.41±3.26	46.45±1.73	47.56±2.08
Xylanase, nmoL/min/mL	100.8±2.75	104.1±3.25	105.7±5.91	106.1±4.14
Protease, µg/h/mL	47.21±5.41	60.36±7.65	56.27±7.15	53.34±7.55
NH_3-N, mg/L	260.2± 4.64	264.9±4.44	270.1± 4.38	272.6±6.63
TVFA,mmoL/dL	4.06± 0.38	4.02±0.14	4.41±0.08	4.20±0.14
Acetate,%	71.71±1.52	70.89±0.50	70.08±0.44	70.41±0.42
Propionate,%	19.54±1.58	20.04±0.48	20.60±0.49	20.91±0.34
Butyrate,%	8.75±0.22	9.07±0.30	9.32±0.23	8.67±0.24
Acetate: Propionate ratio	4.07±0.71	3.55±0.10	3.41±0.10	3.37±0.07

†Compete feeds containing graded levels of urea replacing 0 (U0), 15 (U15), 30 (U30) and 45 (U45) per cent of feed nitrogen.

protease activity was observed in urea containing rations. Ammonia nitrogen content increased with increasing level of urea in the rations, but the differences were not statistically significant (P>0.05). Although hydrolysis of urea by rumen microbes is very rapid but its immediate utilization for synthesis of microbial protein might have occurred due to availability of easily utilizable energy source [29]. In the present study the level of maize grain (source of starch) also increased with the increasing level of urea in the rations.

There was no difference in total VFA production among different rations tested (Table 3). The propionate content was considerably higher at two higher urea levels. The unutilized hydrogen due to reduced methanogenesis upon urea inclusion in the diet might have been diverted for propionate synthesis. This is one of the reasons responsible for 12.78, 16.22 and 17.20% lowering of acetate/propionate ratio with increasing level of urea in the rations, respectively.

The values for total and differential protozoa count as influenced by urea are presented in Table 4. There was no variation (P>0.05) in total protozoa and spirotrich counts. A positive correlation (r = 0.43) was observed between protozoa count and methane production. Finlay *et al*. [30] reported that 37% of methanogenesis in the rumen is due to symbiosis between rumen protozoa and methanogens, as some of the archaea remain attached with the exo-skeleton of protozoa to make interspecies hydrogen transfer

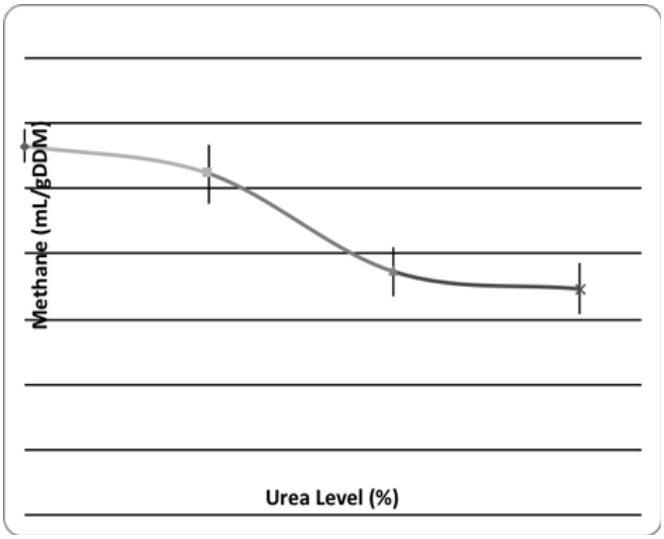

Fig.1. Methane production in buffalo rumen upon inclusion of graded level of urea.

effective. The rations producing more methane also supported higher numbers of protozoa in the present experiment. Our earlier studies have also established that the availability and type of protozoa trigger the fermentation pattern and in turn ruminal methanogenesis [31, 7]. Strategic inhibition of rumen protozoa is often associated with decreased methane output [32, 9].

The results of the present experiment indicated that inclusion of urea in the diet had some impact on the process of methanogenesis without affecting rumen fermentation pattern or digestibility of feed in *in vitro* conditions. Therefore, inclusion of urea in diet can be explored as a feasible nutritional intervention for methane mitigation in ruminants seems to have potential to reduce methane production in the ruminants.

ACKNOWLEDGEMENT

The authors are thankful to the Director, Indian Veterinary Research Institute, Izatnagar, India for providing necessary research facilities and International Atomic Energy Agency, Vienna, Austria for financial assistance to carry out this project.

REFERENCES

1. Bryant MP. Microbial methane production - theoretical aspects. J Anim Sci. 1979; 48: 193-201.

2. Johnson DE, Hill TM, Ward GM, Johnson KA, Branine ME, et al. Principle factors varying methane emissions from ruminants and other animals. In: Atmospheric Methane: Sources, Sinks, and Role in Global Change. NATO ADI Series, 113 (Ed. MAK Khalil). 1993; Springer-Verlag, Berlin, Germany.

3. IPCC. Intergovernmental Panel on Climate Change (Eds. JH Houghton, LG Meria Filho, J Bruce, Hoesung Lee, BA Callander, et al.). 1994; Cambridge University Press, New York, pp. 25-27.

4. Chynoweth DP. Environmental impact of biomethanogenesis. Environ Monit Assess. 1996; 42: 3-18.

5. Moss AR, Jouany JP, Newbold CJ. Methane production by ruminants: its contribution to global warming. Ann Zootech. 2000; 49: 231-253.

6. Chatterjee PN, Kamra DN, Agarwal N. Effect of roughage source, protein and energy levels on *in vitro* fermentation and methanogenesis. Indian J Anim Nutr. 2006; 23: 78-82.

7. Kamra DN, Patra AK, Chatterjee PN, Kumar R, Agarwal N, et al. Effect of plant extracts on methanogenesis and microbial profile of the rumen of buffalo: a brief overview. Aust J Exp Agric. 2008; 48: 175-178.

8. Patra AK, Kamra DN, Agarwal N. Effect of *Terminalia chebula* and *Allium sativum* on *in vivo* methane emission by sheep. J Anim Physiol Anim Nutr. 2011; 95: 187-191.

9. Chatterjee PN, Kamra DN, Agarwal N, Patra A. Influence of supplementation of tropical plant feed additives on *in vitro* rumen fermentation and methanogenesis. Anim Prod Sci. 2014; 54: 1770-1774.

10. Pawar MM, Kamra DN, Agarwal N, Chaudhary LC. Effects of essential oils on *in vitro* methanogenesis and feed fermentation with buffalo rumen liquor. Agric Res. 2014; 3: 67-74.

11. Hamali AY, Manna AL, Owens FN. Effect of energy and nitrogen source on efficiency of microbial protein synthesis in the rumen of steers fed concentrate or roughage diets. J Trop Agric Food Sci. 2001; 29: 223-237.

12. Woyengo TA, Gachuri CK, Wahome RG, Mbugua PN. Effect of protein supplementation and urea treatment on utilization of maize stover by Red Massai sheep. S Afr J Anim Sci. 2004; 34: 23-30.

13. Wahyono T, Sholikin MM, Konca Y, Obitsu T, Sadarman S, et al. Effects of urea supplementation on ruminal fermentation and animal performance in sheep: a meta-analysis. Vet World. 2022; 5(2): 331-340, DOI: 10.14202/vetworld.2022.331-340.

14. Yi S, Zhang X, Zhang J, Pu X, Zhang S, et al. Supplementation of slow-release urea improves milk performance and reduces methane emissions intensity by regulating ruminal fibrolytic bacteria and hydrogen disposal

in dairy cows. J Agric Food Res. 2026; 25: 102584, DOI: 10.1016/j.jafr.2025.102584.

15. AOAC. Official Methods of Analysis (17th ed.). 2000; Association of Official Analytical Chemists, Washington, DC.

16. Menke KH, Steingass H. Estimation of the energetic feed value obtained by chemical analysis and *in vitro* gas production using rumen fluid. Anim Res Dev. 1988; 28: 7-55.

17. Agarwal N, Kamra DN, Chatterjee PN, Kumar R, Chaudhury LC. *In vitro* methanogenesis, microbial profile and fermentation of green forages with buffalo rumen liquor as influenced by 2-bromoethanesulphonic acid. Asian-Australas J Anim Sci. 2008; 21: 818-823.

18. Miller GL. Use of dinitrosalicylic acid reagent for determination of reducing sugar. Anal Chem. 1959; 31: 426-428.

19. Iversen SL, Jorgensen MH. Azocasein assay for alkaline protease in complex fermentation broth. Biotechnol Tech. 1995; 9: 573-576.

20. Weatherburn MW. Estimation of ammonia nitrogen by colorimetric method. Ann Chem. 1967; 39: 971-974.

21. Cottyn BG, Boucque CV. Rapid method for the gas chromatographic determination of volatile fatty acids in rumen fluid. J Agric Food Chem. 1968; 16: 105-107.

22. Kamra DN, Sawal RK, Pathak NN, Kewalramani N, Agarwal N. Diurnal variations in ciliate protozoa in the rumen of black buck (*Antilope cervicapra*) fed green forages. Lett Appl Microbiol. 1991; 13: 165-167.

23. Van Soest PJ, Robertson JB, Lewis BA. Methods for dietary fiber, neutral detergent fiber, and nonstarch polysaccharides in relation to animal nutrition. J Dairy Sci. 1991; 74(10): 3583-3597.

24. SPSS. Statistical Packages for Social Sciences (version 12.0). 2012; SPSS Inc., Illinois, USA.

25. McAllister TA, Okine EK, Mathison GW, Cheng KJ. Dietary, environmental and microbiological aspects of methane production in ruminants. Can J Anim Sci. 1996; 76: 231-243.

26. Benchaar C, Pomar C, Chiquette J. Evaluation of dietary strategies to reduce methane production in ruminants: a modeling approach. Can J Anim Sci. 2001; 81: 563-574.

27. Takahashi J. Nutritional manipulation of methanogenesis in ruminants. Asian-Australas J Anim Sci. 2001; 14: 131-135.

28. Toppo S, Mehra UR, Dass RS. Effect of urea supplementation to urea mineral molasses block (UMMB) lick on nutrient utilization and rumen fermentation pattern in crossbred cattle. Indian J Anim Sci. 2000; 70: 415-418.

29. Dehority BA. Microbial interaction in the rumen. Rev Fac Agron (LUZ). 1998; 15: 69-86.

30. Finlay BJ, Esteban G, Clarke KG, Williams AG, Embley TM, et al. Some rumen ciliates have endo-symbiotic methanogens. FEMS Microbiol Lett. 1994; 117: 157-162.

31. Chatterjee PN. Influence of diet and plant secondary compounds on methanogenesis and rumen fermentation pattern. PhD Thesis, Indian Veterinary Research Institute, Izatnagar, Bareilly, India. 2005.

32. Patra AK, Kamra DN, Agarwal N, Chatterjee PN. Effects of *Terminalia belerica* and *Allium sativum* as feed additives on rumen fermentation, enzyme activities and microbial populations in Murrah buffaloes. Indian J Anim Nutr. 2008; 78: 91-96.

Cite this article as: Chatterjee PN, Kamra DN, Agarwal N and Pal A. Influence of urea on *in vitro* methanogenesis and fermentation of feed with buffalo rumen liquor. Explor Anim Med Res. 2026; 16(1), DOI: 10.52635/eamr/16.1.102-107.

Explor Anim Med Res.
Vol. 16, Issue 1, 2026
DOI: 10.52635/eamr/16.1.108-115

ISSN 2277-470X (Print), ISSN 2319-247X (Online)
Website: www.animalmedicalresearch.org

Published under the CC BY-NC 4.0 license

Research Article

EFFECT OF SHRIMP MEAL ON GROWTH PERFORMANCE, DIGESTIBILITY, CARCASS CHARACTERISTICS, INTESTINAL MORPHOLOGY, AND IMMUNOLOGICAL RESPONSES OF BROILER CHICKEN

P. Mahata[1], S. Soren[1], G. P. Mandal[1], P. Biswas[2], G. Patra[3], S. Biswas[2], A. Roy[4*]

Received 24 March 2025, revised 8 April 2026

ABSTRACT: The purpose of the study was to assess the impact of varying levels of shrimp meal incorporation on the growth performance, nutrient digestibility, carcass traits and immunological responses of broiler chickens. Three groups of 56 chicks each were randomly selected from a total of 168 day-old mixed-sex broiler chicks and divided into seven replicates of eight chicks. There were three experimental groups: SM1 (2.5 percent shrimp meal), SM2 (five percent shrimp meal), and a control group that was given a diet devoid of shrimp meal. Weight gain, intake of feed, and feed conversion ratio were measured on days 0, 7, 14, 21, 28, and 35. At the completion of the trial, carcass characteristics, gut morphology, and antibody titre were assessed. The study found that in SM2 group, final body weights and average daily gain were significantly higher compared to control group and FCR showed better in SM2 group compare to SM1 and control groups. SM2 showed significantly higher DM digestibility compared to SM1 and control. There were no significant effects on carcass traits.The height of duodenal villi (VH), crypt depth (CD), and the ratio of villi height to crypt depth (VH/CD) were not significantly different from each other. The jejunal VH in the SM2 group was significantly higher than that of the control groups (P<0.05). The ileum's VH/CD ratio was significantly higher (P<0.05) in the SM2 and SM1 groups in compare to control group. The results of the study show that shrimp meal can be included at the rate of 5% in a broiler diet without compromising performance.

Keywords: Broiler chickens, Shrimp meal, Growth performance, Gut morphology, Immune response.

INTRODUCTION

The broiler sector is the leading industry in animal output. With the global population expanding and more land allocated to cash crop cultivation, traditional chicken feed ingredients like maize and soybean meal are in short supply. The quality and cost of chicken feed are essential to meet the rising demand. The number of broilers processed annually is increasing, and it is projected that over 73 billion chickens will be processed globally by 2021 [1]. Animal feed is a crucial component of the global food and agriculture industry. It is important to supply animals with clean, high-quality feed to ensure efficient livestock production. High-quality feed provides essential minerals and energy for chicken growth, bone development, and feather production. With the increasing cost of raw materials, attempts are in vogue to identify the potential of several agro-industrial byproducts and bioconverting the community waste to animal wealth in terms of boosting production and health [2, 3, 4]. Kumari [5] reported that shrimp waste meal supplemented diets showed significantly higher body weight gain (P<0.01) compared to those on the control diet throughout the growth phases. Rahman and Koh [6] found that increasing the amount of SM in the diet led to a significant decrease in feed intake. Onbasılar *et al*. [7] suggested that the VH/CD ratio in the jejunum was significantly affected by the addition of shrimp waste to the diet, with the control group showing a lower ratio. Okonkwo *et al*. [8] observed no significant differences

[1]*Department of Animal Nutrition, W.B. University of Animal & Fishery Sciences, Kolkata, India*
[2]*Department of Avian Sciences, W.B. University of Animal & Fishery Sciences, Kolkata, India*
[3]*Department of LPT, W.B. University of Animal & Fishery Sciences, Kolkata, India*
[4]*Department of LFC, W.B. University of Animal & Fishery Sciences, Kolkata, India*
**Corresponding author. e-mail: amitavanutri07@gmail.com*

(P>0.05) in the weights of various body parts across the SWM incorporated groups.Traditional chicken diets often rely on costly and sporadically scarce ingredients like soybean meal (SBM). To deal with this problem, farmers might utilize farm waste and agro-industrial by-products as alternative protein sources. Shrimp meal (SM) is a cost-effective and viable substitute for SBM in poultry diets [9]. SM can be used in poultry feed to reduce reliance on soybean meal, a key protein source with fluctuating prices [10]. SM is a dry, powdered feed ingredient with approximately 40%-62% protein, 3%-8% ether extract, 4%-13% crude fiber, 11%-14% chitin, and 12%-23% minerals [11]. The study aims to investigate the potential use of shrimp meal as a source of protein in broiler diets to reduce environmental pollution. Limited research exists on shrimp meal inclusion in broiler diets. This trial evaluates the effect of shrimp meal on the growth, digestibility, intestinal structure, immunological responses, and carcass characteristics of broiler chickens.

MATERIALS AND METHODS

Experimental design and diets

The experiment was conducted in compliance with the guidelines established by the Institutional Animal Ethics Committee of West Bengal University of Animal & Fishery Sciences under approval no: 763/GO/Re-S/ReRc-L/03/CCSEA/77/2024-25, dated: 12.02.2025. Total 168 one-day-old broiler chicks of mixed sex (Vencobb 400, Venkys, Pune, India) were used in the study. They were divided into three groups based on the shrimp meal content in their diet: 1) basal diet without any shrimp meal (CON), 2) basal diet containing 2.5 % Shrimp meal (SM1), and 3) basal diet containing 5 % Shrimp meal (SM2). Shrimp meal was collected from local markets in West Bengal. Each group of treatment consists of seven replicates of eight birds. The birds included in the treatment were statistically homogeneous in weight and were housed in twenty-one pens. The chicks were housed in pens measuring 90 × 76 cm with litter, following standard management practices.The basal diet, in mash form, was formulated using maize and soybeans to meet the nutritional requirements of Vencobb 400 broiler chicks at different growth stages (starter, grower, and finisher) (Table 1). Experimental birds were given *ad libitum* access to water. The chick starter feed was given from 0–14 days of the 35-day trial period, followed by grower feed from 15–28 days and finisher feed from 29–35 days. From each replicate, two birds were housed for five consecutive days in metabolic cages and fed the respective experimental finisher feed.

Measurement of growth performance, digestibility and carcass traits of experimental birds.

At 0 day, prior to feeding and watering, the birds' body weight was measured, and then weekly throughout the experiment. The feed intake, feed conversion ratio and body weight gain of each replicate were recorded. Two randomly selected broilers were slaughtered following standard protocols from each group at 35 days of age for carcass evaluation. Weight ofabdominal fat, internal organs and the carcass were measured. The different parts of birds' namely prime cuts, edible visceral organs, and lymphoid organs were weighed separately as per standard procedures. For digestibility trial thefecal samples of birds were collected and weighed, along with the total feed given.Digestibility and retention of dry matter, nitrogen, and ash in the feces were analyzed using daily samples stored at -20°C [12].

Determination of intestinal morphology

On the 35th day, broilers were slaughtered for intestinal morphology assessment. Tissue samples from the duodenum, jejunum, and ileum were fixed in 10% buffered formalin for 24-48 hours, processed, and embedded in paraffin. Sections were stained with hematoxylin and eosin, and then examined under a light microscope (Cilika BTE 100 benchtop, MedPrime Technology). Villi with a complete lamina propria and twelve villi per slice were selected. Villus height (VH) and crypt depth (CD) were measured in micrometers (μm). Each sample was analyzed using 10 observations and at least three sections to establish a single observation in micrometers (μm).

Determination of immunological responses

All birds were vaccinated with Newcastle disease (ND) at 5 and 21 days and infectious bursal disease (IBD) at 14 days. Blood was collected from two randomly selected birds from each pen on days 28 and 35. The anti-NDV and anti-AIV antibody response was assessed using the hemagglutination inhibition assay following the methods described by Moghaddam and Jahanian [13]. ELISA was used to detect anti-IBD or anti-IBV responses using machine IDEXX Laboratories Inc., USA.

Statistical analysis

The data was analyzed using SPSS's one-way analysis of variance (ANOVA) in a completely randomized manner [14]. The pen was considered the experimental unit for feed intake, body weight gain, and FCR, while a single bird was the experimental unit for

other parameters. At a significance level of $P < 0.05$, and differences between treatment means were identified using Duncan's test when a significant treatment effect was observed.

RESULTS AND DISCUSSION

Average daily gain, feed intake, feed efficiency and digestibility of nutrients

The SM2 group exhibited a significantly higher ($P<0.05$) average daily gain (ADG) compared to the CON group throughout the 35-day experiment, while the SM1 group did not show significant differences with either the SM2 or CON group (Table 2). However, during the starter (days 1-14), grower (day 15-28), and finisher (day 29-35) phases of the experiment, there were no differences ($P>0.05$) in ADG among the treatment groups. Bird's final body weight was significantly higher in the SM2 group in comparison to the CON group, with no significant difference with SM1 group. The SM1 group exhibited a significantly higher ($P<0.05$) average daily feed intake (ADFI) compared to the CON group, although no significant variation was observed with the SM2 group during the grower period of the broilers. There were no significant variations ($P>0.05$) in ADFI among the treatment groups for the remains of the experiment period or over the entire 35-day experiment period. The feed conversion ratio (FCR) was significantly ($P<0.05$) improved in the SM2 group comparing with the CON group, while the SM1 group did not show any difference with either the SM2 or CON group during the starter phase (day 1-14). Additionally, a significant ($P<0.05$) improvement in

Table 1: Ingredients and composition (%) of the experimental diets.

Ingredients	Starter			Grower			Finisher		
	CON	SM1	SM2	CON	SM1	SM2	CON	SM1	SM2
Maize	61.809	60.634	59.459	64.386	63.215	62.043	66.994	65.819	64.642
Soya DOC Hypro	33.491	32.116	30.741	29.983	28.608	27.232	26.364	24.989	23.617
Shrimp Meal	0	2.500	5.000	0	2.500	5.000	0	2.500	5.000
Oil-veg	0.790	0.963	1.137	2.026	2.198	2.370	3.216	3.389	3.564
Dicalcium phosphate	1.658	1.507	1.356	1.526	1.375	1.224	1.395	1.244	1.093
Limestone powder	0.932	0.962	0.993	0.951	0.982	1.013	0.943	0.974	1.005
Common salt (Nacl)	0.322	0.325	0.328	0.313	0.314	0.315	0.326	0.328	0.331
DL-methionine	0.328	0.322	0.316	0.258	0.252	0.246	0.230	0.224	0.216
L-lysine HCL	0.262	0.264	0.266	0.171	0.173	0.175	0.148	0.149	0.151
L-threonine	0.088	0.086	0.084	0.066	0.064	0.062	0.065	0.064	0.062
Toxin binder	0.050	0.050	0.050	0.050	0.050	0.050	0.050	0.050	0.050
Sodium bi-carbonate	0.100	0.100	0.100	0.100	0.100	0.100	0.100	0.100	0.100
Mineral premix[1]	0.100	0.100	0.100	0.100	0.100	0.100	0.100	0.100	0.100
Vitamin premix[2]	0.050	0.050	0.050	0.050	0.050	0.050	0.050	0.050	0.050
Antioxidant	0.010	0.010	0.010	0.010	0.010	0.010	0.010	0.010	0.010
Phytase 5000	0.010	0.010	0.010	0.010	0.010	0.010	0.010	0.010	0.010
Analysed values (%)									
ME (kcal/kg)*	3000.00	3000.00	3000.00	3100.00	3100.00	3100.00	3200.00	3200.00	3200.00
Crude protein*	22.50	22.50	22.50	20.83	20.83	20.83	19.20	19.20	19.20
Ether extract	3.17	3.50	3.71	1.94	4.23	4.30	4.93	4.60	4.45
Crude fiber	2.23	2.37	2.84	1.99	2.15	2.43	2.12	2.52	2.69
Dry matter	89.09	87.88	87.04	88.56	88.24	87.96	86.55	87.99	87.75
Lysine*	1.25	1.25	1.25	1.09	1.09	1.09	0.98	0.98	0.98
Methionine+Cysteine*	0.90	0.90	0.89	0.80	0.80	0.80	0.74	0.74	0.74
Threonine*	0.77	0.77	0.77	0.70	0.70	0.70	0.65	0.65	0.65
Total ash	6.32	9.09	7.57	6.92	7.19	7.04	6.97	6.93	6.41
Acid insoluble ash	0.31	1.14	1.36	0.44	0.77	0.79	0.51	0.66	0.57
Calcium*	0.94	0.94	0.94	0.91	0.91	0.91	0.87	0.87	0.87

[1]Contains Zn 4.0%, Mn 4.0%, Fe 1.5%, Cu 0.8%, I 0.4%, Se 300ppm, Cr 200ppm;

[2]Contains vitamin E100g, vitamin A 40000000 IU, vitamin D_3 12000000IU, pantothenic acid 60g, vitamin K 8g, vitamin $B_1$120g, vitamin B_2 24g, vitamin B_6 10g, vitamin B_{12} 0.10g, biotin 0.40g, folic acid 4g, niacin 100g

Table 2: Effect of shrimp meal on final body weight (BW), average daily gain (ADG), average daily feed intake (ADFI) and FCR of broiler chickens.

Parameter	Attribute	Treatment			SEM (n=7)	P-Value
		CON	SM1	SM2		
ADG (g/d)	D1-14	27.89	28.52	29.61	0.329	0.091
	D15-28	68.01	72.66	73.05	0.998	0.063
	D29-35	73.14	72.55	76.78	2.122	0.700
	D1-35	52.99^{b}	54.98^{ab}	56.42^{a}	0.503	0.011
	Final BW	1901.15^{b}	1970.36^{ab}	2020.57^{a}	17.625	0.012
ADFI (g/d)	D1-14	32.58	32.58	31.82	0.306	0.533
	D15-28	93.48^{b}	99.86^{a}	96.38^{ab}	0.995	0.023
	D29-35	135.25	135.68	135.53	1.189	0.990
	D1-35	77.47	80.11	78.39	0.489	0.074
FCR (g intake/g gain)	D1-14	1.166^{a}	1.143^{ab}	1.081^{b}	0.015	0.041
	D15-28	1.374	1.376	1.323	0.012	0.137
	D29-35	1.883	1.881	1.806	0.055	0.824
	D1-35	1.464^{a}	1.457^{a}	1.390^{b}	0.013	0.028

^{ab} means bearing different superscripts in the same row differ significantly ($p \leq 0.05$). CON- control diet, SM1- control diet containing 2.5 % Shrimp meal, SM2- control diet containing 5 % Shrimp meal

Table 3: Effect of supplementation of shrimp meal on digestibility of nutrients.

Digestibility %	Treatment			SEM (n=7)	P-Value
	CON	SM1	SM2		
DM	71.83^{c}	74.17^{b}	76.88^{a}	0.761	0.001
CP	77.66^{b}	84.76^{a}	87.16^{a}	1.596	0.008
CF	29.59	26.39	23.76	1.064	0.052
EE	77.06^{c}	82.21^{b}	85.04^{a}	1.170	0.000

^{ab} means bearing different superscripts in the same row differ significantly ($p \leq 0.05$). CON- control diet, SM1- diet containing 2.5 % Shrimp meal, SM2- diet containing 5 % Shrimp meal.

Table 4: Effect of shrimp meal on carcass characteristics of broiler chickens at day 35.

Attributes	Treatment			SEM(n=7)	P-Value
	CON	SM1	SM2		
Final BW (g)	1901.57^{b}	1969.14^{ab}	2020.57^{a}	16.815	0.007
Eviscerated BW (g)	1229.46^{b}	1305.88^{a}	1338.88^{a}	14.469	0.002
Dressing Percentage (%)	64.65	66.27	66.34	0.409	0.165
Breast (g)	484.56	495.28	521.82	6.696	0.056
Frame (g)	238.28	254.59	255.42	3.711	0.100
Thigh (g)	153.10^{b}	166.21^{a}	177.01^{a}	3.029	0.001
Drumstick (g)	178.66	179.34	190.49	2.302	0.053
Wing (g)	104.21	114.75	115.37	2.231	0.064
Neck (g)	49.68^{b}	48.77^{b}	54.30^{a}	0.807	0.005
Gizzard (g)	43.91	47.76	49.64	1.703	0.395
Liver (g)	45.79^{a}	37.59^{b}	39.02^{b}	1.144	0.002
Heart (g)	9.07	9.24	9.30	0.275	0.944
Spleen (g)	1.89	1.76	1.92	0.063	0.554
Bursa (g)	1.29	1.50	1.28	0.090	0.561
Abdominal Fat (g)	32.64	35.17	38.75	1.216	0.117

^{ab} means bearing different superscripts in the same row differ significantly ($p \leq 0.05$). CON- control diet, SM1- diet containing 2.5 % Shrimp meal, SM2- diet containing 5 % Shrimp meal.

Table 5: Effect of shrimp meal on gut morphology of broiler chickens at day 35.

Gut part	Attribute	Treatment			SEM(n=7)	P-Value
		CON	SM1	SM2		
Duodenum	Villi height (VH; µm)	1496.77	1506.55	1541.22	32.147	0.864
	Crypt depth (CD; µm)	212.48	186.72	170.25	7.772	0.065
	VH/CD ratio	7.10	8.09	9.22	0.385	0.061
Jejunum	Villi height (VH; µm)	1006.88^{b}	1089.98^{ab}	1235.85^{a}	37.528	0.021
	Crypt depth (CD; µm)	263.32	259.85	257.48	9.952	0.976
	VH/CD ratio	3.84	4.25	4.90	0.208	0.102
Ileum	Villi height (VH; µm)	687.09	805.03	854.56	34.212	0.114
	Crypt depth (CD; µm)	188.15	179.50	172.28	3.866	0.264
	VH/CD ratio	3.66^{b}	4.48^{a}	4.95^{a}	0.190	0.003

^{ab} means bearing different superscripts in the same row differ significantly ($p \leq 0.05$). CON- control diet, SM1- diet containing 2.5 % Shrimp meal, SM2- diet containing 5 % Shrimp meal

Table 6: Effect of shrimp meal on antibody titre (log_{10}) against infectious bursal disease vaccine (IBDV) and New castle disease vaccine (NDV) of broiler chickens at day 28 & 35.

Disease	Attribute	Treatment			SEM(n=7)	P-Value
		CON	SM1	SM2		
IBDV	d28	2.60^{b}	2.87^{ab}	3.08^{a}	0.063	0.005
	d35	2.52	2.74	2.98	0.083	0.072
NDV	d28	2.71^{b}	2.79^{ab}	2.92^{a}	0.032	0.027
	d35	2.38	2.50	2.59	0.067	0.470

^{ab} means bearing different superscripts in the same row differ significantly ($p \leq 0.05$). CON- control diet, SM1- diet containing 2.5 % Shrimp meal, SM2- diet containing 5 % Shrimp meal.

FCR was seen in the SM2 group when compare with the SM1 and CON groups throughout the experiment (day 1-35). However, during the grower phase (days 15–28) and finisher phase (days 29–35), no significant impact on FCR was noted.

In our study, the group supplemented with 5% shrimp meal showed a significant increase in final body weight in the fifth week and ADG throughout the trial compared to the other groups.There were variations in the average daily weight gain among the groups over the 35-day study period. Previous research [9, 15] has shown that broiler feed containing 5% shrimp waste meal resulted in a significant increase in growth rate ($P < 0.01$). Researcher [5] found that 0.5 g/kg of cricket chitin was more effective in improving broiler growth compared to chitosan. In contrary to researchers' observations [16, 7, 17], which indicated a decrease in broiler growth performance with increased consumption of shrimp waste meal, Okoye et al. [18] observed only minor changes in broiler weight when fed shrimp waste feed during the finisher period. Several experiments have used various shrimp species [19] and segments [20] in experiments, leading to variations in shrimp waste quality. The nutritional composition of shrimp waste varies significantly based on the shrimp species, shell content and processing and storage methods employed [21]. Though the feed intake level did not varied significantly but the lower level of addition of shrimp meal may have increased palatability so birds had a higher intake, but that intake did not translate to proportionally higher weight gain may be due to the nutrient balance at that inclusion was not optimal for growth (limiting amino acids, or the palatability effect increased intake without improving the efficiency than that of SM2 level).

Table 3 shows the impact of an experimental diet on nutrient digestibility after a 35-day trial. Dry matter (DM) digestibility was significantly ($P<0.05$) higher in SM2 compared to SM1 and CON. Crude protein (CP) digestibility was higher ($P<0.058$) in SM2 and SM1 than CON. The ether extract (EE) digestibility of the 5% SM diet was significantly ($P<0.05$) higher than the 2.5% SM diet and the control diet.

Kumar [22] found that nutrients were more digestible during the finisher phase, except for ether extract. According to Birto et al. [23], the inclusion of SWM in

broiler diets led to a significant improvement in protein digestibility (P=0.001). Oduguwa et al. [11] found that adding fishmeal and shrimp waste meal to broiler diets slightly improved ether extract, ash, and dry matter digestibility. They also noted that nutrient digestibility increased as birds matured, with finisher broilers exhibiting higher values than starter broilers and that might be the reasons of showing comparatively better FCR and ADG in finisher period.

Carcass characteristics

Eviscerated weights in the SM1 and SM2 groups were significantly higher (P<0.05) than CON group (Table 4). Significant differences (P<0.05) were also observed in liver, thigh, and neck weights. The results were consistent with researcher [25], showing that broilers fed high amino acid density diets at 35 and 55 days had improvements in various parameters such as fillet weight, tender weight, tender yield, total breast weight, drumstick weight, saddle weight, wing weight, and carcass weight. Likewise, investigator [26] found that increasing lysine content in the diet of 20-week-old pullets to 110% during the rearing phase resulted in higher breast meat production and lower belly fat deposition.The genetic potential of current broiler strains for breast meat production was highlighted by Vieira et al. [24], who found that a high-protein diet increased breast meat yield in broiler carcasses. In a study by Premathilaka et al. [27], broilers fed a diet with 4% FM had higher internal organ weights compared to those on a diet with 2% FM and 3% fortified SBM. The 5% SM incorporated group showed significantly higher slaughter weight, possibly due to increased abdominal fat deposition. However, there were no significant differences (P>0.05) in dressed weight, wing, drumstick, breast, gizzard, spleen, and heart in the group supplemented with SWM [9]. The gizzard, spleen, and heart were not affected, indicating no significant toxicity threat with all the SM incorporated diets [28].

Gut morphology

There were no variations in villi height (VH), crypt depth (CD), or the VH/CD ratio of duodenum among the CON, SM1, and SM2 groups (Table 5). The jejunal VH in the 5% inclusion group was similar to the SM1 group but significantly higher (P<0.05) than the CON group. The VH and CD of the ileum showed no noticeable changes, but the ileum's VH/CD ratio was significantly higher (P<0.05) in both the SM1 and SM2 groups in comparison with the CON group. Overall, the gut morphology of the SM2 group was superior to that of the other groups. According to Li et al. [29], supplementation with chitosan oligosaccharide (COS) may have a beneficial effect on intestinal morphology by increasing villus height and the VH/CD ratio, while decreasing crypt depth. In contrast to the current study, investigator [8] found that adding shrimp waste to the diet significantly affected the VH/CD ratio in the jejunum. Ibitoye et al. [30] found that adding shrimp and cricket chitosan to the diet significantly reduced crypt depth and increased jejunal villus height without affecting body weight.However, the current study did not provide an explanation for the significant improvement in the ileum VH: CD ratio and jejunal VH of broilers fed the 5% SWM-incorporated diet compared to the basal diet. Shrimp meal contains bioactive substances such chitin, chitosan, and astaxanthin, broilers given the 5% SWM diet showed improvements in their ileal VH:CD ratio and jejunal villus height. Through modifying intestinal microbiota, lowering inflammation, and promoting villus growth, these substances are known to improve gut health. By inhibiting harmful bacteria and encouraging advantageous species like *Lactobacillus* spp., chitosan and its oligosaccharides can alter the intestinal microbiota and lower intestinal inflammation and epithelial turnover [29]. A larger VH:CD ratio is a result of the extension of villi and shallower crypts made possible by the decrease in mucosal damage and the need for cellular regeneration.This group's increased growth performance and feed efficiency were likely due to the greater inclusion level (5%) providing enough functional nutrients and antioxidants to enable improved intestinal morphology and nutrient absorption.

Immune response

Our study showed that on day 28, the antibody titers for both IBDV and NDV vaccinations were significantly better in the SM2 group compared to the CON group (P<0.05) (Table 6). But between SM1 and SM2, there was no difference. By day 35, the antibody titers for both IBDV and NDV were comparatively higher (P>0.05) in the SM2 group than other the treatment groups. The post-vaccination antibody levels in broilers increased more with higher doses of shrimp extract, indicating a stronger immune response and overall health. Broiler immune systems can be strengthened with an amino acid-rich diet. Amino acids supplementation has been shown to improve immunological function [31, 32]. Rapidly

growing animals like pigs and broilers require arginine, an essential amino acid present in animal cells, for processes such as immune regulation, protein synthesis, and ammonia detoxification. A deficiency in arginine in broiler diets can lead to reduced spleen and thymus weight, lower antibody levels against NDV, and a decrease in blood heterophil percentage. Research by Tayade *et al*. [32] suggests that arginine enhances the specific immune response against IBD in chickens. Broilers fed the 5% shrimp meal (SM2) diet showed better antibody titers against IBDV and NDV, indicating that shrimp meal boosted immunological competence. High-quality proteins, vital amino acids (particularly arginine), and bioactive substances including chitin, chitosan, and astaxanthin-all of which are known to enhance immunological modulation-are abundant in prawn meal. Arginine is essential for the formation of nitric oxide, antibodies, and lymphocytes, all of which boost immunological responses. Additionally, astaxanthin and chitosan have immunostimulatory and antioxidant qualities that support the integrity of immune organs and improve vaccine response. Therefore, the increased incorporation of shrimp meal in the SM2 group is linked to enhanced nutritional and immunological health, which is reflected in the elevated antibody levels in that group.

CONCLUSION

Recycling animal waste is essential for promoting environmental sustainability. Diet containing 5% shrimp meal has been shown to have positive effects on broiler performance, carcass quality, intestinal morphology, and immunological responses in broiler chickens without any adverse effects. This approach can also help protect the environment by utilizing a waste product. This method utilizes a waste product and contributes to environmental protection.

CONFLICT OF INTEREST

The Authors declares that there is no conflict of interest.

ACKNOWLEDGEMENT

The authors thank the Dean, Faculty of Veterinary and Animal Sciences, West Bengal University of Animal and Fishery Sciences, Kolkata for providing necessary facilities.

REFERENCES

1. Honig H, Haron A, Plitman L, Lokshtanov D, Shinder D, Nagar S, Goshen T, Druyan S. Comparative Analysis of Broiler Housing Systems: Implications for Production and Wellbeing. Animals. 2024 Jun 2; 14(11): 1665

2. Ghosh, S., Chatterjee, P.N., Maity, A., Mukherjee, J., Batabyal, S. and Chatterjee, J.K. 2020. Effect of supplementing pomegranate peel infusion on body growth, feed efficiency, biochemical metabolites and antioxidant status of broiler chicken. Tropical Animal Health and Production, 52:3899-3905.

3. Ghosh S, Chatterjee PN, Maity A, Mukherjee J, Batabyal S and Chatterjee JK, 2020. Effect of supplementing pomegranate peel infusion on body growth, feed efficiency, biochemical metabolites and antioxidant status of broiler chicken. Tropical Animal Health and Production 52(6): 3899-3905. https://doi.org/10.1007/s11250-020-02352-0

4. Ghosh S, Chatterjee PN, Chatterjee J (2020) Supplementing pomegranate peel infusion indrinking water enhances antioxidant quality of broiler meat. Explor Anim Med Res 11(1): 131-134. DOI :10.52635/EAMR/11.1.131-134

5. Kumari, GM. Performance of broilers fed diets containing shrimp waste meal (Doctoral dissertation, Sri Venkateswara Veterinary University, Tirupati-517 502. (AP) INDIA. 2016.

6. Rahman M, Koh K. Effect of shrimp meal made of heads of black tiger (*Penaeus monodon*) and white leg (*Litopenaeusvannamei*) shrimps on growth performance in broilers. The Journal of Poultry Science. 2016; 53(2): 149-52.

7. Onbaşılar EE, Gündoğar UC, Çapar Akyüz H, Yalçın S, Ahlat O, Yüceer Özkul B, Çelebi B, Bundur A, Gebeş ES, Ünal N, Özbeyaz C. The effects of shrimp waste added to broiler diets on growth performance, slaughter and carcass characteristics, intestinal morphology, bone traits, and fatty acids in the meat. Journal of Animal Physiology and Animal Nutrition. 2025 Mar; 109(2): 477-86.

8. Okonkwo AC, Akpan IP, Isaac LJ. Broilers Fed Shrimps Waste Meal. Agricultural Journal. 2012; 7(4): 270-2.

9. Abun A, Widjastuti T, Haetami K. Effect of fermented shrimp shell supplementation of low protein diet on the performance of Indonesian native chicken. Journal of Applied Animal Research. 2022 Dec 31; 50(1): 612-9.

10. Cunha, FS de A., Carlos Bôa-Viagem Rabello, W. M. Dutra Junior, M. do CMM Ludke, RR de S. Loureiro, and CRG de Freitas. "Utilization and effect of shrimp (*Litopenaeus vannamei*) waste meal in the performance and characteristics of broiler carcass." 2006; 273-279.

11. Oduguwa OO, Fanimo AO, Jegede AV. Effect of enzyme supplementation on the utilization of shrimp waste meal based diets by broiler chicken. Nigerian Journal of Animal Production. 2004; 31(2): 167-73.

12. Kareem KY, Abdulla NR, Foo HL, Zamri AN, Shazali N, Loh TC, Alshelmani MI. Effect of feeding larvae meal in

the diets on growth performance, nutrient digestibility and meat quality in broiler chicken. Indian Journal of Animal Sciences. 2018 Oct 1; 88(10): 1180-5.

13. Moghaddam HN, Jahanian R. Immunological responses of broiler chicks can be modulated by dietary supplementation of zinc-methionine in place of inorganic zinc sources. Asian-Australasian journal of animal sciences. 2009 Mar 4; 22(3): 396-403.

14. Hill MA. SPSS missing value analysis 7.5. SPSS Inc.; 1997.

15. Khempaka S, Chitsatchapong C, Molee W. Effect of chitin and protein constituents in shrimp head meal on growth performance, nutrient digestibility, intestinal microbial populations, volatile fatty acids, and ammonia production in broilers. Journal of Applied Poultry Research. 2011 Mar 1; 20(1): 1-1.

16. Khempaka S, Koh K, Karasawa Y. Effect of shrimp meal on growth performance and digestibility in growing broilers. The Journal of Poultry Science. 2006; 43(3): 250-4.

17. Santiago HL, Maldonado LI. The effects of using shrimp meal in broiler diets on live performance and carcass traits. Proceedings in under-graduate research programme. http://academic. uprm. edu/hsantiago/m Paper. pdf. 2005.

18. Okoye FC, Ojewola GS, Njoku-Onu K. Evaluation of shrimp waste meal as a probable animal protein source for broiler chicken. Int. J. Poult. Sci. 2005; 4(5): 458-61.

19. Ngoan LD, An LV, Ogle B, Lindberg JE. Ensiling techniques for shrimp by-products and their nutritive value for pigs. Asian-Australasian Journal of Animal Sciences. 2000 Sep 1; 13(9): 1278-84.

20. Meyers SP. Utilization of shrimp processing waste. Infofish Marketing Digest. 1986; 4: 18-9.

21. Fanimo AO, Oduguwa OO, Jimoh YO, Faronbi AO. Performance and carcass evaluation of broiler chicks fed shrimp waste meal supplemented with synthetic amino acids. Nigerian Journal of Animal Production. 1998; 25(1): 17-21.

22. Kumar MY. *Utilization of shrimp shells containing chitosan as a source of prebiotic in crossbred pigs* (Doctoral dissertation, Sri Venkateswara Veterinary University). 2017.

23. Brito CO, Junior VR, Del Vesco AP, de Castro Tavernari F, Calderano AA, Silva CM, de Lima Maciel JT, de Azevedo MS. Metabolizable energy and nutrient digestibility of shrimp waste meal obtained from extractive fishing for broilers. Animal Feed Science and Technology. 2020 May 1;263:114467.

24. Vieira SL, Lemme A, Goldenberg DB, Brugalli I. Responses of growing broilers to diets with increased sulfur amino acids to lysine ratios at two dietary protein levels. Poultry Science. 2004 Aug 1; 83(8): 1307-13.

25. Kidd MT, Corzo A, Hoehler D, Miller ER, Dozier 3rd WA. Broiler responsiveness (Ross x 708) to diets varying in amino acid density. Poultry Science. 2005 Sep 1; 84(9): 1389-96.

26. Alfaro-Wisaquillo MC, Oviedo-Rondón EO, Cordova-Noboa HA, Caldas JV, Quintana-Ospina GA, Ospina-Rojas IC, San Martin V. Effects of amino acid levels during rearing on Cobb 500 slow-feathering broiler breeders: 1. Growth and development. Poultry Science. 2021 Sep 1; 100(9): 101327.

27. Premathilaka KT, Nawarathne SR, Nambapana MN, Macelline SP, Wickramasuriya SS, Ang L, Jayasena DD, Heo JM. Partial or complete replacement of fishmeal with fermented soybean meal on growth performance, fecal composition, and meat quality in broilers. Journal of Animal Science and Technology. 2020 Nov 30; 62(6): 824.

28. Hossain SM, Blair R. Chitin utilisation by broilers and its effect on body composition and blood metabolites. British poultry science. 2007 Feb 1;48 (1): 33-8.

29. Li J, Cheng Y, Chen Y, Qu H, Zhao Y, Wen C, Zhou Y. Dietary chitooligosaccharide inclusion as an alternative to antibiotics improves intestinal morphology, barrier function, antioxidant capacity, and immunity of broilers at early age. Animals. 2019 Jul 27; 9(8): 493.

30. Ibitoye EB, Lokman IH, Hezmee MN, Goh YM, Zuki AB, Jimoh AA, Danmaigoro A, Nicholas NP. Gut health and serum growth hormone levels of broiler chickens fed dietary chitin and chitosan from cricket and shrimp. Poultry Science. 2019 Feb 1; 98(2): 745-52.

31. Hilliar M, Keerqin C, Girish CK, Barekatain R, Wu SB, Swick RA. Reducing protein and supplementing crystalline amino acids, to alter dietary amino acid profiles in birds challenged for subclinical necrotic enteritis. Poultry Science. 2020 Apr 1; 99(4): 2048-60.

32. Tayade C, Jaiswal TN, Mishra SC, Koti M. L-Arginine stimulates immune response in chickens immunized with intermediate plus strain of infectious bursal disease vaccine. Vaccine. 2006 Jan 30; 24(5): 552-60.

Cite this article as: Mahata P, Soren S, Mandal GP, Biswas P, Patra G, Biswas S, Roy A. Effect of shrimp meal on growth performance, digestibility, carcass characteristics, intestinal morphology, and immunological responses of broiler chicken. Explor Anim Med Res. 2026; 16(1), DOI: 10.52635/eamr/16.1.108-115.

Explor Anim Med Res.
Vol. 16, Issue 1, 2026
DOI: 10.52635/eamr/16.1.116-129

ISSN 2277-470X (Print), ISSN 2319-247X (Online)
Website: www.animalmedicalresearch.org

Published under the CC BY-NC 4.0 license

Research Article

CHITOSAN FILM WITH THYME NANOEMULSION (*THYMUS VULGARIS* L.): A SUSTAINABLE APPROACH FOR MEAT PRESERVATION

Dipanwita Bhattacharya[1*], Dhananjay Kumar[1], Pesingi Pavan Kumar[2], Anshuman Kumar[3], Annada Das[4], Saurabh Karunamay[1], Kaushik Satya Prakash[2], Arun Kumar Das[5], Mahipal Chaubey[6], Mayukh Ghosh[7]

Received 5 September 2025, revised 25 April 2026

Abstract: Recent incidents of meat spoilage and outbreaks of meat-borne pathogens have increased, primarily attributable to breaches in the cold chain and insufficient preservation techniques throughout the supply chain. To address these issues, the current study focused on developing a natural preservation method using a chitosan film. Here, a nanoemulsion of thyme (*Thymus vulgaris* L.) essential oil was prepared, and its morphology was studied by transmission electron microscopy (TEM). Additionally, thyme oil nanoemulsions at concentrations of 0.5%, 1%, and 2% (w/v) were incorporated into various chitosan films for bioactive packaging, and the morphological characteristics of the films were analysed using scanning electron microscopy (SEM). The elongation at break (EAB) and water vapour permeability (WVP) of the chitosan film could be improved by adding the nanoemulsion in a dose-dependent manner. The antimicrobial activity was assessed *in vitro* against *Salmonella* Typhimurium (ATCC 14028) and *Listeria monocytogenes* (ATCC 19111), and the film containing 2% thyme nanoemulsion (T3) exhibited the highest efficacy with the least bacterial counts (2.89±0.10 log CFU/cm² and 2.00±0.00 log CFU/cm², respectively). Similarly, the highest radical-scavenging activity (45.37±1.68%) was observed for T3. Owing to their significant effectiveness as bioactive films, 1% and 2% formulations were applied as aerobic active packaging on chicken drumsticks. The pH, microbiological characteristics, and sensory attributes of the control and different treatment groups were analysed over 15 days of refrigerated storage (4±1°C) to assess the overall meat quality. This study demonstrated that a chitosan film incorporating 2% thyme nanoemulsion significantly extended the shelf life of chicken drumsticks to 15 days during refrigerated storage, without noticeable sensory degradation. This bioactive film serves as an innovative green preservation method for extending the shelf life of uncooked chicken stored at 4±1°C.

Keywords: Bioactive, Nanoemulsion, Antimicrobial, Chitosan, Quality, Shelf-life

INTRODUCTION

Ensuring food safety, especially in meat and meat products, is an important public health issue that must be addressed worldwide. Foodborne illnesses caused by pathogens like Salmonella spp., *E. coli*, *Staphylococcus aureus*, and *Listeria monocytogenes* affect millions annually, resulting in thousands of hospitalisations and many deaths [1]. Addressing these threats with effective measures to safeguard public health is essential. In lower- and middle-income countries, foodborne illnesses

[1]*Department of Livestock Products Technology, Faculty of Veterinary and Animal Sciences, Rajiv Gandhi South Campus, Banaras Hindu University, Mirzapur, 231001.*
[2]*Department of Veterinary Public Health and Epidemiology, Faculty of Veterinary and Animal Sciences, Rajiv Gandhi South Campus, Banaras Hindu University, Mirzapur, 231001.*
[3]*Department of Animal Genetics and Breeding, Faculty of Veterinary and Animal Sciences, Rajiv Gandhi South Campus, Banaras Hindu University, Mirzapur, 231001.*
[4]*Department of Livestock Products Technology, Institute of Veterinary Sciences and Animal Husbandry, Siksha 'O' Anusandhan University, Orissa.*
[5]*Department of Livestock Products Technology, Eastern Regional Station-Indian Veterinary Research Institute, Kolkata*
[6]*Department of Animal Nutrition, Faculty of Veterinary and Animal Sciences, Rajiv Gandhi South Campus, Banaras Hindu University, Mirzapur, 231001.*
[7]*Department of Veterinary Physiology and Biochemistry, Faculty of Veterinary and Animal Sciences, Rajiv Gandhi South Campus, Banaras Hindu University, Mirzapur, 231001.*
**Corresponding author. e-mail: dipanwita.bhattacharya@bhu.ac.in*

incur high costs yearly due to lost productivity, medical expenses, and long-term economic ripple effects on businesses and communities [2, 3]. The meat sector grapples with inadequate cold-chain infrastructure, leading to spoilage and post-harvest losses. These challenges put extra pressure on the economy. The food industry suffers losses due to product recalls, damage to its brand reputation, and lost sales. Meanwhile, healthcare systems and restaurants face high medical and operational costs. For restaurants, a single outbreak can wipe out millions in revenue through lawsuits, lost consumer trust, and legal penalties, highlighting how food spoilage and safety lapses endanger public health and drag down economic vitality across sectors. Hence, meat producers have compulsively implied the abrupt usage of chemical preservatives in the meat food system [4]. These chemical preservatives maintain the meat's quality and sensory attributes but silently damage cellular integrity, have carcinogenic and mutagenic effects, and lead to various health issues over time. Attempts has also been taken to exploit the efficacy of nano-materials to be used for improving the shelf life of meat and meat products [5]. As a result, natural preservation strategies have gained prominence across the industry, government, and research sectors, serving as a sustainable approach in the production and processing of meat and meat products. Bioactive packaging stands out as a leading natural preservation system for extending the shelf life of meat and minimising plastic pollution. Meat producers and sellers use petroleum-derived non-degradable plastic packaging, and it accumulates in nature as a heap of poison that destroys the ecological balance and has a toxic effect on animal and human health [6]. Above all, these cost-effective plastics cannot significantly hasten the shelf life of meat and meat products.

Therefore, introducing biodegradable bioactive packaging in the meat industry has emerged as a means to address plastic pollution and food waste while extending the storage life of muscle foods. Chitosan is an essential source of cationic biopolymers (due to its free amino groups: $–NH_2$), and it is a biodegradable, biocompatible polysaccharide derived from chitin, derived from the exoskeleton of insects, crustaceans, etc. [7]. Chitosan has antimicrobial activity due to its positively charged amino groups ($–NH_3^+$), which interact with the negatively charged membranes of microbial cells, leading to leakage of intracellular contents and ultimately cell death [8]. Nevertheless, their antimicrobial efficiency is insufficient to inhibit or kill pathogens and spoilage organisms in the food matrix [9]. Hence, using essential oils from different plant parts enhances their antimicrobial efficacy. Thyme (*Thymus vulgaris*) is a notable culinary and medicinal herb of the Lamiaceae (mint) family. Essential oils extracted from thyme leaf have potential antimicrobial activity against Gram-positive and Gram-negative microorganisms. Thyme essential oil is a rich source of phenolic components and terpenoids, including carvacrol and thymol, which contribute to its effective free radical scavenging activity, aiding in preserving muscle foods [10, 11]. Several studies have been conducted to enhance the bioefficacy of thyme essential oil in a chitosan film matrix to preserve meat and meat products under refrigeration [12, 13]. However, the strong flavour and intense aroma of free thyme oil can sometimes hinder its acceptance in food preservation. Free essential oil within a chitosan film matrix releases quickly into the food matrix, thereby reducing the long-term protective effect and ensuring only surface protection. The emerging encapsulation technology, specifically nanoemulsions with biopolymers, can address this issue, thereby extending the storage period of meat [14].

The present study developed a chitosan-based bioactive biodegradable film incorporating thyme oil nanoemulsion and assessed its antimicrobial and antioxidant properties. This bioactive, biodegradable packaging can address environmental pollution caused by non-biodegradable plastics, as identified in the existing literature, and sets a future goal for bio-preservation methods for meat. The developed bioactive film was applied to raw chicken drumsticks, which were then stored at 4±1°C for 15 days, and a comprehensive quality assessment was conducted at every 3-day intervals.

MATERIALS AND METHODS

Chemicals and Bacterial strains

The essential oil of *Thymus vulgaris* L. (thyme, 100% purity) was purchased from Sigma-Aldrich, India. Chitosan (75% deacetylated), glycerol, Polysorbate 80 (Tween 80), and other chemicals were procured from Sisco Research Laboratories Pvt. Ltd. (SRL), India. Enrichment broth, selective media and phosphate-buffered saline (PBS) were purchased from Hi-media Laboratories Pvt. Ltd., India. Foodborne pathogens, such as *Salmonella* Typhimurium (ATCC 14028) and *Listeria monocytogenes* (ATCC 19111), were obtained from the Department of Veterinary Public Health and Epidemiology Laboratory at the Faculty of Veterinary and Animal Sciences, Rajiv Gandhi South Campus, Banaras Hindu University, India, for the antibacterial

assay. Chicken drumsticks (lower part of leg) were procured from the Instructional Livestock Farm Complex (ILFC), Faculty of Veterinary and Animal Sciences, Banaras Hindu University, India.

Preparation of nanoemulsion

The nanoemulsion of thyme essential oil was prepared as described by [8, 15] with slight modifications. A coarse emulsion was made by mixing thyme oil with Tween 80 (in a ratio of 1:2) in deionised water at 8000 rpm (5 minutes) using a T18 digital ULTRA-TURRAX® (0003720000) homogeniser, IKA, Germany. Next, the homogenised microemulsion was sonicated (Branson Sonifier SFX250, USA) at 20 kHz, 50% amplitude, and 250 W using a 10 mm probe for 10 minutes to prepare the nanoemulsion. The formulation was stored in the dark at 4°C until used for film formation.

Morphology of nanoemulsion by Transmission Electron Microscopy (TEM)

A transmission electron microscope (TECNAI 20G2, THERMO FISHER, United States, operating at 200 kV) was used to observe the structure, distribution pattern, and size of the nanoemulsion. The emulsion was diluted with added ultra-pure water, and a 5 µl drop of sample was kept onto a carbon-coated copper grid (200 mesh). It was then allowed to dry completely at room temperature. The nano capsule's morphology and size were subsequently analysed under the microscope [16].

Preparation of bioactive chitosan film

Chitosan films incorporating thyme nanoemulsion were prepared using a modified laboratory-based casting method [8, 17, 18] (Fig. 1). 1.5 g chitosan (w/v) was dissolved into 1% acetic acid solution. This mixture was maintained under constant magnetic stirring at 1000 rpm and 30°C for 6 hours for complete dissolution of chitosan. Following this, 0.75% (w/v) glycerol was added to the mixture 30 minutes prior to casting. The thyme nanoemulsion was then blended with the filmogenic suspension at a 1:1 ratio, and the resulting mixture was maintained at concentrations of 0.5%, 1% and 2% (w/v). The active suspension was homogenised using an IKA T18 homogeniser (Germany) at 6000 rpm for 2-3 minutes and subsequently cast into sterile glass petri dishes, each with an 8-inch diameter. For comparison, a control chitosan film was prepared without any nanoemulsion. The suspension was dried in a hot air oven (BST/HAO-1123, Bionics Scientific Technologies, India) at 40°C for 36 hours. Dried films were then carefully collected from plates in a sterile manner and placed in a vacuum chamber for conditioning for a minimum of 72 hours before characterisation.

Characterisation of bioactive film

Surface morphology of film by Scanning Electron Microscopy (SEM)

The surface structure of each film was examined using a scanning electron microscope (ZEISS EV010, ZEISS, Germany). 2-3 mm sized dried films were cut and affixed to copper stubs with double-sided carbon tape. The samples were subsequently treated with gold and examined under an accelerating voltage of 10 kV [7].

Mechanical properties of film

Tensile strength (TS) and elongation ability are crucial measures for assessing mechanical durability. The key properties were evaluated using a texture analyser (ESM 303, MARK-10, USA) in accordance with ASTM D882-91. Each rectangular film specimen, measuring 10 mm by 55 mm, was stretched at a rate of 0.5 mm/s until it broke. The initial distance between the two ends was established at 30 mm. Six samples from each film were tested, and their average results were computed [8, 19].

Water vapour permeability (WVP)

A circular film segment was securely positioned around a 30 ml glass beaker filled with 15 ml of distilled water [8, 20]. The beaker for the experiment was placed inside a desiccator with silica gel to control humidity and stored at 25±1°C for 24 hours. The beaker's weight variation was recorded, and the water vapour permeability was determined using the provided formula.

$$\text{WVP} = \frac{(\Delta W \times T)}{(\Delta t \times A \times \Delta P)}$$

The variance in weight is indicated as ΔW (g), with T symbolising the mean thickness of the film (mm), Δt representing the overall experimental duration (24 h), A denoting the exposed area of film (mm²), and, ΔP (kPa) illustrating the difference in water vapour pressure across both sides of the experimental film.

Antimicrobial property

The antibacterial properties of the films were assessed against *Salmonella* Typhimurium ATCC14028 and *Listeria monocytogenes* ATCC19111 using a growth inhibition test, similar to the methods of Ferreira and

colleagues [21, 22], with appropriate modifications. In 5 ml of Mueller-Hinton broth, a 1 cm^2 UV-treated sterile film sample was placed, and an overnight-grown fresh culture (10 µl, approximately 1×10^6 CFU/ml) of each organism was added. The tubes were then kept at 37 ± 1 °C in a shaker incubator overnight. Serial dilutions were prepared in PBS broth from each tube, and their growth inhibition ability was checked in Hektoen enteric agar (HEA) for *S.* Typhimurium and PALCOM agar medium for *L. monocytogenes* after incubation for 24 hours at 37±1°C. Colony-forming units were counted from a plate with 30 to 300 colonies, and CFU/cm^2 was estimated by multiplying with the dilution factor.

Radical scavenging activity (RSA)

The DPPH (2,2-diphenyl-1-picrylhydrazyl) assay successfully assessed the antioxidant potential of the chitosan film, offering important insights into its effectiveness [8, 23]. Each chitosan film, weighing 100 mg, was immersed in deionised water and stirred continuously in the shaker incubator for 4 hours. Afterwards, 1 mL of this extract was mixed with 0.5 mL methanolic DPPH solution (0.1 mM). The mixed solution was then kept in the dark for another 30 minutes before measuring its absorbance at 517 nm with a UV–Vis spectrophotometer (Spectra Max® M5, Molecular Devices, San Jose, CA, USA). The RSA% of each chitosan film was calculated based on these measurements.

Radical scavenging activity (RSA%) of chitosan film

$$= \frac{Abs_{Control} - Abs_{Sample}}{Abs_{Control}} \times 100$$

Here, *Abs* represents the absorbance values measured with a UV–Vis spectrophotometer for the control and treatments.

Application of bioactive packaging on raw chicken meat

The bioactive films were wrapped around raw chicken drumsticks to evaluate their shelf life under refrigeration conditions (4±1°C). The chicken drumsticks (nearly 200g) were cleaned with sterile deionised water, wrapped with UV-treated bioactive films and the samples were named as CS: meat packed with control chitosan film, TNEF1: meat packed with chitosan film and 1% thyme nanoemulsion, TNEF2: meat sample wrapped with 2% thyme nanoemulsion added chitosan film, and kept in a secondary low-density polyethene (LDPE) package under aseptic conditions. Here, LDPE packaging, as a secondary packaging material, ensures the mechanical strength and water vapour resistance necessary for product safety. The control meat (C) was also examined, which was packed in a sterile LDPE bag and stored at 4±1°C for a total experimental time of 15 days. The pH, microbiological quality, and sensory attributes of the drumsticks were evaluated every three days to monitor their freshness and determine shelf-life.

pH

The meat sample was mixed with deionised water using an ultra-turrax tissue homogeniser (IKAT 18, Germany) for 2 minutes, and its pH was estimated with a digital pH meter (TLPH-3, Trulab, India) [24].

Microbiological assessment of chicken drumsticks

A 25 g sample of the refrigerated drumstick was aseptically blended with 225 mL of sterile peptone water (0.1%) for 2-3 minutes. From the initial dilution (10^{-1}), 1 mL was transferred into a test tube containing 9 mL of sterile 0.1% peptone water and vortexed for 1 minute (10^{-2}). Serial dilutions were subsequently performed carefully. Suitable dilutions were plated on sterile agar media, including plate count agar for measuring total plate count (kept at 37±1 °C for 24 hours), psychrophilic bacteria (incubated for 7 days at 4±1 °C), PALCAM agar for *L. monocytogenes* (stored at 37 °C for 24 hours), and Hektoen enteric agar (HEA) for *S.* Typhimurium (incubated for 24 hours at 37 °C). Colonies from plates with 30 to 300 were counted, and the average was multiplied by the dilution factor to find the log CFU/g of the sample [8, 24]. Each experiment was conducted in triplicate.

Sensory analysis of meat

A group of trained sensory evaluators (n=30), including assistant professors and postgraduate students from the Faculty of Veterinary and Animal Sciences, BHU, assessed the product's sensory attributes. The sensory evaluations were conducted consistently after 3:30 pm. The raw chicken meat (100 g) was evaluated based on colour and odour in a hedonic scale of 9 points, where an extremely preferable sample was scored with 9, and an extremely undesirable sample was scored with 1 [24].

Statistical analysis

Experiments were conducted thrice in duplicate (n=6), except for sensory analysis (n=30), and the data were analysed using SPSS version 20 (IBM, USA). Two-way ANOVA and one-way ANOVA were used to analyse different experimental parameters. Tukey's HSD multiple-range post hoc test was applied to compare and analyse mean ± standard error (SE) values across

treatments. Statistical significance was assessed at the 95% confidence level ($p < 0.05$). Graphs were created using GraphPad Prism (Version 9.0; GraphPad Software, Boston, MA, USA).

RESULTS AND DISCUSSION

Transmission electron microscopy (TEM) of nanoemulsion

Micrographs of nanoemulsions obtained by transmission electron microscopy at different concentrations showed significant morphological features (Fig. 2). The micrograph indicated the presence of irregular, spherical nanosized droplets measuring 19-40 nm; all measurements were within 100 nm. Encapsulations of oil droplets with Tween 80 were confirmed by the presence of dark, dense droplets with a clear outline in the contrast light field [16, 25]. The higher pressure of ultrasonication successfully broke down the coarse emulsion into nanoparticles across all treatments. These reductions in particle size improve stability, surface-to-volume ratio, and potential drug delivery properties compared to free oil [26]. At the same time, noticeable flocculation and clumping occurred in T3 with the higher concentration of (2%) oil. Drying the solvent and flattening the nanoparticles with the grid during experimental processing may influence the shape and size of nanoemulsions [16]. Several studies in the existing literature have confirmed thyme nanoemulsion droplet sizes (<100 nm) using transmission electron microscopy, with Tween 80 used as a solvent [8, 26, 2476]. In a study, thyme nanoemulsion droplets were prepared and characterised by TEM, revealing spherical oil droplets with a size range of 20-55.2 nm [25].

Table 1: Physical, mechanical, antioxidant and antimicrobial properties of bioactive films.

Treatments	TS (MPa)*	EAB (%)*	WVP (g mm m^{-2} day^{-1} kPa^{-1})*	RSA (%)*	*Listeria monocytogenes* (log CFU/cm^2)*	*Salmonella* Typhimurium (log CFU/cm^2)*
C	12.78 ± 0.39^{d}	40.56 ± 1.18^{ab}	2.32 ± 0.02^{c}	5.61 ± 0.69^{a}	3.67 ± 0.02^{c}	4.80 ± 0.02^{c}
T1	9.84 ± 0.70^{c}	39.92 ± 1.78^{a}	2.35 ± 0.05^{c}	17.13 ± 0.68^{b}	3.59 ± 0.01^{c}	4.59 ± 0.01^{bc}
T2	7.15 ± 0.50^{b}	47.26 ± 1.44^{b}	1.92 ± 0.02^{b}	31.11 ± 1.02^{c}	2.69 ± 0.05^{b}	4.44 ± 0.04^{b}
T3	4.70 ± 0.37^{a}	57.56 ± 1.58^{c}	1.64 ± 0.05^{a}	45.37 ± 1.68^{d}	2.00 ± 0.00^{a}	2.89 ± 0.10^{a}

*Data are represented as mean ± standard error (n = 6); and Superscripts with lowercase letters (a, b, c) show significant differences ($p < 0.05$) in the columns; TS= Tensile strength; EAB= Elongation at break; WVP= water vapour permeability; RSA= Radical scavenging activity; C= control chitosan film; T1= chitosan film infused with thyme nanoemulsion (0.5%); T2= chitosan film added with thyme nanoemulsion (1%); T3= chitosan film added with thyme nanoemulsion (2%).

Table 2: Sensory evaluation (colour and odour scores) of raw chicken drumsticks under refrigeration for 15 days.

Treatments	0D	3D	6D	9D	12D	15D
			Colour*			
C_0	8.80 ± 0.05^{Ae}	8.48 ± 0.04^{Be}	6.47 ± 0.06^{Ad}	4.88 ± 0.16^{Ac}	3.61 ± 0.08^{Ab}	2.81 ± 0.12^{Aa}
CS	8.53 ± 0.01^{Ad}	8.31 ± 0.01^{Abd}	6.75 ± 0.10^{Ac}	5.34 ± 0.17^{ABb}	3.81 ± 0.12^{Aa}	3.43 ± 0.09^{Aa}
TNEF1	8.82 ± 0.06^{Ae}	8.22 ± 0.06^{Ae}	7.53 ± 0.01^{Bd}	6.03 ± 0.28^{BCc}	4.41 ± 0.08^{Bb}	3.62 ± 0.06^{Aa}
TNEF2	8.81 ± 0.13^{Ad}	8.44 ± 0.06^{Abcd}	7.70 ± 0.14^{BCc}	6.52 ± 0.01^{Cb}	5.8 ± 0.10^{Cb}	4.86 ± 0.31^{Ba}
			Odour*			
C_0	8.41 ± 0.09^{Af}	7.71 ± 0.02^{Ae}	6.56 ± 0.06^{Ad}	3.88 ± 0.07^{Ab}	3.33 ± 0.03^{Ab}	$2. 6\pm0.06^{Aa}$
CS	8.56 ± 0.12^{ABCe}	8.04 ± 0.15^{Abe}	7.18 ± 0.06^{Bd}	5.91 ± 0.19^{Bc}	4.73 ± 0.13^{Bb}	3.34 ± 0.05^{Ba}
TNEF1	8.83 ± 0.03^{Be}	8.27 ± 0.13^{Abde}	7.7 ± 0.10^{Bd}	6.3 ± 0.16^{Bc}	5.03 ± 0.28^{BCb}	3.66 ± 0.22^{Ba}
TNEF2	8.90 ± 0.05^{Bf}	8.41 ± 0.06^{Abe}	7.55 ± 0.07^{Bd}	6.47 ± 0.07^{Bc}	5.56 ± 0.00^{Cb}	4.7 ± 0.15^{Ca}

*Data are represented as mean ± standard error (n = 30); and Superscripts with lower cases (a, b, c, d) show significant differences ($p < 0.05$) in a row whereas superscripts with other letters (A, B, C, D) shows significant variances ($p < 0.05$) in a column; C_0=control meat; CS= meat wrapped with chitosan film; TNEF1= meat wrapped with 1% thyme nanoemulsion incorporated chitosan film; TNEF2= meat wrapped with 2% thyme nanoemulsion incorporated chitosan film; D= storage days.

Characterisation of chitosan film

Scanning electron microscopy (SEM)

Surface morphology of each film sample from SEM analysis is shown in Fig. 3a to 3d. This experiment presents microstructural observations of the bioactive films, interaction patterns between two phases, and modifications to the nanoemulsion after drying within a chitosan matrix. In the control chitosan film surface (Fig. 3a), noticeable cracks and folds were observed due to improper crystallisation of the chitosan film matrix for its degree of deacetylation with the additive used and the influence of the drying environment [8, 28]. As the nanoemulsion was incorporated, the folds disappeared, and multiple micropores emerged in a non-homogeneous pattern. These micropores ensured the incorporation of oil nanodroplets into the chitosan matrix during drying, followed by evaporative loss. As the concentration was increased to 1% and 2% (Fig. 3c to 3d), a few large clumps and flocculations were noticed on the surface, but higher concentrations improved the surface roughness and compactness of the film [29, 30].

The cross-sectional study (Fig. 3e-3h) showed that adding essential oil nanoemulsion improved the smoothness of control chitosan films. With higher concentrations, the films became more compact and denser. This study demonstrates a compatible integration of thyme essential oil nanoemulsion within the chitosan film matrix [31]. The amalgamation depends on the type of essential oil used and on the film properties. This structural compactness improves the film's moisture- and gas-barrier properties. Still, limitations in tensile strength may arise from perforated microstructures and flocculation at higher oil concentrations in bioactive films [32]. Similar structural arrangements of chitosan films with essential oil nanoemulsions have been reported in various studies [16, 23, 33].

Mechanical properties of chitosan film

Measuring the mechanical properties of the film, especially Tensile Strength (TS) and Elongation at Break (EAB), is essential for assessing its suitability in food applications. The study found that the TS of the chitosan film was 12.78±0.39 MPa, but it dropped after adding the essential oil nanoemulsion, reaching 4.70±0.37 MPa in T3 (see Table 1). Tensile strength indicates the maximum stress a biopolymer can withstand before breaking or fracturing. This property is

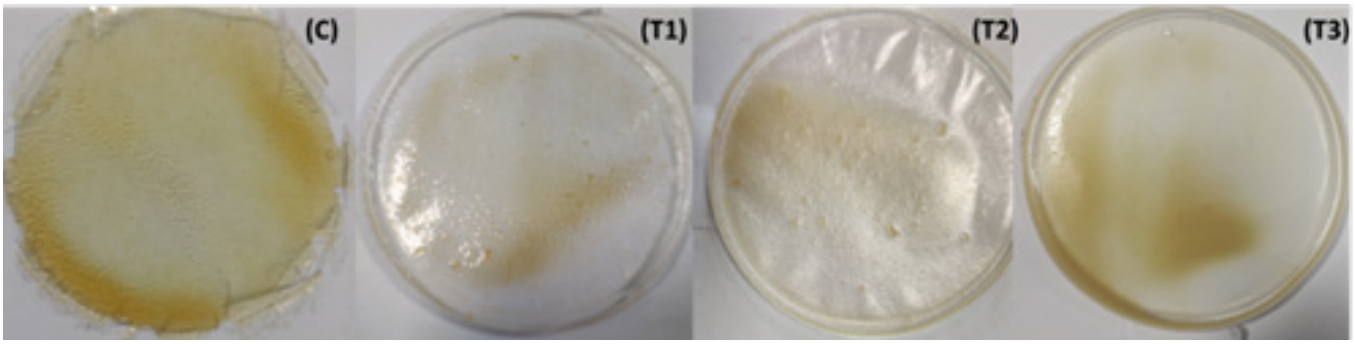

Fig. 1. Prepared bioactive films; C = Chitosan film, T1= Chitosan film and thyme nanoemulsion (0.5%), T2= Chitosan film and thyme nanoemulsion (1%), T3 = Chitosan film and thyme nanoemulsion (2%).

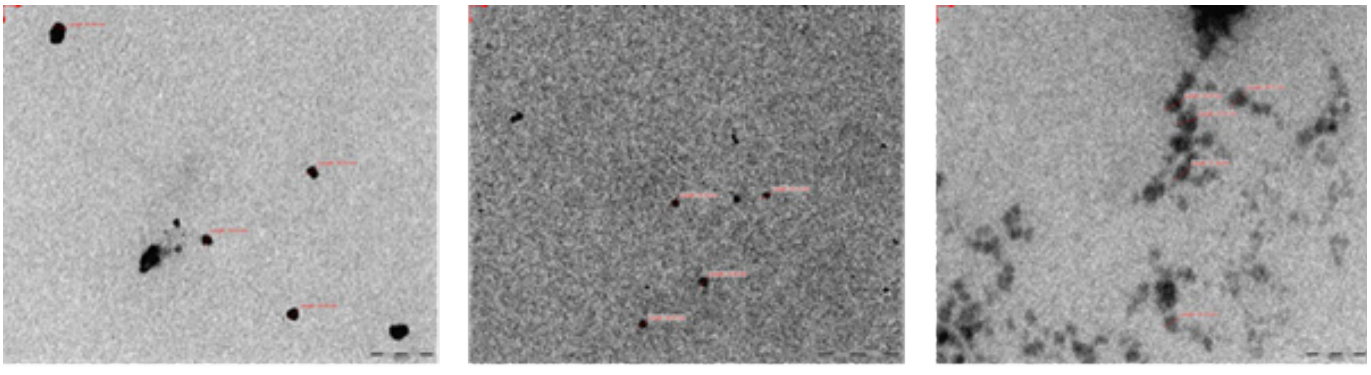

Fig. 2. Morphology of nanoemulsions by Transmission electron microscopy (TEM);(a) image of T1 (b) image of T2 (c) image of T3.

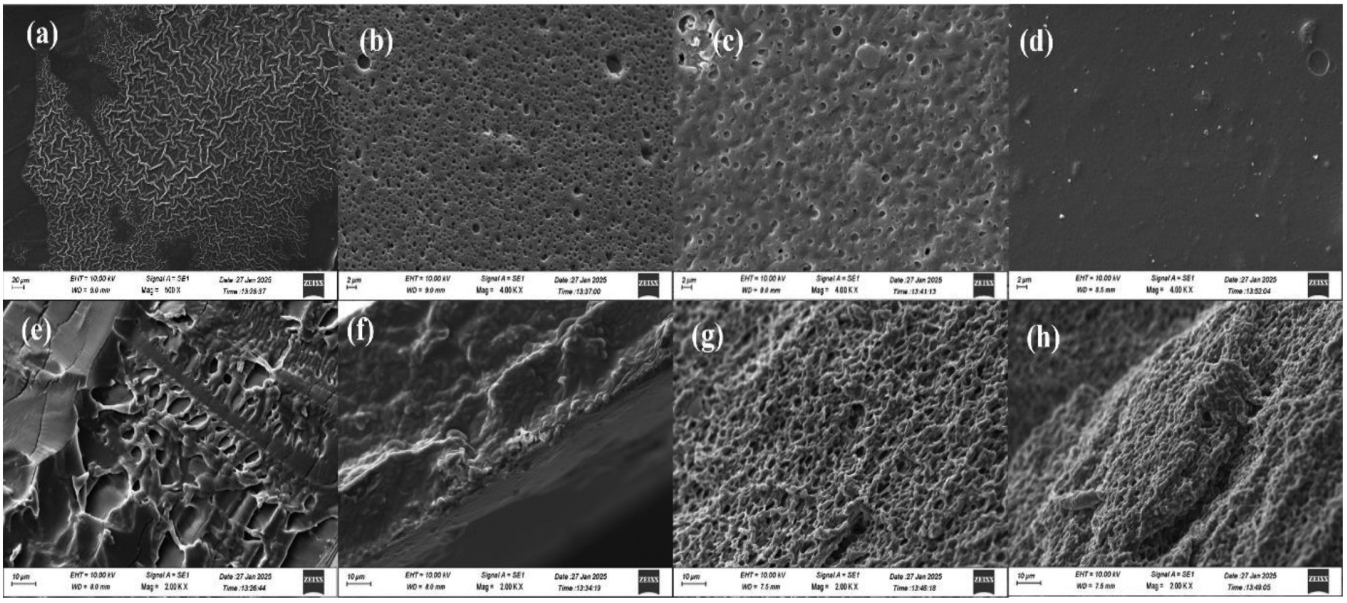

Fig. 3. Surface morphology (from left to right a-d) and cross-section (from left to right e-h) study of chitosan biopolymer with different concentrations of thyme nanoemulsion; SEM images were taken at 10 kv and 500 X, 2000 X and 4000X magnifications; (surface morphology: a = C, b = T1, c = T2, d = T3; Cross section: e= C, Cross section f = T1, g = T2, h = T3)**.**

essential for understanding the limits of a biopolymer's mechanical performance. TS has decreased during treatment due to weak intermolecular interactions between the nanoemulsion and the chitosan matrix. Additionally, evaporative damage to oil nanodroplets during film drying, with multiple holes and pores, weakens the biopolymer's internal cohesive properties. Similar findings were analysed in different literature where TS was compromised after the addition of essential oil nanoemulsion [33, 34].

Conversely, the elongation at break (EAB) increased (Table 1) by adding the essential oil nanoemulsion into the control film. Elongation at break (EAB) is a critical measure representing a film's ability to stretch or deform before it ultimately fractures under tensile stress. This property reflects the material's flexibility and resilience, indicating how much strain it can tolerate before reaching its breaking point. The highest EAB was measured in T3 at 57.56±1.5%, which differed significantly ($p<0.05$) from the others. C and T1 showed no significant difference ($p > 0.05$), exhibiting minimal variation in values. The increase in the bioactive film's stretchability is likely attributed to hydroxyl groups in thyme essential oil nanoemulsions, which could improve the film's plasticising properties [35]. Various studies have reported an increase in EAB of bioactive films, mainly influenced by essential oils and their nanoemulsions [7, 36].

Water vapour permeability (WVP)

Water vapour barrier properties are crucial for food packaging, particularly for muscle foods. In this study, T1 exhibited a higher water vapour permeability (WVP) compared to the control film, although the difference was not statistically significant ($p > 0.05$) (Table 1). This observation can be explained by the presence of multiple heterogeneous pores in T1, which can facilitate increased water vapour transmission. The water vapour permeability (WVP) decreased significantly ($p < 0.05$) in T2 and T3, suggesting that higher nanoemulsion concentrations in films are more effective. A similar analysis showed that a chitosan biopolymer with a higher concentration of thyme oil exhibited improved physical cohesion due to intermolecular chain interactions, thereby enhancing its water-vapour barrier properties.

Radical scavenging activity assay (RSA)

Estimation of the antioxidant property of bioactive films is important to justify their bio-preservative nature. The DPPH (2,2-diphenyl-2-picrylhydrazyl) assay is an important method for assessing the free radical scavenging activity (RSA) of a film and is acknowledged as one of the most reliable techniques for determining antioxidant capacity. In this study, the chitosan film infused with a 2% thyme oil nanoemulsion exhibited greater electron-donating capability and free radical scavenging activity (45.37±1.68%) than the other samples (Table 1). In contrast, the control chitosan

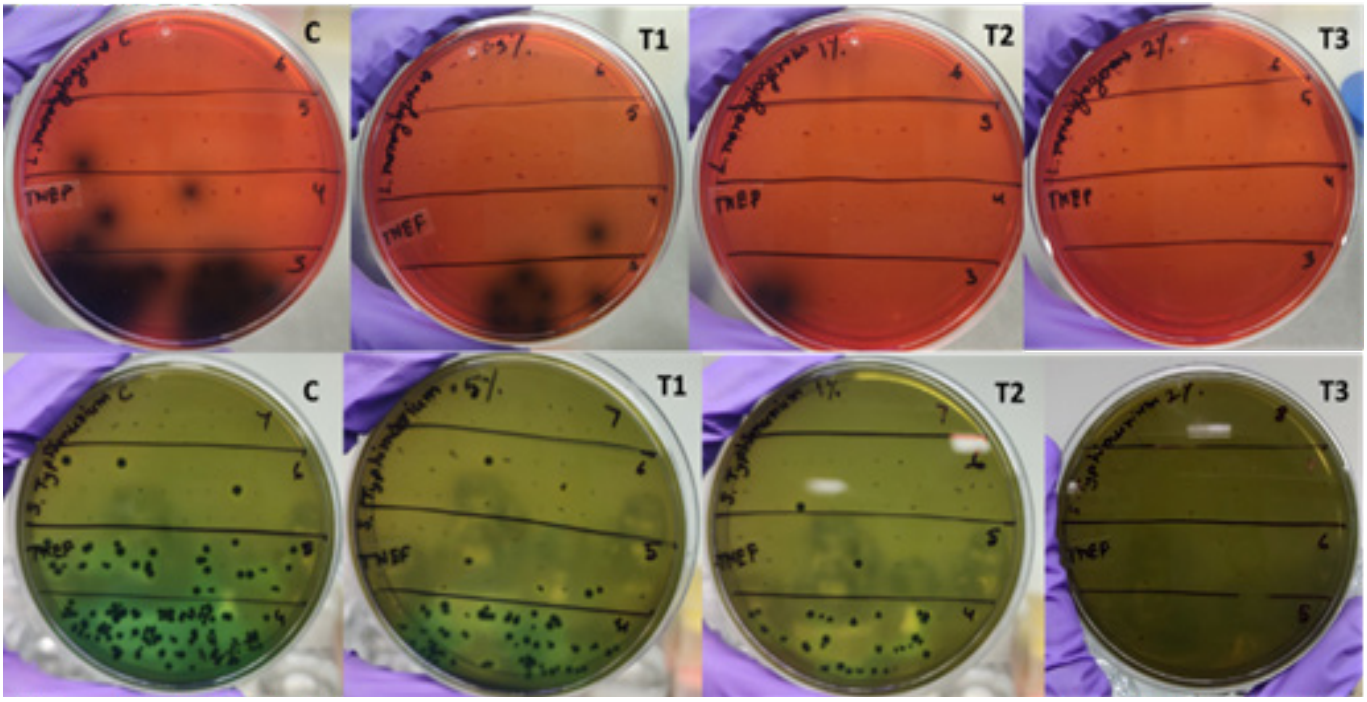

Fig. 4. Antimicrobial activity of thyme nanoemulsion film (TNEF); (C= chitosan film, T1= TNEF with thyme nanoemulsion (0. 5 %), T2= TNEF with thyme nanoemulsion (1 %), T3= TNEF with thyme nanoemulsion (2 %) against *Salmonella* Typhimurium (ATCC 14028) and *Listeria monocytogenes* (ATCC 19111).

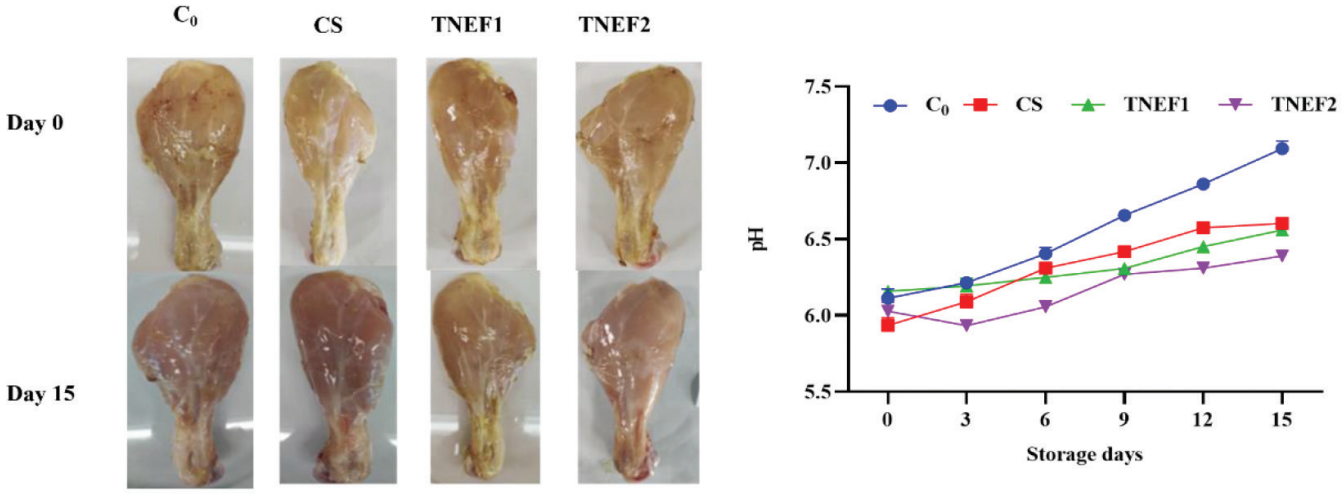

Fig. 5. (a) Biopreservation of raw chicken drumsticks with bioactive films with different concentrations of thyme nanoemulsion under refrigerated Storage for 15 days; (b) pH estimation of meat samples stored at 4±1°C for 15 days; C_0 = control sample without bioactive film, CS= sample packed with chitosan control film, TNEF1= meat wrapped with chitosan film infused with 1% thyme nanoemulsion, TNEF2= meat sample wrapped with chitosan film and 2% thyme nanoemulsion.

film exhibited limited antioxidant properties, likely due to the presence of amine and hydroxyl groups in its fundamental structural unit and a significant degree of deacetylation [9]. In contrast, the thyme nanoemulsion is rich in thymol and carvacrol, key phenolic compounds that enhance the antioxidant efficacy of the chitosan film [8, 11]. Several studies support the current findings regarding the emerging free radical scavenging properties of chitosan film after the inclusion of thyme nanoemulsion [37, 39].

Antimicrobial property

The antimicrobial properties of bioactive biopolymers represent a significant biofunctional

characteristic that may demonstrate their efficacy in bio-preservation applications. The antimicrobial activity of bioactive films is shown in Table 1 and Fig. 4. It was observed that the Chitosan film with 1% and 2% thyme nanoemulsions exhibited significantly higher ($p < 0.05$) antimicrobial efficacy than the control chitosan film. However, the T1 and control films did not differ significantly ($p > 0.05$) for Gram-negative and Gram-positive organisms. Thymol and carvacrol in thyme nanoemulsion contribute to the antimicrobial effectiveness observed in bioactive films, while chitosan films exhibit antimicrobial properties due to their polycationic nature. It was noted that increasing the nanoemulsion concentration within the biopolymer enhanced antimicrobial properties. Similar antimicrobial activity of thyme essential oil was depicted in different literature [26, 40]. Additionally, bioactive films exhibited greater sensitivity to Gram-positive bacteria than to Gram-negative bacteria. This phenomenon can be explained by the outer membrane of Gram-negative bacteria, which acts as a strong protective barrier made up of Lipopolysaccharide (LPS). Due to their hydrophobic nature, essential oils find it difficult to pass through the LPS barrier of Gram-negative bacteria, leading to reduced effectiveness against Gram-negative organisms compared to Gram-positive ones. The principal bioactive components in thyme essential oil disrupt the cell structure integrity of microorganisms, leading to leakage of ions and intracellular components, disruption of proton motive force, alteration of DNA, and sometimes chelation with microbial enzymes, interfering with cellular metabolism and resulting in cellular death [25, 41].

Application of biopolymer on chicken drumsticks preservation

pH

Evaluating pH levels is essential for assessing the degradation of meat quality during storage investigations. In this research, four sample groups were refrigerated and examined: one group included chicken drumsticks without any preliminary wrapping (C_0), another group utilised a control film, and the rest two groups were covered in chitosan films infused with 1% and 2% thyme nanoemulsion, respectively (Fig. 5a). It was observed that the pH of each meat sample increased over time due to changes in meat quality. In C_0, the pH rose notably ($p < 0.05$), from 6.11±0.06 on day 0 to 7.09±0.05 at the endpoint (see Fig. 5b). In TNEF2, the pH level started at 6.02±0.06 on day 0 and rose to 6.39±0.00 by day 15 ($p < 0.05$), which remained below the control level. It was further observed that in C_0 and CS, starting from day 6, pH values increased significantly ($p < 0.05$). In the treatment groups, this significant enhancement was maintained during later storage stages. When alkaline metabolites accumulate in the meat matrix, including ammonia, non-nitrogenous substances, etc., pH increases, indicating meat quality deterioration by microbial spoilage and enzymatic

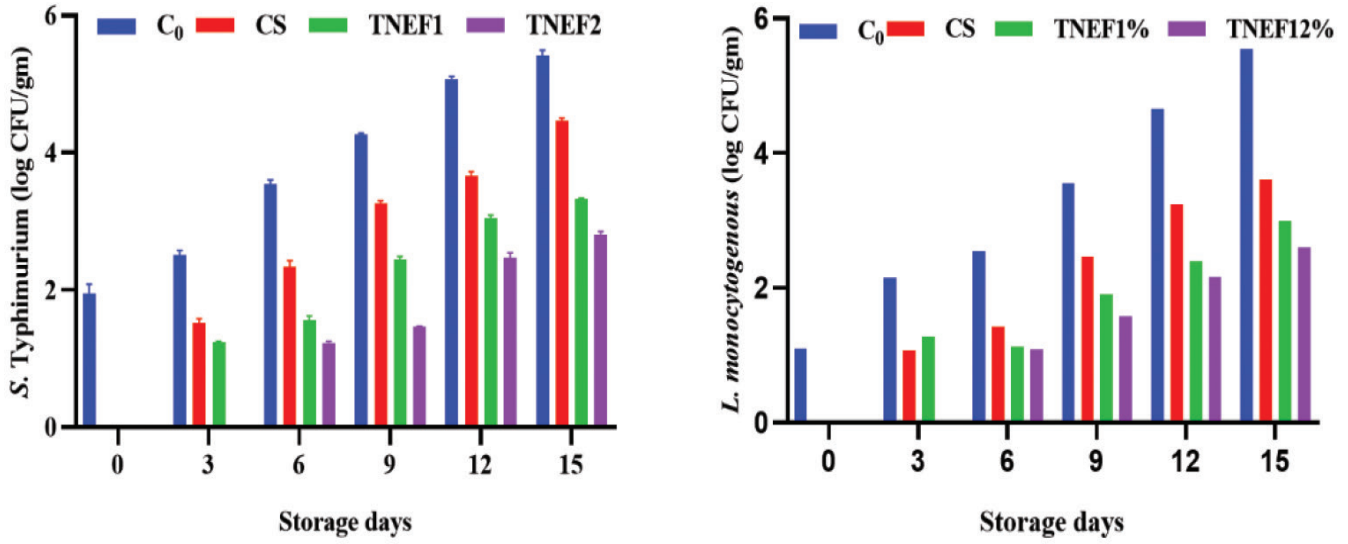

Fig. 6. Microbiological analysis of chicken drumsticks under refrigeration storage for 15 days (a) Total plate count (TPC); (b) Psychrophilic bacterial count (PBC); C_0= chicken drumstick without any wrapping; CS= chicken drumstick wrapped with chitosan film; TNEF1= chicken drumstick wrapped with chitosan film with 1% thyme nanoemulsion; TNEF2= chicken drumstick wrapped with chitosan film with 2% thyme nanoemulsion.

decline [39]. In the treatment samples, the prolonged release of thyme nanoemulsion from the bioactive film slows down the microbial spoilage of meat because of the effective polyphenolic antimicrobial compounds, namely carvacrol and thymol [8, 42].

Microbiology of the meat sample

In the current experiment, total plate count (TPC) increased from 4.95±0.03 log CFU/g on day 0 to 7.63±0.02 log CFU/g on the 15th day of storage in the control meat sample ($p < 0.05$), indicating that microbial spoilage could not be prevented under refrigeration for up to 15 days (Fig. 7a). Meanwhile, chicken drumsticks wrapped in chitosan films failed to preserve meat quality after 6 days of storage due to the chitosan film's insufficient antimicrobial activity. TNEF1 and TNEF2 initially reduced the microbial count, followed by a gradual increase in bacterial numbers up to the 15th day. The TNEF2 started with an initial microbial count of 4.44±0.11 log CFU/g on day 0, which rose to 5.39±0.09 log CFU/g on day 15 (not exceeding the acceptable limit of 5 log CFU/g as per the Food Safety Standards Authority of India). In TNEF1, microbial loads were significantly higher ($p < 0.05$) than in TNEF2 because of a lower concentration of thyme essential oil nanoemulsion in the biopolymer. The bioactive compounds embedded within the biofilm diffuse out effectively, inhibiting bacterial growth by disrupting cellular membranes and interfering with enzymatic systems. This disruption leads to a loss of ions and fluids, thereby adversely affecting the bacteria [7, 43]. [44] reported a similar outcome, showing that garlic nanoliposomes embedded in a chitosan film could prolong the storage of chicken meat for up to 14 days at 4±1°C. In this experiment, 2% garlic essential oil nanoliposomes exhibited the most effective antimicrobial activity against chicken fillets. A 1.5-log reduction in aerobic counts was observed in the 2% nanoliposome sample compared to the control sample.

Similar findings were observed in the psychrophilic bacterial counts (PBC) (Fig. 6b). Here, the control sample exhibited an exponential increase ($p < 0.05$) in microbial counts, reaching 7.30±0.04 log CFU/g on the 15th day from 4.44±0.05 log CFU/g loads on day 0. A decreasing pattern of microbial counts was observed in the treatment groups (CS and TNEF1) up to the 3rd day, and in TNEF2 up to the 6th day, followed by sluggish growth towards the end of storage. In TNEF2, PBC counts increased from 3.24±0.03 log CFU/g on the 0th day to 4.88±0.08 log CFU/g at the end of the meat storage. Gram-negative psychrophiles are the key organisms responsible for aerobic spoilage of muscle food under refrigeration. Importantly, they are less sensitive to essential oils due to their lipopolysaccharide-based cell wall structure [44, 45]. Thyme essential oil nanodroplets effectively prevented microbial spoilage compared to control samples without any protective bioactive films. The current study aligns with [44], which noted that applications of whey protein isolate- and cinnamon essential oil-based coatings suppressed the growth of psychrophiles in chicken breasts. In a separate study, the nanoemulsion of *Eryngium campestre* essential oil at a concentration of 2.5% effectively reduced the total psychotropic counts in ostrich meat to 1.37±0.06 log CFU/g. This was in contrast to the control group, which showed 7.31±0.55 log CFU/g after 12 days of storage period at 4±1°C [46].

Compared with gram-negative organisms (*S.* Typhimurium), the thyme essential oil nanoemulsion demonstrated potential antimicrobial activity against gram-positive microorganisms *(L. monocytogenes*) in a meat model system, which aligns with the in vitro antimicrobial activity of the bioactive biopolymer (Fig. 8a and 8b). In this study, chicken drumsticks packaged with chitosan films containing a 2% thyme essential oil nanoemulsion exhibited superior antimicrobial effects against both microorganisms compared with other treatments. In the case of *S.* Typhimurium and *L. monocytogenes*, microbial growth was absent until the 3rd day of refrigerated storage, at which point the bacteria were treated with TNEF2. The microbial load increased to 2.81±0.04 log CFU/g (*S.* Typhimurium) and 2.60±0.04 log CFU/g (*L. monocytogenes*) by day 15, from initial counts of 1.23±0.02 log CFU/g (*S.* Typhimurium) and 1.09±0.03 log CFU/g (*L. monocytogenes*) in TNEF2. Moreover, TNEF1 yielded comparable results in extending the shelf life of raw chicken drumsticks. Thymol and carvacrol are the active antimicrobial components in the bioactive film with a 2% thyme nanoemulsion, which reduces the numbers of spoilage and pathogenic microbes in meat [47–49].

Sensory evaluation of meat samples

Sensory attributes are a vital factor influencing consumer acceptance or rejection of food. In this study, trained evaluators were assembled to assess the sensory aspects of raw chicken drumsticks (Table 2). Colour is an important parameter in fresh meat preservation studies, as it indicates freshness. In this current study, colour scores decreased as days passed. Up to day 3, higher scores were observed ($p > 0.05$) across all samples, followed by a decline. This deterioration was observed

more slowly ($p > 0.05$) in treatment samples, especially in TNEF2. It was also noted that TNEF1 and TNEF2 did not differ significantly ($p > 0.05$) until day 9 of storage. Colour differences were noticeable between treatments and the control ($p < 0.05$), indicating that essential oil nano droplets significantly help maintain meat freshness. Similar observations were reported in the literature, where essential oil nanoemulsion delayed microbial spoilage as well as oxidative depletion in meat myoglobin and extended storage life [50, 51]. Sensory scores correlated with microbiological analysis and pH studies. Decreased color scores can be attributed to chemical changes in myoglobin pigment and the production of metmyoglobin during storage due to unavoidable oxidation [8, 52].

The odour of raw chicken drumsticks was assessed throughout the storage period by sensory panelists (Table 2). It was observed that odour scores decreased over time, with foul odour becoming more prominent in the later stages of storage. The shift from meaty to foul odour was caused by proteolytic degradation and the release of volatile nitrogenous and non-nitrogenous metabolites. Microbial growth and enzymatic activity are key factors behind these odours [53]. The odour score dropped from 8.41±0.09 on day 0 in the control sample (C_0) to 2.56±0.06 at the termination of the storage period ($p < 0.05$). Conversely, treatment samples suppressed the foul smell during storage due to the mild aromatic fragrances of essential oil, which consumer panelists appreciated. Additionally, these bioactive films inhibited microbial growth and chemical oxidation in the meat samples. In the treatment groups, odour scores also decreased with storage time but remained higher than those in the control group, reflecting consumer preference. The highest score was recorded for TNEF2, starting at 8.90±0.05 and decreasing to 4.7±0.15. The odour scores below 4 on the hedonic scale were deemed objectionable. The control sample was discarded after day 6 based on odour scores; the CS sample exhibited a major objectionable odour by day 12, and the TNEF1 sample was rejected at day 15 due to off-odours. These rising off-odour scores indicate significant microbial spoilage. A pleasant aromatic fragrance, masking the meaty smell of raw chicken that sometimes consumers dislike, was preferred over all other treatments in TNEF1 and TNEF2, owing to their consistent release of EO nanoemulsion onto the chicken drumsticks [50]. Different authors have reported similar works in their literature, where it was stated that the application of micro or nano emulsions of essential oils in meat preservation systems consistently achieved higher acceptance compared to control samples in terms of odour and other sensory attributes [50, 54–56]. In another study, it was found that the odour and colour scores of meat emulsion treated with thyme and oregano essential oil nanoparticles (500 ppm each) remained satisfactory for up to 9 days of refrigerated storage, with scores exceeding 3.5. In contrast, the control meat samples, which were packaged aerobically without any treatments, only remained satisfactory for 3 days [57].

CONCLUSION

The present study successfully developed chitosan-based bioactive films infused with thyme essential oil nanoemulsions at concentrations of 0.5%, 1% and 2% (v/w). The structural characteristics and mechanical properties of the developed films were analysed. Chitosan film with 2% thyme nanoemulsion (T3) exhibited potent radical-scavenging and antimicrobial activities, especially against *S.* Typhimurium and *L. monocytogenes*. Notably, the T3 film formulation, containing a 2% thyme essential oil nanoemulsion, demonstrated significant improvements in elongation at break and water-vapour barrier performance, indicating strong potential for use in bioactive packaging. Scanning electron microscopy (SEM) images revealed greater compactness and structural stability in the T3 formulation than in the other films. Further, during *in situ* application to raw meat, the bioactive film containing 2% thyme nanoemulsion (TNEF2) extended the shelf life of refrigerated (4±1°C) drumsticks to 15 days, compared with 6 days for the control meat without any biopolymer. Furthermore, the chitosan film containing the 1% thyme nanoemulsion produced comparable microbiological results. Therefore, based on these findings, a chitosan film containing a 2% thyme oil nanoemulsion can be considered an excellent biopreservation strategy, particularly for the meat packaging industry, as it may improve meat quality and prolong shelf life during refrigerated storage.

ACKNOWLEDGEMENT

The authors would like to thank the Banaras Hindu University, Varanasi, Uttar Pradesh, for providing the facilities for this research work.

REFERENCES

1. Bintsis T. Foodborne pathogens. AIMS Microbiol. 2017;3(3):529–63.

2. Lianou A, Panagou EZ, and Nychas G-JE. Meat Safety—I Foodborne Pathogens and Other Biological Issues. *Lawrie's Meat Science*. Elsevier; 2017.

3. Das A, Bhattacharya D, Nanda PK, Nath S, and Das AK. *Biopreservation in Meat and Meat Products*. 2024.

4. Guerra AF. Update on the use and abuse of preservatives in meat products. Food Control. 2024;166:110775.

5. Mahato A, Chatterjee PN, Sarkar S, Sen AR, Pal A, Roy S, Patra AK. Effects of Chemically and Green Synthesized Zinc Oxide Nanoparticles on Shelf Life and Sensory Quality of Minced Fish (*Pangasius hypophthalmus*). Foods. 2024; 13(17):2810.

6. S. Bhuvaneshwari*, D.Sruthi*, V. Sivasubramanian*, and Niranjana kalyani** and J. Sugunabai **. Development and characterization of chitosan film. Int J Eng Res Appl. 2011;1(2):292–9.

7. Elshamy S, Khadizatul K, Uemura K, Nakajima M, and Neves MA. Chitosan-based film incorporated with essential oil nanoemulsion foreseeing enhanced antimicrobial effect. J Food Sci Technol. 2021;58(9):3314–27.

8. Bhattacharya D, Kumar D, Pavan Kumar P, Das AK, Nanda PK, Das A, Karunamay S, Satyaprakash K, Singh Parmar A, and Kumar A. Development and characterization of chitosan–thyme essential oil nanoemulsion films for active packaging of raw chicken drumsticks. AIMS Agric Food. 2025;10(4):1004–38.

9. López-Mata MA, Ruiz-Cruz S, Silva-Beltrán NP, Ornelas-Paz J de J, Ocaño-Higuera VM, Rodríguez-Félix F, Cira-Chávez LA, Del-Toro-Sánchez CL, and Shirai K. Physicochemical and Antioxidant Properties of Chitosan Films Incorporated with Cinnamon Oil. Int J Polym Sci. 2015;2015:1–8.

10. Loizzo MR, Tundis R, Menichini F, and Duthie G. Anti-rancidity effect of essential oils, application in the lipid stability of cooked turkey meat patties and potential implications for health. Int J Food Sci Nutr. 2015;66(1):50–7.

11. Tohidi B, Rahimmalek M, and Arzani A. Essential oil composition, total phenolic, flavonoid contents, and antioxidant activity of Thymus species collected from different regions of Iran. Food Chem. 2017;220:153–61.

12. Satora P, Michalczyk M, and Banaś J. Impact of Thyme Essential Oil on the Aroma Profile and Shelf Life of Vacuum-Packed Minced Turkey Meat. Molecules. 2024;29(15):3524.

13. Marzlan AA, Hussin ASM, Bourke P, Chaple S, Barroug S, and Muhialdin BJ. Combination of Green Extraction Techniques and Essential Oils to Develop Active Packaging for Improving the Quality and Shelf Life for Chicken Meat. Food Rev Int. 2023;39(7):3783–805.

14. Das S, Singh VK, Dwivedy AK, Chaudhari AK, Upadhyay N, Singh P, Sharma S, and Dubey NK. Encapsulation in chitosan-based nanomatrix as an efficient green technology to boost the antimicrobial, antioxidant and in situ efficacy of *Coriandrum sativum* essential oil. Int J Biol Macromol. 2019;133:294–305.

15. Amiri E, Aminzare M, Azar HH, and Mehrasbi MR. Combined antioxidant and sensory effects of corn starch films with nanoemulsion of *Zataria multiflora* essential oil fortified with cinnamaldehyde on fresh ground beef patties. Meat Sci. 2019;153:66–74.

16. Xavier LO, Sganzerla WG, Rosa GB, da Rosa CG, Agostinetto L, Veeck AP de L, Bretanha LC, Micke GA, Dalla Costa M, Bertodi FC, *et al*. Chitosan packaging functionalized with *Cinnamodendron dinisii* essential oil loaded zein: A proposal for meat conservation. Int J Biol Macromol. 2021;169:183–93.

17. Gómez-Estaca J, López de Lacey A, López-Caballero ME, Gómez-Guillén MC, and Montero P. Biodegradable gelatin-chitosan films incorporated with essential oils as antimicrobial agents for fish preservation. Food Microbiol. 2010;27(7):889–96.

18. Bhattacharya D and G. K. Selection of biopolymers to develop a biodegradable and ediblefilm for packaging of luncheon chicken meat slices. Asian J Dairy Food Res. 2017;36(01).

19. Fallah M, Rouhi M, Soltani M, Mohammadifar MA, Bahrami R, Davachi SM, Abbaspourrad A, and Mohammadi R. Physico-mechanical, Antimicrobial, and Antioxidant Properties of Gelatin Edible Films Incorporated with *Olibanum* Essential Oil and Sodium Hexametaphosphate on the Rainbow Trout Fillet Under Refrigerated Conditions. J Polym Environ. 2021;29(7):2174–84.

20. Haghju S, Beigzadeh S, Almasi H, and Hamishehkar H. Chitosan films incorporated with nettle (*Urtica dioica L.*) extract-loaded nanoliposomes: I. Physicochemical characterisation and antimicrobial properties. J Microencapsul. 2016;33(5):438–48.

21. Ferreira RR, Souza AG, and Rosa DS. Essential oil-loaded nanocapsules and their application on PBAT biodegradable films. J Mol Liq. 2021;337.

22. Santos M, Fonseca A, Mendonça P, Branco R, Serra A, Morais P, and Coelho J. Recent Developments in Antimicrobial Polymers: A Review. Materials (Basel). 2016;9(7):599.

23. Almasi H, Azizi S, and Amjadi S. Development and characterization of pectin films activated by nanoemulsion and Pickering emulsion stabilized marjoram (*Origanum majorana L.*) essential oil. Food Hydrocoll. 2020;99.

24. Das A, Biswas S, Satyaprakash K, Bhattacharya D, Nanda PK, Patra G, Moirangthem S, Nath S, Dhar P, Verma AK, *et al*. Ratanjot (Alkanna tinctoria L.) Root Extract, Rich in Antioxidants, Exhibits Strong Antimicrobial Activity against Foodborne Pathogens and Is a Potential Food Preservative. Foods. 2024;13(14):2254.

25. Doghish AS, Shehabeldine AM, El-Mahdy HA, Hassanin MMH, Al-Askar AA, Marey SA, AbdElgawad H, and Hashem AH. *Thymus Vulgaris* Oil Nanoemulsion: Synthesis, Characterization, Antimicrobial and Anticancer Activities. Molecules. 2023;28(19):6910.

26. Gupta P, Preet S, Ananya, and Singh N. Preparation of *Thymus vulgaris* (L.) essential oil nanoemulsion and its chitosan encapsulation for controlling mosquito vectors. Sci Rep. 2022;12(1):4335.

27. El-Sayed SM and El-Sayed HS. Antimicrobial nanoemulsion formulation based on thyme (*Thymus vulgaris*) essential oil for UF labneh preservation. J Mater Res Technol. 2021;10:1029–41.

28. Muñoz-Núñez C, Hevilla V, Zágora J, Plachá D, Muñoz-Bonilla A, and Fernández-García M. Functionalization of Chitosan-Chitin Nanowhiskers Films By Impregnation With Essential Oils Via Supercritical CO2. J Polym Environ. 2025;33(1):96–111.

29. Guo S, Li T, Chen M, Wu C, Ge X, Fan G, Li X, Zhou D, Mi L, Zhao X, *et al*. Sustainable and effective Chitosan-based edible films incorporated with OEO nanoemulsion against apricots' black spot. Food Control. 2022;138:108965.

30. Sayadi M, Abedi E, and Oliyaei N. Effect of Persian gum-gelatin based-pickering emulsion film loaded with Thyme essential oil on the storage quality of Barred mackerel (*Scomberomorus commerrson*) fillet. LWT. 2025;215:117241.

31. Norcino LB, Mendes JF, Natarelli CVL, Manrich A, Oliveira JE, and Mattoso LHC. Pectin films loaded with copaiba oil nanoemulsions for potential use as bio-based active packaging. Food Hydrocoll. 2020;106:105862.

32. Gharibi S, Tabatabaei BES, and Saeidi G. Comparison of Essential Oil Composition, Flavonoid Content and Antioxidant Activity in Eight *Achillea* Species. J Essent Oil Bear Plants. 2015;18(6):1382–94.

33. Shen Z and Kamdem DP. Development and characterization of biodegradable chitosan films containing two essential oils. Int J Biol Macromol. 2015;74:289–96.

34. Çoruhlu P, Rayman Ergün A, and Baysal T. Characterization of chitosan films incorporating thyme oil and its effect on black olives. Ital J Food Sci. 2025;37(1):307–18.

35. Ferreira RR, Souza AG, and Rosa DS. Essential oil-loaded nanocapsules and their application on PBAT biodegradable films. J Mol Liq. 2021;337:116488.

36. Al-Ali RM, Al-Hilifi SA, and Rashed MMA. Fabrication, characterization, and anti-free radical performance of edible packaging-chitosan film synthesized from shrimp shell incorporated with ginger essential oil. J Food Meas Charact. 2021;15(4):2951–62.

37. Lian H, Shi J, Zhang X, and Peng Y. Effect of the added polysaccharide on the release of thyme essential oil and structure properties of chitosan based film. Food Packag Shelf Life. 2020;23:100467.

38. Almasi L, Radi M, Amiri S, and McClements DJ. Fabrication and characterization of antimicrobial biopolymer films containing essential oil-loaded microemulsions or nanoemulsions. Food Hydrocoll. 2021;117.

39. Ghani S, Barzegar H, Noshad M, and Hojjati M. The preparation, characterization and in vitro application evaluation of soluble soybean polysaccharide films incorporated with cinnamon essential oil nanoemulsions. Int J Biol Macromol. 2018;112:197–202.

40. Zehra A, Wani SM, Jan N, Bhat TA, Rather SA, Malik AR, and Hussain SZ. Development of chitosan-based biodegradable films enriched with thyme essential oil and additives for potential applications in packaging of fresh collard greens. Sci Rep. 2022;12(1):16923.

41. Kanatt SR. Development of active/intelligent food packaging film containing Amaranthus leaf extract for shelf life extension of chicken/fish during chilled storage. Food Packag Shelf Life. 2020;24:100506.

42. Amiri H. Essential oils composition and antioxidant properties of three thymus species. Evidence-based Complement Altern Med. 2012; 2012.

43. Elsherief MF, Devecioglu D, Saleh MN, Karbancioglu-Guler F, and Capanoglu E. Chitosan/alginate/pectin biopolymer-based Nanoemulsions for improving the shelf life of refrigerated chicken breast. Int J Biol Macromol. 2024;264:130213.

44. Kamkar A, Molaee-aghaee E, Khanjari A, Akhondzadeh-basti A, Noudoost B, Shariatifar N, Alizadeh Sani M, and Soleimani M. Nanocomposite active packaging based on chitosan biopolymer loaded with nano-liposomal essential oil: Its characterizations and effects on microbial, and chemical properties of refrigerated chicken breast fillet. Int J Food Microbiol. 2021;342:109071.

45. Sheerzad S, Khorrami R, Khanjari A, Gandomi H, Basti AA, and Khansavar F. Improving chicken meat shelf-life: Coating with whey protein isolate, nanochitosan,

bacterial nanocellulose, and cinnamon essential oil. LWT. 2024;197:115912.

46. Moadab FR and Azizkhani M. The Effect of Chitosan Edible Coating Containing Nanoemulsion of <scp> *Eryngium campestre* </scp> Essential Oil on the Quality of Ostrich Meat During Storage in Refrigerator. Food Sci Nutr. 2025;13(5).

47. Karam L, Roustom R, Abiad MG, El-Obeid T, and Savvaidis IN. Combined effects of thymol, carvacrol and packaging on the shelf-life of marinated chicken. Int J Food Microbiol. 2019;291:42–7.

48. Kiprotich S, Mendonça A, Dickson J, Shaw A, Thomas-Popo E, White S, Moutiq R, and Ibrahim SA. Thyme Oil Enhances the Inactivation of *Salmonella enterica* on Raw Chicken Breast Meat During Marination in Lemon Juice With Added *Yucca schidigera* Extract. Front Nutr. 2021;7.

49. Gholami-Ahangaran M, Ahmadi-Dastgerdi A, Azizi S, Basiratpour A, Zokaei M, and Derakhshan M. Thymol and carvacrol supplementation in poultry health and performance. Vet Med Sci. 2022;8(1):267–88.

50. Wang W, Zhao D, Xiang Q, Li K, Wang B, and Bai Y. Effect of cinnamon essential oil nanoemulsions on microbiological safety and quality properties of chicken breast fillets during refrigerated storage. LWT. 2021;152:112376.

51. Noori S, Zeynali F, and Almasi H. Antimicrobial and antioxidant efficiency of nanoemulsion-based edible coating containing ginger (*Zingiber officinale*) essential oil and its effect on safety and quality attributes of chicken breast fillets. Food Control. 2018;84:312–20.

52. Wang X, Wang Z, Zhuang H, Nasiru MM, Yuan Y, Zhang J, and Yan W. Changes in color, myoglobin, and lipid oxidation in beef patties treated by dielectric barrier discharge cold plasma during storage. Meat Sci. 2021;176:108456.

53. Bleicher J, Ebner EE, and Bak KH. Formation and Analysis of Volatile and Odor Compounds in Meat—A Review. Molecules. 2022;27(19):6703.

54. Y. Youssef D. Assessment of the Impact of Rosemary Chitosan Microemulsion Effect on *Escherichia coli* and *Listeria monocytogenes* Dipping in Chicken Meat Stored at 4˚C. Int J Agric Biol. 2022;27(01):69–76.

55. Khorshidi S, Mehdizadeh T, and Ghorbani M. The effect of chitosan coatings enriched with the extracts and essential oils of *Elettaria Cardamomum* on the shelf-life of chicken drumsticks vacuum-packaged at 4 °C. J Food Sci Technol. 2021;58(8):2924–35.

56. Xiang H, Liao J, Tang Y-T, Wen P, and Wang H. Development of cinnamon essential oil-loaded core-shell nano film for the preservation of chilled flesh foods. Food Packag Shelf Life. 2024;45:101310.

57. Hussain SA, Wani SA, Rafeh S, Adil S, Sofi AH, Ghamry HI, and Wani M. Enhancing Meat Emulsion Quality and Storage Stability During Refrigeration Using Thyme and Oregano Essential Oil Nanoparticles. Foods. 2025;14(6):1076.

Cite this article as: Bhattacharya D, Kumar D, Kumar PP, Kumar A, Das A, Karunamay S, Prakash KS, Das AK, Chaubey M, Ghosh M. Chitosan film with thyme nanoemulsion (*Thymus vulgaris* L.) : A sustainable approach for meat preservation. Explor Anim Med Res. 2026; 16(1), DOI: 10.52635/eamr/16.1.116-129.

Explor Anim Med Res.
Vol. 16, Issue 1, 2026
DOI: 10.52635/eamr/16.1.130-139

ISSN 2277-470X (Print), ISSN 2319-247X (Online)
Website: www.animalmedicalresearch.org

Published under the CC BY-NC 4.0 license

Research Article

IDENTIFICATION OF PRIMORDIAL GERM CELLS IN EARLY PHEASANT (*PHASIANUS COLCHICUS*) EMBRYO

Entekhab Hameed Abed Al-Shuwaili [1,2], Azam Hosseini [1], Abolghasem Nabipour[1]

Received 7 June 2025, revised 27 April 2026

ABSTRACT: The aim of this study is identification of primordial germ cells during their circulation in the blood stream and migration to the primary gonads in pheasant embryo. The blood was taken from stages 14-17 and genital ridge tissue was taken from stages 20-21 Hamburger & Hamilton. Primary gonads were acquired from stages 28-30 Hamburger & Hamilton. Primordial germ cells have been recognized by using histochemical and immunostaining methods. The current article specified that these cells are distinguishable based on their relatively large size, large nuclei and cytoplasm with defined boundaries. In blood smear, such cells were negative for alkaline phosphatase, while the circulating primordial germ cells were negative for stage-specific embryonic antigen-1 (SSEA-1). Further, the Periodic Acid-Schiff staining was negative or very weak. These cells showed a very weak or negative reaction to staining with Alcian blue. At stages 20-30 Hamburger & Hamilton, primitive germ cells might not be distinguished by alkaline phosphatase and SSEA-1 immunostaining. Alcian blue and Periodic Acid-Schiff staining was either negative or very weak in these cells. According to the results of this study, primordial germ cells in all stages showed very weak or negative reactions to different histochemical and immunostaining techniques. We recommend that the use of routine hematoxylin and eosin staining yields better results for primordial germ cells identification.

Keywords: Germ cells, Immunohistochemistry, Alkaline phosphatase, Identification.

INTRODUCTION

The cells that produce spermatogonia or oogonia are known as primordial germ cells (PGCs). These cells arise from the epiblast within the central area of the blastoderm (area pellucida). As the primitive streak forms, these cells migrate to the anterior extra-embryonic region known as the germinal crescent. Following vascularization, PGCs enter the bloodstream and travel to the genital ridges, where they settle and contribute to gonad formation [1, 2]. PGCs are germline stem cells and are beneficial in the genetic information transfer between generations [3, 4]. Depending upon signals from their circumstance, PGCs differentiate into gametes of either sex [5]. In the ostrich, turkey and chick embryo, the primordial germ cells have been recognized by large nuclei, large size, and cytoplasmic granules [6, 7, 8]. The cells were recognized by several methods such as: histochemical staining, immunohistochemistry and enzyme histochemistry [alkaline phosphatase (ALP)]. Periodic Acid-Schiff (PAS) staining is a standard technique for detecting polysaccharides, such as glycogen, in cells and tissues. Immunohistochemistry staining is used to detect cell-surface antigens in various tissues [8]. Also, ALP known as an important diagnostic technique that could be used for identification of embryonic stem cells and PGCs [9]. The antibody against stage-specific embryonic antigen (SSEA1) is used to recognize PGCs in different species [10, 11, 12]. Researchers found that PGCs can generate germline chimeric chickens in laboratory conditions. These cells migrate toward blood vessels at stage 11-12 H&H, peak at stage 14 H&H, and decline at stage 18H&H, making stage 12-17 H&H (45h-64h of incubation) the optimal time for their isolation. [2, 13]. Although pheasants are an important economical species [14], but there are very few studies on pheasant embryos. In order to study primordial germ cells, they require special stains and methods to be distinguished from other embryonic cells. PGCs derived from a variety of the embryonic tissues are characterized and

[1]*Department of Basic Sciences, Faculty of Veterinary Medicine, Ferdowsi University of Mashhad, Mashhad, Iran*
[2]*Department of Biology, College of Education for Pure Science ibn Al-Haitham, University of Baghdad, Iraq*
**Corresponding Author. e-mail: nabipour@um.ac.ir*

examined afterwards by using a specific antibody, ALP and other histochemical techniques. Therefore, this study aimed to identify primordial germ cells in pheasant using histochemical and immunohistochemical techniques and to determine which method provides the most accurate detection.

MATERIALS AND METHODS

Fertile pheasant (*Phasianus colchicus*) eggs (28 eggs) were collected from commercial poultry farm. The eggs were placed in an incubator. During incubation, optimal conditions were maintained at 37˚C and 60% humidity, and the eggs were rotated at one-hour intervals.

Separation of embryos

At the end of the incubation period for each stage (stage 14-17, stage 20-21 and stage28-30 H&H), the eggs were removed from the incubator, and placed under a stereomicroscope. Then, the eggshell was cut at the location of the embryo and the embryonic stages were determined using the Hamburger and Hamilton (H&H) criteria [15]. At stage 14-17 H&H, with Using a fine heparinized glass needle, blood samples were obtained from extraembryonic vessels and, in some cases, the dorsal aorta (Monoject scientific, Ireland). After that, blood samples were mixed with phosphate buffer saline (PBS) to maintain an isotonic environment and to prepare a uniform cell suspension on the slide. The blood sample, previously diluted with PBS, placed on slides with adhesive coating (Poly-L-lysine). The blood smears were directly treated with paraformaldehyde solution (PFA), 4% in PBS. The slides were washed with PBS and allowed to dry at the room temperature. They have been stored in PBS at 4^{o}C for upcoming usage.

The stages 20-21 H&H (3.5-4 days of incubation) and stages 28-30 H&H (6-7 days of incubation) eggs were opened as described earlier. The embryos were taken from the yolk then embedded in 4% PFA for 24 h at 4^{o}C. Some embryos immediately immersed in Gender's fixative and fixed for 8 hours at room temperature. Gender's fixative (alcoholic bouin's fluid) was employed to more effectively preserve glycogen particles within the cells [16]. After fixation, the embryos were washed with 80% ethanol. The embryos were dehydrated in series of ascending ethanol, cleared in xylene and embedded in paraffin. 5 µm thick paraffin sections were obtained with a rotary microtome (Leica RM 2145; Germany). The sections were photographed on an BX-51 light microscope with digital Olympus camera (DP-12) after histochemical and immunohistochemical staining.

Immunohistochemical staining

For immunohistochemistry, paraffin sections were dewaxed, hydrated in an ethanol series and washed in phosphate buffered saline (PBS). The sections were incubated with 0.30% H_2O_2 in PBS at room temperature for 15min to block any endogenous peroxides. then, the slides formerly washed with PBS. A 10% bovine serum albumin in PBS was prepared. Tissue sections and blood smears were incubated in it in a humid chamber. Slides were incubated with the primary antibody SSEA-1 (R&D; US), followed by a donkey anti-mouse IgM secondary antibody conjugated to horseradish peroxidase (Jackson Immunoresearch, US). Concentration 1:300 was used for the primary antibody overnight at 4^{o}C and the secondary antibody was used at a concentration of 1:500 for one hour at room temperature. After washing with PBS, peroxidase label was revealed by reaction with Diaminobenzidine (DAB) for 5 min at room temperature. The sections were counterstained with hematoxylin and mounted using Entellan (Merck; Germany). Negative controls were prepared by omitting the primary antibodies [7,17].

Alkaline phosphatase staining

Tissue sections were deparaffinized and hydrated by graded alcohol series. Sections and blood smears were incubated for 30 min at room temperature in ALP substrate solution (stock 5% BCIP in 100%. Dimethylformamide (33µl), stock 5% NBT in 70% Dimethylformamide (66µl) and 10ml of buffer substrate. Deionized water was utilized in order to wash the slides. Lastly, the sections were dehydrated and then mounted by using Entellan. BCIP: Bromo-4-Chloro-3-indolyphosphate (Thermo scientific; USA), NBT: Nitro-blue tetrazolium chloride (Thermo scientific; USA) and the buffer substrate consisted of 10 mM NaCl (Merck; Germany), 5 mM Magnesium chloride ($MgCl_2$) (Merck; Germany) and 100 mM hydroxymethyl aminomethane (Sigma Aldrich-TM; USA) with PH 9.5 [7,17].

Paraffin sections were stained with hematoxylin and eosin (H&E), PAS and Alcian blue stains. PAS and Alcian blue stains detect glycogen granules and acidic mucosubstances, respectively, in the cytoplasm [18].

RESULTS AND DISCUSSION

The pheasant PGCs at stages14-17 of H&H had a large and eccentric nucleus which occupied the majority of cytoplasm (Fig. 1A). These cells in blood slides were not stained with SSEA-1 antibody, and the reaction was negative (Fig. 1B, 1C), despite that, PGCs were easily diagnosed. The cells appeared spherical, containing a

large compact nucleus and a terminal site, and could be differentiated from light/pale blood cells (Fig. 1B). Some PGCs were imaged during division (Fig. 1D), and some appeared in clusters (Fig. 1E). PGCs did not react to ALP staining. These cells, after ALP staining, appeared clear, with a brown cytoplasm, with the nucleus lighter than the cytoplasm (Fig. 1F). Results of PAS (Fig. 1G) and Alcian blue staining (Fig. 1H) were also negative or weak, while the cytoplasm and nucleus showed blue and white color, respectively.

Detection of PGCs in genital ridge

During the formation of genital ridge, PGCs were observed in a migratory state. These cells were placed

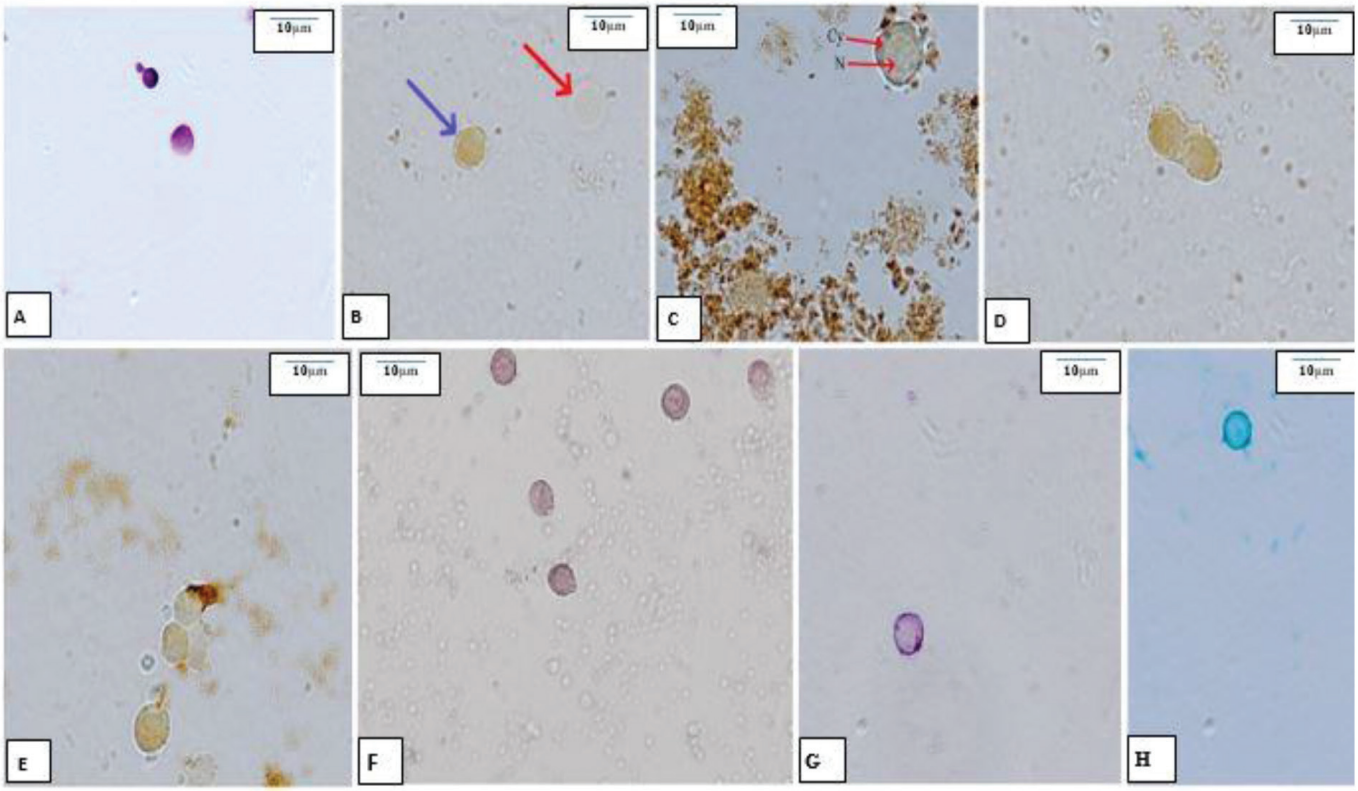

Fig. 1. Photomicrograph of blood smear from stage (14-17 H&H) pheasant embryo (1000×). A) PGCs stained with H&E, **B**) PGCs treated with SSEA1 antibody (blue arrow), blood cell (red arrow), **C**) PGCs stained with SSEA1 antibody demonstrate nucleus (N), cytoplasm (Cy), **D**) PGCs in division state, **E**) clusters of PGCs stained with SSEA1 antibody, **F**) ALP activity, **G**) PAS stain, **H**) Alcian blue stain.

inside the blood vessels of the embryo or attached to the vessel wall (Fig. 2A). Also, by using H&E, it was possible to distinguish the difference in shape between the primordial germ cells in the migratory state, which had dark pink nuclei (Fig. 2B), and white nuclei in the genital ridge in stage 20 H&H (Fig. 2C). The PGCs could easily be detected by examining the paraffin sections stained with H&E. These cells were larger than the mesenchymal cells, had a large white and compact nucleus occupying most of the cell volume, and a narrow cytoplasm appeared pink at both stages 20 (Fig. 2C) and 21 H&H (Fig. 2D). It was noticed that the genital ridge in stage 21 H&H was thicker than in stage 20 H&H, possibly due to the accumulation of PGCs at stage 21 H&H (Fig. 2D).

The majority of the primordial germ cells migrated through dorsal mesentery in order to reach the genital ridge. They could be observed using different staining methods. In this study, they were observed in tissue sections stained with hematoxylin and eosin (Fig. 3A), as well as SSEA-1 immunolabeling (Fig. 3B). Although the reaction was negative with SSEA1, the shape of the cells helped in their diagnosis. During migration toward and within the genital ridge, primordial germ cells displayed a negative reaction to SSEA-1 immunostaining at both 20 (Fig. 3C) and 21 H&H (3D) stages. At stages 20-21 H&H, the pheasant PGCs showed a negative reaction with the alkaline phosphatase enzyme (Fig. 3E and 3F). Histological specimen of liver from chick with one-day-old were

utilized as negative control for enzyme histochemistry method (ALP staining) through revealing them to a 60°C temperature for 1 hr without straining the nucleus (Fig. 3G). The liver from the similar stage was utilized as well for the ALP enzyme staining as a positive control (Fig. 3H). PGCs in pheasant embryos at 20-21 stages of H&H stained with Alcian blue (Fig. 3I and 3J) and PAS stains (Fig. 3K and 3L) showed a weakly positive or negative reaction. Histological samples of ovine trachea were utilized as a positive control for Alcian blue stain (Fig. 3M) and PAS stains (Fig. 3N).

Detection of PGCs in the primary gonad

At stages 28, 29 and 30 H&H, the gonads were formed on the ventromedial surface of the mesonephros. In the current work, in the transverse sections, the gonads formed two ovals or circular structures (Fig. 4A, 4B, and 4C). The PGCs settled in the area could be easily differentiated from gonad mesenchymal cells by their phenotypic characteristics mentioned in the previous stages. In H&E staining, the cells might be easily recognized by their white nucleus, big size, and pink cytoplasm (Fig. 4D, 4E, and 4F). In the slides stained with anti-SSEA1 antibody, the PGCs in all stages had been negative (Fig. 4G, 4H, and 4J), while only in some cases did, they react very weakly (Fig. 4G and 4I). These cells, had no positive staining with the SSEA-1 but, were easily distinguished by their morphology. PGCs were spherical, large size with large nucleus that lodging the majority of cytoplasm. A number of slides were prepared from chick embryo gonad samples and had been utilized as positive control for the SSEA1 antibody. Germ cells at this stage countered positively to SSEA-1 staining (Fig. 4K). The similar stage had also been utilized as negative control by neglecting primary antibody and using only the secondary antibody (Fig. 4L). The PGCs in stages 28, 29, and 30 H&H, were negative or weakly positive with PAS staining (Fig. 4M, 4N, and 4O). In the embryo of stages 28, 29, and 30 H&H, the PGCs reacted negatively with alkaline phosphatase enzyme (Fig. 4P, 4Q, & 4R). In entirely three embryonic stages, primordial germ cells displayed negative or very weak reaction with Alcian blue (Fig. 4S, 4T, and 4U).

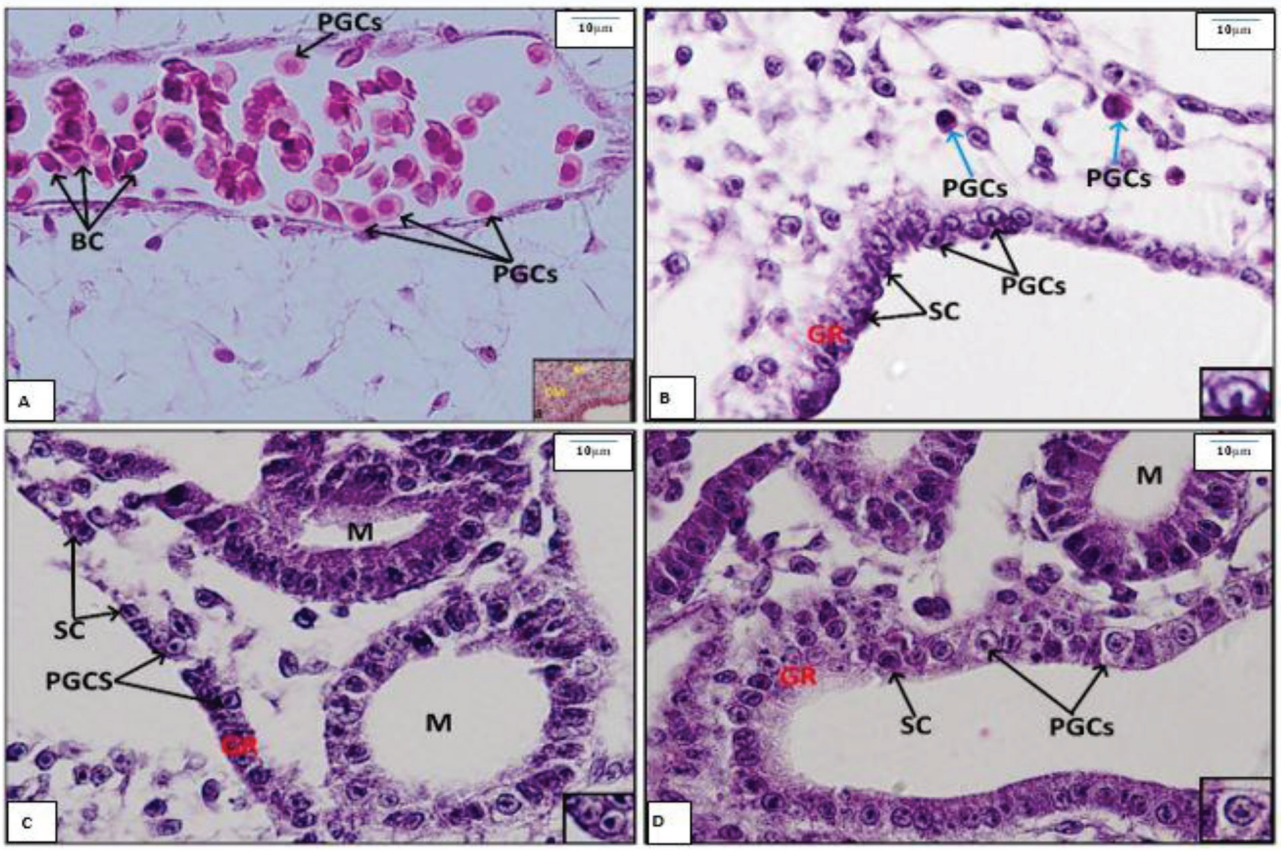

Fig. 2. Identifying the pheasant PGCs, migration toward the genital ridge at stage 20-21 H&H (1000×). A) PGCs in dorsal aorta and some of PGCs adhered to the wall of the dorsal aorta, or in dorsal mesentery (a). **B**) PGCs migrate from blood vessel to genital ridge (blue arrows), **C**) PGCs in genital ridge of stage 20 H&H, **D**) stage 21 H&H (D). Genital ridge (GR), primordial germ cell (PGCs), somatic cells (SC), mesonephros (M), dorsal mesentery (DM). H&E stain.

The transfer of PGCs between embryonic blood vessels represents a common approach for establishing germline chimeric [18, 19]. The chromosomal sex and germ cell competition's role in differentiating avian germ cells was studied by [20]. In the past, methods of freezing eggs were used to preserve embryos, which was an impractical method. At present, the freezing of primordial germ cells allows preserving the offspring of male and female animals [21]. The process by which primordial germ cells enter blood vessels is similar to that occurs during the inflammation and the movement of lymphocytes to the sites of inflammation and tumor [22, 23]. PGCs in birds have an epiblastic origin [1]. They migrate through blood vessels, enter the dorsal mesentery, and reach the genital ridges. At stage 17 H&H, they settle down in the genital ridges [8], where they finally differentiate into oogonia or spermatogonia [1, 2]. Germ cells can be observed in the bloodstream from stage 10 onward [24]. They are characterized by being migratory cells, the origin and migration of which are important topics that have attracted the attention of researchers [25]. The PGCs concentration in the bloodstream reaches its peak at stage 14 H&H and then begins to decline at stage 15 H&H because of the presence of PGCs in the network of capillaries that supply the gonads [26]. Histochemical and immunohistochemical staining facilitate cell detection, as PAS staining is widely recognized as an effective

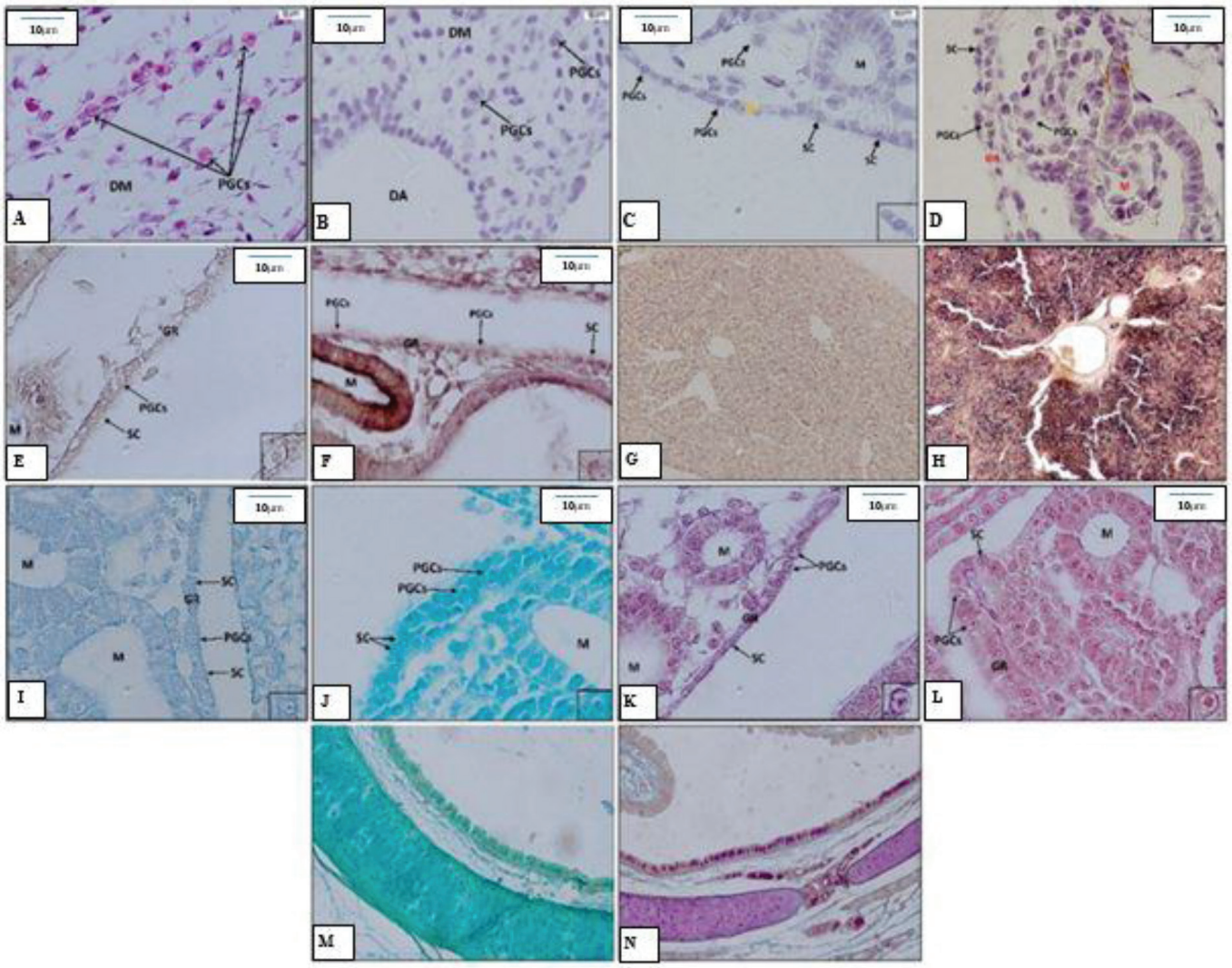

Fig. 3. Identifying the pheasant PGCs, migration toward the genital ridge at stage 20 (C, E, I, K), and stage 21 H&H (D, F, J, L). A) Some of the PGCs seen in dorsal mesentery by using H&E stain (1000×), **B**) SSEA-1 antibody (1000×), **C, D**) The PGCs were identified by SSEA-1 antibody (1000×), **E, F**) ALP activity (1000×), **G**) ALP negative control (100×), **H**) ALP positive control (400×), **I, J**) Alcian blue stain (1000×), **K, L**) PAS stain (1000×), **M**) Alcian blue control (400×), **N**) PAS stain control (100×). Primordial germ cells (PGCs), somatic cells (SC), dorsal mesentery (DM), dorsal aorta (DA), genital ridge (GR), mesonephros (M).

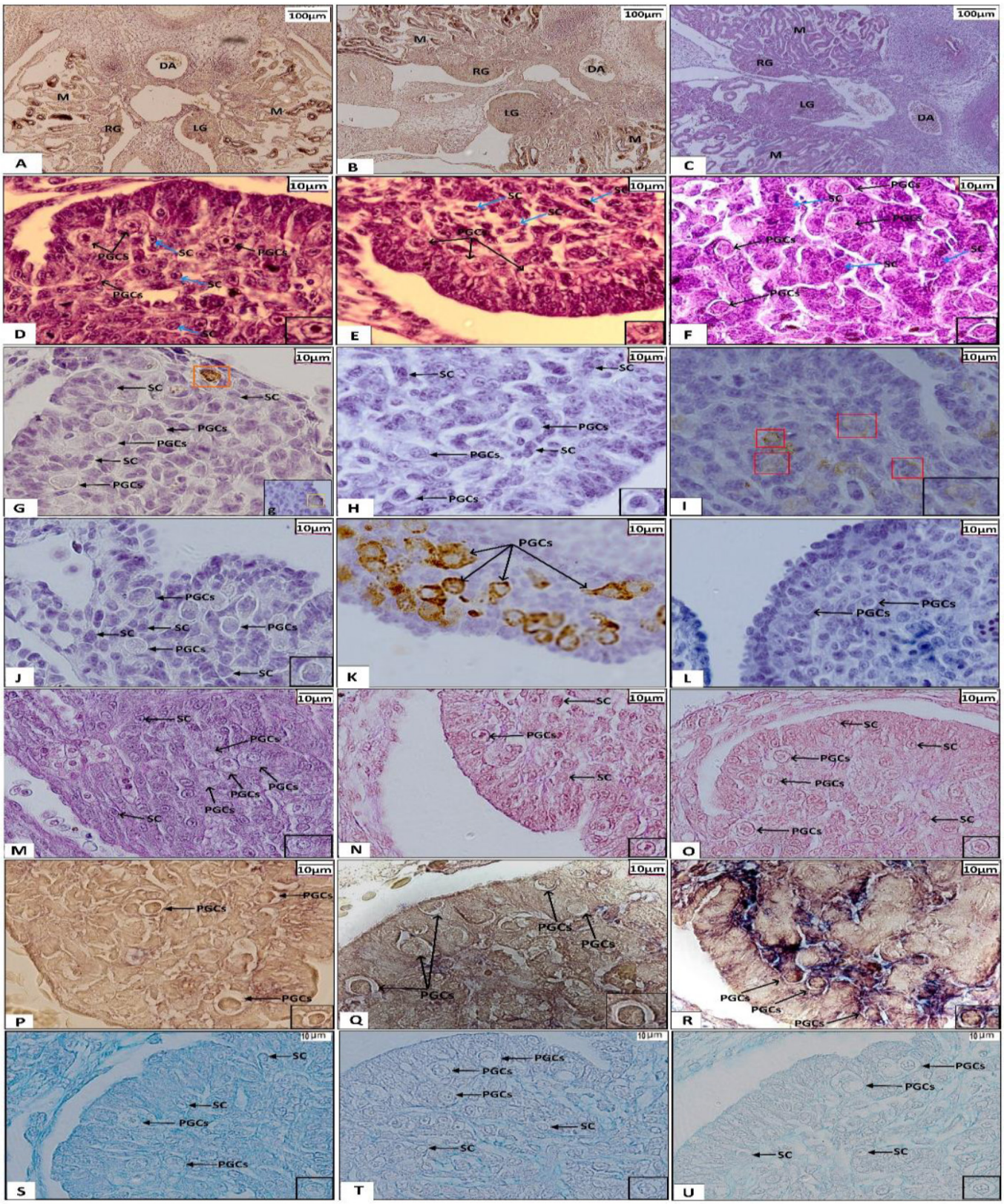

Fig. 4. Identifying the pheasant PGCs in the primary gonad. **A, B, C**) Site of gonads inside body in stages 28-30 H&H (100×), **D, E, F**) the PGCs were identified by H&E (1000×), **G, H, I, J**) SSEA-1 antibody (1000×), **M, N, O**) PAS stain (1000×), **P, Q, R**) ALP activity (1000×), **S, T, U**) Alcian blue stain (1000×), **K**) SSEA-1 positive control of chick embryo (1000×), **L**) SSEA-1 negative control of chick embryo (1000×). Primordial germ cells (PGCs), somatic cells(SC), PGCs weak reaction with SSEA-1in stage28-29 H&H (A, C), left gonad (LG), right gonad (RG), dorsal aorta (DA), mesonephros (M).

method for differentiating PGCs from surrounding cells [27]. The PGCs are demonstrated to contain abundant glycogen by the PAS reaction [24]. England and Matsumura showed the PGCs in chicks to be distinguished in the germinal crescent by the PAS stain [28]. Reported that PGCs in blood smear and genital ridge of turkey embryo were PAS-positive because the PGCs contain high glycogen granules in turkey embryo (*Meleagris gallopavo*) [7]. While chicken and turkey PGCs contain glycogen and can be detected with the PAS stain, pheasant cells have very little glycogen. This may indicate that the aldehyde groups or carbohydrates in pheasant PGCs are very low or negligible and therefore, the PAS method is less effective for identifying PGCs in pheasants [7, 29, 30]. At stages 20-21 H&H of the chick embryo, observed that PGCs were settled in the genital ridge and these cells have been localized within the mesenchyme [31]. The present study showed that PGCs in pheasant embryos from stage 20-21 H&H were found in genital ridge, as well as the dorsal mesentery and blood vessels. PAS stain is a promising approach to identifying PGCs in blood smears and paraffin slices of the primitive gonad of an ostrich embryo [6]. PGCs in the blood and genital ridge of chick embryos were investigated using the PAS stain by [13, 32]. The present study's findings in pheasant embryos differ from those reported in chick embryos. PAS staining and anti SSEA-1 antibodies are routinely employed to identify chicken PGCs [8, 24]. Somatic cells are PAS-negative, and germ cells are PAS-positive since PGCs have a high glycoprotein content. Further, PAS technique is utilized for demonstrating the neutral mucins [33]. In the present study, PGC reactivity to PAS has been too weak to clearly detect PGCs, due to the absence or decreased amount of glycogen in the cytoplasm of pheasant PGCs. The findings of this study are inconsistent with those reported by Naeemipour & Bassami, and contradict the results reported by Meyer [17, 34]. A histochemical method was developed for detecting proteoglycans and acidic carbohydrates using Alcian blue-silver staining by [35]. According to [11], the ovomucin-like protein (OLP), cell surface mucin, on migrating chick and rat PGCs enhances the cells broad migration to vaginal ridges by blocking adherence of PGCs to the walls of blood vessel and mesenchyme. Alcian blue has been used to demonstrate various kinds of acid glycoconjugates and sulfomucins [36]. Sulfomucins are a subclass of mucins characterized by a high content of sulfate groups and play an important role in histopathological evaluations. Alcian Blue selectively interacts with the sulfated moieties of sulfomucous secretions, enabling the identification of cells that produce these mucins in abundance. In addition, the combined application of Alcian Blue and PAS staining provides a valuable diagnostic approach for differentiating cell types and tissue structures based on their specific mucin secretion profiles [16, 35, 36]. In this study, an Alcian blue stain was used to prove if the cells contain mucosubstances sulfomucins in PGCs. The present study agrees with [37] but disagrees with [7]. Since these cells are migratory, cell migration could result in an alteration in cellular parts containing carbohydrates which may be a reason why cells show no positive reaction with PAS and Alcian blue. According to [38], once the PAS and Alcian blue stain were used, the germ and epithelial cells in the right ovary in chicken embryos showed more intense reaction than in the left ovary. The reason was attributed to the increase of materials in mucinous in the advanced stages of the formation of the gonads, playing a vital role in cell migration. SSEA-1 is antigenic epitope on the cell surface that is deployed as a specific antibody for stem cell detection [24]. Other researchers identified PGCs using SSEA-1 and EMA-1 [39]. There are numerous disagreements about the SSEA-1 marker; certain articles consider SSEA-1 a PGCs marker, while others view it a pluripotency marker. PGCs are easily recognized utilizing monoclonal antibody SSEA-1[40]. In this study, the SSEA-1 was negative in PGCs of a blood smear, the same result was detected by [41] and [6]. In the current

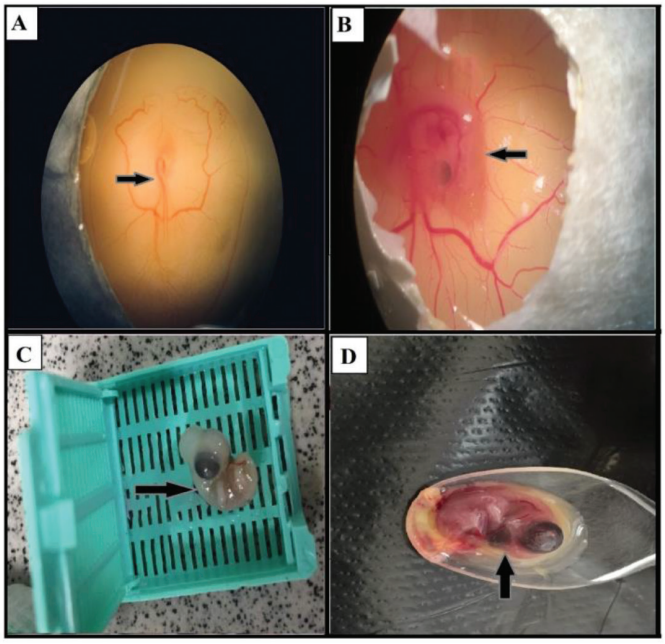

Fig. 5. Photograph of Pheasant embryos at four developmental stages. A) Pheasant embryo at stage 15 H&H, **B**) stage 21 H&H, **C**) stage 28 H&H, **D**) stage 30 H&H. Black arrows in all panels indicate the embryo.

research, the pheasant PGCs were SSEA-1 negative at stage 20-21 H&H and was very weak or negative in PGCs of gonad at stages 28, 29, and 30 H&H. These results disagree with previous studies [7, 42, 43]. Some researchers reported that, PGCs from the Chinese Meiling chicken were SSEA-1 positive. Previous studies show that, SSEA1 has not been detected during the cleavage and gonadal ridge stages in the bovine embryo [10]. In the turkey embryo, primordial germ cells that migrate to genital ridge at stage 20 H&H did not express SSEA1 epitope; however, an SSEA-1 positive reaction could be detected in PGCs of chick embryo after they settled in the gonad [44]. The current research is in line with those mentioned above in that the PGCs in pheasants are incapable of expressing the SSEA1 epitopes, and with the help of this method, PGCs are not identified, although a very weak reaction of cells appears in the 28th and 29th stage. The reasons behind the negative results of identifying PGCs with SSEA-1 in the pheasant are unclear. The absence of SSEA-1 marker expression in pheasant PGCs may indicate that these cells are intrinsically unable to express this marker, suggesting that their cell type dose not correspond to SSEA-1- positive profiles. This could be due to species-specific differences between chicken and pheasant. ALP enzyme expression appears in many cells, like the osteoblasts and odontoblasts, as well as in undifferentiated embryonic stem cells and pluripotent stem cells; its enzymatic activity indicates differentiation in cells [45]. The cytoplasm of PGCs differs from somatic cells in that alkaline phosphatase activity (enzymatic properties) is higher in PGCs [46]. In zebra fish, the PGCs show a high alkaline phosphatase activity in peripheral cytoplasm [47]. During passive and active migration phases, ALP has been shown to play a vital part in enzymatic activity [48]. In this article, in blood, the PGCs were not detected by ALP; a different finding was reported in turkey and chicken PGCs [7, 24]. In the genital ridges and primary gonads in the pheasant embryo, the PGCs did not react positively with the ALP enzyme. The findings in this study agree with those in the turkey and chicken embryo but inconsistent with the study of Swarts in chickens [7, 17, 48]. The reason may be the change in the metabolic activities of PGCs or the synthesis of alkaline phosphatase [48].

CONCLUSION

Primordial germ cells in blood smear showed a negative reaction with alkaline phosphatase, and circulating PGCs in the blood were negative for SSEA-1. The PAS staining has been negative or very weak. These cells showed a very weak or negative reaction to staining with Alcian blue. At stages20-30 H&H, primitive germ cells cannot be distinguished by alkaline phosphatase, and cannot be detected by SSEA-1 immunostaining. Those cells showed negative or very weak staining with Alcian blue and PAS. The results of this study showed that PGCs in all stages studied had very weak or negative reactions to different histochemical and immunostaining techniques. Conventional H&E staining provides a reliable method for the microscopic identification of these cells. Morphologically, pheasant PGCs resemble those of birds; however, species-specific differences led to negative reactions in histochemical and immunohistochemical staining.

ACKNOWLEDGEMENT

The authors gratefully acknowledge the support of the research council of the Ferdowsi University of Mashhad for this study. (Grant No. 3/49497)

ETHICAL APPROVAL

All experiments were approved by the Ethics Committee of Ferdowsi University of Mashhad (IR. UM.REC.1399.136).

REFERENCES

1. Barton L, Roa-de la Cruz L, Lehmann R, Lin B. The journey of generation: advances and promises in the study of primordial germ cell migration. Dev. 2024; 151(7): 1-19, Doi: 10. 1242/dev.201102.

2. Altgilbers S, Klein S, Diedrks C, Weigend S, Kues WA. Cultivation and characterization of primordial germ cells from blue layer hybrids (*Araucana crossbreeds*) and generation of germline chimeric chickens. Sci Rep. 2021; 11: 1-12, Doi: 10.1038/s41598-021-91490-y.

3. Porras-Gómez TJ, Villagrán-SantaCruz M, Moreno-Mendoza N. Biology of primordial germ cells in vertebrates with emphasis in urodeles amphibians. Mol Rep Dev. 2021; 88(12): 773-792, Doi: 10. 1002/ mrd.23533.

4. Cheng H, Shang D, Zhou R. Germline stem cells in human. Signal Transduct Target Ter. 2022: 1-22, Doi: 10.1038/s41392-022-01197-3.

5. Mizushima Sh, Ogawa Y, Kuroiwa A. Initial formation of and sex differences in primordial germ cells in Japanese quail. Reprod Biol. 2024; 24(3): 1-5, Doi: 10.10.1016/j. repbio.2024.100922.

6. Hassanzadeh B, Nabipour A, Dehghani H. Ostrich (*Struthio camelus*) primordial germ cells in embryonic

blood and presumptive gonad: characterization by PAS and immunohistochemistry. Iran J Vet Res. 2019; 20(4): 299-303.

7. Hosseini A, Nabipour A, Dehghani H. Characterizing primordial germ cells in the turkey (*Meleagris Gallopavo*) embryo. Anat Sci J. 2020;17(2): 63-72.

8. Szczerba A, Kuwana T, Bednarczyk M. Concentration and total number of circulating primordial germ cells in green –legged partidgelike chicken embryos. Poult Sci. 2020; 100(1): 319-324, Doi: 10.1016/j.psj.2020.08.016.

9. Liu CH, Ma Z, Cai Z, Zhang F, Liu Ch, Chen T, Peng D, Xu X, Lin H. Identification of primordial germ cell-like cell as liver metastasis initiating cells in mouse tumor models. Cell Dis. 2020; 6(15): 2-14, Doi: 10.1038/s41421-020-0145-3.

10. De Melo Bernardo A, Sprenkels K, Rodrigues G, Noce T, Chuva De Sousa Lopes SM. Chicken primordial germ cells use the anterior vitelline veins to enter the embryonic circulation. Biol open. 2012; 1(11): 1146-1152, Doi: 10.1242/bio.20122592.

11. Halfter W, Schurer B, Hasselhorn HM, Christ B, Gimpel E, Epperlein HH. An ovomucin-like protein on the surface of migrating primordial germ cells of the chick and rat. Dev. 1996; 122(3): 915-923, Doi:10.1242/dev.122,3.915.

12. Yön ND, Akbulut C. Identification of primordial germ cells: cytological, histological and immunohistochemical aspects. Hum Anim Health. 2015; 58(2): 115-121, Doi: 10.1590/s1516-8913201500335.

13. Tajima A, Hayashi H, Kamizumi A, Ogura J, Kuwana T, Chikamune T. Study on the concentration of circulating primordial germ cells (cPGCs) in early chick embryos. J Exp Zool. 1999; 284(7): 759-764, Doi:10.1002/(sici)1097-010x (19991201)284:7<759: aid-jez5>3.0.co;2-6.

14. Adamski M, Kuźniacka J. The effect of age and sex on slaughter traits of pheasants (*Phasianus colchicus L.*). Anim Sci Pap Rep. 2006; *24*(2): 11-18.

15. Hamburger V Hamilton HL. A series of normal stages in the development of the chick embryo. Dev Dyn. 1951;195(4): 231-272.

16. Culling CFA. A handbook of histopathological and histochemical techniques (3th edn), 1974; Oxford: Butterworth Heinemann. https://doi.org/10.1016/c2013-0-04011-x.

17. Naeemipour M, Bassami MR. Isolation, culture and characterization of chicken primordial germ cells. JCMR. 2013; 5(2): 48-53, Doi: 10.22067/JCMR.V512.24558.

18. Naito M, Harumi T, Kuwana T. Long-term culture of chicken primordial germ cells isolated from embryonic blood and production of germline chimeric chickens. Anim Reprod Sci. 2014; 153: 50-61, Doi: 10.1016/j.anireprosci.2014.12.003.

19. Sritabtim K, Prukudom S, Piyasanti Y, Chaipipat S, Kuwana T, Jurutha J, Sinsiri R, Tirawattanawanich Ch, Siripattarapravat K. First study on repeatable culture of primordial germ cells from various embryonic regions with giant feeder cells in Japanese quail (*coturnix japonica*). Theriogen. 2024; 213: 43-51, Doi: 10.1016/ j.theriogenology.2023.09.020.

20. Ballantyne M, Taylor L, Hu T, Meunier D, Nandi S, Sherman A. Avian primordial germ cells are bipotent for male or female gametogenesis. Front Cell Dev Biol. 2021; 9: 101-111, Doi: 10.3389/fcell.2021.726827.

21. Chaipipat S, Prukudom S, Sritabtim K, Kuwana T, Piyasanti Y, Sinsiri R, *et al.* Primordial germ cells isolated from individual embryos of red jungle fowl and indigenous pheasants of Thailand. Theriogenol. 2021; 165: 59-68, Doi: 10.1016/j.theriogenology.2021.02.010.

22. Alsayed YH, Ngo J, Runnels X, Leleu UK, Singha CM, Pitsillides JA, *et al*. Mechanisms of regulation of CXCR4/SDF-1 (CXCL12)–dependent migration and homing in multiple myeloma. J Blood. 2007;109(7): 2708-2717, Doi:10.1182/blood-2006-07-035857.

23. Ueda Y, Yang K, Foster SJ, Kondo M, Kelsoe G. Inflammation controls B lymphopoiesis by regulating chemokine CXCL12 expression. J Exp Med. 2004; 199(1): 47-58, Doi: 10.1084/jem.20031104.

24. Fujimoto T, Ukeshima A, Kiyofuji R. The origin, migration and morphology of the primordial germ cells in the chick embryo. Anat Rec. 1976; 185(2): 139-153, Doi: 10.1002/ar.1091850203.

25. Pilato G, D'urso V, Viglianisi F, Sammartano F, Sabella G, Lisi O. The problem of the origin of primordial germ cells (PGCs) in vertebrates: historical review and a possible solution. Int J Dev Biol. 2013; 57(11-12): 809-819, Doi:10.1387/ijdb.120261gp.

26. Szczerba A, Kuwana T, Bednarczyk M. Concentration and total number of circulating primordial germ cells in Green-legged Partridgelike chicken embryos. Poult Sci. 2021; 100(1): 319-324, Doi: 10.1016/j.psj.2020.08.016.

27. Chojnacka-Puchta L, Kasperczyk K, Płucienniczak G, Sawicka D, Bednarczyk M. Primordial germ cells (PGCs) as a tool for creating transgenic chickens. Pol J Vet Sci. 2012; 1: 55-61, Doi: 10.2478/v10181-011-0132-6.

28. England MA, Matsumura G. Primordial germ cells in the primitive streak stages chick embryo as studied by scanning electron microscopy. J Anat. 1993;183(pt1): 67-73.

29. Jung JG, Kim DK, Park TS, Lee SD, Lim JM, Han JY. Development of novel markers for the characterization of chicken primordial germ cells. Stem Cells. 2005; 23(5): 689-698, Doi:10.1634/stemcells.2004-0208.

30. Mozdziak PE, Angerman-Stewart J, Rushton B. Isolation of chicken primordial germ cells using fluorescence-activated cell sorting. Poult Sci. 2005; 84(4): 594-600, Doi: 10.1093/ps/84.4.594.

31. Nakamura Y, Kagami H, Tagami T. Development, differentiation and manipulation of chicken germ cells. Dev Growth Differ. 2013; 55(1): 20-40, Doi:10.1111/dgd.12026.

32. Zuo Q, Zhou J, Wag M, Zhang Y, Chen G, Li B. Study on the function and mechanism of Lin28B in the formation of chicken primordial germ cell. Anim. 2021; 11(1): 43, Doi:10.3390/ani11010043.

33. Shedge S, Roy P, Shedge A, Doshi MA. Periodic Acid Schiff (PAS) staining: a useful technique for demonstration of carbohydrates. Medico Leg Upd. 2020; 20(2): 353-357, Doi: 10.37506/mlu. v20i2.1129.

34. Meyer DB. Application of the periodic acid-Schiff technique to whole chick embryos. Stain Technol. 1960; 35(2): 83-89, Doi: 10.3109/10520296009114721.

35. Moller HJ, Heinegard D, Poulsen JH. Combined alcian blue and silver staining of subnanogram quantities of proteoglycans and glycosaminoglycans in sodium dodecyl sulfate-polyacrylamide gels. Anal Biochem. 1993; 209: 169-175, Doi: 10.1006/abio.1993.1098.

36. Padra JT, Lindén SK. Optimization of Alcian blue pH 1.0 histo- staining protocols to match mass spectrometric quantifications of sulfomucins and circumvent false positive results due to sialomucins. Glycobiol. 2021; 32(1): 6-10, Doi: 10.1093/glycob/ cwab091.

37. Mohamed GK, Selim AA, Abdelhafeez HH, Mohamed MB. Histomorphological developmental studies of the left ovary in the Japanese quail (*Coturnix Coturnix Japonica*). M J Cyto. 2017; 1 (1): 1-21.

38. Avila RE, Samar ME, De Fabro SP. Evolution of germinal epithelium in the chick ovary during embryogenesis. Revista de la Facultad de Ciencias Medicas (RFCM). 1991; 49(1): 11-15.

39. Park TS, Han JY. Derivation and characterization of pluripotent embryonic germ cells in chicken. Mol Reprod Dev. 2000; 56(4): 475-482, Doi:10.1002/1098-2795(200008)56:4<475: AID-MRD5>3.0.CO;2-M .

40. Dehdilani N, Yousefi Taemeh S, Rival-Gervier S, Montillet G, Kress C, Jesn Ch, Goshayeshi L, Dehghani H, Pain B. Enhanced cultivation of chicken primordial germ cells. Sci Rep. 2023; 13: 1-13, Doi: 10.1038/s41598-023-39536-1.

41. Wade AJ, French NA, Ireland GW. The potential for archiving and reconstituting valuable strains of turkey (*Meleagris gallopavo*) using primordial germ cells. Poul Sci. 2014; 93(4): 799-809, Doi: 10.3382/ps.2013-03629.

42. Gooi HC, Feizi T, Kapadia A, Knowles BB, Solter D, Evans MJ. Stage-specific embryonic antigen involves alpha l to 3 fucosylated type 2 blood group chains. Nature. 1981; 292: 156-158, doi: 10.1038/292156a0.

43. Yu F, Zhu Z, Chen X, Huang J, Jia R, Pan J. Isolation, characterization and germline chimera preparation of primordial germ cells from the Chinese Meiling chicken. Poult Sci. 2019; 98(2): 566-572, Doi: 10.3382/ps/pey410.

44. Fox N, Damjanov I, Martinez-Hernandez A, Knowles BB, Solter D. Immunohistochemical localization of the early embryonic antigen (SSEA-1) in post implantation mouse embryos and fetal and adult tissues. Dev Biol. 1981;83(2): 391-398, doi: 10.1016/0012-1606(81)90487-5.

45. Nonoyama S, Karakida T, Chiba-Ohkuma R, Yamamoto R, Ujiie Y, Nagano T, Yamakoshi Y, Gomi K. Development and characterization of alkaline phosphatase-positive human umbilical cord perivascular cells. Cells. 2021; 10(11): 3011, Doi: 10.3390/cells10113011.

46. Chiquoine AD. The identification, origin, and migration of the primordial germ cells in the mouse embryo. Anat Rec. 1954; 118(2):135-146, Doi: 10.1002/ar.1091180202.

47. Koc ND, Rikap Yüce R. A light- and electron microscopic study of primordial germ cells in the zebra fish *(Danio rerio)*. Biol Res. 2012; 45: 331-336, Doi: 10.4067/S0716-97602012000400001.

48. Swartz WJ. Acid and alkaline phosphatase activity in migrating primordial germ cells of the early chick embryo. Anat Rec. 1982; 202(3): 379-385, Doi:10.1002/ar.1092020310.

Cite this article as: Al-Shuwaili EHA, Hosseini A, Nabipour A. Identification of primordial germ cells in early pheasant (*Phasianus colchicus*) embryo. Explor Anim Med Res. 2026; 16(1), DOI: 10.52635/eamr/16.1.130-139.